UNIVERSITA' DEGLI STUDI "ROMA TRE"
SCUOLA DOTTORALE IN GEOLOGIA DELL'AMBIENTE E DELLE RISORSE (SDIGAR)
SEZIONE GEOLOGIA DELLE RISORSE NATURALI
- XXV CICLO-

CENOZOIC GEOMETRIC AND KINEMATIC EVOLUTION OF THE TUSCAN-UMBRIAN TECTONO-STRATIGRAPHIC UNITS (NORTHERN APENNINES): PALEOTHERMOMETRIC AND PALEOMAGNETIC CONSTRAINTS

PhD Candidate
Chiara Caricchi

Advisor: Prof. Sveva Corrado

Co-advisors: Prof. Massimo Mattei
Dr. Francesca Cifelli
Dr. Luca Aldega

Head of the Doctoral School:
Prof. Domenico Cosentino

UNIVERSITA' DEGLI STUDI "ROMA TRE"
SCUOLA DOTTORALE IN GEOLOGIA DELL'AMBIENTE E DELLE RISORSE
(SDIGAR)
SEZIONE GEOLOGIA DELLE RISORSE NATURALI
- XXV CICLO-

CENOZOIC GEOMETRIC AND KINEMATIC EVOLUTION OF THE TUSCAN-UMBRIAN TECTONO-STRATIGRAPHIC UNITS (NORTHERN APENNINES): PALEOTHERMOMETRIC AND PALEOMAGNETIC CONSTRAINTS

PhD Candidate
Chiara Caricchi

Advisor**: Prof. Sveva Corrado**

Co-advisors **: Prof. Massimo Mattei**
Dr. Francesca Cifelli
Dr. Aldega Luca

Head of the Doctoral School**:**
Prof. Domenico Cosentino

A.A. 2012/2013

A mio nonno

-Teatro di dossi, ebbri, calcinati,
muto, è la muta luna che ti vive-
L'Appennino
Pier Paolo Pasolini

-Vedere di nuovo un greppe dell' Appennino dove risuona
fra gli alberi un' usata e semplice tramontana-
Vorrei
Francesco Guccini

Table of contents

Acknowledgements

This dissertation would not have been possible without the guidance and the help of several individuals who in one way or another contributed and extended their valuable assistance in the preparation and completion of this study.

First and foremost, my utmost gratitude to my supervisor Prof. Sveva Corrado for her guidance and support during these years, for her notable teaching and help throughout this project's development.

It is with heartfelt gratitude that I acknowledge the support and help of my co-supervisor Prof. Massimo Mattei. I thank him, for his teaching, precious advices and for listening to my concerns, solving my problems with patience and always with a smile.

I am deeply indebted to Francesca Cifelli, without her generous help, this work would not have been possible. I thank her for guiding me through the work in the paleomagnetic laboratory and for always being there during these years for discussions, teachings and advising always the right way.

My sincere gratitude goes to Luca Aldega for introducing me to lab work in clay analysis, for his precious help in the field work, for his support and scientific contributions. Moreover, I am grateful to Sergio lo Mastro for his help in X-ray analyses.

Thanks to Fabio Speranza for his help and useful discussions regarding this project. I owe my deepest gratitude to Leonardo Sagnotti for spending so much quality time in the lab with me. I wish to thank also all the other members of the paleomagnetic laboratory at INGV, in particular Aldo Winkler.

Flavia Botti and Prof. Federico Sani are acknowledged for facilitating my fieldwork and for helping clarify several points.

I have also benefited greatly from discussions with Prof. Massimiliano Barchi, who offered me new challenging ideas for my research. I wish to thank the whole PRIN Project team and in particular Francesco Mirabella, Fausto Pazzaglia, Francesco Brozzetti, for

facilitating my field work and for their helpful advices. Thanks to Massimiliano Zattin for providing the thermocronological analyses and for valuable suggestions.
I owe my deepest gratitude to Domenico Grigo and Eni s.p.a. for permission to access to large amounts of wells data, very important to my work.

Special thanks go to the Prof. Giovanni Muttoni and Maria Laura Balestrieri for their careful revision of my thesis.

Thanks to Prof. Simonetta Cirilli for our nice friendship, for her important advices and her continuous presence.

I am indebted to my many colleagues with whom I shared the office or who I met in these years at Roma Tre. First of all, thank to those who well welcomed me on my arrival: Lea (for her help and nice conversation), Danilo, Matteo, Valerio, Massimetto e Luca (thanks for our friendship, thanks to Beatrice too), Andrea Bollati, Lilli, Luigi, Gabriele, Stella, Irene, and still Fabio, Stefano, Francesco, Andrea, Silvia (Ringraziamenti vari), Roberta, Marco and Gabriele “topomod”.

Thanks to Alessandro who supported, helped and resisted, especially in these last months…. as someone said there is nothing to explain, jigsaws falling into place.

Ringrazio Alessandra and Emilia con le quali ho passato dei momenti meravigliosi nella casa di Pilar, grazie per le indimenticabili giornate passate insieme, per avermi aiutato e ascoltato quando ne avevo bisogno.

Grazie di cuore ai miei genitori per il supporto morale e per essermi stati accanto in ogni momento… ringrazio anche il resto della mia numerosa e bella famiglia.

Un grande ringraziamento va ai miei amici per essermi stati sempre vicini anche se lontani. In questi anni la vostra presenza è stata fondamentale, grazie per esserci sempre. In particolare grazie ad Ale, Maurizio, Nicola, Andrea, Luigiloro, Marialuce, Luca, Stefi, Lucia ed al distaccamento romano Fabrizio, Fabio, Lara e Tommaso, manca solo una parola per voi… pa ne tto ne….

Abstract

In the past decades, paleothermal, thermochronological and paleomagnetic methodologies have been widely adopted for the reconstruction of orogenic belts evolution. Paleothermal and thermochronological analyses have allowed the reconstruction of the vertical paths (burial and exhumation path) of the sedimentary successions involved in the orogenic belts, providing thermal and time constraints on their evolution. Besides, paleomagnetic analysis are an excellent tool to assess kinematic models of curved orogenic systems because of its great potential to quantify vertical axis rotations.

In this framework, a multidisciplinary approach was adopted in this thesis in order to understand the geometric and kinematic evolution of the Tuscan-Umbria-Marche Domain, in the inner portion of the Northern Apennines, during the Cenozoic time. In this sector of the Apennines, some issues on the deformation history are still unexplored. By integrating paleothermal, thermochronological and paleomagnetic results, it was possible to provide new data and constraints to reconstruct the tectonic evolution of this portion of the Apennine chain.

Two key areas of Northern Apennines have been investigated. An inner sector, from the Trasimeno Lake to the south to the Garfagnana area to the north, where sedimentary succession of the Tuscan Domain units were analysed. An outer sector, in the Umbria-Marche-domain, where the analyses were concentrated in the area affected by the low angle normal faults Altotiberina system, from Massicci Perugini to east of the Gubbio fault.

In chapter 1, the aim of the thesis, the methodology and the main phases of the research are illustrated. The methodological approach is based on the integration of common methods used in basin analysis, such as thermal analysis (organic matter optical analysis -vitrinite reflectance: R_o%, clay mineralogy by means of X-ray analyses) and thermochronological analyses (dating by fission track and (U-Th)/He in apatite). The optical studies of organic matter and X-ray diffraction analysis allowed defining the thermal maturity level reached by sedimentary succession. The thermochronological data define the age and rates of the exhumation. Paleothermal and thermochronological data were used to calibrate 1D thermo-structural models used to reconstruct the burial history and quantify the tectono-stratigraphic loads now removed.

The paleomagnetic analyses were conducted in order to reconstruct the rotational history of the internal part of Northern Apennines. Besides paleomagnetic analysis, magnetic mineralogy analysis was carried out in order to identify the carriers of the natural remnant magnetization. The anisotropy of magnetic susceptibility (AMS) analysis was also carried out in the analysed sediments. This method constitutes an unique tool in defining the deformation pattern in poorly deformed sedimentary sequences, whose tectonic setting can't easily be defined using classical structural methods.

Chapter 2 illustrates the paleothermal analyses carried out in the internal sector (Tuscan Domain). Results show two main maturity trends: one perpendicular and the other parallel to the strike of the chain. In the first case, the paleothermal indicators record a decrease in thermal maturity from inner to outer sectors of the chain. In detail, Ro% values of the internal sector range from 0.6 to 0.9% indicating early-mid mature stages of hydrocarbon generation. Moving toward the external areas of the fold-and-thrust belt, values range from 0.3% to 0.5% indicating an immature stage of hydrocarbon generation. These data are in agreement with those obtained by the semi-quantitative analysis of clay fraction which shows a decrease of illite content in mixed layers from 89% (maximum temperature of 120-130 °C) to 38% (temperature below 100 °C) from hinterland towards foreland. Following the method proposed by Hillier (1995), a low heating rate, typical of foredeep basins, was obtained from the comparison between R_o% and I% in I/S mixed layers. A geothermal gradient of about 23 °C/Km is derived combining calculated heating and burial rates and used for thermal modelling. The second trend shows a thermal maturity increase, along the strike of the chain from the SW (Trasimeno lake area) toward the NW (Pratomagno area) where vitrinite reflectance maturity reaches values up to 0.95% and illite 87-89% in agreement with thermal maturity distribution derived from Ro% data. According to the performed one dimensional modelling, maximum burial and thermal maturity of the Tuscan Nappe succession decrease from the inner toward the outer sector with a corresponding reduction of the eroded thicknesses related to a reduction of the allocthonous (Ligurian Unit) which takes place from north to south along the chain, from hinterland towards foreland.

Chapter 3 is focused in the area characterized by the low-angle Altoriberina normal fault system. Paleothermal (surface and well water) and thermochronological data were integrated, in order to develop an exhumation history model for this sector of the chain.

The main evidence is an increase in the exhumation age from the innermost sector affected by the Altotiberina normal fault system (Massicci Perugini, 3 Ma) to the most external area affected by this system (to the east of the fault of Gubbio, 4.3 Ma). Significant novelty derives also from the rates of exhumation, suggesting quicker exhumation of Massicci Perugini (0.8 mm/yr) when compared to the area to the east of the Gubbio fault (0.5 mm/y). Therefore, these data suggest that most of the exhumation in the Massicci Perugini may be related to the recent activity of the normal faults and not only to the old compression phase and subsequent erosion. Thus the extensional activity of the Altotiberina Fault system may account for the younger exhumation age in the internal sector compared to the external one. Moreover the quicker erosion rate of about 0.8 mm/yr in the internal sector may be related to tectonic activity.

In chapter 4, results obtained from paleomagnetic studies carried out in the Tuscan Domain, along the innermost arc, are shown. The rotational pattern recorded in Eocene-Oligocene sediments, shows a decrease of rotation values from lower (area of Trasimeno Lake) towards higher (Garfagnana area) latitude. In fact, mean rotations values recorded in the Trasimeno Lake area are 96° ± 25° counterclockwise, passing through 81° ± 35° counterclockwise for the Mt. Chianti area, up to 37° ± 16° counterclockwise in Garfagnana. These data do not fit into an oroclinal model, proposed for the external sector of the chain (Umbria-Marche domain). In this study I propose a new model that takes into account the contribution of the rotation of the Corsica-Sardinia block to the structural architecture of this sector of chain. This model predicts that the main tectonic phases of the internal sector of the chain occurred between Oligocene and early Miocene times, during the drift of the Corsica-Sardinia block. The Tuscan Domain units recorded rotation of the Corsica-Sardinia block during their incipient deformation. This block rotation occurred around a pole placed at 43.5° N and 9.5° E. At this time, the Northern Apennines and Corsica-Sardinia block were two different sectors of the upper plate of the Central Mediterranean subduction system, whereas the Umbria domain still represented the undeformed foreland. The contribution of the Corsica-Sardinia to the rotation of the Tuscan Domain depended on the position respect to the rotation pole. In fact, the amount of the Corsica-Sardinia block rotation is recorded in the southern areas (Lake Trasimeno) and tends to decrease at higher latitude (Mt. Chianti) until to the area at north of rotation pole where the contribution of Corsica Sardinia block rotation is not recorded (Garfagnana area).

In chapter 5, the AMS carried out on the same deposits analyzed for paleomagnetic reconstructions, are illustrated. AMS data show that the sediments are characterized by a dominant magnetic foliation parallel to the bedding plane, suggesting that the magnetic fabric is due to the compaction process during the diagenetic process that the sediments undergone. Moreover, a distinct magnetic lineation was observed, indicating an incipient deformation related to a compressional deformation, overprinted on to the original magnetic fabric. In most of the cases the lineation is parallel to the fold axes and thrust fronts, in agreement with previous results in the Umbria Marche domain.

In chapter 6, a general discussion is developed and final remarks are illustrated.

Riassunto

Negli ultimi decenni, studi paleotermici, termocronologici e paleomagnetici sono stati utilizzati come strumenti d'indagine nella ricostruzione della storia evolutiva delle catene orogeniche. Le analisi paleotermiche e termocronologiche permettono di ricostruire i percorsi verticali, di seppellimento e di esumazione, delle successioni sedimentarie che costituiscono le catene orogeniche, fornendo vincoli termici e temporali per la ricostruzione dell'evoluzione delle stesse. Le analisi paleomagnetiche, permettono di quantificare rotazioni intorno ad assi verticali, e permettono di definire la storia rotazionale di un'area, fornendo degli importanti vincoli per la ricostruzione dell' evoluzione cinematica delle catene arcuate.

Lo scopo di questa tesi è quello di comprendere, con approccio multidisciplinare, l'evoluzione geometrica e cinematica, durante il Cenozoico, delle unità tettono-stratigrafiche del dominio Tosco-Umbro-Marchigiano nel settore più interno dell'Appennino Settentrionale, un'area ad oggi tuttora inesplorata dal punto di vista paleotermocronologico e paleomagnetico. Mediante questo lavoro, ci si prefigge di fornire nuovi dati e porre dei vincoli alla ricostruzione dell'evoluzione di questa porzione dell'Appennino.

Sono stati indagati due settori chiave dell'Appennino Settentrionale: un settore più interno di pertinenza toscana e un settore più esterno che interessa il dominio Umbro-Marchigiano. Nel settore interno sono state analizzate le successioni sedimentarie delle unità toscane dall'area del lago Trasimeno a sud fino alla Garfagnana a nord, mentre nel settore nel dominio Umbro-Marchigiano, le analisi sono state concentrate nell'area interessata dal sistema di faglie normali a basso angolo della valle Altotiberina, dai Massicci Perugini a ovest fino a est della dorsale di Gubbio.

Nel Capitolo 1, vengono illustrate le finalità della tesi, le metodologie impiegate e come è stata articolata l'attività di ricerca.

L'approccio metodologico, di tipo integrato, ha previsto l'utilizzo di metodi di uso comune nell'analisi di bacino, quali le analisi termiche (analisi ottiche della materia organica- quali la riflettanza della vitrinite: R_o%; analisi diffrattometriche a raggi X delle argille) e termocronologiche (datazioni con tracce di fissione e con il metodo U-Th/He in apatite). Lo studio ottico della materia organica e le analisi diffrattometriche ai raggi-X

hanno permesso di definire il grado di maturità raggiunto dalle successioni sedimentarie e dettagliare il carico tettonico e/o stratigrafico subìto dalle successioni analizzate. I dati termocronologici hanno permesso inoltre di definire l'età e i tassi di esumazione in diversi settori. I dati paleotermici e termocronologici sono stati utilizzati per effettuare modellazioni monodimensionali della storia del seppellimento e di esumazione delle successioni in esame, attraverso il software Basin Mod 1-D.

Le analisi paleomagnetiche sono state condotte al fine di valutare le entità delle rotazioni a cui sono andati incontro durante la strutturazione della catena.
Tali analisi sono state affiancate da quelle di anisotropia della suscettività magnetica (AMS) e di mineralogia magnetica. Le prime hanno permesso di identificare i processi sedimentari e/o tettonici subiti dai sedimenti. Le seconde hanno permesso da un lato di identificare i minerali magnetici portatori della magnetizzazione e comprendere quindi le relazioni tra questi e la componente di magnetizzazione caratteristica rimanente individuata, dall'altro di distinguere il contributo di ferromagnetici e paramagnetici alla suscettività magnetica.

Le analisi paleotermiche (Capitolo 2) condotte nel settore interno (Dominio Toscano) mostrano due principali *trend* di maturità termica: uno perpendicolare ed uno parallelo all'asse della catena. Nel primo caso, gli indicatori paleotermici evidenziano una diminuzione di maturità termica verso i settori esterni. I valori di riflettenza della vitrinite (R_o%) variano da 0.6 a 0.9 % (stadio iniziale e intermedio della generazione d'idrocarburi) a 0.3-0.5% (livello di immaturità termica). Tali dati sono in accordo con quelli ottenuti dalle analisi semi-quantitative della frazione argillosa che hanno mostrato un andamento simile con diminuzione del contenuto di illite nell'interstratificato illite-smectite dall'89% (temperatura massima raggiunta di 120-130 °C) al 38% (temperatura inferiore ai 100 °C). Il secondo *trend* osservato consiste in un incremento della maturità termica lungo lo *strike* della catena da SE verso NW, con un salto nei valori di riflettenza della vitrinite fino a 0.95% ed un corrispettivo contenuto di illite pari all'87-89% (a NW della Val Marecchia, area di Pratomagno). Questo *pattern* di maturità termica, come dimostrato dalla modellazione termica del bacino, è legato ad una diminuzione dello spessore delle unità alloctone (Unità Ligure) che si esplicita in una riduzione dello spessore del cuneo orogenico che si registra sia spostandosi da NW a SE lungo la catena, sia dai settori interni a quelli esterni della stessa.

Gli studi focalizzati nell'area del sistema di faglie a basso angolo dell'Altotiberina (Capitolo 3) hanno visto l'integrazione di dati paleotermici (superficiali e di pozzo) e termocronologici, finalizzati allo sviluppo di un modello della storia di esumazione di questo particolare settore di catena. I risultati ottenuti dalle analisi di datazione termocronologica di (U-Th)/He in apatiti mostrano un aumento delle età di esumazione dalle aree più interne della catena (Massici Perugini, 3 Ma) verso i settori esterni (ad est della faglia di Gubbio, 4.3 Ma). Variazioni significative si registrano anche nei tassi di esumazione, che suggeriscono una più rapida esumazione dei Massicci Perugini (0.8 mm/a) rispetto alle aree a est della faglia di Gubbio (0.5 mm/a). Questi dati suggeriscono quindi che la maggior parte dell'esumazione in questo settore sia legata alla recente attività delle faglie normali e non solo alla vecchia fase di compressione e relativa erosione. Così l'attività estensionale del sistema Altotiberina può spiegare l'età più giovane dell'esumazione nel settore interno rispetto a quello esterno. Inoltre la maggiore velocità di erosione di circa 0.8 mm/a nel settore interno può essere correlato all'attività tettonica. L'attività estensionale potrebbe rendere ragione del fatto che i settori interni mostrino sia un tasso di erosione maggiore (intorno a 0.1 mm/a) che una età di esumazione più giovane rispetto agli esterni.

I risultati ottenuti dagli studi paleomagnetici (Capitolo 4) condotti nel Dominio Toscano, lungo l'arco più interno, hanno permesso di formulare un nuovo modello tettonico per questo settore di catena. La distribuzione delle rotazioni ottenuta su sedimenti eocenici e oligocenici mostra un *trend* di diminuzione dai settori a più basse latitudini (area del Lago Trasimeno) verso i settori a latitudini maggiori (area della Garfagnana). Sono state registrate rotazioni antiorarie medie di 96° ± 25° per l'area del Trasimeno, passando per 81° ± 35° per l'area dei Monti del Chianti, fino a 37° ± 16° nell'area della Garfagnana. Questi dati, in disaccordo con il modello dell'oroclino avanzato per il settore esterno (Dominio Umbro-Marchigiano), suggeriscono il contributo della rotazione del blocco Sardo-Corso nella strutturazione di questo settore di catena. Si propone un nuovo modello nel quale le principali fasi di evoluzione tettonica del settore interno dell'Appennino settentrionale si ipotizza siano avvenute tra Oligocene e il Miocene inferiore, quando il Dominio Toscano entra in catena e avviene la rotazione antioraria di 45° del blocco Sardo-Corso attorno ad un polo di rotazione posto a 43.5°N e 9.5°E. In questa fase, l'Appennino Settentrionale e il blocco Sardo-Corso costituiscono due settori della placca superiore del sistema di subduzione quando il Dominio Umbro rappresenta ancora l'avampaese

indeformato. Il trasferimento dell'entità di rotazione del blocco Sardo-Corso è evidente nei settori meridionali (Lago Trasimeno) e tende a diminuire all'aumentare della latitudine (Monti del Chianti) fino a non essere registrata nei settori a nord del polo di rotazione (Area della Garfagnana).

Nella medesima area, gli studi di anisotropia della suscettività magnetica (Capitolo 5) mostrano come i sedimenti siano caratterizzati da una dominante foliazione magnetica parallela al piano di stratificazione, suggerendo un *fabric* magnetico legato principalmente ai processi diagenetici dei sedimenti. È stata inoltre osservata una distinta lineazione magnetica disposta parallelamente al fronte dei *thrust* principali, caratteristica indicativa di una sedimentazione in regime compressivo, in accordo con i dati già presenti in letteratura, nel settore Umbro-Marchigiano.

Nel capitolo 6, vengono infine discussi i risultati ottenuti nelle diverse fasi del lavoro e vengono esposte le considerazioni conclusive.

Chapter 1

Introduction

1.1 Aim of thesis and methodology

The studies carried out in this thesis are aimed to the reconstruction of the geometric and kinematic evolution of the Tuscan-Umbria tectono-stratigraphic units, an area located in the more internal sector of the Northern Apennines.

The research is based on a multidisciplinary approach based on the integration of different methodologies: thermal and thermo-chronological analyses, paleomagnetism, and anisotropy of the magnetic susceptibility (AMS) analyses.

The thermal and thermochronological approach is typical of the Basin Analyses field, mainly developed by oil companies for exploration. Thermal analyses consist of the optical analyses of the organic matter dispersed in sediments correlated to the X-ray diffraction study of clay minerals, and allow quantifying the maximum sedimentary and/or tectonic loads that studied successions have undergone. The thermo-chronological methods (apatite fission tracks and (U/Th)/He dating) implement the analyses providing the definition of the exhumation timing, rates and magnitudes of exposed successions. Results were uses to build mono-dimensional thermal and burial models.

Paleomagnetic studies have been used to reconstruct the tectonic and rotational history of the curved Northern Apennines. In particular, a quantitative analysis of the distribution and magnitude of vertical axis rotations was used to define the timing of the bending and to discriminate the different tectonic processes that concurred to shape its present-day curvature. Results from this study and

integration with other published data were used to build a suitable model to explain the tectonic evolution of Northern Apennines.

The anisotropy of magnetic susceptibility (AMS) analyses were carried out in order to reconstruct the deformational history of fine-grained sediments exposed in the internal sector of the Northern Apennine chain. In particular, the magnetic fabric analysis on these sediments helped in discriminate the effects of sedimentary processes (e.g., compaction) from tectonic processes. Moreover, integrating data from this study with previous data, it was possible to reconstruct the timing of the deformation of this portion of the Apennine chain at local and regional scale.

Furthermore paleo-thermal and paleomagnetic data reported in this thesis represent the first results collected in this sector of the Northern Apennines, filling a pre-existing gap in the internal sector of the chain.

1.2 Thesis Organization

Following this introductory part (Chapter 1), this thesis is divided into other four parts.

In Chapter 2 the thermal evolution models of the Tuscan Nappe units are illustrated, and a reconstruction of the architecture of the thrust wedge is proposed.

In Chapter 3 a possible model for the kinematic evolution of the Altotiberina Fault system is described, based on the collected paleo-thermal and thermo-chronological data.

In Chapter 4 the rotational pattern in the Tuscan Nappe, as deduced by paleomagnetic analysis, is illustrated. A new reconstruction of the tectonic evolution of the area is proposed, in the general framework of the Cenozoic Mediterranean evolution.

In Chapter 5 the anisotropy of magnetic susceptibility (AMS) data are presented and a reconstruction of the pattern of the deformation in this sector of the chain is described.

In Chapter 6 final remarks on the main results achieved by the entire research are presented.

1.3 Main phases of the research

The thesis was developed in three main phases.

Phase one was mainly devoted to the bibliographic research. Previous studies on regional geology, and methodological papers were collected in order to guarantee an up-to-date knowledge on the study area and on the methodologies used in this research.

Phase two was mainly dedicated to fieldwork and sampling. Moreover, laboratories analyses accompanied and alternated with the fieldwork.

Phase three was related to data processing. Results were then correlated and used to reconstruct new possible models on the geological and geodynamic evolution of the Northern Apennines Chain.

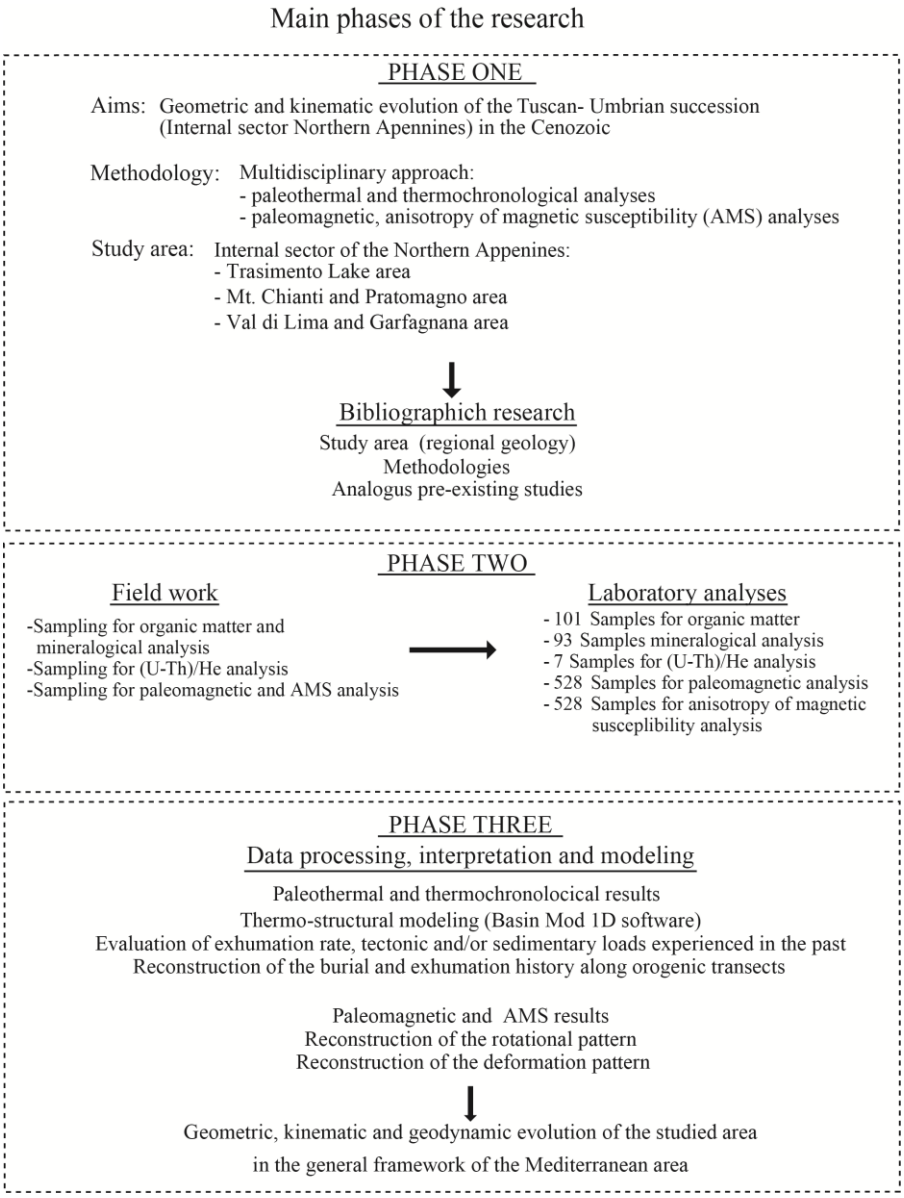

Fig. 1.1. Flowchart of the thesis.

Chapter 2

Along strike variations in the architecture of a thrust wedge detected by means of indicators of thermal exposure: an example from the Northern-Central Apennines boundary (Italy)

2.1 Introduction

Fold-and-thrust belts (FTBs) frequently show lack of cilindricity along strike (Marshak *et al*., 2004). This feature may be expressed in terms of variations of the amount and rates of shortening and tectonic transport as well as of structural styles. These along strike variations can be gradual and easily honour the principle of kinematic compatibility (Butler *et al.* 2006 and references therein) or abrupt (Marshak *et al.* 2004 and references therein). In the last case, changes are marked by strike-slip faults that may be detectable at various scale from lithospheric to shallow crustal levels. These faults frequently show a complex and long-lived activity within the FTBs and their depth of formation and evolution are generally debated in kinematic reconstructions. This is the case of the Italian Apennines that is strongly segmented by transverse faults (Patacca and Scadone 2001, Tavarnelli *et al.,* 2004). Nevertheless these faults may mark variations in the exposure of different structural levels. Such evidences occur at the boundary between the Northern and the Central Apennines where the uppermost structural unit of the thrust pile, the Ligurian Nappe, is preserved from erosion as a result of variations of structural culminations along strike. Nevertheless very faint features are exposed on main transverse faults. To understand these variations despite of the incomplete sedimentary record preserved in the field, it is possible to attempt the reconstruction of regional cross sections on different blocks separated by transverse faults that take into account reliable evaluations of the

missing portions of the section now eroded and/or removed by tectonics (e.g., Zattin *et al*., 2002; Corrado *et al*. 2010a; Mirabella *et al.*, 2011). This approach allows to substantially reduce the number of acceptable geometric and kinematic models on the basis of the amount of exhumation and maximum burial that characterize different areas of the wedge.

Thermal modelling of sedimentary successions, constrained by paleothermal and low temperature thermochronological indicators, has been frequently performed in the external areas of fold-and-thrust belts (see Roure *et al.*, 2010 for a review) with several examples for the Apennines and Sicily (see, Corrado, 1995; Corrado *et al.* 1998; 2009; 2010b; Botti *et al.*, 2004; Mazzoli *et al.*, 2008; Aldega *et al.*, 2011; Di Paolo *et al.*, 2012) (Fig. 2.1). Nevertheless in the area to the south of the Val Sillaro and to the north of the peri-tyrrhenian volcanic complexes cropping out in Southern Tuscany-Northern Latium, studies of burial and thermal history are very scarce as well as the outcrops of the uppermost units overriding the wedge (Ligurian and Sub-ligurian Units).

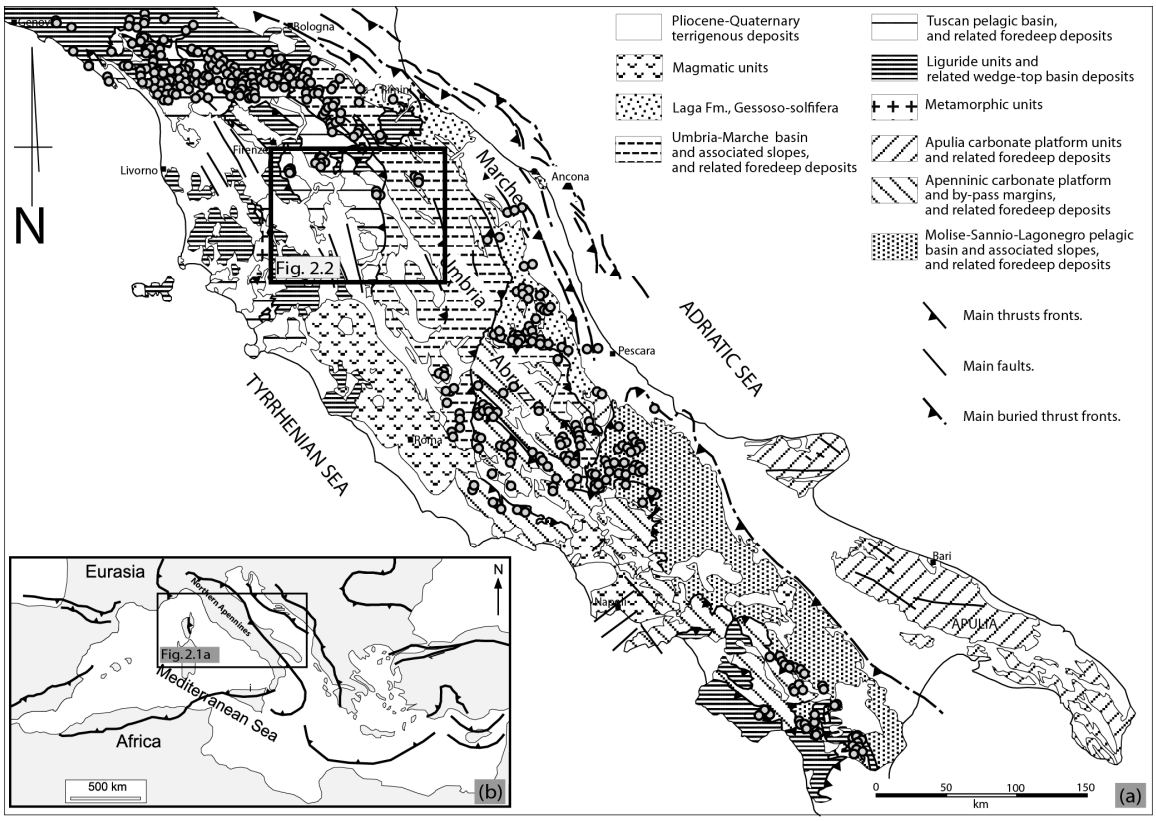

Fig. 2.1 Geological sketch map of the Italian peninsula showing the location of main sampling sites for thermochronological and paleothermal studies data along the Apennines (modified after Corrado *et al.* 2010a). Simplified main geological features from APAT(2004) and Butler *et al.*, (2004). Coordinates in UTM European Datum 1950 33N.

The aim of this chapter is to provide quantitative data on (sedimentary or tectonic) burial evolution during thrust wedge building in order to unravel changes across transverse

faults at the boundary between the Northern and the Central Apennines. In this chapter, I present a series of thermal models performed along five geological cross-sections across the Tuscan Nappe in an area located between Chianti and Cetona Mts. to the SW and the Trasimeno Lake and the Mugello Basin to the NE. These models allowed me to reconstruct the areal distribution of the eroded structural portion of the wedge and to draw the thrust belt evolution during Neogene times.

2.2 Geological setting

The Northern Apennines is the result of the development of the east to northeast orogenic wedge, above the subduction of the Ligure-Piemontese ocean. This process was followed by continental collision between the European plate (Corsica-Sardinia block) and Adriatic microplate (of African affinity) and by the opening of the Tyrrhenian Sea back-arc basin (Boccaletti *et al*.,1980*;* Malinverno and Ryan, 1986; Dewey *et al*., 1989; Boccaletti *et al*., 1990; Faccenna *et al*., 2004). Since the Oligocene, after continental collision, the evolution of the Northern Apennines proceeded by intra-continental deformation with a progressive migration of the orogenic system toward east. The deformation of ocean and passive margin paleogeographic domains brought to the structuring of different tectonic units (Barchi *et al.*, 1998a). Thrust and fold belt geometry were modified by extensional tectonics, that took place in Tortonian times and is still active (Barchi *et al.*, 1998b; Mirabella *et al.*, 2011).

The Northern Apennines is composed of a series of stacked structural units accreted onto the Adriatic microplate, whose litostratigraphic and structural features reflect the evolution of this sector of the chain (Baldacci *et al.*, 1967; Elter, 1975; Boccaletti *et al.*, 1980; Principi and Treves, 1984; Barchi *et al*., 1998b; Costa *et al*., 1998, Molli *et al*., 2002).

The innermost tectonostratigraphic unit is the Ligurian Unit (Etler, 1975; Bortolotti *et al.*, 2001; Cerrina Ferroni *et al.*, 2002). This unit is the remnants of the Ligurian Ocean and consists of a mix of ophiolite, sedimentary rocks and flysch deposits ("helminthoid flysch") (Etler, 1975; Marroni *et al.*, 2001; Festa *et al.*, 2010).

Onto the Ligurian Unit, the Epiligurian Unit unconformably overlie as was deposited in marine thrust-top basins (Ricci Lucchi, 1975; Barchi *et al.*, 2001; Cibin *et al.*, 2001). Deposition of the Epiligurian Unit occurred simultaneously with the east and northeast migration of the thrust and fold belt (Festa *et al.*, 2010). Underneath the Ligurian Unit there is the Subligurian unit, made up of Paleocene to Eocene shales and limestones

(Bortolotti *et al.*, 2001) and of thick early Oligocene siliciclastic deposits. The Subligurian Unit is considered as the first and oldest Apennines foredeep deposit indicating the onset of collision of the Ligurian accretionary wedge and the continental passive margin of the Adria microplate (Catanzariti *et al.*, 2003). The Ligurian and sub-Ligurian Units can be grouped together into a larger Ligurian Nappe which was then thrust north-eastward over more external units (Ventura *et al.*, 2001).

During the continental collision the Ligurian Nappe was obducted on to the western Adriatic margin, and the other accreted structural units (Ricci Lucchi, 1986; Boccaletti *et al.*, 1990, Argagni and Ricci Lucchi, 2001). These latter units are characterized by stratigraphic sequences, that consist of Paleozoic basement rocks unconformably overlain by Mesozoic evaporitic and carbonate deposits. These sequences are covered by Oligocene-Miocene thick and extensive syn-orogenic foredeep deposits. These deposits are progressively younger towards north-east and were deposited in eastward-migrating foredeep basins along the front of avalanching Ligurian Nappe and progressively incorporated in the fold and thrust system (Abbate *et al.*, 1970; Ricci Lucchi, 1986; Boccaletti *et al.*, 1990, Ventura *et al.*, 2001, Mirabella *et al.*, 2011). Two main tectono-stratigraphic units are recognized: the Tuscan Unit and the Umbria-Marche-Romagna Unit.

The Tuscan Unit is the main object of analyses in this work. Samples were collected from two main areas located respectively to the SE and to the NW of the Marecchia Valley lineament (MVL, see Fig. 2.2). The first sampling area is located at the boundary between Tuscany and Umbria regions. It is characterized by contractional architecture that consists of four structural units, piled up during Miocene times (Mirabella *et al.*, 2011). Some authors (e.g., Abbate and Bruni, 1989; Brozzetti, 2007) have regarded the outermost part of the Tuscan Nappe as belonging to a more external tectonic unit (Falterona-Cervarola Unit or Falterona Nappe). In this chapter, for this area, the Falterona-Cervarola Unit is interpreted as belonging to the Tuscan Nappe according to Plesi *et al.* (2002). The analysed stratigraphic succession of the Tuscan Nappe consists of pelagic foreland ramp deposits (Scaglia Toscana Fm.) and foredeep turbidite deposits (Macigno Fm.). The former consists of calcareous-marly turbidites and varicoloured shales. It can be divided into the Calcareniti di Dudda (Sto_4) and the Monte Filoncio (Sto_6) members (Ypresiano-Luteziano NP11-NP15; Rupeliano-Chattiano MNP25a) according to Geological Cartography Project, Sheets 299 Umbertide, 310 Passignano and 289 Città di Castello. The Macigno Fm. consists of thick-bedded coarse-grained siliciclastic turbidites alternating with siliciclastic thin and fine grained beds. Three members have been distinguished, referred, from bottom

to top, as Molin Nuovo (Mac_1), Poggio Belvedere (Mac_2) and Lippiano members (Mac_3) (Chattiano-Aquitaniano MNP25a-MNP25b-MN1d; Barsella *et al.*, 2009). Since Aquitanian time, the Tuscan Domain started being involved in compressive deformation to form the Tuscan Nappe detached at the level of the Scaglia Fm.. This tectonic unit is subdivided into minor tectonic elements delimitated by secondary thrust faults. In this area, moving from the west to the east, they are: Terontola Element, Tuoro Element, Portole Element, Ansina Element, Scarzola Element e Marcignano-Gioiello Element (Geological Cartography Project, 2011 a, b, c).

Regarding to the area to the north of MVL, the analyses have been carried out along Pratomagno ridge, Chianti ridge and around the Mugello Basin (Fig. 2.3). In detail, the structure of the Chianti Mountains has been interpreted as a result of thrust-and-fold deformation (Bonini, 1999) and is characterized by extensive outcrop of the Tuscan Nappe succession. In this sector of the chain, the Scaglia Toscana Fm. crops out down to its most ancient member from the Argille di Brotolo Member (Sto_2) (Albian-Turonian); to the Calcareniti di Dudda Member (Sto_4) (Upper Cretaceous-Lower Eocene). On top of it the Macigno Fm. has a thickness of about 3,000 m and consists of turbidite sandstones that evolve to pelites at the top of succession. This formation has been subdivided into five members (Geological Cartography Project 2011d)

The main structural feature of this region is an E-NE vergent, steeply to moderately dipping, overturned anticline folding the Macigno sandstones and exposing Cretaceous-Oligocene marls and shales (Scisti a Policromi or Scaglia Toscana Fm.) in its core (Bonini *et al*., 2012). Referring to Sagri *et al.* (2012), the Tuscan Nappe in this sector thrust onto more external Cervarola-Falterona Unit. This unit crops out in the Pratomagno ridge and includes a stratigraphic succession that consists of Rupelian-Chattian varicoloured clays alternating with mudstone layers (Villore Marls) at the bottom, silicoclastics turbidite of Falterona Mts. Sandstone (Chattian-Burdigalian) and Burdigalian-Langhian Vicchio Marls. In detail the Falterona Fm. consists of five members, distinguished by layer thickness and arenites/pelites ratio that decreases toward the top of the succession. From bottom to the top, there are the M. Falco Member (Fal_1); the Camaldoli Member (Fal_2); the Montalto Member (Fal_3); the Lonnano Member (Fal_4) (Bortolotti *et al.*, 2012).

The second area extends to south-southeast of the Mugello Basin and is characterized by Monte Falterona and Acquerino Units that thrust on to the Umbria–Romagna domain. The Acquerino Unit consists of Chattian-Aquitanian varicolours marls (Marne di Villore Fm.) at the bottom followed by Chattian-Budigalian turbiditic deposits of the Aquerino

Fm. (Bettelli *et al.*, 2002). Many authors consider this unit such as a sub-unit of the Falterona-Cervarola Unit (Abbate *et al*., 1969; Boccaletti and Coli, 1982; Guenther and Reutter 1985). Recently other authors have interpreted this unit as independent (Bettelli *et al.*, 2002; Cerrina Feroni *et al*., 2002; Cibin *et al.*, 2004). From Oligocene time the compressive phase, during the collisional stage, deformed the foredeep Tuscan successions with the migration toward north-east of the deformational front. This deformation determined the present-day configuration of the chain with a structure of thrust and associate folds.

2.3 Methods and materials

2.3.1 Organic matter optical analyses

To the south of MVL, in the area located at the boundary between Tuscany and Umbria regions, a suite of 48 samples for vitrinite reflectance analyses was collected from the Tuscan Nappe, mainly from the Macigno Fm.. In detail, samples were collected in the different tectonic elements, recognized in this area, along four cross-sections perpendicular to the chain axis (see A-A', B-B', C-C' and D-D' in Fig. 2.2).

From hinterland to foreland the following tectonic thrust sheets were sampled: the Terontola Element, the Tuoro Element, the Portole Element, the Ansina Element, the Scarzola Element and the Marcignano-Gioiello Element. These elements are constituted by rocks belonging to the Tuscan succession that, in the internal sector, consists of the Scaglia Toscana Fm. at the bottom, followed by three members of the Macigno Fm. with a thickness of about 1,700-1,800 meters. In the external sector (Marcignano – Gioiello element) the sedimentary succession consists of the youngest member of the Scaglia Toscana formation (Sto_6) and two members of the Macigno Fm. (Mac_2 and Mac_3) for about 1,200 m of total thickness (Fig. 2.3). The samples were collected from the three members of the Macigno Fm., from both thick arenaceous-pelitic beds and thin-fine turbiditic beds. Samples were mainly composed by coal seams and well preserved wooden fragments 1 to 3 cm-long dispersed in the arenaceous sediments (Tab. 2.1).

Other samples are from the areas to the north of the MVL. In detail, five samples were collected across the Pratomagno ridge, along section E-E' (Fig. 2.2) from the base of arenaceous levels of the Falterona Fm. (Fal_2, Fal_3 members). These samples consist of wooden fragments dispersed in sediments. Three further samples were collected in the area to the south-southeast of the Mugello Basin, two of these in the Falterona Fm. (Fal_3

member) and the one from a fine and laminated arenaceous layer of the Aquerino Fm. (Tab. 2.2).

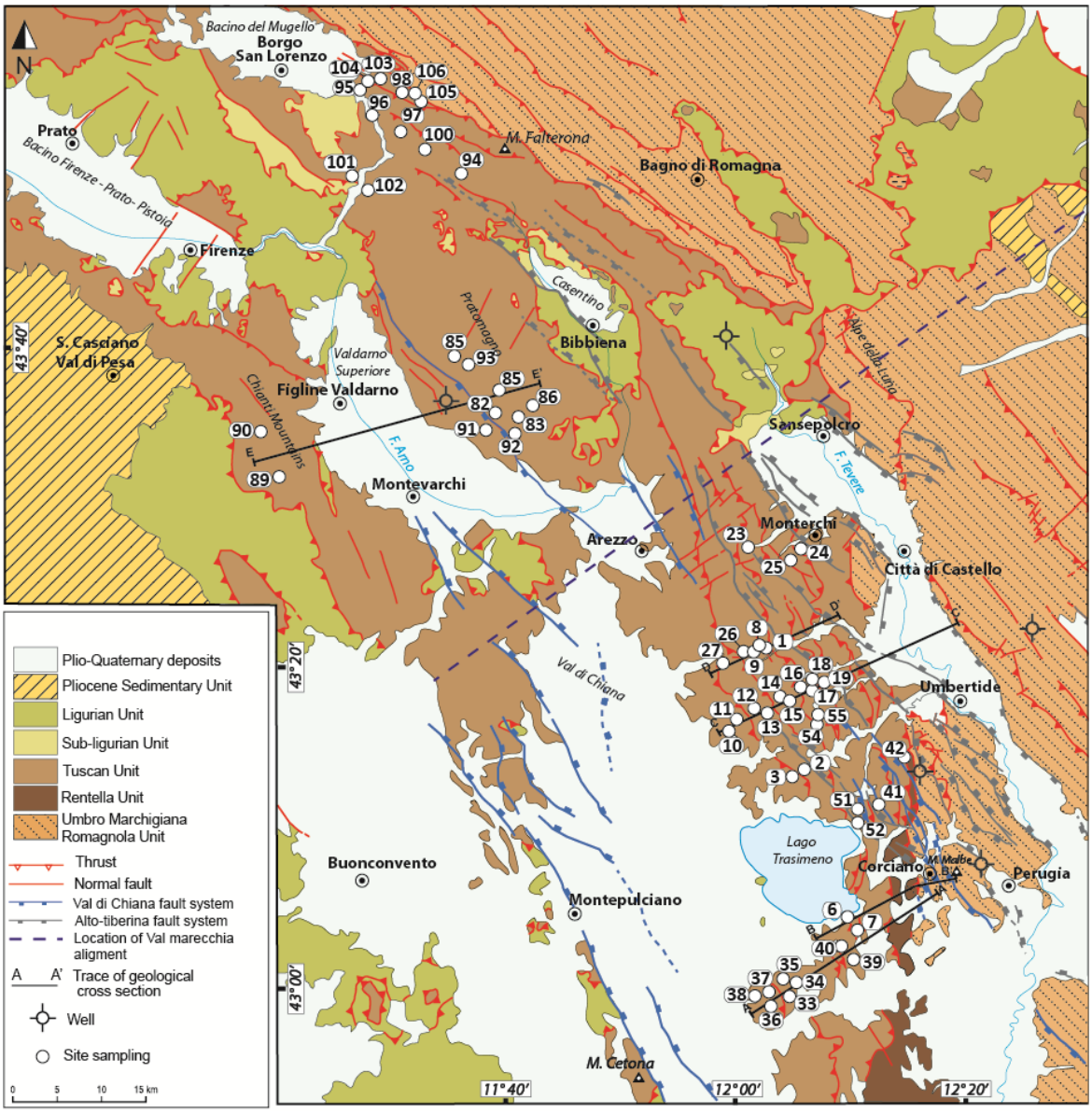

Fig. 2.2 Tectonic sketch map of the study area with sample sites. Compiled after Mirabella *et al*., (2011) and Geological Cartography Project (2011), Umbertide, in Carta Geologica d'Italia, sheet 299, scale 1:50,000, Ist. Super. per la Prot. e la Ric. Rome.

Whole-rock samples were mounted in epoxy resin and polished according to standard procedures (Bustin *et al*., 1990). Vitrinite Reflectance (Ro%) was then performed on randomly oriented grains using a Zeiss Axioplan microscope, under oil immersion in reflected monochromatic non-polarised light. The number of measurements that were performed on vitrinite fragments ranges from 20 for samples with small amounts of organic matter to 100 for coal seams and samples rich in well preserved fragments. Mean reflectance and standard deviation values were calculated for all measurements identifying the indigenous population.

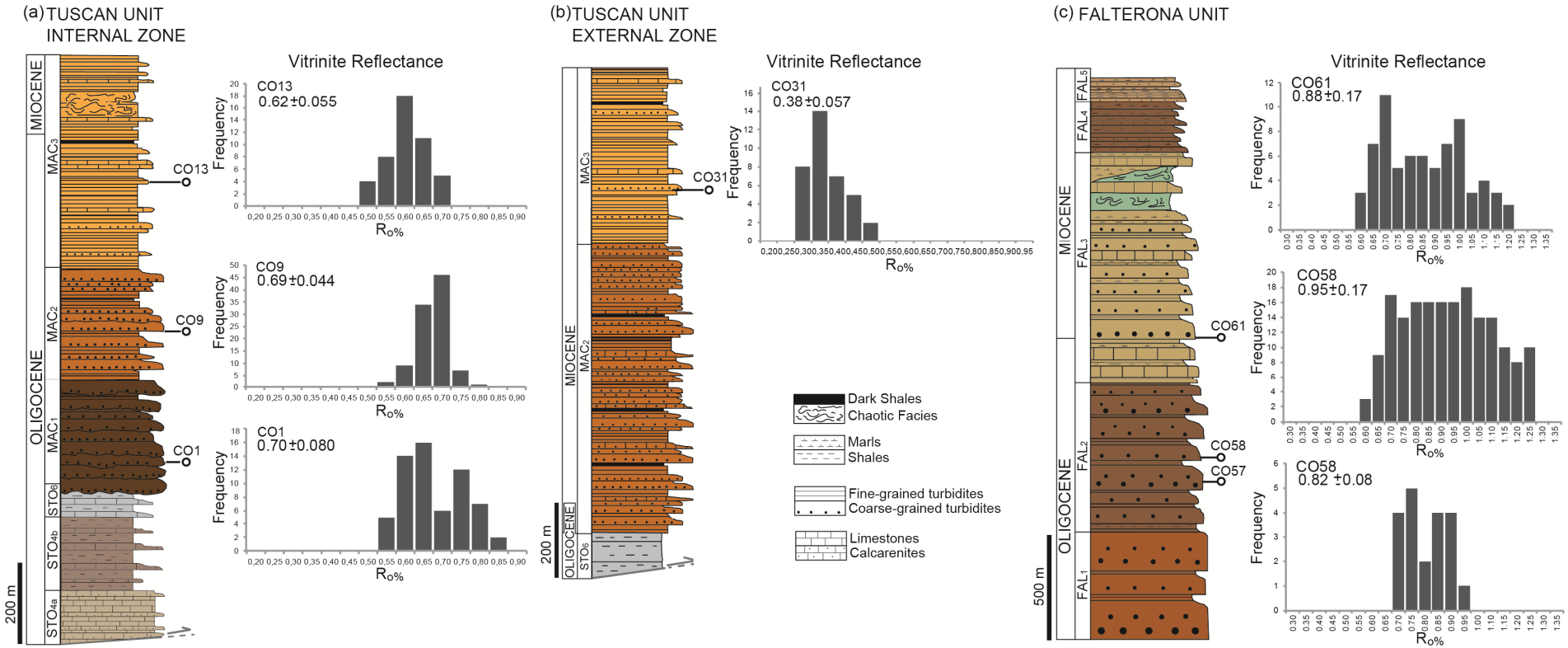

Fig. 2.3 Simplified stratigraphic columns of the study area ((a) and (b) for the area to the SE of the Val Marecchia Line and (c) to the North of it) with representative histograms of distribution of vitrinite reflectance data.

Table 2.1. Organic matter maturity and clay mineralogy data from the area to the south of the MVL

Site	Coordinates (Lat-Long)	Fms	Age	Lithology	Samples for Vitrinite Analyses	R_o% (±s.d.)	Samples for XDR Analyses	X-ray quantitative analysis of the <2µm grain-size fraction (%wt.)	%I in I-S	%C in C-S	S.O.
01	43° 21' 22.6", 12° 03' 16.2"	Macigno	Aquitanian	SDT/LMS	CO1	0.7 (±0.08)	CM1	I_{51} I/S_{14} C/S_{25} Cl_{10}	86	85	
02	43° 14' 49.4", 12° 06' 28.1"	Macigno	Aquitanian	SDT/LMS	CO5	0.6 (±0.06)	CM5	I_{30} C/S_{36} Cl_{34}	75	75	R1
03	43° 14' 32.3", 12° 04' 54.9"	Scaglia Toscana	Eocene	Mudstone			CM6a, CM6b, CM6c	I_{54} I/S_{20} C/S_{23} Cl_4 I_{64} I/S_{29} C/S_6 Cl_6 I_9 I/S_{41} $C/S_{27}K_6Cl_6$	84/ 84/ 60	65/ 65/ 65	R1 R1 R1
06	43° 05' 14.2", 12° 10' 50.0"	Scaglia Toscana	Eocene	Mudstone			CM9a, CM9b, CM9c	I_{31} I/S_{53} C/S_{13} Cl_3 I_{55} I/S_{40} C/S_5 I_{48} I/S_{48} $C/S_3K_1Cl_1$	73/ 74/ 74	70	R1 R1 R1
07	43° 04' 17.7", 12°11.1' 22.6"	Scaglia Toscana	Eocene	Mudstone			CM10a, CM10b	I_{40} I/S_{34} K_{18} Cl_9 I_{47} I/S_{23} K_{20} Cl_{10}	74/ 77		R1 R1
08	43° 21' 06.3" , 12° 02' 37.3"	Macigno	Aquitanian	SDT/LMS	CO9	0.7 (±0.04)	CM11	I_{48} $I/S_{15}C/S_{20}$ Cl_{17}	85		
09	43° 20' 48.3" , 12° 02' 09.2"	Macigno	Aquitanian	SDT/LMS	CO13	0.6 (±0.06)	CM3/ CM4	I_{67} I/S_9 C/S_6 Cl_{18} I_{63} I/S_{20} Cl_{17}	86/ 85		
10	43° 17' 22.6", 12° 00' 51.9"	Macigno	Aquitanian	SDT/LMS	CO14	0.5 (±0.06)	CM12	I_{74} I/S_{17} C/S_5 Cl_4	84	75	R1
11	43° 17' 20.4", 12° 01' 27.5"	Macigno	Aquitanian	SDT/LMS	CO16	0.6 (±0.07)	CM13	I_{71} I/S_{14} C/S_{10} Cl_5	84		R1
12	43° 17' 53.5", 12° 02' 22.6"	Macigno	Aquitanian	SDT/LMS	CO17	0.8 (±0.07)	CM14	I_{53} I/S_2 Cl_{45}	82		R1
13	43° 17' 50.9" , 12° 02' 40.5"	Macigno	Aquitanian	SDT/LMS	CO18	0.6 (±0.05)	CM15	I_{38} $I/S_4C/S_{39}Cl_{18}$	82	75	R1
14	43° 17' 50.9" , 12° 04' 34.9"	Macigno	Aquitanian	SDT/LMS	CO19	0.6 (±0.07)					
15	43° 18' 13.8", 12° 05' 29.1"	Macigno	Aquitanian	SDT/LMS	CO20	0.4 (±0.07)	CM16	I_{79} $I/S_{16}C/S_5Cl_1$	81	59	R1
16	43° 18'49.45", 12° 08' 3.80"	Macigno	Aquitanian	SDT/LMS	CO21	0.7 (±0.05)	CM17	I_{48} $I/S_7C/S_{17}Cl_{29}$	80	75	R1
17	43° 19' 4.3", 12° 07' 12.24"	Macigno	Aquitanian	SDT/LMS	CO22/23	barren					
18	43° 19' 4.95", 12° 07' 38"	Macigno	Aquitanian	SDT/LMS	CO24a,b	barren					
19	43° 19' 1.06", 12° 08' 3.80"	Macigno	Aquitanian	SDT/LMS	CO25	barren	CM18	I_{70} $I/S_{26}C/S_2Cl_2$	85	60	R3
23	43° 27' 43.6", 12° 01' 5.14"	Macigno	Aquitanian	SDT/LMS	CO30	0.6 (±0.04)	CM22	I_{47} $I/S_5C/S_{17}Cl_{31}$	80	70	R1 R3
24	43° 27' 46.8" , 12° 07' 40.63"	Macigno	Aquitanian	SDT/LMS	CO31	0.4 (±0.05)	CM23	I_{51} $I/S_{11}Kl_{39}$	50		R0
25	43° 27' 5.54", 12° 06' 18.13"	Macigno	Aquitanian	SDT/LMS	CO32	0.3 (±0.05)	CM24	I_{57} $I/S_{11}C/S_{25}K_7$	49	59	R0
26	43° 20' 40.7", 12° 1.4' 24.3"	Macigno	Aquitanian	SDT/LMS	CO33	0.9 (±0.08)	CM25	$I_{35}I/S_4Cl_{61}$	89		R3
27	43° 20' 20.1" , 12° 0' 20.14"	Macigno	Aquitanian	SDT/LMS	CO34	0.7 (±0.05)	CM26	I_{44} $I/S_{10}C/S_{15}K_{31}$	82	60	R3
28	43° 20' 2.96", 11° 59' 40.32"	Macigno	Aquitanian	SDT/LMS			CM27	I_{46} I/S_6K_{48}	87		R3
33	43° 0' 25.48", 12° 05' 50.38"	Macigno	Aquitanian	SDT/LMS	CO39	0.4 (±0.10)	CM30	I_{61} $I/S_{14}C/S_{19}Cl_6$	85	59	R3
34	43° 1' 4.26", 12° 05' 45.42"	Macigno	Aquitanian	SDT/LMS	CO40	0.5 (±0.10)	CM31	I_{70} I/S_{30}	84		R3
35	43° 1' 21.10", 12° 04' 45.47"	Macigno	Aquitanian	SDT/LMS	CO41	0.6 (±0.07)					
36	43° 1' 0.06", 12° 03' 15.78"	Macigno	Aquitanian	SDT/LMS	CO42	0.6 (±0.08)	CM32	I_{69} I/S_{31}	86		R3
37	43°16'46.62", 12° 8'44.83"	Macigno	Aquitanian	SDT/LMS	CO43	0.4 (±0.06)					
38	43° 1' 0.30", 12° 02' 54.96"	Macigno	Aquitanian	SDT/LMS	CO44a,b	0.6 (±0.10)	CM33	I_{71} I/S_{29}	84		R3
39	43° 2' 38.70", 12° 09' 54.42"	Scaglia Toscana	Eocene	Mudstone			CM34	I_{56} $I/S_{24}K_{20}$	77		R1
40	43° 3' 2.58", 12° 10' 15.60"	Macigno	Aquitanian	SDT/LMS	CO45	0.5 (±0.08)					
41	43° 12' 0.48", 12° 14' 44.22"	Macigno	Aquitanian	SDT/LMS	CO46	0.5 (±0.08)	CM35	$I_{57}I/S_{15}C/S_{22}Cl_6$	79	70	R1
42	43° 15' 6.05", 12° 15' 26.54"	Scaglia Toscana	Eocene	Mudstone			CM36	$I_{30}I/S_{29}K_{41}$	75		R1
51	43°11'16.02", 12°11'41.58"	Macigno	Aquitanian	SDT/LMS	CO52	0.4 (±0.90)					
52	43°11'1.74", 12°11' 6.60"	Macigno	Aquitanian	SDT/LMS			CM42	$I_{60}I/S_{25}C/S_{21}Cl_{18}$	80	80	R3
54	43°16'46.62", 12° 8'44.83"	Scaglia Toscana	Eocene	Mudstone			CM43	$I_{79}I/S_{17}C/S_3$	82	80	R3
55	43°19'8.82", 12° 8' 23.58"	Macigno	Aquitanian	SDT/LMS	CO54	0.5 (±0.08)					

Acronyms: SDT=sandstone; LMS= Limestone; I=illite; I/S=mixed layer illite-smectite; C/S=mixed layer clorite-smectite; K= Kaolinite; Cl=Clorite; S.O.= stacking order

Table 2.2. Organic matter maturity and clay mineralogy data from the area to the north of the MVL

Site	Coordinates (Lat-Long)	Fms	Age	Lithology	Sampled for Vitrinite Analyses	R_o (±s.d.)	Sampled for XDR Analyses	X-ray quantitative analysis of the <2µm grain-size fraction (%wt.)	%I in I-S	%C in C-S	S.O.
82	43° 37' 28.7", 11°40' 43.8"	Falterona	Aquitanian	SDT/LMS	CO57	0.8 (±0.08)					
83	43° 37' 23.7", 11°40' 59.1"	Falterona	Aquitanian	SDT/LMS	CO58	0.9 (±0.17)					
84	43° 38' 13.5", 11°40' 30.8"	Falterona	Aquitanian	SDT/LMS	CO59	0.6 (±0.94)					
85	43°40' 33.66", 11° 39' 47.70"	Falterona	Aquitanian	SDT/LMS	CO60	0.6 (±0.08)					
86	43° 37' 40.2", 11° 41' 00.1"	Falterona	Aquitanian	SDT/LMS	CO61	0.9 (±0.16)					
89	43° 32' 19.8", 11° 24' 32.9"	Scaglia Toscana	Pal-Eocene	Mudstone			CM48	$I_{55}I/S_{25}K_{10}C_{10}$	83	---	R3
90	43° 36' 09.0", 11° 22' 21.2"	Scaglia Toscana.	Pal-Eocene	Mudstone			CM49	$I_{46}I/S_{13}C/S_{26}C_{15}$	87	60	R3
91	43° 37' 14.6", 11° 40' 9.9"	Falterona	Aquitanian	SDT/LMS			CM50	$I_{43}I/S_{11}C/S_{37}Cl_9$	88	55	R3
92	43° 37'21.01", 11° 41' 9.1"	Falterona	Aquitanian	SDT/LMS			CM51	$I_{44}I/S_5C/S_{26}Cl_{25}$	87	85	R3
93	43° 40'40.37", 11° 39' 46.3"	Falterona	Aquitanian	SDT/LMS			CM52	$I_{47}I/S_4C/S_{33}Cl_{16}$	88	85	R3
94	43° 50' 32.01", 11° 38' 42.8"	Falterona	Aquitanian	SDT/LMS	CO62	0.4 (±0.79)	CM53	$I_{47}I/S_{16}K_{23}Cl_{14}$	70		R1
95	43° 55' 5.1", 11° 29' 41.8"	Marne di Vicchio	Burdig.	Marls			CM54	$I_{60}I/S_{17}K_5Cl_{18}$	70	--	R1
97	43° 53' 50.81", 11° 32' 54.52"	Falterona	Aquitanian	SDT/LMS			CM56	$I_{61}I/S_{17}K_5Cl_{18}$	80	--	R3
98	43° 55' 31.31", 11° 33' 29.8"	Aquerino	Aquitanian	SDT/LMS	CO63	0.3 (±0.07)	CM57	$I_{59}I/S_{15}K_{12}Cl_{15}$	55		R0
100	43° 51' 52.43", 11° 34' 46.3"	Falterona	Aquitanian	SDT/LMS	CO65	0.5 (±0.07)	CM59	$I_{58}I/S_9C/S_8K_9Cl_{16}$	83	80	R3
101	43° 51' 5.8", 11° 30' 10.19"	Falterona	Aquitanian	SDT/LMS			CM60	--	--	--	--
102	43° 49' 21.64", 11° 29' 29.88"	Falterona	Aquitanian	SDT/LMS			CM61	$I_{63}I/S_7C/S_{16}K_4Cl_{11}$	83	80	R3
103	43° 57' 1.48", 11° 31' 45.7"	Aquerino	Aquitanian	SDT/LMS			CM62	$I_{45}I/S_{29}K_{15}Cl_{11}$	50	--	R0
104	43° 56' 43.75", 11° 35' 11.78"	Aquerino	Aquitanian	SDT/LMS			CM63	$I_{70}I/S_9C/S_{11}Cl_{10}$	52	65	R0
105	43° 55' 35.10", 11° 30' 51.95"	Carigiola	Aquitanian	SDT/LMS			CM64	$I_{62}I/S_1C/S_{16}K_4Cl_{17}$	77	80	R1
106	43° 55' 14.25", 11° 34' 13.88"	Aquerino	Aquitanian	SDT/LMS			CM65	$I_{35}I/S_{34}K_{15}Cl_{16}$	57/ 75		R0

Acronyms: SDT=sandstone; LMS= Limestone; I=illite; I/S=mixed layer illite-smectite; C/S= mixed layer clorite-smectite; K= Kaolinite; Cl=Clorite; S.O.= stacking order

2.3.2 XRD analyses

To the south of Marecchia Valley lineament, a suite of 36 samples for mineralogy X-ray semi-quantitative analyses were collected from the Tuscan succession, mainly along the same four cross section and in the same sites where collection of samples for vitrinite reflectance analyses was performed too (Fig. 2.2 and Tab. 2.1).

Samples were collected from both Scaglia Toscana and Macigno Fms.. In particular in the first, varicoloured clays were collected from layers of clay and marls interbedded to calcareous layers. Whereas gray siltites and pelites were collected from fine, laminated turbiditics beds of Macigno Fm..

In the area to the north of Marecchia Valley lineament further 21 samples have been collected from both Tuscan Nappe succession in the Chianti Mountains and Mt. Falterona succession at Pratomagno ridge along cross section E-E' and Mt. Falterona succession and Aquerino succession in an area to the south-est of Mugello Basin (Tab. 2.2). In detail, 5 samples of varicoloured clays were collected from Scaglia Toscana Fm., 9 samples consist of gray siltites from fine turbiditics beds of Falterona Fm., 1 sample was collected from a

fine laminated gray marls of Marne di Vicchio Fm. and 3 derive from varicoloured clays of Marne di Villore Fm. of Aquerino Unit.

Qualitative and semi-quantitative analyses of the < 2μm grain fraction (equivalent spherical diameter) were performed by Scintag X1 X-ray diffractogram system (CuKa radiation, solid state detector, spinning sample). After centrifugation, the suspension containing the < 2μm grain-size fractions was decanted, pipetted, and dried at room temperature on glass slides to produce a thin highly oriented aggregate. Oriented air-dried samples were scanned from 1 to 48°2θ with a step size of 0.05°2θ and a count time of 4 s per step at 40 kV and 45 mA. The presence of expandable clays was determined for samples treated with ethylene glycol at 25 °C for 24 h. Ethylene-glycol-solvated samples were scanned at the same conditions as air-dried aggregates, with a scanning interval of 1-48°2θ. Expandability measurements were determined according to Moore and Reynolds (1997) by using the Δ2θ method after decomposing the composite peaks between 9 – 10 and 16 – 17 °2θ using the Scintag X1 software program with a split Pearson VII function.

2.4 Results

2.4.1 Organic matter analyses

Organic matter dispersed in the Macigno Fm., to the south of Marecchia Valley lineament, is generally abundant, homogeneous and mainly made up of well-preserved macerals. The predominant macerals belong to huminite-vitrinite group, the inertinite group is present such as subordinate macerals. In some samples pyrite, either finely dispersed or in small globular aggregates, is locally present, associated with both groups. Most of data generally show one main cluster identifiable by a Gaussian distribution, which represents the indigenous population of huminite-vitrinite macerals (see for example CO1; CO9; CO13 and CO31 in Fig. 2.3). R_o% data generally indicate immature to early-middle mature stage of hydrocarbon generation, with some variations. It is possible to identify two main trends of vitrinite reflectance: the first one along the stratigraphic succession in every single element and the latter one across the chain, at a regional scale. Generally there is an increase of R_o% values from top to the bottom of Macigno formation. In particular, in the most internal element (Terontola Element, Tuoro Element, Portole Element, Ansina Element) the R_o% values range from 0.60 to 0.80%; in Scarzola Element from 0.5 to 0.6% and in the most external element (Marcignano-Gioiello) from 0.30 to 0.50% (Fig. 2.4).

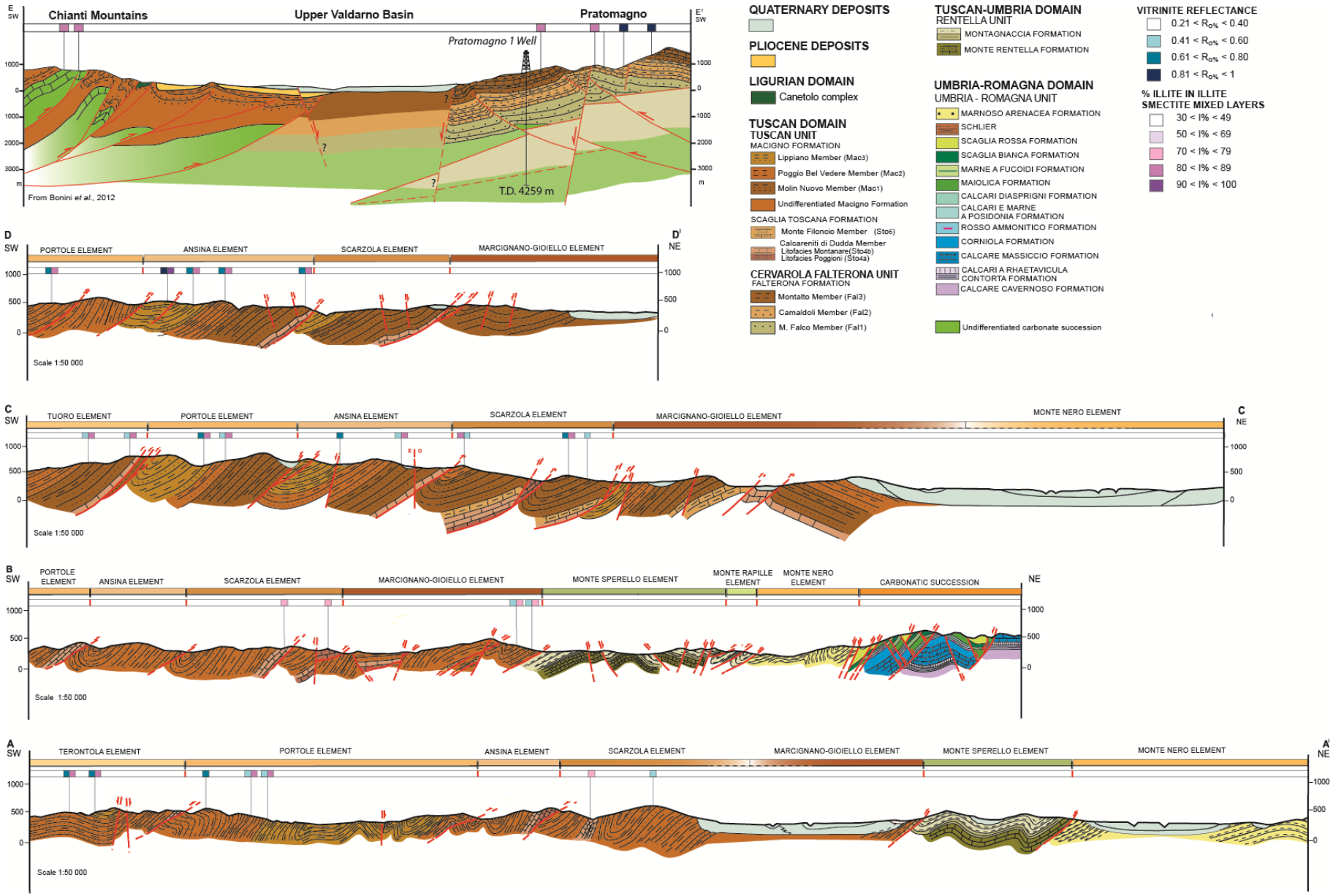

Fig. 2.4 Geological sections across the study area: redrawn and modified after Bonini *et al.*, (2012). Geological Cartography Project (2011c), this study. Sampling sites (in brackets), vitrinite reflectance and illite content in mixed layers I-S are plotted. Traces of cross sections are given in Fig. 2.2

Locally there is an anomalous increase of organic matter maturity at the top of successions that are preserved at the footwall of the secondary thrusts that delimitate the tectonic elements (i.e. Ansina element in D-D' in Fig. 2.4b).

At regional scale, in the analyzed area, moving along the cross sections, from internal to external sectors of the Tuscan Nappe, it is possible to observe a general decrease of thermal maturity of organic matter dispersed in sediments (Fig. 2.5)

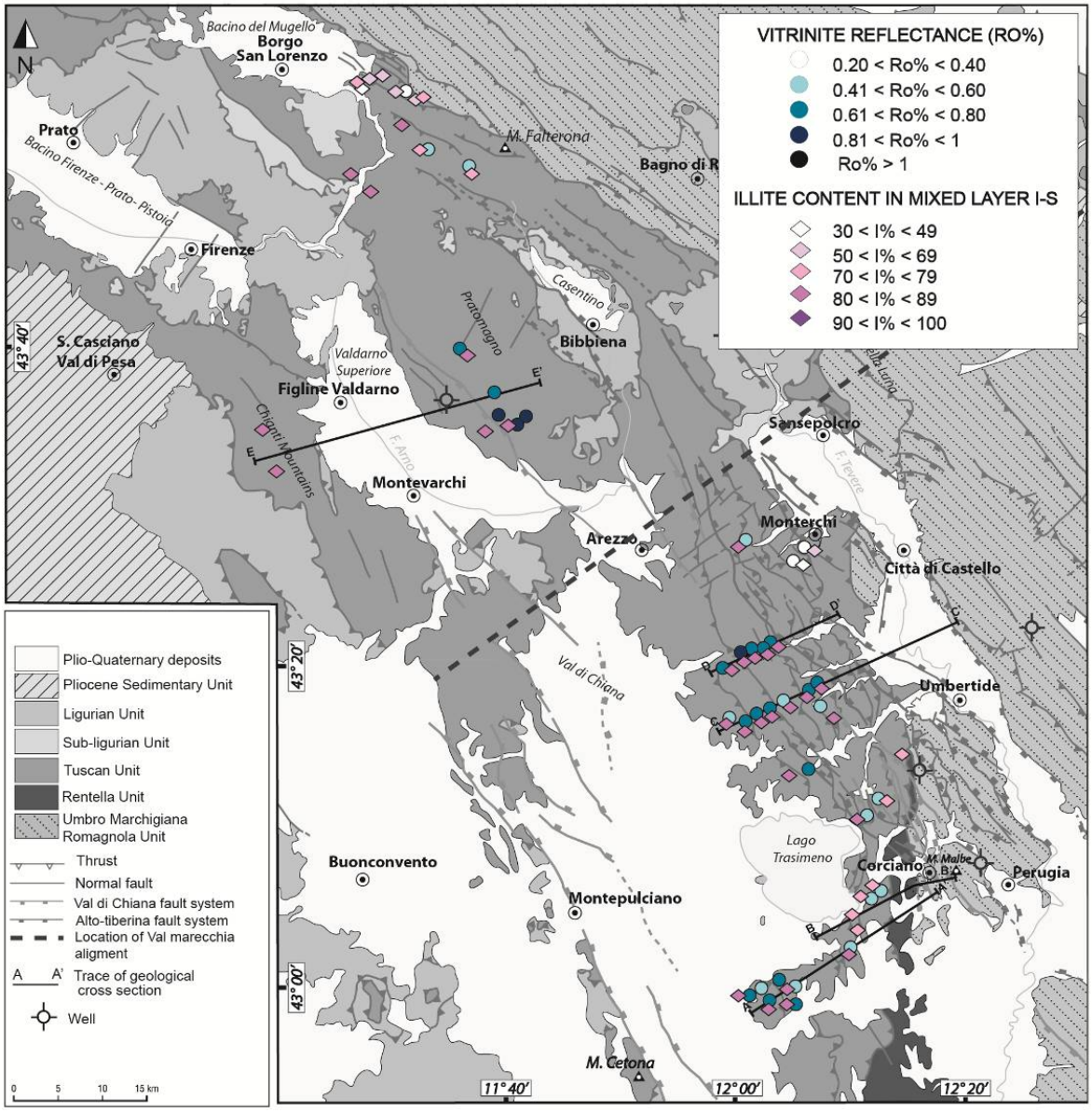

Fig. 2.5. Distribution of vitrinite reflectance and I% in I-S mixed layers data performed in this study and plotted on the simplified tectonic scheme of Fig. 2.2. Note the gradual decrease in thermal maturity moving from hinterland to foreland and the abrupt trend moving from the Se to the NW.

Regard to organic matter dispersed in the Mt. Falterona Fm., at Pratomagno ridge, it is possible to observe an unimodal distribution identifiable by a Gaussian distribution (see Fig. 2.3) that indicates the presence of predominant macerals belonging to the huminite-vitrinite group. The inertinite group is present such as subordinate macerals, in a few samples fusinite is present. In some samples pyrite, either finely dispersed or in small globular aggregates, is locally present, associated with both groups. The Ro% values range from 0.60% to 0.95% indicating middle mature stage of hydrocarbon generation.
Moving toward the north-east in the area to the south-east of the Mugello Basin, a decrease of thermal maturity has been observed. In this sector of the chain the samples, collected from Fal_3 member, have recorded lower Ro% values ranging from 0.45 to 0.50% (Fig. 2.5 and Tab. 2.2).

2.4.2 Clay mineralogy analyses

Regarding to the area to the south of the MVL the quantitative analyses of <2 μm grain-size fraction show mainly the presence of illite, chlorite, mixed layers illite-smectite (I-S) and subordinate amounts of kaolinite and mixed-layers chlorite-smectite (C-S). Non-clay minerals: such as quartz, plagioclase, calcite have been recognized as well. In addition, gypsum is also present in samples from the Scaglia Toscana Fm. (see Tab. 2.1). In this area, the stacking order of mixed layers I-S shows a thermal maturity trend similar to that shown by vitrinite reflectance. In fact, from the inner to the outer element of the Tuscan Nappe, the I-S stacking order changes, passing from long-range ordered structures (R3) in the most internal element to short-range (R1) and random-ordered structures (R0) in the easternmost Marcignano-Gioiello element. A variation in the illite content in mixed layers I-S from 89% to 38% moving toward the foreland is also observed (Fig. 2.5).

At the scale of the whole succession, a slight increase of illite layers in mixed layers I-S with depth occurs within the same element. In the internal elements (Terontola, Tuoro , Portole, Ansina Elements), the I% in I-S ranges from 80% to 89%, whereas it increases from 70% to 79% in the Scarzola Element and from 40 to 50% in the most external element (Marcignano-Gioiello) (Fig. 2.4). Data interpreted according to Merriman and Frey (1999) indicate that the internal sector of the Tuscan units experienced maximum temperatures ranging between 120-130° in the late diagenetic zone whereas toward the external sector temperature decreases below 100°C.

To the north of MVL in the Chianti Mts. and Pratomagno area, semi-quantitative analyses of the < 2 μm grain-size fraction show illite as major mineral and subordinate

amounts of mixed layers I-S and C-S, and chlorite (Tab. 2.2). The illite content in long range ordered mixed layer I/S is about 87-88% for both the Scaglia Toscana and Falterona Fms., indicating late diagenetic conditions in agreement with vitrinite reflectance data. These data correspond to a higher maturity level than that recorded for formation of similar age to the south of the MVL. Moving toward the NE, in the Mugello area (Fig. 2.5) a decrease of thermal maturity has been observed. Mixed layers I/S show a progressive increase of expandable layers (from 27 to 43% of smectite layers) from the internal to the external units, which correspond to changes in the staking order. Long range ordered (R3) mixed layers passes to short (R1) and the random ordered (R0) structures suggesting a decrease of tectonic/sedimentary loads.

2.5 Discussion

2.5.1 Geothermal gradient

The paleogeothermal gradient active during the deposition of the Macigno formation, has been reconstructed using the following equation: Geothermal Gradient (°C/Km) = Heating rate (°C/Ma) / Burial rate (Km/Ma). According to the method proposed by Hillier *et al*. (1995) the heating rate values have been determined by the correlation of vitrinite reflectance and Illite content in mixed layer I-S, in relation to thermal history and sedimentary basin types. Fig. 2.6 shows two main data clusters: the first (squares) and corresponding to more external samples in the thrust belt, yields heating rate ranging from 0.375-1.5 °C/Ma The latter (circles) corresponds to more internal samples and indicates heating rates comprised between 0.357 – 4.000 °C/Ma The highest values of heating rate (triangles) correspond to samples collected at the top of succession at the footwall of secondary thrust. The burial rate has been calculated for the outcropping successions of each tectonic element, using thickness and age of each stratigraphic member of the Macigno Fm. For burial rates ranging from 0.04 to 0.07 Km/Ma the paleo-geothermal gradient obtained for the various elements ranges from 21 to 23 °C/Km.

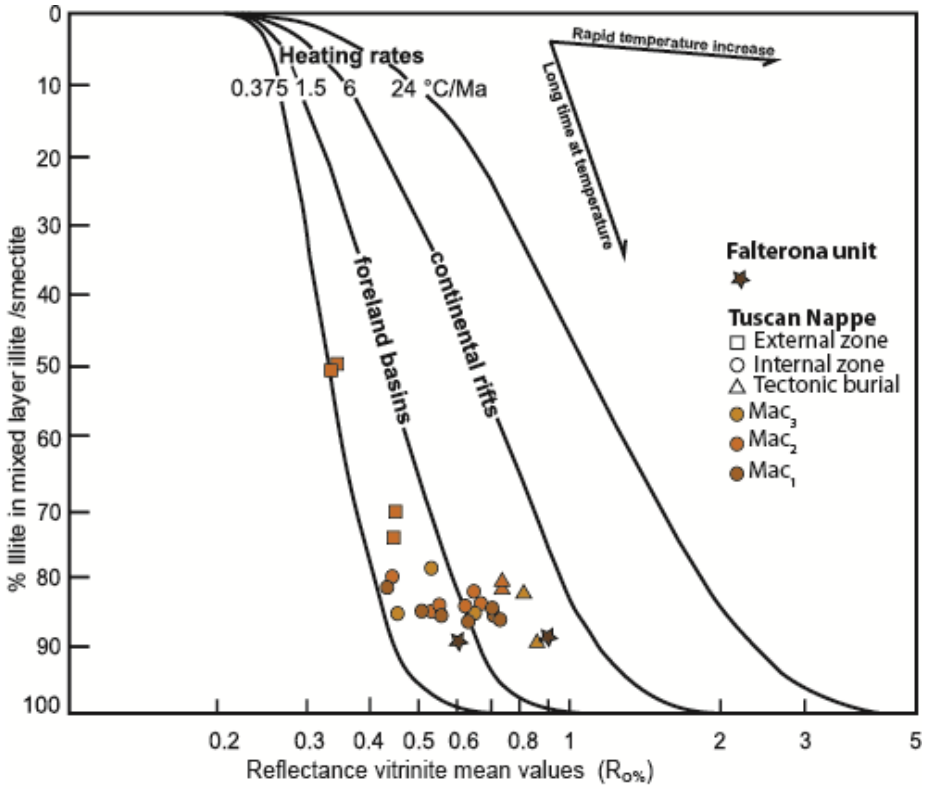

Fig. 2.6 Heating rate values for the Falterona Fm. and Tuscan Nappe extracted from the correlation of vitrinite reflectance and illite content in illite-smectite (I-S) data based on the kinetic model of vitrinite maturation of Burnham and Sweeney (1989) and the kinetics of the I-S reaction determined by Hillier *et al.* (1995). Modified and redrawn after Hillier *et al.* (1995)

2.5.2 Thermal modelling

The obtained geothermal gradient is an essential constraint to perform burial and thermal models. The models of the Tuscan Units were carried out using BASIN MOD-1D software (1996). The main assumption for the modelling are: (1) correction for decompaction of the burial curves according to Sclater and Christie's method (1980); (2) sea level changes, have been neglected, as the thermal evolution is influenced more by sediment thickness than water depth (Butler, 1992); (3) thrusting is considered instantaneous when compared with the duration of sedimentation, as generally suggested in theoretical models (Endignoux and Wolf, 1990); (4) calculated geothermal gradient (23 °C/Km) has been adopted for the modelling; thickness, lithology and age of sediments are derived from geological maps (Geological Cartography Project (2011a, b, c, d, e). The exhumation rate is assumed constant and burial curves have been calibrated against Ro% and I% in I/S (reported in the previous section).

Regarding the study area to the south of the MVL, various models were performed for the different tectonic elements, eight of these are presented and discussed in this

chapter. In detail the modelled elements are Terontola, Portole, Scarzola and Marcignano-Gioiello for the cross sections A-A' and B-B'; Portole, Ansina, Scarzola for the sections C-C' and D-D' (Fig. 2.7). Constraints and results are reported in Table 2.2. From Fig. 2.7 it is evident that the deposition started during Eocene times with the sedimentation of pelagic limestone of the Scaglia Toscana Fm. and continued until Aquitanian times with the deposition of the Macigno Fm.. In the lower-middle Miocene, the emplacement of a regional thrust sheet caused a tectonic loading that persisted for about 15 Ma, during compressional deformation. This load brought the succession at maximum depths that differ in each tectonic element, decreasing toward the external sector of the unit, from 5.7 km experienced by the Terontola element to 3.5 km for the Marcignano-Gioiello element. The maximum recorded paleo-temperatures, corresponding to the different depths of burial, are about 120-130 °C for the internal element such as Terontola, Portole and Ansina and decrease moving toward the eastern sector reaching 110° C for the Scarzola and about 95 °C for the Marcignano-Gioiello element (Fig. 2.7 see Burial History). Therefore in this sector of the chain, the Tuscan unit succession experienced a thermal evolution compatible with late diagenetic conditions in the early and middle stages of hydrocarbon generation (Fig. 2.7 see Maturity vs Depth Diagram). The calculated tectonic load, currently eroded, is characterized by lateral variations showing a decrease toward the external sector of this portion of the chain where the Tuscan Nappe thrust onto the Umbria–Romagna Domain.

In detail, in the most internal area, to the east of Val di Chiana, a load of about 3.7 Km emplaced onto the Terontola element decreasing down to 2.3 Km onto the Marcignano-Gioiello element. Exhumation started in early Pliocene times.

In the area to the north of the Marecchia Valley in Pratomagno area (see E-E'), one model has been performed (Tab. 2.2). Fig. 2.8 shows that deposition started in this area during Oligocene times and went on until Aquitanian-Burdigalian time with the sedimentation of the turbidite deposits of the Falterona Unit. In the lower-middle Miocene, the emplacement of a regional thrust sheet caused a tectonic loading which persisted for about 13 Ma, during the compressional phase. This event brought the succession at maximum depths of about 6.5 km, recording maximum temperatures of about 150 °C. In this portion of the chain, the sedimentary succession reached the late mature stage of hydrocarbon generation. The calculated tectonic load, presently eroded, is of about 3.7 km.

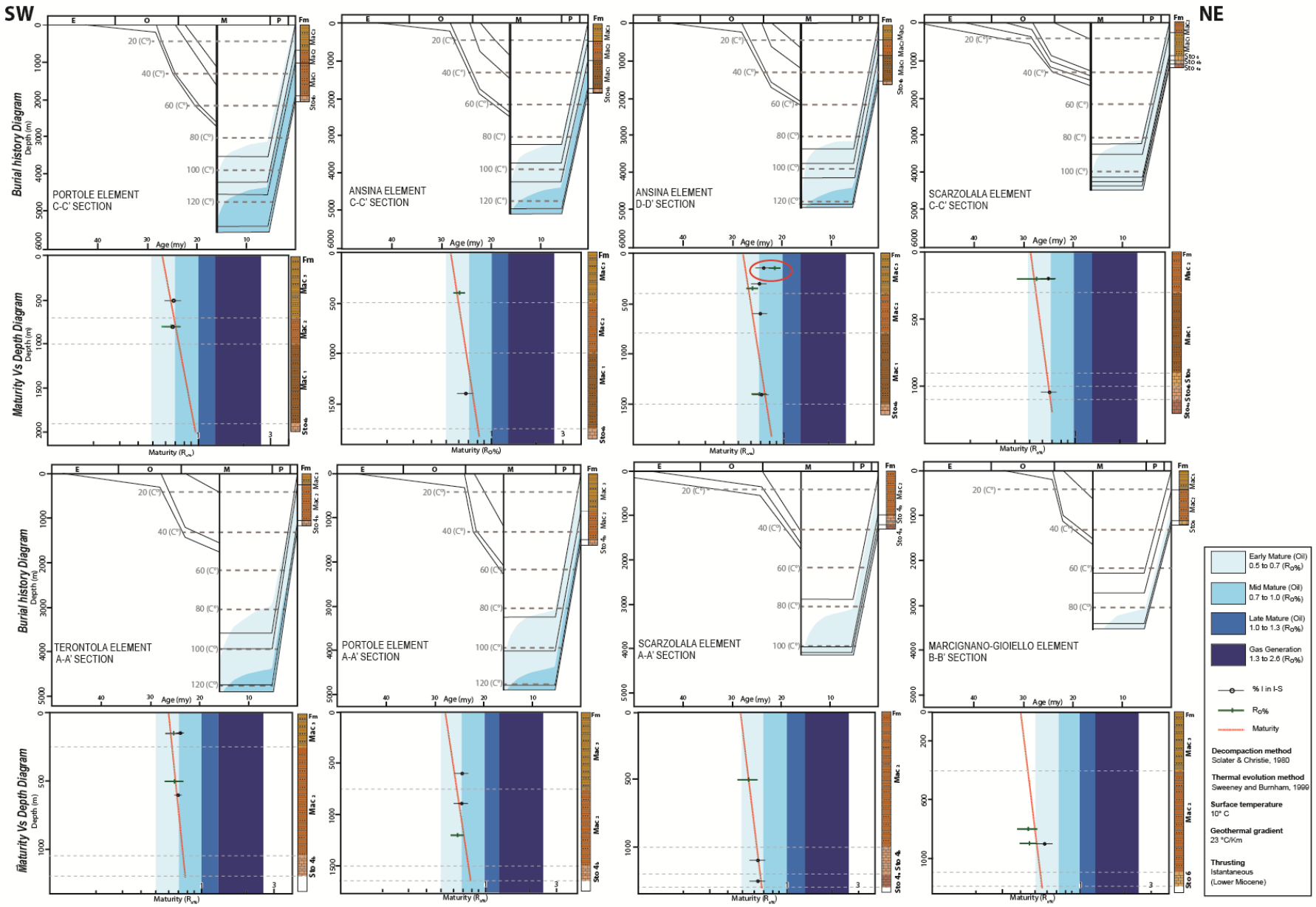

Fig. 2.7 Representative one-dimensional burial and thermal modeling of the Tuscan Nappe succession in the southern area of MVL and related present-day thermal maturity data.

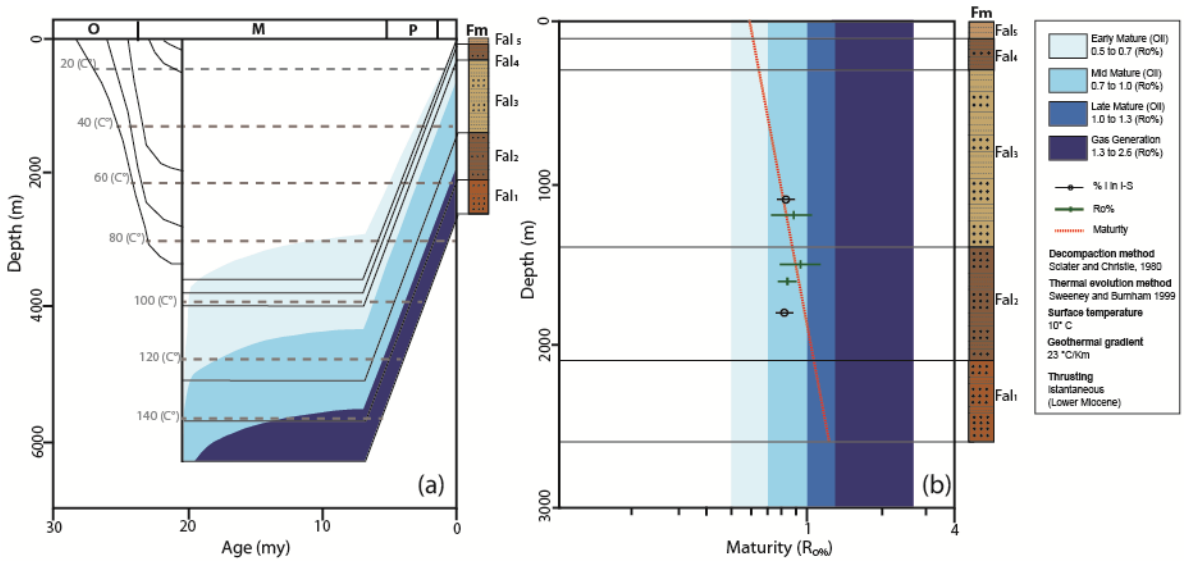

Fig. 2.8 (a) Representative one-dimensional burial and thermal modelling of the Falterona Fm. in the northern area of MVL. (b) Present-day thermal maturity data plotted against calculated thermal maturity curve. Depth for each sample is derived from outcrop sample distribution.

2.5.3 Tectonic model

The organic and inorganic indicators of the thermal exposure of the sediments and thermal modelling allowed me to reconstruct the amount of the tectono-sedimentary load the Tuscan and Falterona Units underwent and to speculate on its origin. On this basis I traced a tectonic evolutionary model during the Neogene time, and propose a possible deformation model for this sector of the chain, reconstructing of the missing portion of the tectonic wedge, now eroded.

In the area to the south of the MVL, the investigated successions underwent a differential tectono-sedimetary load, higher in the internal portion compared to the external one, ranging from about 3.7 km to 2.3 Km. These loads have been reported above the reconstructed sections and highlighted a reduction of the wedge thickness moving toward more external sectors of this portion of the chain (Fig. 2.9). In order to understand which units composed the wedge, a reconstruction of the missing portion of the chain has been attempted, in agreement with the tectono-sedimentary loads derived from thermal data. In this area, the thickness of the Tuscan successions ranges from a maximum of 1.8 to a minimum of 1.2 km, considering that the top of the Mac_3 member is eroded and its complete thickness cannot be univocally evaluated. However, the maximum outcropping thickness recognized in published maps is of about 400 m and Barsella *et al*. (2009) reported a value of about 600 m, on the basis of stratigraphic and biostratigraphic analyses.

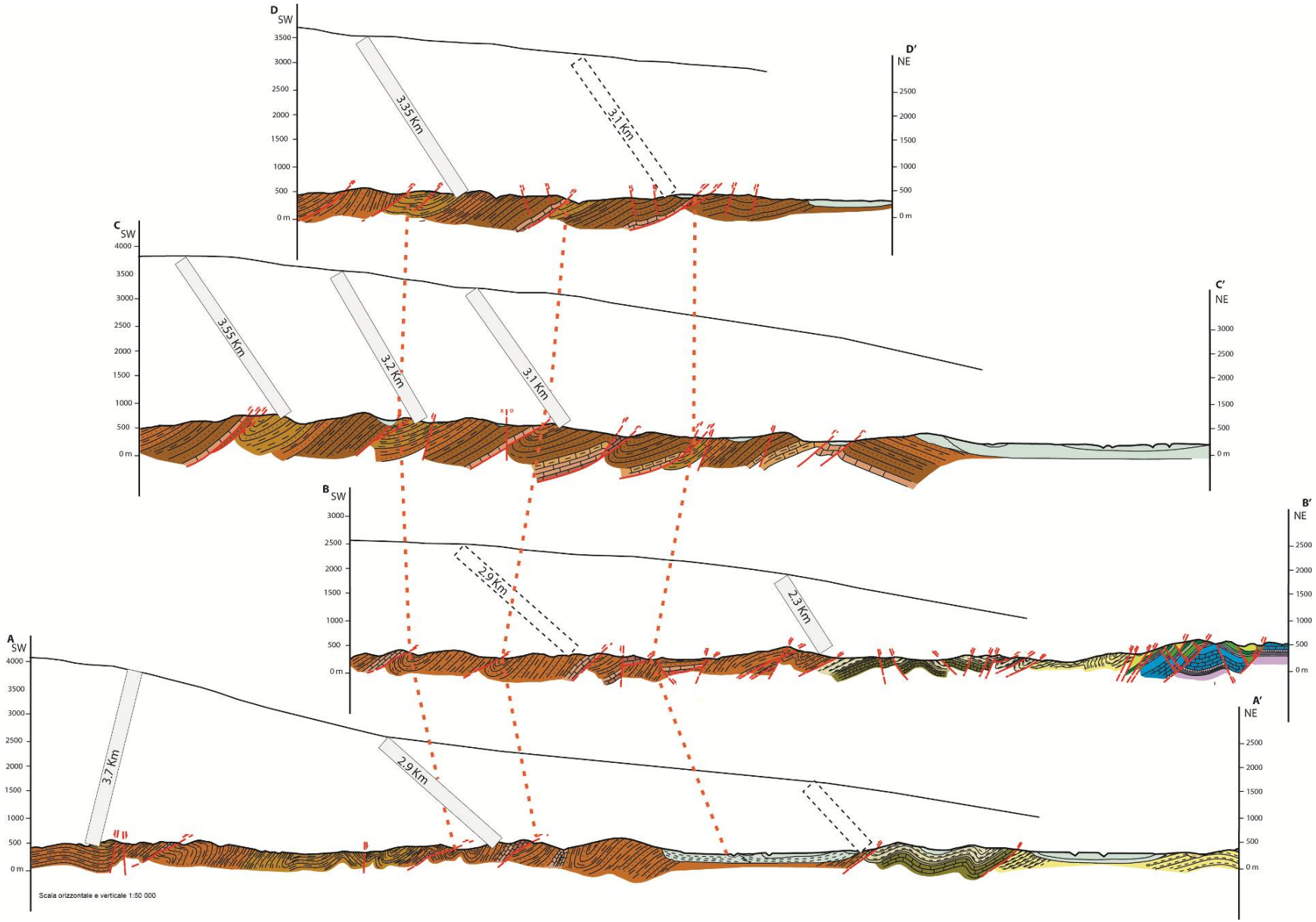

Fig. 2.9 Geological cross-sections with the calculated tectonic-sedimentary loads.

An upper bound to the Mac_3 thickness can be obtained by comparison with the coeval Fal_3 member, that has a maximum measured thickness of 1,100 m (Geological Cartography Project, 2011 d, e).

In detail, a reconstruction of the missing section has been carried on for the C-C' section assuming for the Mac_3 two alternative thickness values: 600 and 1,100 m (Fig. 2.10).

Fig. 2.10a shows the possible reconstruction with either 600 or 1,100 m; in both cases, especially for the most internal portion, stratigraphic thicknesses of the missing portion of the Macigno Fm. cannot totally justify the total amount of calculated tectonic load.

Thus, to compensate the calculated tectonic loads values, it is necessary to hypothesize that the missing thickness is partially due to the emplacement of the allochthonous Ligurian Unit (now completely eroded), on top of the total thickness of the Tuscan Nappe succession. The thickness of Ligurian Unit can be derived by subtracting the estimated thickness of Macigno Fm. from the thickness of the total calculated sedimentary-tectonic load. The derived thicknesses of the Ligurian allochtonous units are shown in Fig. 2.10 b, c and decrease toward the front of the chain. In particular, if I considered a total thickness of Mac_3 of 1,100, the Ligurian Unit is about 2 km thick and it tapers onto more internal element to zero. Whereas if a thickness of 600 m for the Mac_3 is considered the Ligurian Unit front is located in a more external position and its maximum thickness is higher (Fig. 2.9c).

Another piece of information that I obtained from these data is that an anomalous thermal maturity level is recorded in the immediate footwall of each tectonic element for the youngest member of the Macigno Fm., in apparent contradiction with the general trend of increasing of maturity moving toward the oldest member of the stratigraphic succession. This effect is probably related to the internal imbrication of the Tuscan Unit and to the stacking of secondary thrusts.

On the other hand, in the sector to the north of MVL, and in particular in the Pratomagno area, the modelling shows that the Falterona succession reached higher burial depths, with a total maximum load of about 3.7 km. The reconstruction of the missing section in this sector, with the same method mentioned above, shows that the load corresponds entirely to the thickness of Ligurian Unit.

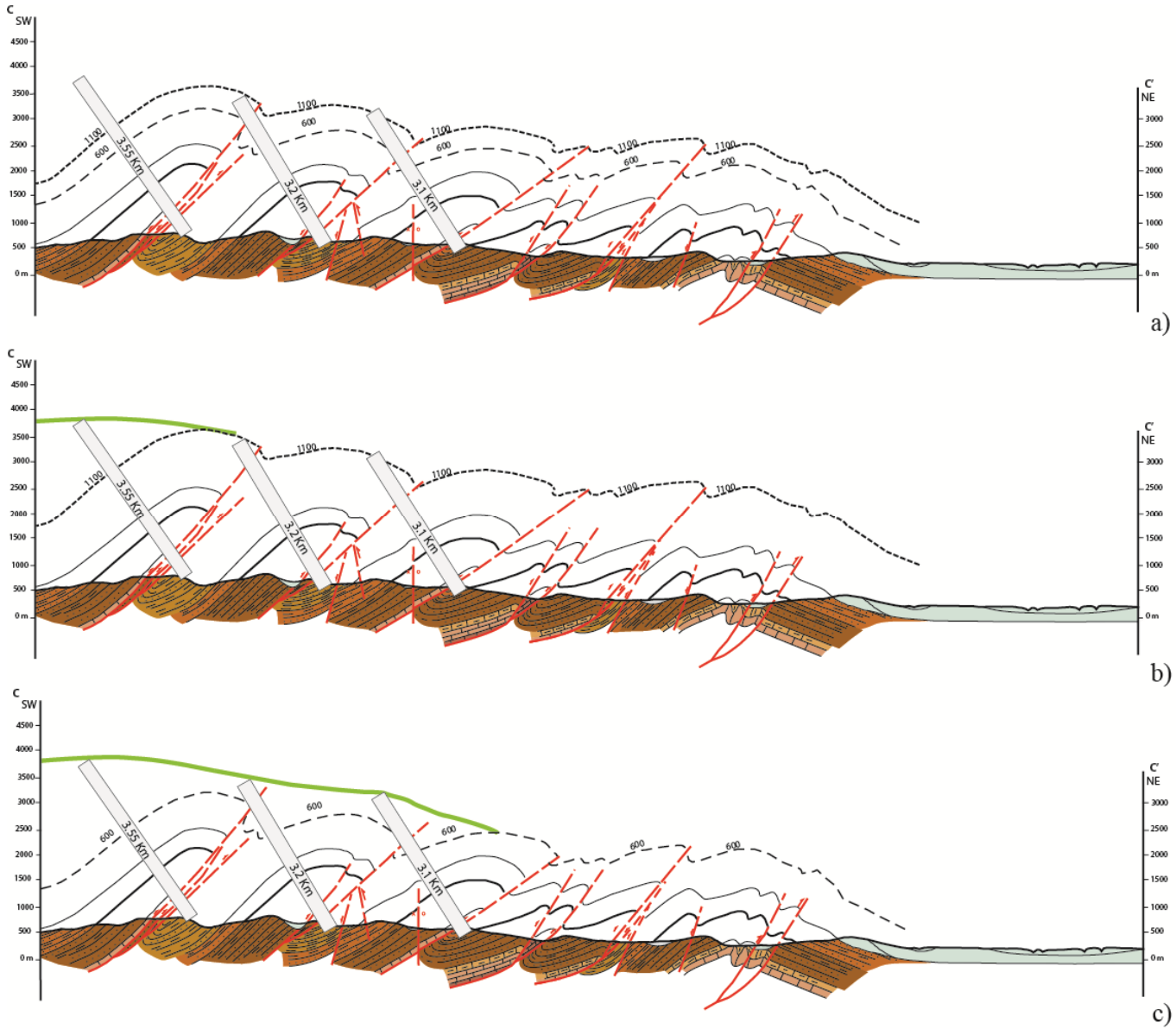

Fig. 2.10 Different versions of the geological cross section C-C' for the reconstruction of the eroded portion of the chain: (a) with projected punctual maximum loads experienced by present-day outcropping units and assuming for the Mac_3 two alternative thickness values: 600 and 1,100 m; (b-c) assuming for the Mac_3 1,100 m (in b) or 600 m (in c) and a possible thickness for the Ligurian Unit (whose envelope is indicated by the green line) derived from the exceeding thickness of the total load in cross section.

Therefore a variation in the thickness of the Ligurian Unit moving both perpendicular and parallel to the strike of the chain is evident with respectively either gradual or abrupt changes. In detail, the Ligurian Unit had maximum thickness of up to 3.7 km to the north of the MVL in the Pratomagno area and up to about 1.5 km to the south of the MVL in the Trasimeno Lake area. Thus, the two sectors are abruptly separated by the MVL that exerts a structural control on the original position of the Ligurian thrust front.

In detail, as shown in map of Fig. 2.11, to the north of the MVL it can be noticed that there is a higher degree of preservation from erosion of the Ligurian Unit when compared to that of the southern sector, where it crops out only in an area of limited extension to the W-SW of the Trasimeno Lake.

Moreover an increase of organic matter maturity in the units preserved at the footwall of the regional nappe of the Ligurian Unit is evident moving further to the north-west, in agreement with paleothermal data distribution published in previously works (see Corrado *et al*., 2010a for a review).

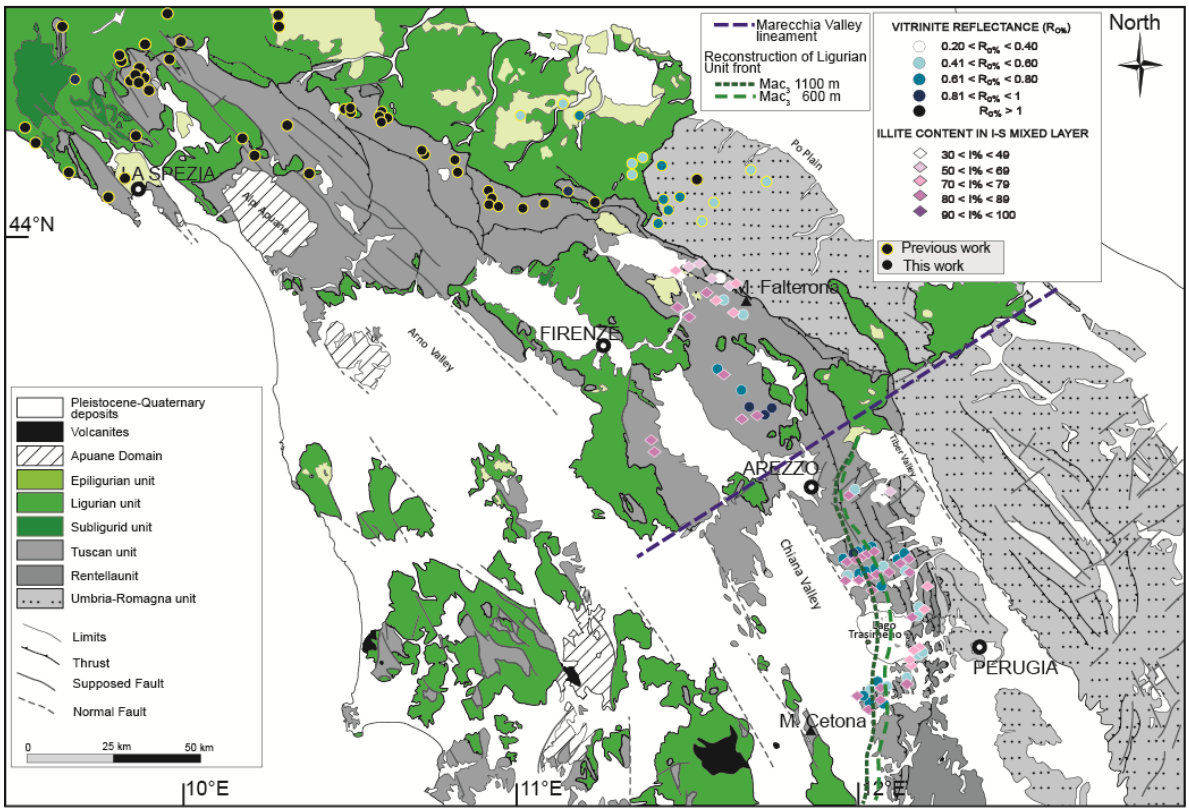

Fig. 2.11. Distribution of vitrinite reflectance and I% in I-S mixed layers data performed in this study and previously published (see Corrado *et al*., 2010a) projected on the simplified tectonic scheme with present-day outcrops of the Ligurian Unit. Note the abrupt increase in thermal maturity to the north of the Marecchia Valley Lineament.

The Ligurian Unit to the south of MVL has been totally eroded probably because of its original reduced thickness than that preserved to the north of the MVL, as confirmed by presented thermal modelling. This reduced thickness may be related to a reduced propagation of the Ligurian Unit towards the foreland moving from the NW to the SE along the chain and approaching the bulge of Carbonate Platform of the Central Apennines where the allochtonous units never propagated toward the most external areas (Corrado, 1995; Corrado *et al*., 1998). Furthermore, the maximum thickness of the Ligurian wedge in the northern area may have triggered the emplacement of huge volumes of Ligurian Unit (such as in the Marecchia Valley) that are absent in the southern area.

Some recent studies (Cerrina Feroni *et al*., 2001; Zattin *et al*., 2002) proposed that to the North of the study area, the Sillaro – Livorno line marks a jump in the erosional level in the Northern Apennines with bigger volumes of preserved Ligurian Unit moving towards the NW. On the basis of my reconstruction (high preservation of the Ligurian Unit to north of MVL compared to the southern sector) it is possible to assume that the MVL marks a further change in the erosional level along the Apennines chain. In this framework the culmination occurred progressively toward the south-west with discrete steps ruled by the main lineaments such as the Sillaro-Livorno and Marecchia Valley lineaments moving towards the Central Apennines.

2.6 Conclusion

Vitrinite reflectance and mixed-layered clay minerals data allowed me to trace the thermal evolution of the Tuscan Nappe sedimentary sequences during the evolution of orogenic wedge.

I identified two main trends of thermal maturity of the sedimentary succession. One perpendicular to chain axis, with organic and inorganic thermal indicators decreasing toward the external sector of the chain. The second one, moving along the strike of the chain, from the SE (Trasimeno Lake) toward the northeastern sector (Pratomagno area). In this case an abrupt increase of thermal maturity has been recorded and this jump corresponds to the Marecchia Valley lineament.

This pattern of thermal maturity is due to a variation of the original thickness of the allochthonous Ligurian Nappe.

Chapter 3

Paleothermal and Thermochronological constraints to the Neogene-Quaternary kinematic evolution of the extensional system of the Altotiberina fault system

3.1 Introduction

In the Northern Apennines several paleothermal and low T thermocronological studies have been performed to investigate the burial and exhumation history of the main tectonic units that compose the Northern Apennines. The aim of these studies was to constrain vertical motions of the fold-and-thrust belt during the whole chain building (Boettcher and McBride, 1993; Balestrieri *et al*,. 1996, 2000, 2003; Abbate *et al.*,1999; Zattin *et al.*, 2000; 2002; Ventura *et al.*, 2001; Corrado *et al.*, 2010a; Thomson *et al.*, 2010; Bonini *et al.*, 2012). Nevertheless, less attention has been paid to the evolution of vertical motions, with special regard to exhumation due to localised extensional tectonics in the late stages of chain evolution.

The present study focuses on the presentation of a new dataset of low T thermochronological - (U-Th)/He and AFT - and paleothermal data - vitrinite reflectance and illite content in mixed layers illite-smectite - for the Marnoso Arenacea Fm. to reconstruct the burial and exhumation history in the area where the Altotiberina fault system (ATF): one of the most active extensional fault systems of the northern-central Apennines (Barchi *et al*., 1998a,b; Mirabella *et al*., 2011). In detail, the investigated area is located in a sector of the Northern Apennines at the boundary between Tuscan and Umbria domains. It extends from the Massicci Perugini to the west, to the Gubbio ridge to the east, across the Tiber Valley (Fig. 3.1).

Furthermore data from two deep wells - S. Donato 01 and Monte Civitello 01- drilled respectively close to Perugia and Gubbio towns, are shown at the end of the "3.5 Results" section. Stratigraphy and tectonic evolution of these wells are briefly described and data concerning organic matter dispersed in sediments (e.g., percentage distribution of main terrestrial and marine components) as well as thermal maturity indicators (e.g. vitrinite reflectance and Thermal Alteration Index) are extensively discussed.

For the Monte Civitello 01 well, 1D burial and thermal modelling has been also performed and results from modelling compared with surface data to derive a final tectonic model.

3.2. Geological setting

The study area is located in a sector of the Northern Apennines at the Tuscany-Umbria boundary (Fig. 3.1) and is characterized by Neogene contractional architecture affected by a severe Neogene - Quaternary extensional activity.

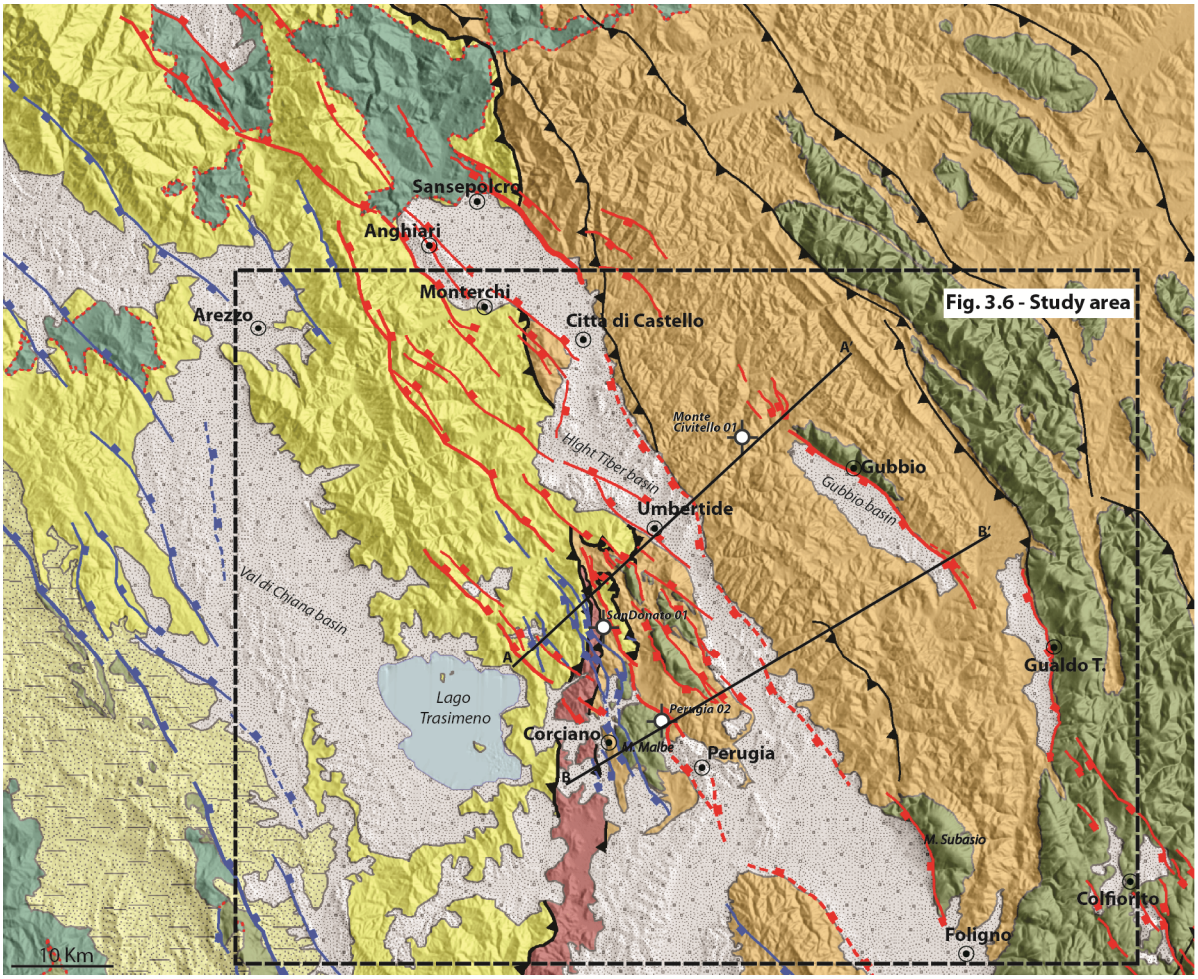

Fig. 3.1. Geological sketch map of the study area showing the outcropping tectono-stratigraphic units, main thrusts and normal fault systems (modified after Mirabella *et al.*, 2011).

The contractional architecture consists of four structural units that were piled up during Miocene times (Mirabella *et al.*, 2011). Some authors (e.g., Abbate and Bruni, 1989; Brozzetti, 2007) considered the outermost part of the Tuscan Nappe as belonging to a more external tectonic unit (Falterona-Cervarola Unit or Falterona Nappe, *Auct.*). For the study area, the Falterona-Cervarola Unit is interpreted as belonging to the Tuscan Nappe according to Plesi *et al.* (2002).

The structural setting, from top to the bottom, consists of:

(1) Ligurian Unit, made up of ophiolites, sedimentary covers and flysch deposits ("helminthoid flysch" *Auct.*) (Elter, 1975; Marroni *et al.*, 2001; Festa *et al.*, 2010);

(2) The Tuscan Nappe, an east-verging imbricate thrust-stack formed by pelagic foreland ramp deposits (Scaglia Toscana Fm.) and foredeep turbidite deposits (Macigno Fm.) (Plesi *et al.*, 2002; Barsella *et al.*, 2009);

(3) Mt. Rentella Unit, interposed between the Tuscan and Umbria-Marchigiana-Romagnola Units (Barsella *et al.*, 2009), that consists of Rupelian-Aquitanian varicoloured pelagic and hemipelagic marls (Monte Rentella Fm.) followed by Aquitanian-Burdigalian siliciclastic turbidites (Montagnaccia Fm.). This succession is arranged in a stack of thin imbricate slices bounded by N-S striking thrusts with ramp-and-flat geometry (Barsella *et al.*, 2009; Meneghini *et al.*, 2012);

(4) the western Umbria-Marchigiana-Romagnola Unit characterized by a Triassic-Early Miocene calcareous-marly-siliceous succession and Early to Middle Miocene foredeep turbidites (Marnoso Arenacea Fm.) at the top (Ricci Lucchi and Pialli, 1973).

Subsurface data show that, at deeper levels, contractional deformation involves the entire sedimentary successions of the Umbria domain, including the lowermost sedimentary units (Triassic in age) and the upper part of the phyllitic basament (Mirabella *et al.*, 2008a; Barchi *et al.*, 2010). In detail, logs of Perugia 02 and S. Donato 01 wells indicate a tectonic doubling of the Burano Anhydrites and the underlying phyllites by means of a regional thrust to the west of the Tiber River (the so called Perugia Mountains thrust, Minelli and Menichetti, 1990; Anelli *et al.*, 1994; Barchi *et al.*, 1998a, Mirabella *et al.* 2011) (Fig. 3.2a).

The age of the foredeep deposits provides the timing of compressional deformation that gets younger moving eastward. Recent biostratigraphic data for this portion of the chain, indicate that the deformation of the Tuscan Nappe, Rentella Unit and Umbria-Marche Unit occurred during Aquitanian, Burdigalian and Langhian times, respectively (Barsella *et al.*, 2009). In addition, scattered "klippen" of the Ligurian Units are identified

at the top of the Tuscan Nappe, as testified to the west of Trasimeno Lake (Meneghini *et al.*, 2012).

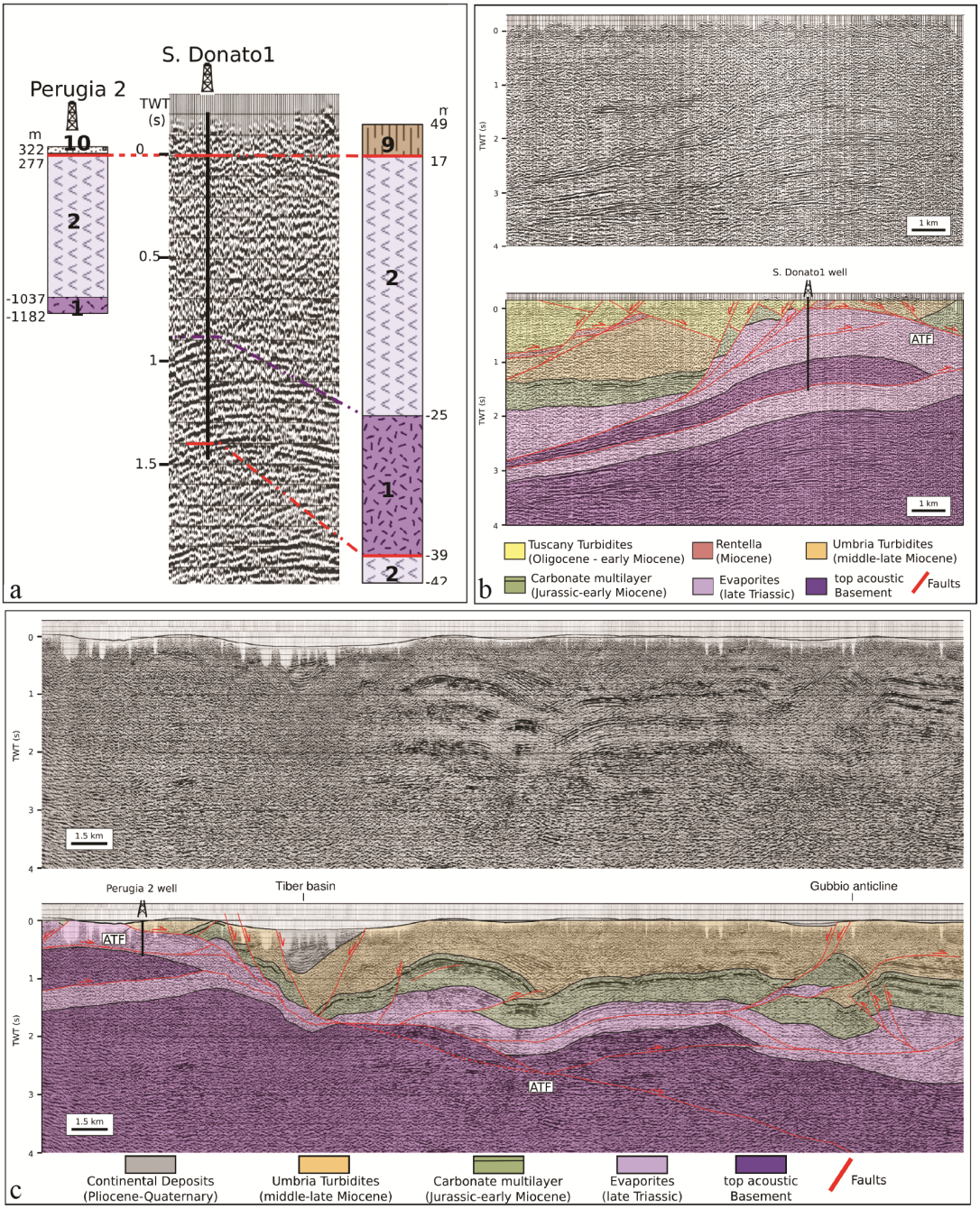

Fig. 3.2. (a) Simplified stratigraphy of the Perugia- 02 well, and related seismic image and geological sketch of the San Donato-01 well (Mirabella *et al.*, 2011); (b) seismic section (top) with geological interpretation (bottom) across Mt. Acuto area, (section L3 in Mirabella *et al.*, 2011); (c) seismic section (top) with geological interpretation (bottom) from Mt. Malbe to Gubbio town, (section L4 in Mirabella *et al.*, 2011)

The described compressional setting has been severely dissected by extensional tectonics since Late Pliocene by a complex pattern of normal faults. Several Authors have provided an early and detailed surface description for the Perugia Mts. area such as Dessau (1962), Ghelardoni (1962), Minelli and Menichetti (1990), Brozzetti (1995). The Perugia-02 and S. Donato-01 wells drilled a tectonic contact separating the Miocene Marnoso-Arenacea Fm. at the top from the Triassic Anidriti di Burano Fm. at the bottom (Martinis and Pieri, 1964; Anelli *et al.*, 1994; Keller *et al.*, 1994). This tectonic elision has been interpreted as a regional low-angle extensional fault.

More recent studies integrating field geology and seismic lines (CROP 03 profile and other commercial seismic lines) indicated that the previously described extensional features are the surface and subsurface expression of the Altotiberina fault system (ATF) (Barchi *et al.*, 1998b, 1999, 2006; Pialli *et al.*, 1998; Boncio *et al.*, 1998, 2000; Mirabella *et al.*, 2011) (Fig. 3.2 b, c).

The ATF system has been acting since Late Pliocene (about 3 Ma ago) as testified by geological, geodetic and seismological data. The geological and geomorphological evidence of faults activity are located along the Monterchi and Anghiari fault segments (Cattuto *et al.*, 1995; Delle Donne *et al.*, 2007; Brozzetti *et al.*, 2009, Mirabella *et al.*, 2011). Geodetic data testify a SW-NE extension (with rates in the order of 2.5–3.0 mm/yr) from Perugia to Città di Castello towns, along the high Tiber basin (D'Agostino *et al.*, 2009; Hreinsdóttir and Bennett, 2009; Mirabella *et al.*, 2011).

Nowadays, different and extremely rich dataset about extensional faults developed along the ATF system are described in the existing literature. Some structures such as Malbe, Tezio and Acuto Mts. normal faults, have been identified since the 50's (Dessau, 1956; Ghelardoni, 1962; Barnaba, 1958), whereas some others, such as the Mt. Favalto, Monterchi, Anghiari, Città di Castello and Umbertide faults, have been more recently studied (Cattuto *et al.*, 1995; Barchi *et al.*, 1998b; Boncio *et al.*, 2000; Brozzetti *et al.*, 2009). This regional scale extensional system is driven by the low-angle normal Altotiberina fault (ATF), (angles of dip <30° at depth) with the east-dipping structures that have been generally interpreted as synthetic splays of the ATF, whereas the west-dipping faults, developed mainly on the eastern side of the Tiber Valley, are interpreted as antithetic subsidiary structures (i.e. Sansepolcro and the Gubbio faults in Boncio *et al.*, 1998, 2000; Barchi *et al.*, 1999; Mirabella *et al.*, 2004, 2008b; Barchi and Ciaccio, 2009).

This NNW-SSE fault system is characterized by a great along-strike continuity and relevant exhumation of the footwall block, in the Mt. Malbe area. Nevertheless the amount

and timing of the possible footwall uplift of the ATF system is still matter of scientific debate as the area where the AFT developed was first the locus of intense shortening and subsequent denudation due to erosion and then of extensional deformation due to the evolution of the Val di Chiana fault system. In other words the contribution of either each of these older tectonic events, or of the ATF evolution, or simply of the regional erosion due to final uplift of the peninsula to the exhumation of Mesozoic cores in the area of Perugia is still strongly debated. In this chapter I will contribute to this debate with new thermochronological and paleothermal data to provide quantitative dating and amounts of exhumation in this area.

A tectonic regional scheme showing geometric relationships between the older compressive structures and the Pliocene-Quaternary normal fault systems has been reported in Fig. 3.1 in agreement with Mirabella *et al.* (2011). There are two Pliocene-Quaternary normal fault systems: the older Val di Chiana fault system (in blue in Fig. 3.1); and the Altotiberina fault system (in red in the Fig. 3.1)

In the area between the Trasimeno Lake to the West and Gubbio - Gualdo Tadino towns to the east, these two fault systems have been described with further detail by Mirabella *et al.* (2011). The authors highlighted four main arrays of NW-SE normal faults that can be variously attributed to either the younger and eastern ATF or to the older and western Val di Chiana system (in blue in the Fig. 3.1). From west to the east, secondary synthetic and antithetic faults have been defined as follows:

(1) the east-dipping Lisciano-Pian di Marte-Magione Fault set (LMF belonging to the ATF System),

(2) the west-dipping Corciano-Preggio Fault set (COF belonging to the Val di Chiana System),

(3) the east-dipping Altotiberina Fault (ATF),

(4) the west-dipping Sansepolcro-Gubbio alignment (Antithetic and belonging to the Altotiberina Fault System). The east-dipping ATF and LMF have a very similar geometry and kinematics, as a consequence LMF has been interpreted as the westernmost part of the ATF displaced by COF (Mirabella *et al*., 2011, Fig. 3.3).

The throw produced by the activity of COF decreases toward the N-NW, moving from Corciano village to Mt. Acuto area. In the same direction a displacement decrease of the ATF is also recorded. Mirabella *et al.*, (2001) interpreted the extensive outcrop of the Triassic unit in the MT. Malbe - Mt. Torrazzo area, as the locus of the maximum exhumation occurring at the footwall both the ATF and COF (Fig. 3.3).

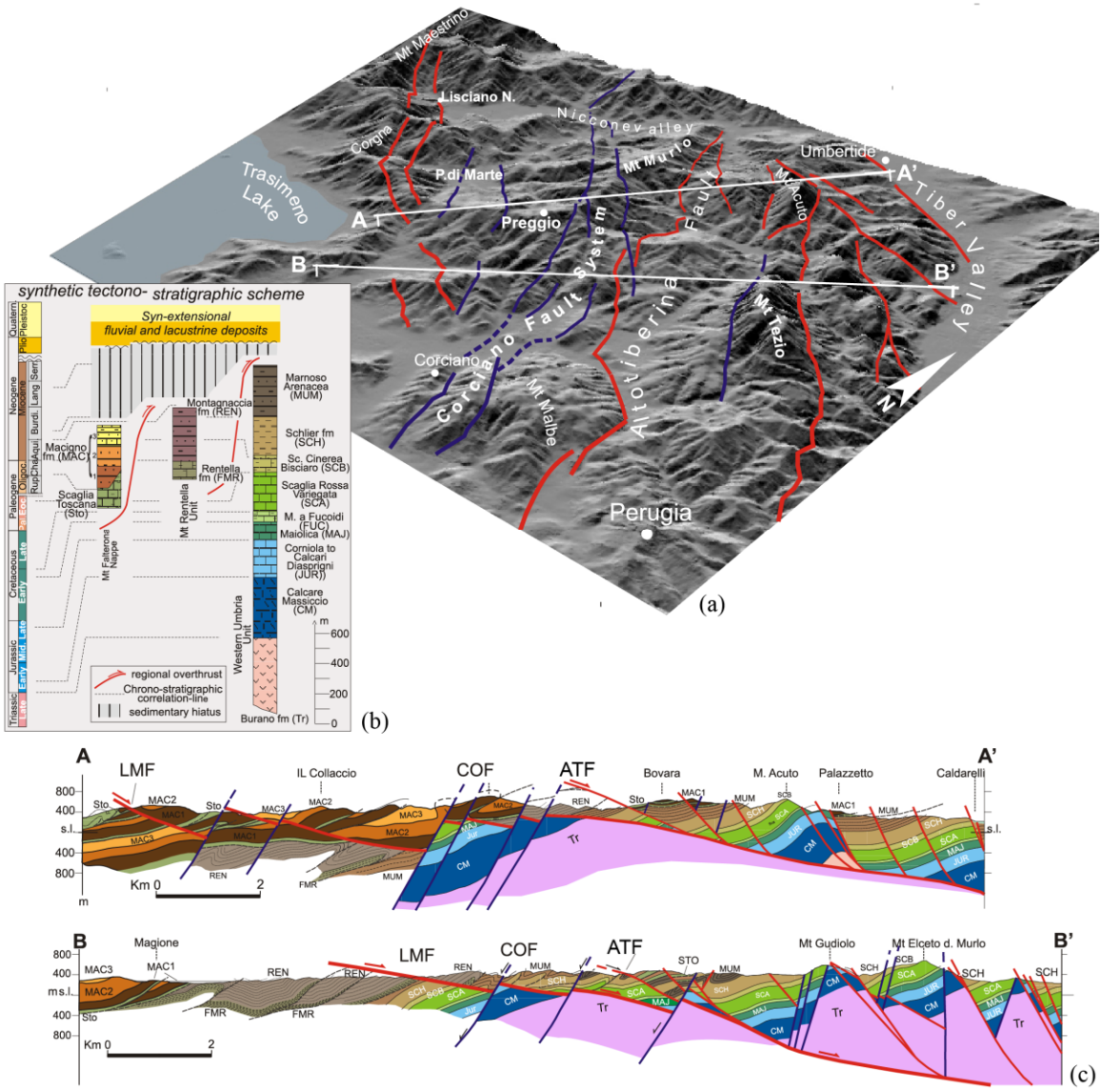

Fig. 3.3. (a) DTM (25m resolution) of the southwestern part of the study area showing the trace of the normal faults belonging to the LMF, COF and ATF fault-alignments, red traces refer to E-NE-dipping faults, dark-blue traces to SW-dipping faults. The traces of the A-A' and B-B' sections (white thin lines); (b) tectono-stratigraphic scheme of the study area showing the superposition relationships occurring among the main units and their internal stratigraphy; (c) cross-sections drawn along the A-A' and B-B' lines, based on surface data (modified after Mirabella *et al*., 2011).

3.3 Methods and materials

Integrated paleothermal and low-T thermocronological analyses have been performed to investigate the burial and exhumation history of the Altotiberina Fault system.

A synthetic description of the thermocronological methods has been reported below; while for the paleothermal methods description see chapter 2.

3.3.1 Generalities of Apatite fission-track method

Apatite fission-track analysis on sedimentary successions has been the object of many studies since the early eighties because of its implications for hydrocarbon exploration (Fig. 3.4, Gleadow *et al.*, 1983).

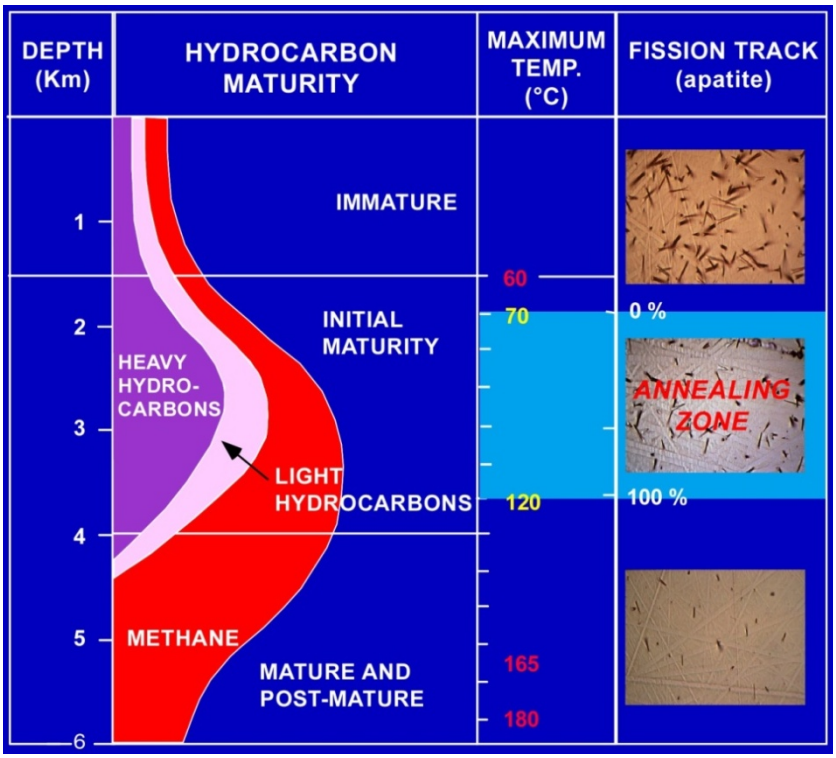

Fig. 3.4 Application of Apatite fission tracks to the hydrocarbon exploration. After Gleadow e Duddy (1981*)*

This methodology has been widely applied to the Apennines as it provides constraints to the thermal history of the sedimentary successions involved in the chain building (Zattin *et al.*, 2002; Thomson *et al.*, 2010). The most important difference with other low-temperature indicators (such as vitrinite reflectance and I-S mixed layers) is that this methodology provides timing and amount of exhumation whereas the other methods constrain only maximum paleo-temperatures and burials. The other difference is that apatite fission-track (AFT) studies can reflect multiple cooling and heating events as a

function of sample age and track length distribution as based on reversible processes. AFT dating is based on the spontaneous fission of ^{238}U which produces a damaged zone or a linear defect (spontaneous track) in the crystal lattice (Fleischer *et al.*, 1965).

AFT dating is very similar to other isotopic dating methods based on the decay of an unstable parent to a stable daughter atom. The age is function of the proportion between the abundance of the new stable isotope and the parent unstable atom. In AFT dating methodology, these two quantities are substituted by the number of observable tracks and the amount of Uranium present in the sample. The Uranium content is determined by the number of induced tracks obtained by irradiation with a known dose of thermal neutrons in a nuclear reactor. This irradiation causes the fission of ^{235}U which isotopic ratio with ^{238}U is constant in nature. Therefore, the age of the sample can be estimated by the ratio between spontaneous and induced tracks.

The most important parameter affecting the stability of tracks is temperature. As temperature increases, a decreasing number of tracks and a reduction of their length is visible. This process is known as annealing. The AFT annealing rate depends on the chemical composition of apatite (Green *et al.*, 1986) and on cooling or heating rate (Gleadow and Duddy, 1981). It generally occurs between about 60 °C and 125 °C for heating time of about 10 Myr and can be used to reconstruct the thermal history of basins, from deposition and burial of sediments through subsequent cooling related to uplift and erosion. The temperature range in which reduction of lengths occurs is known as Partial Annealing Zone (PAZ; Wagner and Van den Haute, 1992). According to this concept, temperatures of any geological setting can be divided into three zones with respect to fission-track annealing: (1) the total annealing zone, in which spontaneous tracks are immediately erased after any fission event; (2) the partial annealing zone, in which reduction of lengths occurs with the increase of temperature; (3) the stability zone, where tracks are stable.

AFT record the age of cooling and the exhumation rate of rocks from the total annealing zone, evaluate the thermal history of a sedimentary succession in the partial annealing zone and assess the age of the source rock in the stability zone giving information on the provenance of the sediments.

The annealing temperatures depend on the rate of the geological process and the PAZ temperature range cannot be univocally defined. Gleadow and Duddy (1981) noted a reduction of the FT density as a function of temperature in drill-hole samples from the Otway Group sandstones (Fig. 3.5).

For apatite, temperatures between 140 and 120 °C are cited for the bottom whereas 70 to 40 °C for the top of the PAZ. More precisely, Gleadow and Duddy (1981), on the basis of 36 data obtained from drill holes samples in the Otway basin, suggest a PAZ between 145 and 80 °C for heating events 1 Myr long, and between 110 and 45 °C for events 1 Gyr long.

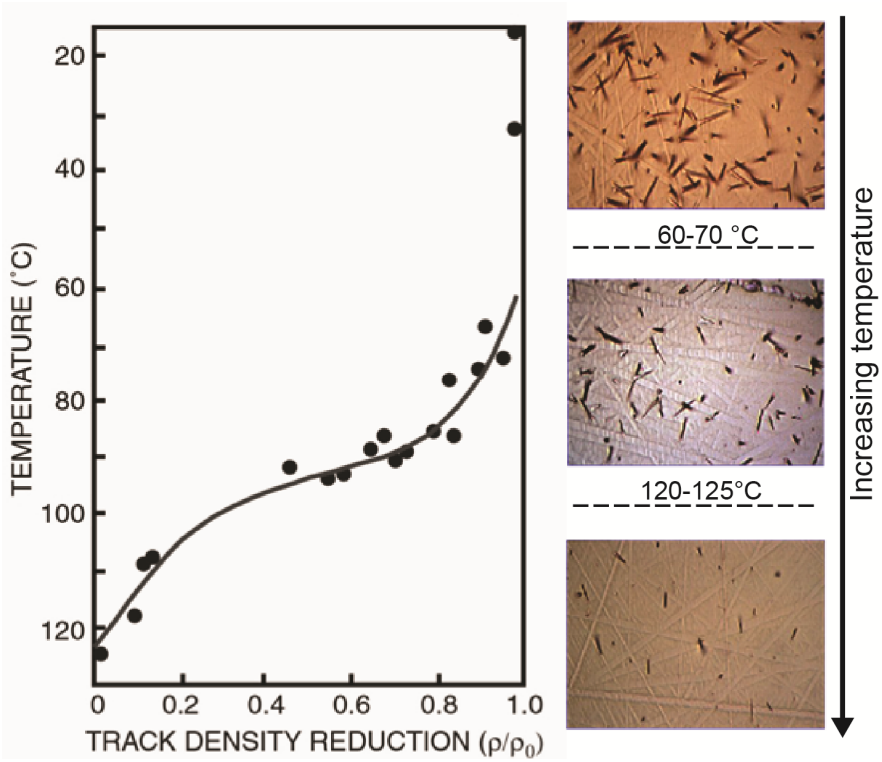

Fig. 3.5 Reduction of spontaneous traces with increasing temperature in a deep well in the Otway Basin (Australia). After Gleadow e Duddy (1981).

The cooling range in the PAZ has been simplified in a single temperature value to which the age has to be referred. This temperature value was defined by Dodson (1973) as the closure temperature. Wagner and Reimer (1972) suggest that the closure temperature correspond to temperature at which 50% of the track are retained. In conclusion, the best assessments of the closure temperature are 128 °C, 112 °C, 98 °C and 85 °C for cooling rates of 100 °C/Myr, 10 °C/Myr, 1 °C/Myr and 0.01 °C/Myr, respectively (Brandon *et al.*, 1998).

Most of the limitations of this method are due to the young age of sediments (< 10 Myr). In fact in such a short period of time, the accumulation time of tracks can be too short to produce an acceptable number of measurable tracks with a “normal” uranium content (about 35 ppm) causing relevant errors in the age determination (Zattin, 2003). A different problem derives from the relationships between the apatite chemistry and the

annealing degree. In terrigenous rocks, it is very probable to analyse apatites crystals coming from different source rocks with different chemical composition. Finally, different source areas may record different cooling age. As a consequence, the pre-depositional history of apatites crystals can differ for the single grains within each samples. Therefore quantitative modelling of data can be very difficult given the heterogeneity in the thermal history of single grains. Radial plots and/or peak-fitting statistical method can be used to discriminate different inherited populations and overcome this problem (Gailbraith, 1988; Brandon and Vance, 1992; Brandon *et al.*, 1998).

3.3.2 Generalities of (U-Th)/He method

(U-Th)/He dating of apatite has attracted considerable interest as a potential low-temperature thermochronometer (e.g., Zeitler *et al.*, 1987; Lippolt *et al.*, 1994; Wolf *et al.*, 1996a). Differently from Apatite Fission Tracks dating, laboratory He-diffusion experiments suggest that this system should be sensitive to crustal temperatures of ~ 40–80 °C (Wolf *et al*., 1996b, 1998).

(U/Th)/He dating is based on the α emission during the decay of ^{235}U, ^{238}U, and ^{232}Th series nuclides. The (U-Th)/He dating method is based on the measurement of the isotopic abundances present in the following equation:

$$He = 8\ ^{238}U\ (e^{\lambda_{238}t} - 1) + 7\ (^{238}U/137.88)\ (e^{\lambda_{235}t} - 1) + 6\ ^{232}Th\ (e^{\lambda_{232}t} - 1)$$

(U/Th)/He age is the result of the thermal history experienced by a rock in the region where radiogenic He is at least partially retained (Wolf *et al.*, 1998). Therefore a knowledge of He diffusivity (and retention) at a given temperature is fundamental to understand the concept of (U-Th)/He dating. Extrapolation of laboratory volume-diffusion kinetic parameters to geologic time scales indicates that He is completely expelled from apatite above ~80 °C and almost totally retained below ~40 °C (Wolf *et al.*, 1996, 1998). Diffusion experiments further suggest that the apatite (U-Th)/He system has a closure temperature (T_c) of ~65–75°C, assuming a constant cooling rate of 10 °C/Myr. (Farley, 2000). He diffusivity correlates with the physical dimensions of Durango apatite, indicating that the diffusion domain is the grain itself, so grain size has a small effect on the closure temperature (Farley, 2000). Grain shape-dimension, cooling rate and U-Th distribution within the grain itself are parameters influencing T_c (Lippot *et al.*, 1994; Wolf

et al., 1996; Warnock *et al.*, 1997; Wolf *et al.*, 1998; Farley, 2000; Meester and Dunay, 2002a,b).

A continuous proliferating of literature has demonstrated that (U-Th)/He dating on apatite crystals represent an useful tool to solve a large variety of geological questions at shallow crustal levels (House *et al.*, 1998; Stockli *et al.*,2000; Farley *et al.*, 2001).

In this study (U-Th)/He dating on apatite from the Marnoso Arenacea Fm. is used to constrain both the thermal evolution and in particular vertical movements in the Altotiberina fault system area. The thermochronological contribution to this thesis comes from a collaboration with Prof. Massimiliano Zattin (Padova University) who provided (U-Th)/He analyses performed on samples which I collected during field work.

For the same sample of Marnoso Arenacea Fm. from one to 5 crystals have been analysed. This procedure allows to verify whether burial temperatures exceeded the reset temperature of about 80 °C for (U-Th)/He system. Exceeding this temperature is easily recognizable when the ages of the individual crystals are all younger than stratigraphic age of the sample.

The apatite crystals, with characteristics suitable for dating (minimum diameter > 60 µm, ehuedrale form, absence of fractures parallel to the c axis and abrasions, absence of inclusions), have been separated and concentrated from rock samples. Samples have been analyzed at Department of Geosciences University of Arizona, using Nd-YAG laser. The samples were than degassed and the concentration of ^{4}He measured by the ratio $^{4}He/^{3}He$ by dilution with ^{3}He in a quadrupole mass spectrometer. The amount of U, Th and Sm were then measured by isotope dilution mass spectrometry in plasma.

3.4 Sampling strategy

Samples have been collected at different structural levels in the ATF system. The first set of samples is located in the ATF footwall, in the western part of the Tiber Valley (Box A in Fig. 3.6) and the second set in the eastern part of the Tiber Valley in the hangingwall of the ATF system (Box B in Fig. 3.6). For this last dataset samples have been collected both in the Gubbio Basin (to the west of the antithetic Gubbio fault) and to the east of the Gubbio ridge (to the east of the antithetic Gubbio fault).

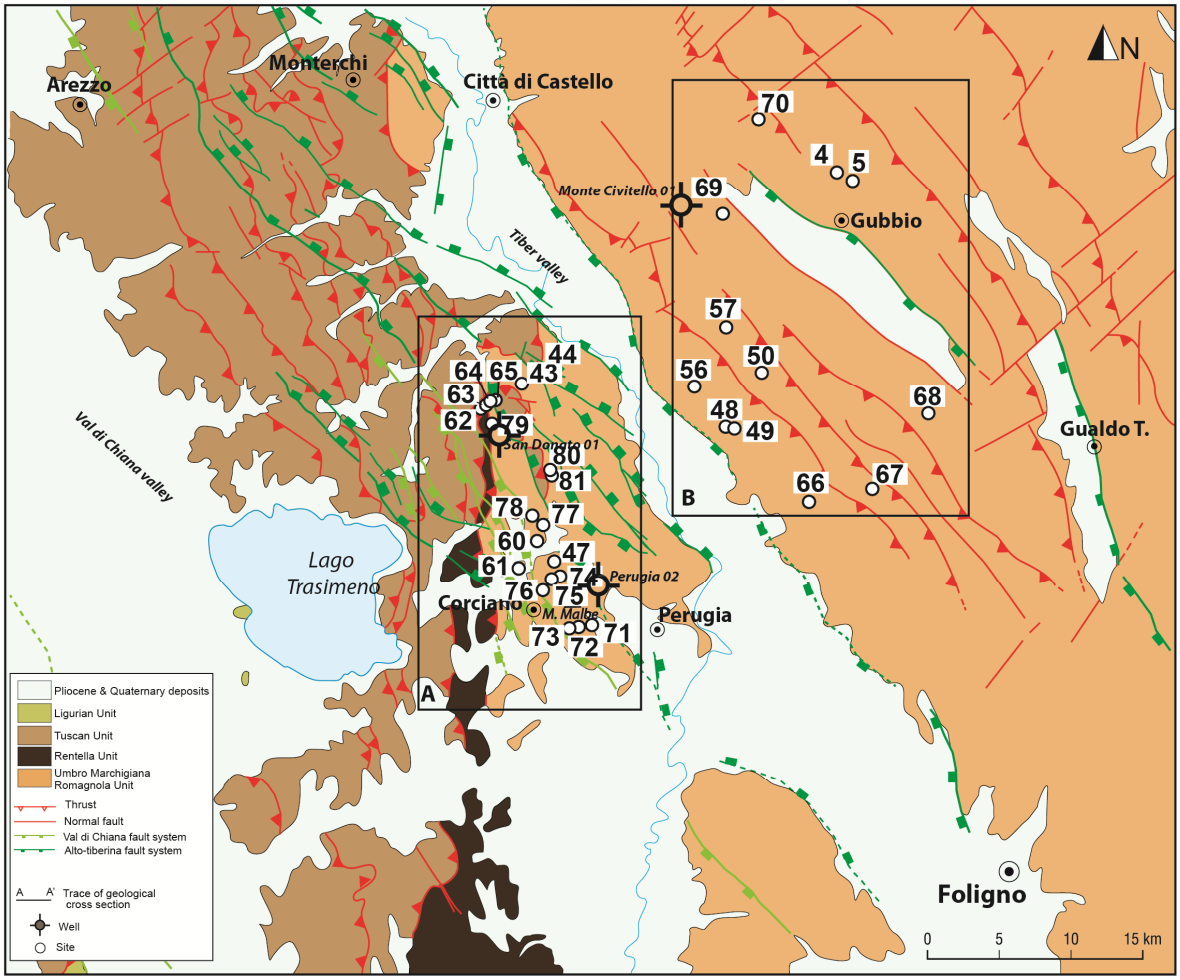

Fig. 3.6 Tectonic sketch map of the study area with sample sites. Compiled after Mirabella *et al.*, (2011) and sheet Umbertide 299, scale 1:50,000; in Carta Geologica d'Italia. Ist. Super. per la Prot. e la Ric. Rome; (Carg Project , 2011).

Generally, samples for the different analytical techniques were collected in the same sites to allow direct correlation among indicators of maximum burial and paleo-temperature and to calculate exhumation rates. A total of 32 sites have been sampled and a total of 58 samples have been analyzed at Roma Tre and Padova Universities.

3.4.1 Sampling for Paleo-thermal (Ro% and I% in I-S) and thermochonometric (U-Th/He) analyses

Sampling sites are located in the footwall of the ATF to the West of the Tiber Valley where the oldest stratigraphic units crop out (box A in Fig 3.6). Three sites have been sampled to the north of the San Donato-01 well from the foredeep turbidites of the Marnoso Arenacea Fm.. Ten samples have been collected from Mt. Malbe exhumed Triassic units, one sample from the Aptian-Albian Marne a Fucoidi Fm.. Two additional

sites are located on the Schlier and Marnoso Arenacea Fms. in the footwall of the most external klippen of the Tuscan Nappe.

To the East of the Tiber Valley (box B in Fig. 3.6) sampling has been concentrated mainly on the Marnoso Arenacea Fm., both at the hangingwall and at the footwall of the Gubbio fault. Eleven sites have been analyzed in the Marnoso Arenacea Fm. and one in the Schlier Fm..

The sampled intervals in the Marnoso Arenaca Fm. have different ages in the different sectors. In the sector to the west of the Tiber Valley, the Burdigalian-Langhian member has been sampled (Barsella *et al.*, 2009). Whereas in the Gubbio basin, between the Tiber Valley and the Gubbio ridge, the Marnoso Arenacea Fm. is as young as Serravallian age (Ridolfi *et al.*, 1995; Ricci Lucchi and Pialli 1973). In the end, to the east of the Gubbio ridge the older member (Burdigalian-Langhian time) crops out again (Ridolfi *et al.*, 1995).

The sampling sites for the U-Th/He analyses are concentrated only on the Marnoso Arenacea Fm..

In detail a suite of 28 samples has been collected for the organic matter optical analyses (Ro%); 23 for the XRD studies, and 5 samples for the (U-Th)/He analyses (Tabs. 3.1, 3.2).

3.5 Results

3.5.1 Surface results

3.5.1.1 Organic matter analyses

In this section samples from different formations will be described separately. Moving along the stratigraphic succession (Umbria-Romagna-Marche domain) from the bottom to the top, significant results have been obtained from Triassic Rhaetavicula contorta Fm.; Aptian-Albian Marne a Fucoidi Fm. and Burdigalian-Langhian-Serravallian Marnoso Arenacea Fm..

The organic matter dispersed in the Rhaetavicula contorta Fm. is generally abundant, the predominant macerals belong to the huminite-vitrinite group, present in small fragments, whereas the inertinite group macerals are less abundant. Only in one sample pyrite is present.

Table 3.1. Organic matter maturity and clay mineralogy data from the study area

Site	Coordinates (Lat-Long)	Lithology	Samples for Vitrinite Analyses	Ro% (± s.d.)	N°	Samples for XDR Analyses	X-ray quantitative analysis of the <2µm grain-size fraction (%wt.)	%I in I-S	%C in C-S	S.O.
Triassic Rhaetavicula contorta Fm.										
47	43°9'25.62" 12°19' 2.60"	Marls/lms	CO49	1.03 (±0.150)	22	CM39	I_{68} I/S_{31} Cl_1	83		R3
60	43° 9'52.14" 12°18'22.92"	Marls/lms	CO69	barren						
71	43°7'50.58" 12°20' 3.78"	Marls/lms	CO79	1.22 (±0.086)	20	CM76	Sm_{48} I_{46} I/S_5 Cl_1	77		R1/R3
72	43°05' 4.2", 12° 0' 3.36"	Marls/lms	CO80	barren		CM77	I_{83} I/S_{14} K_2 Cl_1	85		R3
73	43°7'57.00" 12°11.1'22.6"	Marls/lms	CO81	barren		CM78	I_{56} I/S_{18} K_8 Cl_{18}	72		R1
74	43° 8' 34.62" 12°19' 14.10"	Marls/lms	CO82	barren						
75	43° 20' 48.3" 12°17'54.42"	Marls/lms	CO83	barren						
76	43°8'31.32" 12°17'54.42"E	Marls/lms	CO84	1.03 (±0.150)	22	CM79	I_{70} I/S_{29} K_1	84		R3
77	43°10'4.80" 12°18'26.82"	Marls/lms	CO85	barren		CM80	I_{69} I/S_{29} K_2	84		R3
78	43°10'17.94" 12°18'23.94"	Marls/lms	CO86	barren						
Albian Marne a Fucoidi Fm.										
61	43° 9'12.47", 12°17'20.28"	Marls	CO70	0.78 (±0.140)	6	CM68	I_{87} I/S_{13}	75		R1
Burdigallian Schlier Fm.										
80	43°13'43.98" 12°19'19.50"	Sdt/lms				CM82	I_{50} I/S_{13} Cl_{37}	70		R1
4	43°23'10.04" 12°33'25.70"	Sdt/lms				CM07	I_{41} I/S_{38} Cl_{21}	38		R0
Burdigallian-Langhian-Serravallian Marnoso Arenacea Fm.										
43 44	43°15'52.44" 12°17'22.38"	Sdt/lms	CO47a CO47b	0.37 (±0.132)	10	CM37	I_{62} I/S_{21} C/S_7 Cl_{11}	40	70	R0
48	43°14'2.52" 12°28'54.30"	Sdt/lms	CO50	0.35 (±0.063)	26	CM40a	I_{67} I/S_{27} K_3 Cl_3	40		R0
49	43°14'2.52" 12°28'54.30"	Sdt/lms				CM40b	I_{59} I/S_{36} K_4 Cl_1	50		R0
50	43°15'22.80" 12°31'24.00"	Sdt/lms	CO51	0.26 (±0.050)	76	CM41	I_{57} I/S_{24} K_7 Cl_{12}	45		R0
56	43°14'32.32" 12°26'46.61"	Sdt/lms	CO55	0.42 (±0.068)	35					
57	43°17'0.54" 12°29'11.22"	Sdt/lms	CO56	barren		CM44	I_{56} I/S_{16} K_9 Cl_{20}	40		R0
62	43°15'16.37", 12°15'40.81"E	Sdt/lms				CM69	I_{59} I/S_{18} Cl_{23}	70		R0-R1
63	43°15'16.12" 12°15'44.33"	Sdt/lms	CO71	barren						
64	43°15'16.05" 12°15'26.54"	Sdt/lms	CO72	barren		CM70	I_{64} I/S_{18} K_5 Cl_{13}	55		R0
65	43°15'22.79" 12°15'51.13"	Sdt/lms	CO73A, CO73B	0.46 (±0.069)	14					
66	43° 9'56.70" 12°33'47.94"	Sdt/lms	CO74	barren		CM71	I_{56} I/S_{40} K_3 Cl_1	54		R0
67	43°10'17.88" 12°39'9.48"	Sdt/lms	CO75	0.28 (±0.057)	66	CM72	I_{55} I/S_{38} Cl_7	50		R0
68	43°15' 3.55" 12°37' 0.77"	Sdt/lms	CO76	0.32 (±0.058)	36	CM73	I_{54} I/S_{30} K_5 Cl_{11}	50		R0
69	43°22'24.90" 12°28'46.62"	Sdt/lms	CO77	barren		CM74	I_{57} I/S_{19} K_8 Cl_{16}	50		R0
70	43°25'45.51" 12°26'5.16"	Sdt/lms	CO78	barren		CM75	I_{53} I/S_{18} K_9 Cl_{20}	38		R0
79	43°14'6.96", 12°16'50.76"	Sdt/lms	CO87	0.40 (±0.076)	132	CM81	I_{57} I/S_8 C/S_{17} K_8Cl_{10}	60	60	R1
81	43°12'29.40" 12°19'3.96"	Sdt/lms	CO88	0.37 (±0.066)	20	CM83	I_{57} I/S_6 Cl_{37}	65		R1
05	43°23'1.00" 12°33'52.40"	Sdt/lms	CO08	0.39 (±0.045)		CM08	I_{51} I/S_{19} K_{11} Cl_{19}	44		R0

Acronyms: SDT=sandstone; LMS= Limestone; I=illite; I/S=mixed layer illite-smectite; C/S= mixed layer clorite-smectite; K= Kaolinite; Cl=Clorite; S.O.= stacking order

Table 3.2. (U-Th)/He analytical details and results

Site	Grain no.	raw age (Ma)	±σ (Ma)	radius (µm)	U (ppm)	Th (ppm)	Sm (ppm)	^{4}He (nmol/g)	eU (ppm)	FT ^{238}U	FT ^{235}U	FT ^{232}Th	FT ^{147}Sm	Fully FT correct. age (Ma)	±σ (Ma)	mean age (Ma)	±σ (Ma)
63	FT47_Ap1	1.58	0.11	42.03	27.16	96.09	402.92	0.43	49.74	0.67	0.62	0.62	0.75	2.44	0.17	**2.40**	**0.06**
	FT47_Ap2	1.22	0.09	37.59	29.14	56.61	313.89	0.28	42.45	0.63	0.59	0.59	0.71	1.96	0.15		
	FT47_Ap4	1.51	0.06	32.46	55.05	102.88	319.83	0.64	79.23	0.58	0.53	0.53	0.65	2.66	0.11		
	FT47_Ap5	1.41	0.06	34.80	72.97	93.71	134.15	0.71	94.99	0.61	0.56	0.56	0.68	2.37	0.10		
64	FT71_Ap1	3.19	0.13	60.52	6.08	25.70	172.78	0.21	12.12	0.76	0.73	0.73	0.85	4.26	0.18	**3.56**	**0.13**
	FT71_Ap2	2.19	0.16	46.52	7.76	49.16	104.32	0.23	19.31	0.70	0.66	0.66	0.78	3.25	0.23		
	FT71_Ap4	1.48	0.19	42.79	7.76	27.55	85.84	0.11	14.24	0.67	0.63	0.63	0.75	2.26	0.28		
	FT71_Ap5	173.78	3.05	36.62	44.63	78.14	304.40	59.19	62.99	0.63	0.58	0.58	0.70	282.34	5.01		
65	FT73_Ap1	1.79	0.15	47.70	5.31	38.75	185.57	0.14	14.41	0.70	0.66	0.66	0.79	2.63	0.21	**2.50**	**0.10**
	FT73_Ap2	4.91	0.13	53.62	32.78	21.44	451.56	1.00	37.82	0.73	0.70	0.70	0.82	6.72	0.18		
	FT73_Ap3	1.36	0.09	43.03	14.04	57.01	173.41	0.20	27.44	0.68	0.63	0.63	0.76	2.07	0.14		
	FT73_Ap4	1.48	0.15	36.28	6.50	42.16	181.06	0.13	16.41	0.62	0.57	0.57	0.70	2.50	0.26		
	FT73_Ap5	2.43	0.16	51.26	12.24	10.33	84.81	0.19	14.67	0.72	0.69	0.69	0.81	3.39	0.22		
79	FT87_Ap1	3.33	0.14	46.64	42.80	59.10	475.25	1.01	56.69	0.70	0.66	0.66	0.78	4.83	0.20		
	FT87_Ap2	2.42	0.06	48.27	51.88	108.73	196.60	1.00	77.43	0.71	0.67	0.67	0.79	3.48	0.09	**3.77**	**0.06**
	FT87_Ap3	2.48	0.11	48.22	17.88	51.58	118.23	0.40	30.01	0.71	0.67	0.67	0.79	3.59	0.16		
	FT87_Ap4	3.16	0.09	63.74	12.32	27.99	100.51	0.32	18.90	0.77	0.74	0.74	0.87	4.14	0.12		
	FT87_Ap5	4.29	0.23	61.66	4.20	10.23	33.37	0.15	6.61	0.77	0.73	0.73	0.86	5.68	0.31		
67	FT75_Ap1	6.67	0.43	52.43	3.21	15.65	97.90	0.25	6.88	0.73	0.69	0.69	0.82	9.39	0.61		
	FT75_Ap2	19.00	0.48	35.31	13.63	69.75	664.81	3.14	30.02	0.61	0.56	0.56	0.69	32.29	0.81		
	FT75_Ap4	5.09	0.23	48.97	20.63	45.89	324.87	0.86	31.41	0.71	0.67	0.67	0.80	7.29	0.33		
	FT75_Ap5	0.86	0.27	33.82	5.99	23.51	58.21	0.05	11.52	0.60	0.55	0.55	0.67	1.49	0.47		
66	FT74_Ap1	20.30	0.37	60.66	48.30	18.67	120.10	5.67	52.69	0.76	0.73	0.73	0.85	26.69	0.48		
	FT74_Ap2	33.97	0.52	51.54	34.36	49.22	173.80	8.34	45.93	0.72	0.69	0.69	0.81	47.47	0.73		
	FT74_Ap4	45.51	0.85	44.75	52.28	23.06	97.86	13.94	57.70	0.69	0.64	0.64	0.77	66.60	1.25		
	FT74_Ap5	8.37	0.15	54.83	29.10	102.76	734.77	2.42	53.25	0.74	0.70	0.70	0.83	11.55	0.21		

Raw age: not correct age.
Radius: radius of crystal.
U, Th, Sm: concentrations estimated on the basis of the volume of the crystal and the content of U, Th and Sm
^{4}He: concentration di ^{4}He
eU: *effective Uranium* calcolated as [U] + 0.235[Th]
FT: correlation factors for l'*α-ejection.*

The frequency histograms in Fig. 3.7(a, b) show an indigenous population of huminite-vitrinite macerals. R_o% values for the Rhaetavicula contorta Fm. range between 1.03 and 1.22% indicate that the Triassic unit is in the thermal maturity range of the oil window.

The analyzed sample of Marne a Fucoidi Fm. is characterized by a scarce content of unaltered vitrinite fragments. The histogram distribution shows one population, whose mean value is 0.78. This unit is in the catagenetic zone as well, but values are substantially lower than those of the Triassic unit (Fig. 3.7 c).

In the end, the Marnoso Arenacea Fm. is characterized by rich palinofacies, with small and medium-sized fragments of the huminite-vitrinite group and a scarce presence of inertinite. In these samples pyrite is also observed, either in globular aggregates or finely dispersed.

In Fig. 3.7 stratigraphic samples distribution in the Marnoso Arenacea Fm. allow us to distinguish three separate stratigraphic sequences: (1) to the west of the Tiber Valley, (2) in the Gubbio basin and (3) to the east of the Gubbio fault.

The majority of the histograms is characterized by a Gaussian distribution, except for one to the east of the Gubbio fault that shows a second population probably related to reworked vitrinite fragments. These data generally indicate a low thermal maturity of the hosting succession.

In detail the reflectance values in the area around the San Donato-01 well, range between 0.37and 0.46% and testify the immature stage of the hydrocarbon generation.

Moving to the east of the Tiber Valley, in the Gubbio basin, the sedimentary succession that is up to Serravallian in age shows R_o% values ranging from 0.42 to 0.26%.

In the end, to the east of the Gubbio fault the only reliable sample has Ro% of 0.39%.

In Fig. 3.7 Ro% histograms related to the distribution of thermal maturity from bottom to top of the stratigraphic succession indicate a strong decrease of thermal maturity from the middle portion of the oil window (at the bottom) down to the immature stage of hydrocarbon generation (at the top).

In Fig. 3.8 Ro% distribution is plotted in map views. In summary in this map data related to the Marnoso Arenacea Fm., are slightly higher to the west (0.4-0.5%), decrease in the Gubbio basin (mainly 0.2-0.3%) and slightly increase again to the east of the Gubbio fault (0.4%) where sample is referred to the lowermost member of the Marnoso Arenacea Fm..

3.5.1.2 Clay mineralogy analyses

Significant results have been obtained from Triassic Rhaetavicula contorta Fm., Aptian-Albian Marne a Fucoidi Fm., Langhian Schlier Fm. and Burdigalian-Langhian and Serravallian Marnoso Arenacea Fm. by X-Ray diffraction analyses (Fig. 3.7).

In Fig. 3.7 (g-k) selected XRD oriented patterns of the <2μm grain-size fraction have been reported. In Table 3.1 analytical details are given.

The semi-quantitative analyses of <2μm grain-size fraction for the Triassic Rhaetavicula contorta Fm. show mainly the presence of illite, chlorite, mixed layers illite-smectite (I-S) and subordinate amounts of kaolinite. Non-clay minerals such as quartz, calcite, gypsum and plagioclase, have been recognized as well (see Tab. 3.1). The illite-smectite mixed layers (I-S) display both short (R1) and long (R3) range staking order. The illite content in mixed layer I-S range from 72% to 85% corresponding to an increase in the stacking order. The sediments of the Raetavicula contorta Fm. reached the late diagenetic zone, and experienced a maximum paleotemperature of about 120-130 °C according to Merriman and Frey (1999) (Fig. 3.7 g, h and Tab. 3.1).

The only sample coming from the Marne a Fucoidi Fm. is characterized by the presence of illite and I-S mixed layers. Among the non-clay minerals, calcite, quartz and traces of chlorite have been recognized. The illite content in the short range-ordered mixed layers I-S is about 75%, suggesting that also this unit experienced late diagenetic conditions and presumably maximum paleo-temperatures higher than 100-110 °C (Merriman and Frey, 1999).

In the <2μm grain-size fraction of the Schlier Fm., quartz, calcite, gypsum and plagioclase has been recorded among the non-clay minerals, whereas mixed layers chlorite-smectite and illite-smectite constitute the clay fraction. The samples collected show, in the area, variable stacking order and illite content in the mixed layers I-S.

In detail, the samples collected in the Schlier Fm. area to the west of the Tiber Valley, at the front of the most advanced klippen of the Tuscan Unit (site 80 in Fig. 3.5) are characterized by short range ordered I-S with an illite content of 70%. Moving toward the external sector, to the east of the Tiber Valley, samples collected at the footwall of the Gubbio normal fault display a random ordered of the I-S mixed layer and the illite content decrease down to 38%.

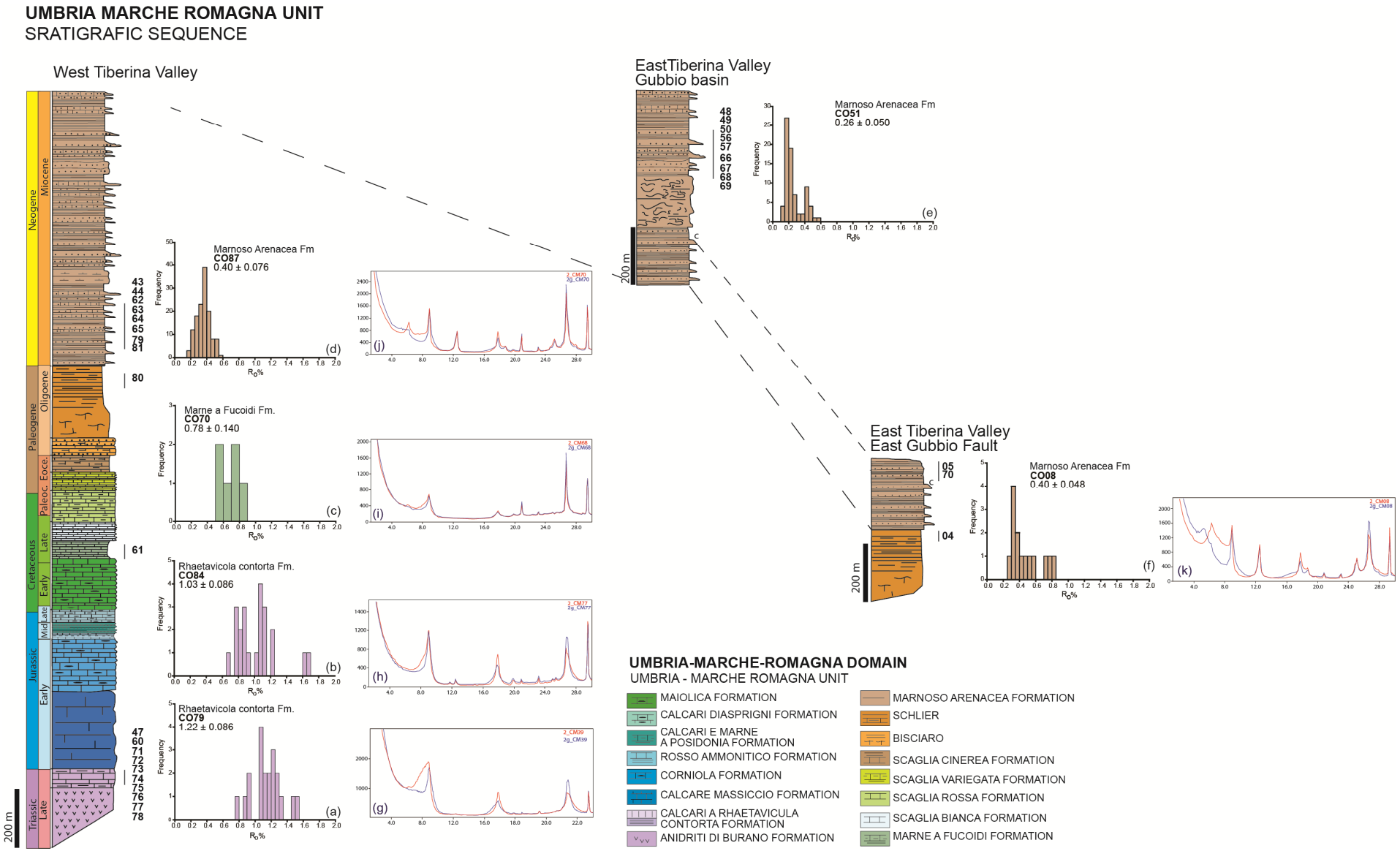

Fig. 3.7 Simplified stratigraphic columns of the study area with representative histograms of distribution of vitrinite reflectance data and XRD oriented patterns of the <2µm grain-size fraction.

In general, a decrease of the thermal maturity along the stratigraphic succession has been recorded from bottom to top by I% in I-S mixed layer data, similarly to what recognized by means of the organic matter analyses (Fig. 3.7).

In plain view (Fig. 3.8), a general regional decrease of thermal maturity from the west to the east is highlighted by illite content data distribution.

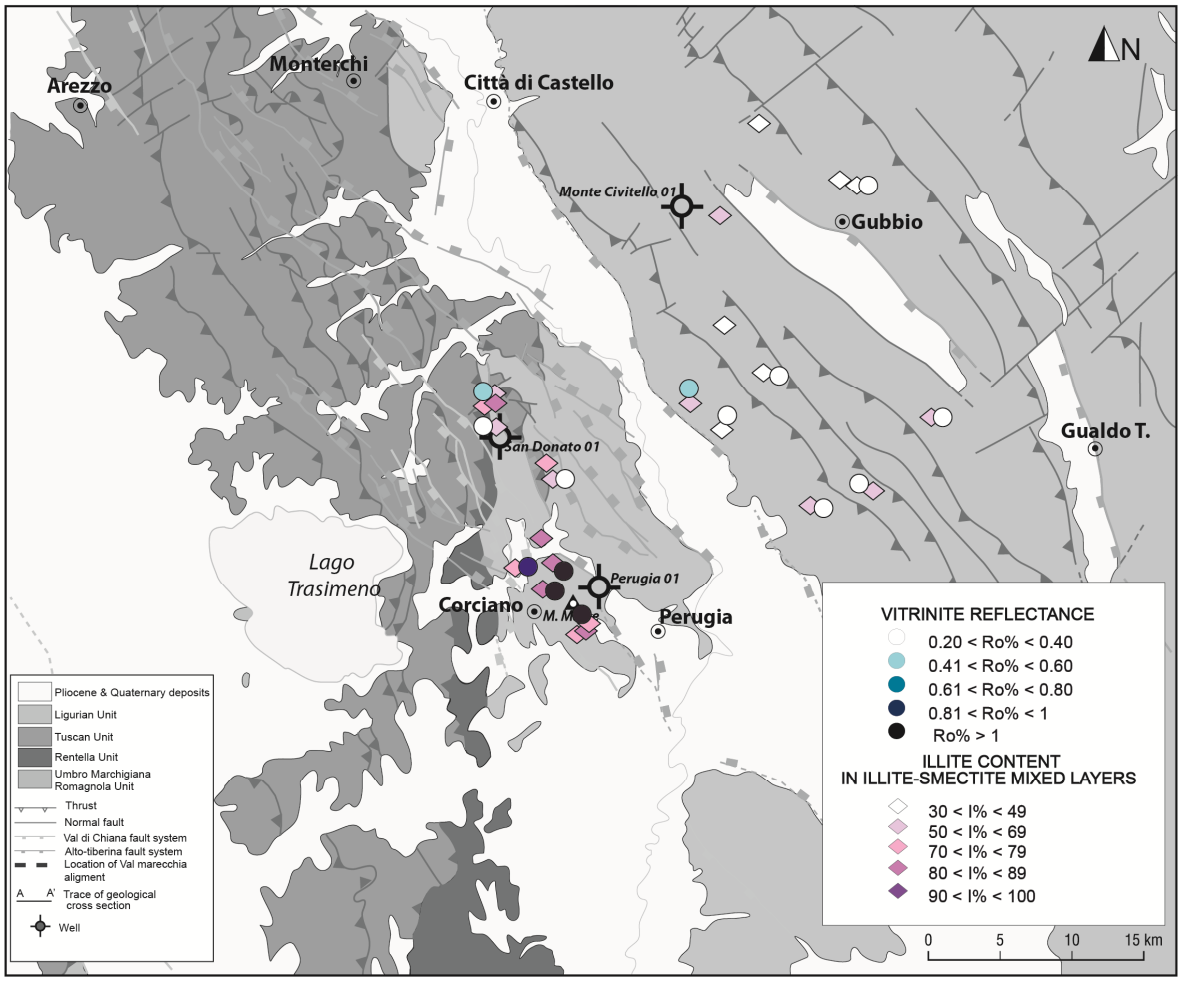

Fig. 3.8 Distribution of vitrinite reflectance and I% in I-S mixed layers data performed in this study and plotted on the simplified tectonic scheme of Fig. 3.6.

3.5.1.3 (U-Th)/He analyses

A total of 24 ages was obtained from 6 samples of the Marnoso Arenacea Fm. (Fig. 3.6 and Tab. 3.2).

In samples FT47 and FT87, the ages obtained onto single crystals of apatite are mutually comparable, taking into account the error bars. Thus, the mean age of these two sample has been calculated by the arithmetic mean among every single crystals in each sample (Tab. 3.2).

For samples FT71 and FT73, one crystal shows a significantly greater age than the others (especially in the case of ample FT71). For this reason they were not considered in the averaging process.

The remaining two samples (FT74 and FT75) show a very high age variability. Probably, both samples were subject to temperatures of maximum burial lower than those required to reset the (U-Th)/He system (80 °C). Therefore the ages are not representative of cooling during exhumation but describe a pre-depositional history.

In sample FT75, the age obtained for one crystal is extremely recent (1.49 Ma), this value must be considered with caution, because the He content is close to the limit of the analytical methodology.

The obtained mean age for each site has been reported in Fig. 3.9 together with the other data of U-Th/He dating and Apatite Fission Tracks ages already published by Zattin *et al.* (2002) and Thomson *et al.* (2010) (Tab. 3.3) and will be discussed in the discussion section.

Table 3.3 U-Th/He dating and Apatite Fission Tracks ages published by Zattin *et al.* (2002) and Thomson *et al.* (2010)

Site	Coordinates (Lat-Long)	Lithology	Formation	Age	Age(Ma) ± 1σ	
Apatite fission tracks ages (Zattin *et al*., 2002)						
AP19	43° 17' 54" 12° 19' 04"	Sdt/lms	Marnoso Arenacea	Burdigalian-Langhian	20.4±2.0	NR
AP20	43° 16' 59" 12° 18' 0.4"	Sdt/lms	Marnoso Arenacea	Burdigalian-Langhian	12.3±1.4	PR
AP21	43° 16' 41" 12° 21' 13"	Sdt/lms	Marnoso Arenacea	Burdigalian-Langhian	3.7±1.0	R
AP22	43° 22' 41" 12° 18' 45"	Sdt/lms	Marnoso Arenacea	Burdigalian-Langhian	40.7±4.3	NR
AP23	43° 24' 29" 12° 32' 58"	Sdt/lms	Marnoso Arenacea	Serravallian	41.3±4.7	NR
AP25	43° 23' 0.8" 12° 33' 0.8"	Sdt/lms	Marnoso Arenacea	Serravallian	34.1±2.6	NR
AP28	43° 25' 15" 12° 36' 17"	Sdt/lms	Marnoso Arenacea	Serravallian	72.5±8.4	R
(U-Th)/He ages (Thomson *et al*., 2010)						
AP19	43° 17' 54" 12° 19' 04"	Sdt/lms	Marnoso Arenacea	Burdigalian-Langhian	5.83	R
AP20	43° 16' 59" 12° 18' 0.4"	Sdt/lms	Marnoso Arenacea	Burdigalian-Langhian	1.85	R
AP21	43° 16' 41" 12° 21' 13"	Sdt/lms	Marnoso Arenacea	Burdigalian-Langhian	1.85	R
AP22	43° 22' 41" 12° 18' 45"	Sdt/lms	Marnoso Arenacea	Burdigalian-Langhian	2.62	R
AP23	43° 24' 29" 12° 32' 58"	Sdt/lms	Marnoso Arenacea	Serravallian	4.18	R
AP25	43° 23' 0.8" 12° 33' 0.8"	Sdt/lms	Marnoso Arenacea	Serravallian	4.63	R
AP28	43° 25' 15" 12° 36' 17"	Sdt/lms	Marnoso Arenacea	Serravallian	7.5	R

Regarding both original and already published U-Th/He data, the majority of samples are totally reset with the exception of two samples (one partial reset AP20 and one no reset AP21).

Moving from the west (ATF system in the area of Mt. Acuto) to the east (Gubbio ridge) four clusters of data can be distinguished. To the west of the Tiber Valley and in particular to the east of the Rentella Unit thrust front, in the more internal portion of the Marnoso Arenacea Fm., the ages range between 2.5 and 3.6 Ma (Fig. 3.9a). Whereas, in the portion of the Marnoso Arenacea Fm. cropping out between the Tiber Valley and the front of the Tuscan Units (Fig. 3.9b) the age are younger and range between 1.85 and 2.4 (the age value of 5.83 Ma is probably an outlier and should be discharged). To the east of the Gubbio fault the mean age is 4.4 Ma, considering the 7.5 and 2.5 Ma as outliers thus not reliable (Fig. 3.9d).

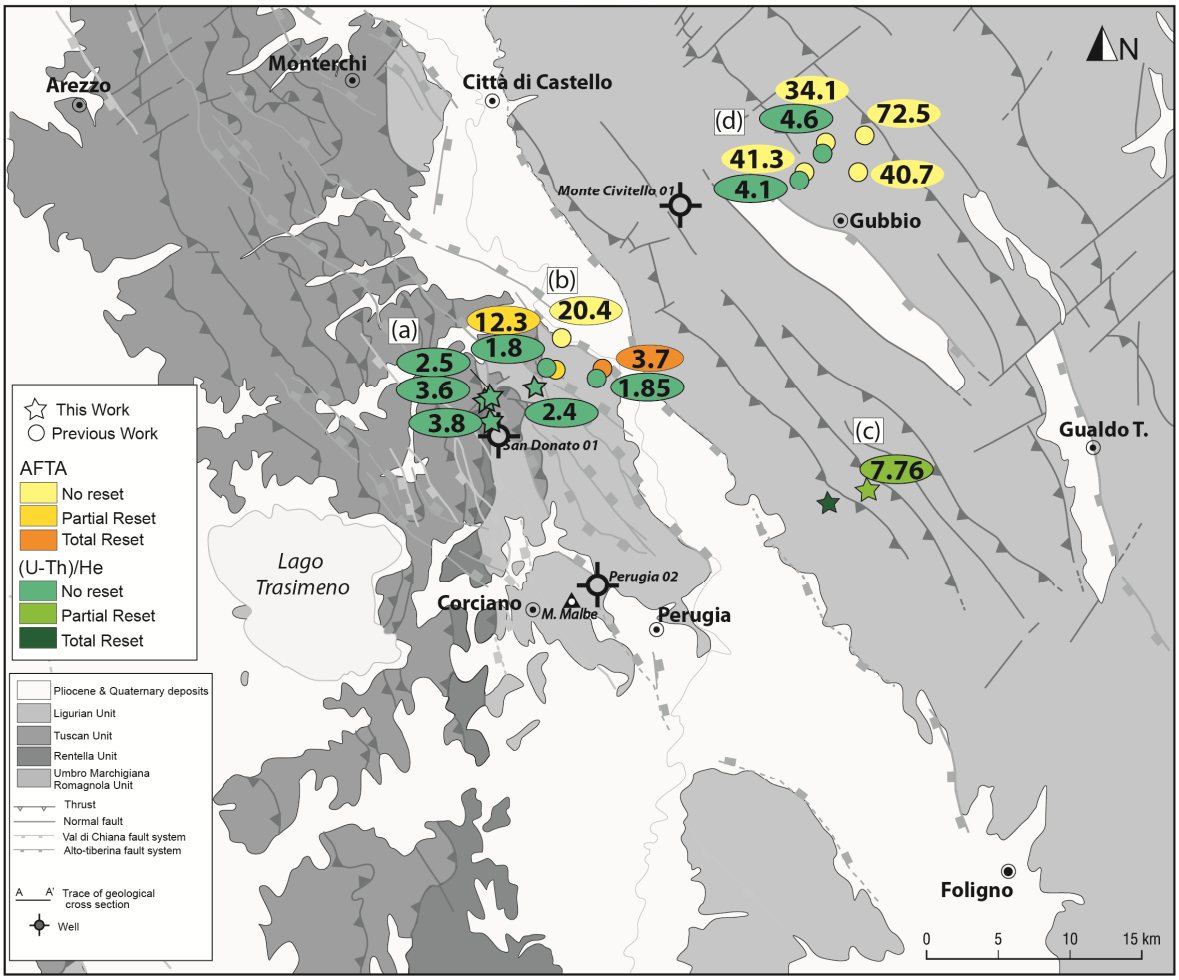

Fig. 3.9 Distribution (U/Th)/He ages performed in this study and plotted on the simplified tectonic scheme (Fig. 3.6) together with (U/Th)/He and AFT ages already published by Zattin *et al.*, (2002) and Thomson *et al.*, (2010).

To the east of the Tiber Valley in the Gubbio basin and in the hangingwall of the Gubbio fault, data indicate partial retention and no retention of He.

Summing up the western portion of Marnoso Arenacea Fm. exhumed more recently than the external one of about 1.5 Ma. Between these two sector an area that experienced lower paleotemperatures is preserved (e.g., Gubbio basin).

3.5.2 Subsurface data from deep wells

The stratigraphic and thermal maturity data of the Monte Civitello 01 well and San Donato 01 wells have been reported in Fig. 3.10.

ENI spa is kindly acknowledged for providing these data.

3.5.2.1 Monte Civitello 01

Monte Civitello 01 well is located to the NW of the Gubbio town and reaches depths down to about 5,600 m. From the top to the bottom, the stratigraphic succession starts from the Marnoso Arenacea Fm. (1,070 m thick) and evolves down to the carbonatic succession of the Umbria-Marche-Romagna domain (2,000 m thick) and then down to the Triassic Anidrite di Burano Fm. (2,500 m thick).

The optical analyses of palynofacies and thermal maturity investigation (T.A.I.-Thermal Alteration Index and R_o%) were performed by ENI lab on cuttings analyses. The results have been obtained for: four samples of the Marnoso Arenacea Fm.; three samples of the carbonatic succession (from Scaglia Fm., Marne a Fucoidi Fm., Rhaetavicula contorta Fm.) and two from the evaporates of the Anidriti di Burano Fm..

The analyses of the palynofacies are summarised in Fig. 3.11a in which the composition of kerogen has been plotted against depth; whereas in Fig 3.11b the thermal maturity of organic matter, expressed as T.A.I. and Ro%, has been reported.

The palynofacies of the Marnoso Arenacea Fm. consist of 50-60% of the continental wooden fragments, 30% of continental herbaceous fragments and subordinate amounts of marine and amorphous organic matter (Fig. 3.11a). The colorimetric variation of the palynomorph (T.A.I.) indicates a value of 1.7 in the immature stage of hydrocarbon generation, in agreement with R_o% values ranging from 0.42 to 0.44 (Fig. 3.11b). These results do agree with surface data sampled in the Gubbio basin described in the previous paragraph.

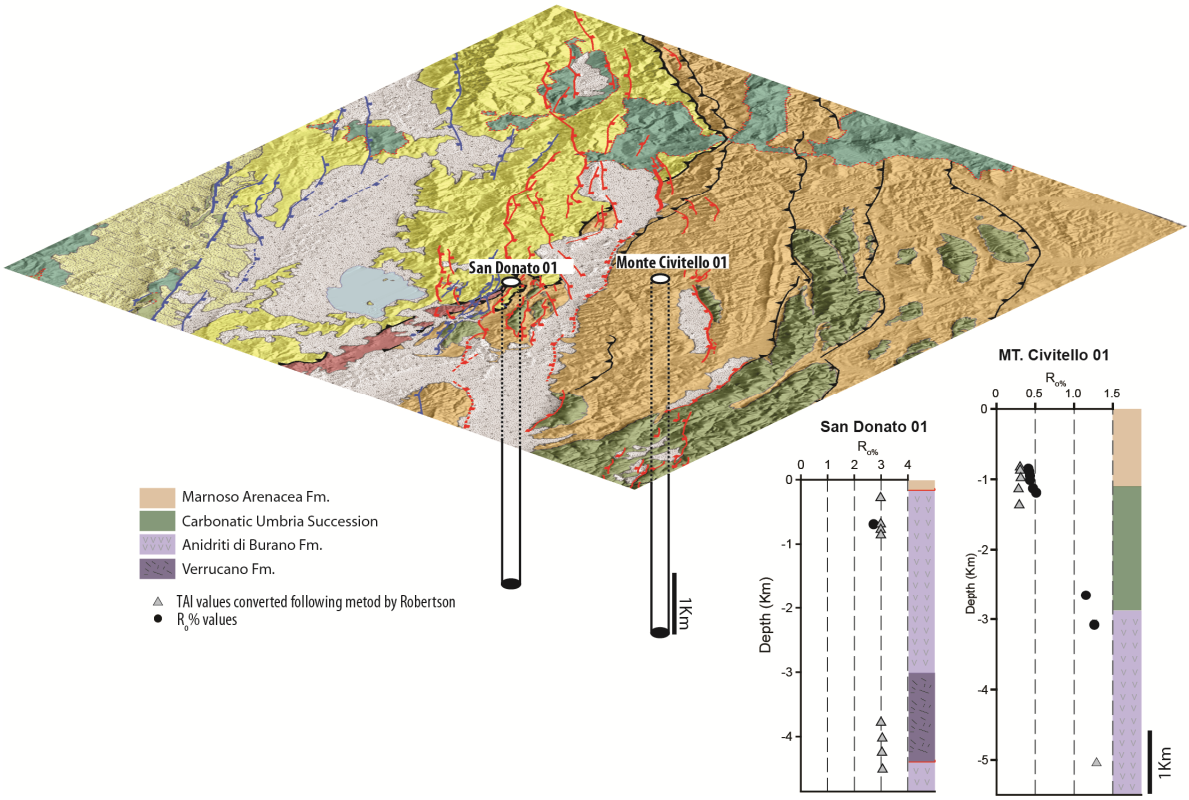

Fig. 3.10 (a) Structural map with wells location**;** (b) simplified stratigraphic logs with R_o% and T.A.I values: data refer to San Donato 01 well and Monte Civitello 01 well.

For the carbonatic succession, samples from the Scaglia Fm. show a palynofacies consisting of 50% of continental wooden fragments and 40% of herbaceous continental fragments and marine organic matter for the remaining percentage (10%). Amorphous organic matter is absent. R_o% values range from 0.48% to 0.52%, indicating the boundary between the immature and mature stages of hydrocarbon generation. T.A.I. value is 1.5, in the immature stage of hydrocarbon generation.

In the palynofacies of the Marne a Fucoidi Fm., the marine organic matter is totally absent, whereas continental fragments are mainly constituted by wooden fragments (70%). The remaining 30% consists of herbaceous fragments and amorphous organic matter. Only T.A.I. analysis has been performed on this unit and indicates the immature stage of hydrocarbon generation, with a value of 1.5. The Corniola Fm. consists of mainly continental organic matter, with wooden fragments ranging between 65-80% and herbaceous fragments ranging from about 20 to 35%. A small percentage of amorphous organic matter is present. The organic matter optical analyses are absent.

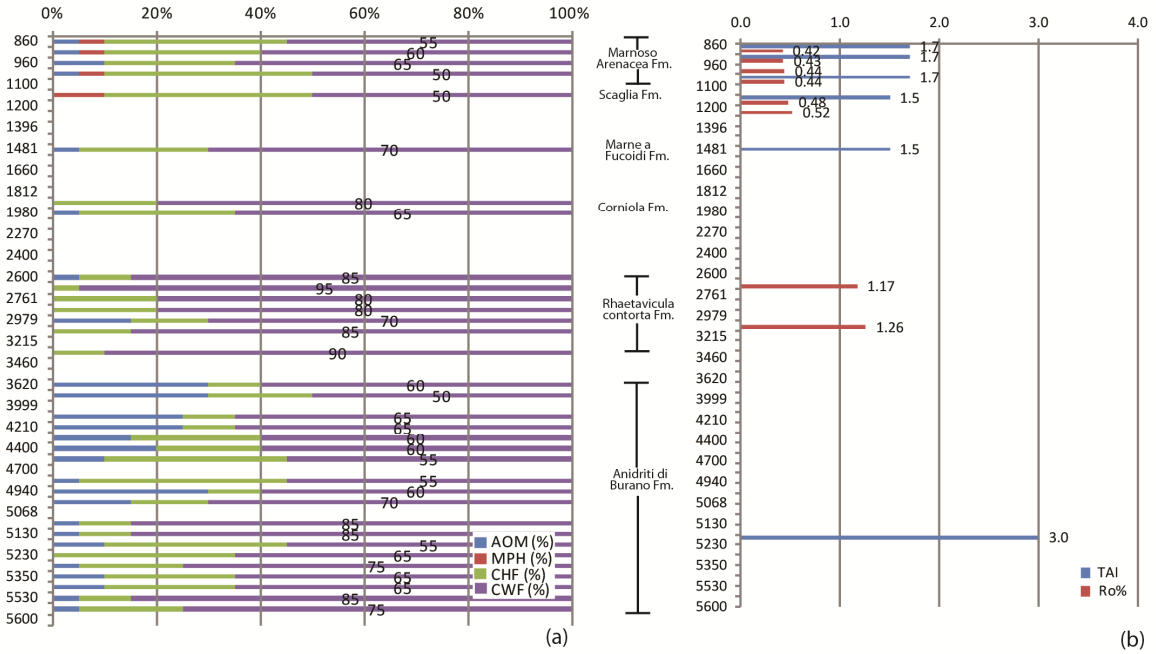

Fig. 3.11 (a) Diagram representing the kerogene composition of the sedimentary succession in Monte Civitello 01- well. AOM stands for amorphous om, MPH for marine phytoplankton; HCF for continental herbaceous om; CWF for continental wooden om whose percentage are indicated on each bar; (b) Diagram representing the Thermal Alteration Index (T.A.I.) and R_o% versus the depth.

The Rhaetavicula contorta Fm. is characterized by the prevalence of continental organic matter. The wooden fragments cover the 70-95% of the total content, whereas the remaining amount consists of herbaceous fragments and amorphous organic matter. The organic matter optical analyses suggest that sediments have reached the late mature stage of hydrocarbon generation (R_o% = 1.17%) (Fig. 3.11a,b).

In the end, the Triassic Anidriti di Burano Fm. consists of mainly continental organic matter, with wooden fragments ranging between 55-85% and herbaceous fragments ranging between 10-40%. A small amount (5-10%) of amorphous organic matter is present (Fig. 3.11a). R_o% value is of 1.26% in the late mature stage of hydrocarbon generation. The colorimetric variation of the palynomorph (T.A.I.=3) indicate a mature stage of hydrocarbon generation in agreement with R_o% values (Fig. 3.11b).

Summarizing, the Monte Civitello 01 well is characterized by an almost regular thermal maturity trend with an increase of R_o% values from 0.42 to 1.26 in good agreement with T.A.I. values. The abundance of data available for this well allowed to perform 1D thermal modelling (see the Discussion in this chapter).

3.5.2.2 San Donato 01 well

The San Donato 01 well is located to the NNW of Perugia town reaching a depth of 4,750 m. The stratigraphy of the well is characterized by the Marnoso Arenacea Fm. (326 m thick) at the top, in tectonic contact by means of an extensional fault with the Triassic Anidriti di Burano Fm. (Fig 3.10) (Minelli and Menichetti, 1990; Anelli *et al.* 1994). The Anidriti di Burano Fm. is about 2,700 m thick and stratigraphically evolves downwards to the Verrucano Fm. (1,420 m thick). At the depth of 4,500 m, a thrust affects the stratigraphic sequence superimposing the Verrucano Fm. onto Anidriti di Burano Fm..

Organic palinofacies and organic matter maturity data expressed both by T.A.I. and Ro % are plotted against depth in Fig. 3.12a and Fig. 3.12b, respectively.

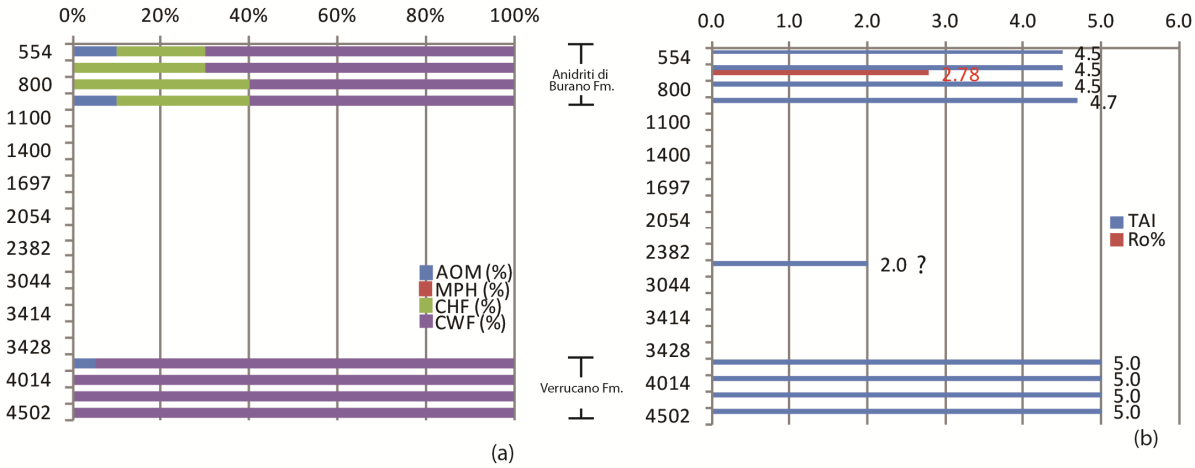

Fig. 3.12 (a) Diagram representing the kerogene composition of the sediments in the San Donato 01- well. AOM stands for amorphous om, MPH for marine phytoplankton; HCF for continental herbaceous om; CWF for continental wooden om; (b) Diagram representing the Thermal Alteration Index (T.A.I.) and R_o% versus the depth in the San Donato 01- well

The main results of the analyses have been obtained for the Anidriti di Burano and Verrucano Fms..

The Anidriti di Burano Fm. is mainly characterized by continental organic matter consisting of wooden fragment for a 60-70% and herbaceous fragments for 20-40%. In a few samples, small amounts of amorphous organic matter is also present. The colorimetric variation of the palynomorphs indicates T.A.I. values ranging from 4.5 to 4.7 suggesting a post-mature stage of hydrocarbon generation according to Staplin (1969). These data are in agreement with Ro% values that reach 2.78%, typical of over-mature stages of the hydrocarbon generation.

The palynofacies of the Verrucano Fm. consists only of wooden fragments of continental origin. The T.A.I. analyses provide a value of 5, suggesting an over-mature carbonification

level. Summarizing the palinofacies in the S. Donato 01 well consists of mainly wooden fragments of continental origin, and to a lesser extent herbaceous fragments and amorphous organic matter. The marine organic matter is totally absent. Regarding the organic matter maturity analyses, sediments have reached the anchizone and the metagenetic stage of hydrocarbon generation.

3.6 Discussion

3.6.1 Comparison between indicators of maximum thermal exposure (Ro% and mixed layers I-S)

In Fig. 3.13 the correlation between vitrinite reflectance and illite content in illite-smectite (I-S) mixed layer data has been reported. This diagram has been produced on the basis of the kinetic model of vitrinite thermal evolution performed by Burnham and Sweeney (1989) and the kinetics of the I-S reaction determined by Hillier *et al.* (1995).

Violet circles represent the Triassic Rhaetavicula contorta Fm., blue stars the Albian Marne a Fucoidi Fm. and triangles indicate Marnoso Arenacea Fm.. Different colours for triangles indicate different locations and structural positions with respect to the Tiber Valley and the main elements of the Altotiberina fault system: red triangles pertain to data from the sector to the west of the Tiber Valley, whereas yellow ones indicate data to the east of the Tiber Valley.

A decrease in the heating rate from the Triassic to the Miocene turbidites is evident. The Rhaetavicula contorta Fm. is characterized by high heating rates typical of continental rifts. A strong decrease in the heating rate is recorded in the Marnoso Arenacea Fm. where most of samples show values ranging from 1.5 to 0.375, and three sample show even lower values (<0.375) typical of cold basins (e.g. foredeep basins). In the case of data for the literature (Meneghini *et al.*, 2012) both Ro% and I% in I-S are slightly higher than those sampled in this work. I cannot exclude that this last evidence is due to the local heating effect of thrusting of the Tuscan unit and/or Rentella unit on thermal maturity of the thrust footwall.

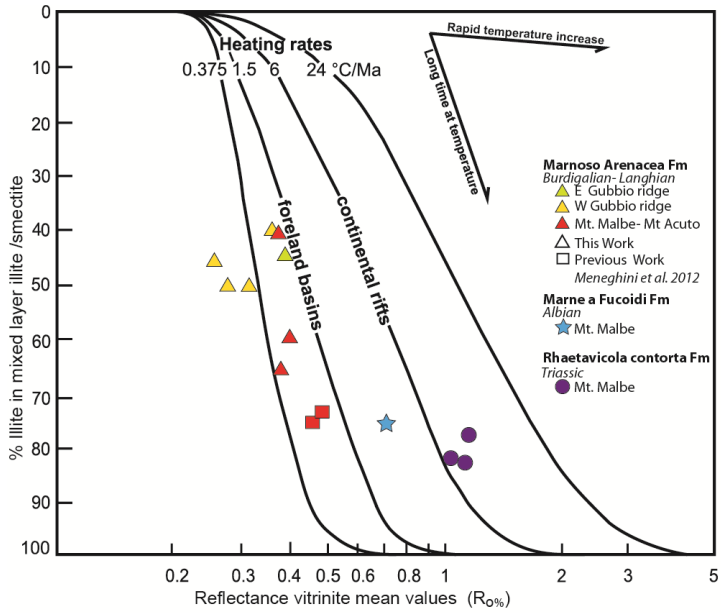

Fig. 3.13 Heating rate values for the Marnoso Arenacea Fm. (triangles), Marne a Fucoidi Fm. (stars) and Rhaetavicula contorta Fm. (cirles) extracted from the correlation of vitrinite reflectance and illite content in illite-smectite (I-S) data based on the kinetic model of vitrinite maturation of Burnham and Sweeney (1989) and the kinetics of the I-S reaction determined by Hillier *et al.* (1995). Modified and redrawn after Hillier *et al.* (1995)

The heating rate decrease from Triassic to Miocene times can be easily ascribed to the different geodynamics settings experience by the different stratigraphic units: from Tethyan rift and post-rift stages to the Alpine convergence and collision.

3.6.2 Tectonic evolution by means of paleothermal and thermochronological constraints

The integration of organic and inorganic thermal and thermocronological indicators allowed us to distinguish three main sectors in the study area which experienced different amounts of sedimentary/tectonic loads and exhumation as well as variable timing and rates of exhumation.

3.6.2.1 Area to the west of the Tiber Valley

The sector to the west of the Tiber Valley is quite complex from a structural point of view because of several closely spaced Pliocene-Quaternary normal faults dissecting the main thrust contact between the Tuscan and the Umbria-Marche-Romagna domains and their strong along strike variations. This sector is limited to the west by the roughly N-S Rentella and Tuscan Unit regional thrust fronts and to the east by the alluvial deposits of the Tiber Valley. It is characterized from west to east by the outcrop of a NNW-SSE narrow corridor of Langhian-Burdigalian Marnoso Areancea Fm. bounded toward the east

by west dipping normal faults belonging to the Val di Chiana extensional system. In their footwall the regional NNW-SSE ridge of the Mt. Malbe, crops out and is made up of pre-orogenic carbonates that plunge towards the north. Moving to the East this structural high is downthrown by the ATF east dipping segments. Their hangingwall hosts more advanced and thin klippen of the Tuscan Nappe that in turn overthrust the Langhian-Burdigalian Marnoso-Arenacea Fm. This last is dissected by NNW-SSE of the ATF that creates a further structural high (Mt. Tezio-Mt. Acuto) where the carbonates crop out again (Fig. 3.1). Thus the most exhumed structures of this sector are represented by the two structural highs where carbonates crop out uplifted by both the Corciano (COF) and ATF normal fault segments dipping in opposite directions.

Fig. 3.14 shows in detail R_o% data (Fig. 3.14a), I% in I-S values (Fig. 3.14b), AFTA data from Zattin *et al.* (2002) (Fig. 3.14c) and (U-Th)/He ages from this work and Thomson *et al.* (2010) (Fig. 3.14d) for this sector.

Focusing up on data, the pre-orogenic units cropping out in correspondence of the structural high of Mt. Malbe (such as the Triassic Rhaetavicula contorta and the Marne a Fucoidi Fms.) acquired the highest thermal maturity values (oil window and late diagenetic zone of clay minerals zonation) recorded in the entire study area and these values are analogous to those recorded for the same units preserved at depth in Monte Civitello 01 well. This evidence suggests that this structure subdued exhumation in quite recent times, otherwise I would expect in the Monte Civitello 01 much higher values than in the outcropping Mt. Malbe area. In the case of an early exhumation in Mt. Malbe it is highly probable that it did not evolve thermally at the same level of the buried equivalent unit now preserved at depth in Monte Civitello 01 well.

This evidence seems to be confirmed by U-Th/He dating between 3.8 and 2.5 Ma along the northern plunge of the Mt. Malbe structure and by exhumation ages younger than 2 Ma to the east of both Mt. Malbe and Mt. Acuto-Mt. Tezio ridges on totally reset samples of the Marnoso-Arenacea Fm..

All thermochronometric data are generally younger than data recorded a few tens of km to the east of the Tiber Valley, in more external position (ages higher than 4.5 Ma along the Contessa section).

This evidence suggests that other than the typical pattern of rejuvenation of exhumation towards the external portions of a thrust belt, is recorded in the study area with younger exhumation probably enhanced by extensional tectonics in this western sector with respect to the eastern one. Vitrinite reflectance for the Marnoso Arenacea Fm. has

slightly higher values (up to about 0.5%) at footwall of the Rentella thrust and values lower than 0.4 % at the footwall of the most external klippen of Tuscan thrust front. This slight variation may mark the actual position of the Tuscan front before erosion (more internal with respect to 0.39, 0.37 values of R_o%) and also with respect to Mt. Malbe.

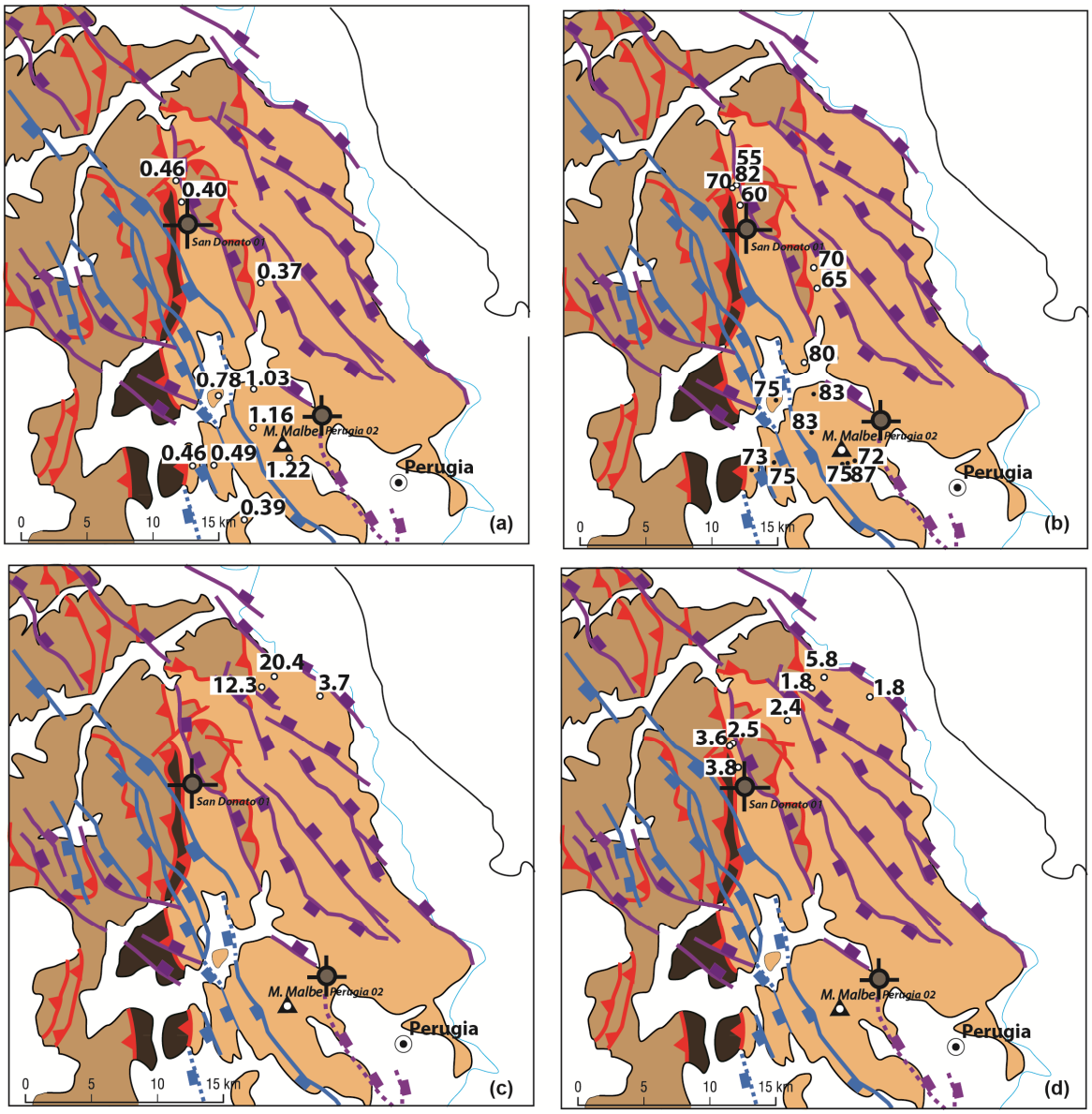

Fig. 3.14 Detail of the area at west of Tiber Valley with: (a) distribution of vitrinite reflectance (b) I% in I-S mixed layers data performed in this study; (c) distribution of (U/Th)/He ages by Thomson *et al.* (2010) and (d) AFT ages published by Zattin *et al.* (2002).

The evidence that Mt. Malbe was never overthrust by the Tuscan Nappe is supported by the strong difference between thermal maturity acquired by Triassic units in both Mt. Malbe cropping out succession and the same units preserved in the S. Donato 01 well along the northern plunge of Mt. Malbe. Here R_o% and T.A.I. values indicate overmature conditions of HC generation, corresponding to anchizone. Nevertheless the extremely high

values, detected in S. Donato 01 well, deserve further investigations, and new analyses are required to confirm existing data. If confirmed, they can be explained considering either very high tectonic load due to the Tuscan unit emplacement, or hot fluid circulation at depth that may have enhanced thermal maturity. We can exclude that this high thermal maturity is the effect of Triassic thermal regime, because if it would have been the case, I should have recorded similar values also in Monte Civitello 01 well and in the outcrops of Mt. Malbe.

Illite % in mixed layers I-S do not show significant changes in thermal maturity of the Marnoso Arenacea Fm. in this sector, probably because of a strong detritical signal that cannot totally disregard in semi-quantitative analysis of <2µm fraction.

. Furthermore data from this sector are always higher than those to the east of the Tiber Valley indicating a higher amount of exhumation. Whereas mineralogical data (R1 stacking order and I% in mixed layers higher than 80%) on the pre-orogenic succession strongly agree with vitrinite reflectance and reset of U-Th/He data.

To test the hypothesis of a contribution of extensional tectonics to exhumation, exhumation rates from all U-Th/He and reset AFT data were calculated using different geothermal gradients.

Data from AFT analyses derive only from the external corridor of the Marnoso Arenacea Fm. outcrops to the east of Mt. Acuto - Mt. Tezio structural high and at footwall of the most advanced klippen of the Tuscan Unit. These data indicate differing thermal conditions. One sample is totally reset with a 3.7 Ma exhumation age; one is partially reset with a 12.3 Ma age, and the last one is not reset and shows ages older than the stratigraphic age of the Marnoso Arenacea Fm (20.4 Ma) (Zattin *et al.*, 2002). For the last two samples (partial and no reset) the Marnoso Arenacea did not reach a burial temperature higher than 120 °C (total annealing temperature of AFT system) (Fig. 3.14c). Thus, for the reconstruction of the exhumation history, the age of 3.7 Ma related to reset sample was used.

The evaluation of the exhumation rate has been performed taking into account heat advection, using as input two values of geothermal gradient (20 °C/Km in Fig. 3.15a and 30 °C/km in Fig. 3.15b). For a geothermal gradient of 20 °C/Km, the exhumation rates range between 0.63 and 0.95 mm/yr, with a mean rate of about 0.8 mm/yr. In contrast, exhumation rates are lower, from 0.45 mm/yr to 0.67 mm/yr, with a mean rate of about 0.56 mm/yr if a geothermal gradient of about 30 °C/km is applied.

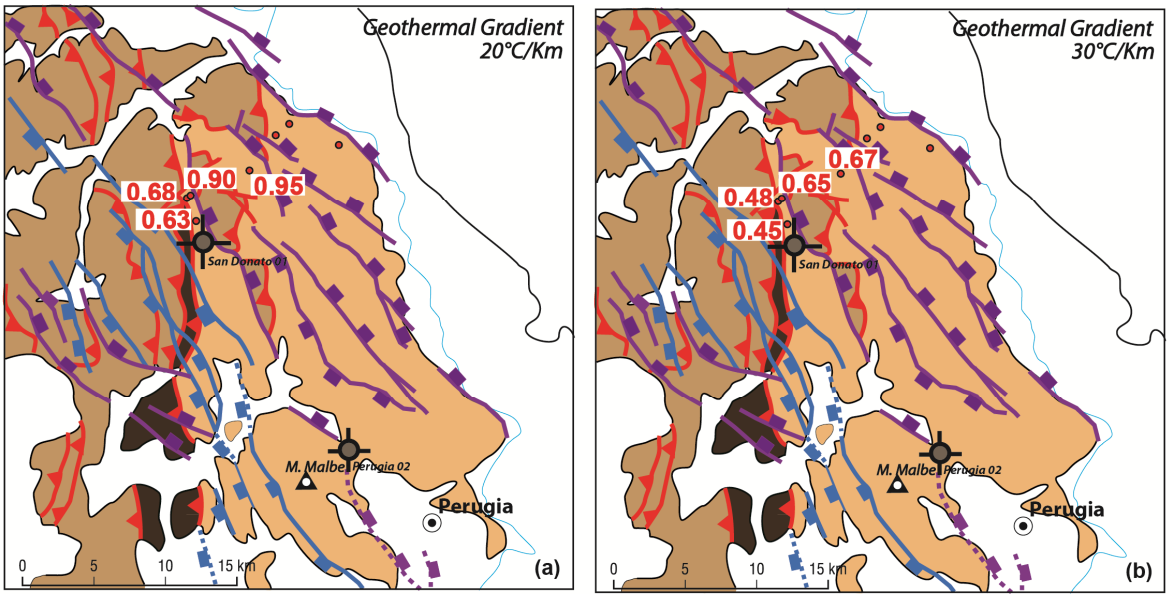

Fig. 3.15 Detail of the area to the west of Tiber Valley with exhumation rates calculated from a geothermal gradient of 20 °C/Km (a) and 30 °C/Km (b). Both tests took into account advection processes.

As the AFTA are commonly not-reset, it is not possible to determine if stepwise or continuous exhumation took place in the last part of the cooling history from 120 °C down to surface temperature (about 10 °C) using both thermochronometers. However considering the only site where both thermochronometers gave reliable results with (U-Th)/He age at 1.85 Ma (Thomson *et al.*, 2010) and AFT age of 3.7 Ma (Zattin *et al.*, 2002) there is no significant change in the exhumation rate in the last 3.7 Ma (Fig. 3.16 a,b).

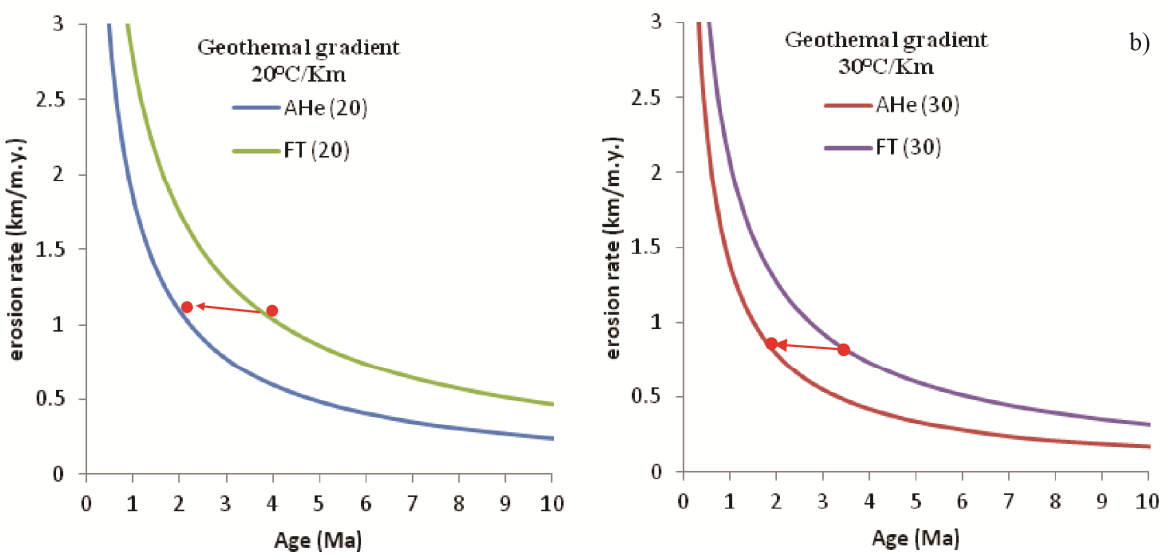

Fig. 3.16 Diagram of erosional rate considering a gradient of 20 °C/Km (a) and 30 °C/Km (b).

3.6.2.2 Area to the east of the Tiber Valley

The sector to the east of the Tiber Valley extends towards the east to the Scheggia-Foligno line. It is mainly separated by the Mt. Semonte - Mt. Foce ridge bounded by the SW dipping Gubbio fault, an antithetic segment of the ATF system. To the SW of the Gubbio fault and to the east of the Tiber Valley a series of thrust sheets with top to the NE sense of transport develop deforming the so-called Gubbio basin and reaching maximum thicknesses of about 1,200 m and Serravallian ages for the top of preserved Marnoso-Arenacea Fm. (Ridolfi *et al.*, 1995). Whereas to the NE of the Gubbio ridge only the lower portion of the Marnoso-Arenacea is preserved (Burdigalian-Langhian in age).

A synthetic map with data has been reported in Fig. 3.17.

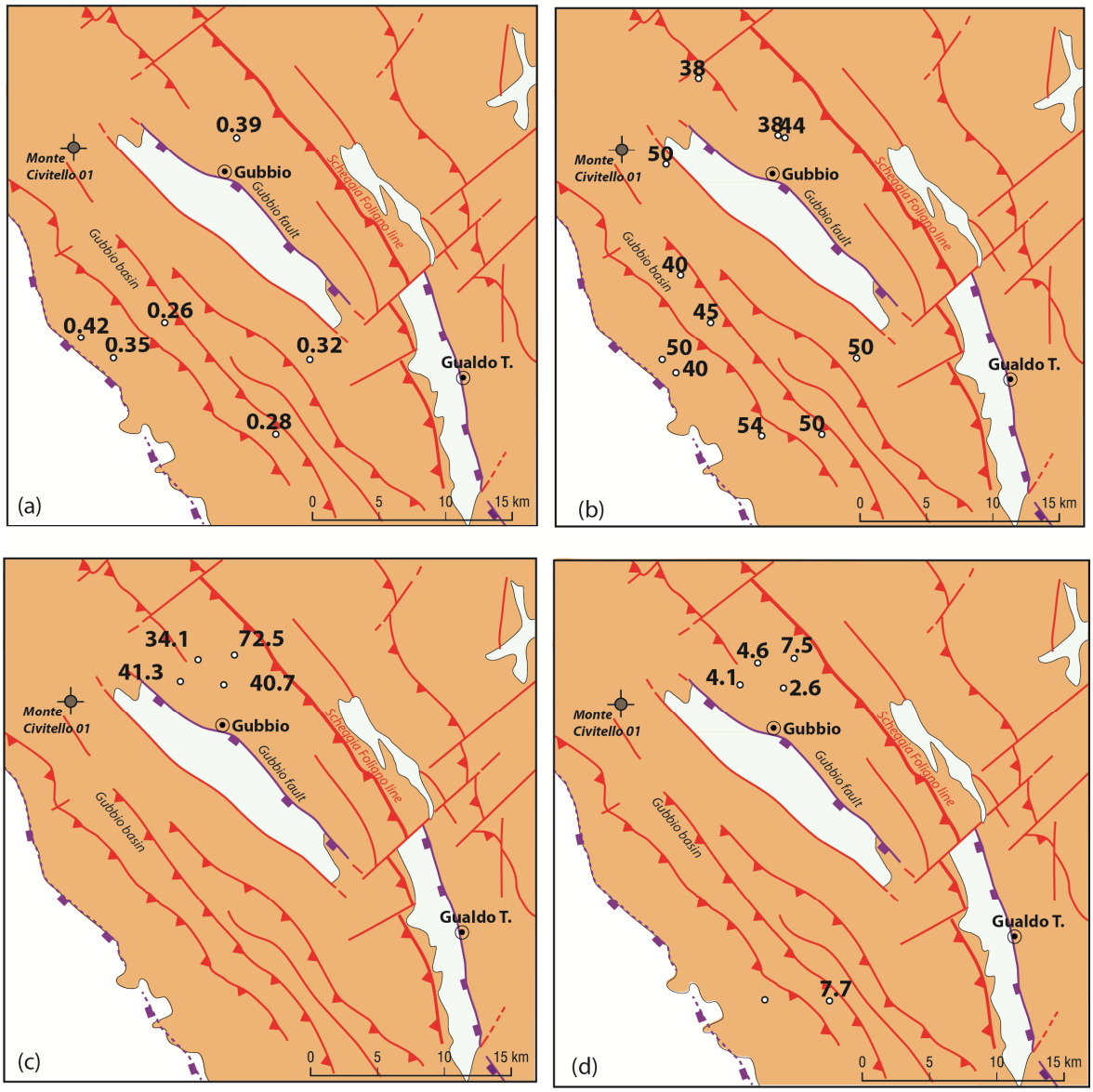

Fig. 3.17 Detail of the area to the east of Tiber Valley with: (a) distribution of vitrinite reflectance; (b) I% in I-S mixed layers data performed in this study; (c) distribution of (U/Th)/He ages by Thomson et al. (2010) and (d) AFT ages already published by Zattin *et al.* (2002).

In the Gubbio basin, only the Marnoso Arenacea Fm. crops out and (U-Th)/He data indicate no-reset or partial reset. These data are consistent with R_o% data which show very low thermal maturity with values between 0.25 and 0.40 and I% in mixed layers I-S between 40 and 50%, from younger to older stratigraphic levels indicating that the youngest portion of the Marnoso Arenacea Fm. never experienced maximum burial temperatures higher than 70 °C. Furthermore in the Gubbio basin, at the latitude of the north-western tip of the Gubbio fault, the Monte Civitello 01 well is located.

The high quality of the dataset of R_o% and T.A.I. values (Fig. 3.11) and their coherence with surface data coupled with the information obtained by plotting Ro% against mineralogical data on Hillier *et al.*'s diagram (1995, Fig. 3.13) allowed me to constrain thermal modelling for Monte Civitello 01 well. The models have been carried out using BASIN MOD-1D software (1996). The main assumption for the modelling are: (i) correction for decompaction of burial curves according to Sclater and Christie's method (1980); (ii) sea level changes, have been neglected, as the thermal evolution is influenced more by sediment thickness than water depth (Butler, 1992); (iii) thickness, lithology and age of sediments are derived from literature (Ricci Lucchi and Pialli 1973; Ridolfi *et al*, 1995). The exhumation rate is considered constant and burial curves have been calibrated against Ro% and T.A.I. values.

Different models were performed using both geothermal gradient and heat flow as an input. The first test has been performed considering the present-day total thickness of the succession (from the Marnoso Arenacea Fm. to the Anidriti di Burano Fm.) and a gradient of about 23 °C/Km. The diagram of thermal maturity versus depth has been reported in Fig. 3.18a. It is evident that this input did not match the regression line of thermal maturity data. In the second test the thickness of the succession was increased, adding the missing (e.g. eroded) portion of the Marnoso Arenacea Fm. (about 1,200 m thick). Also in this case a good fit of the data has not been obtained (Fig. 3.18b). The difficulty to fit together the upper portion of succession with the lower portion led me to separate the succession and perform two distinct models to fit the synorogenic and both the pre-orogenic sections. For the upper part (Fig. 3.18c) the modelling shows a good fit of data assuming as input the total thickness of the succession (including the missing portion of the Marnoso Arenacea Fm.) and a higher gradient of 25 °C/Km. In contrast, for the lower portion (Fig 3.18d) the best fit of data is obtained with the total thickness (Preserved succession+Missing Marnoso Arenacea Fm. section) and a higher geothermal gradient (35 °C/Km).

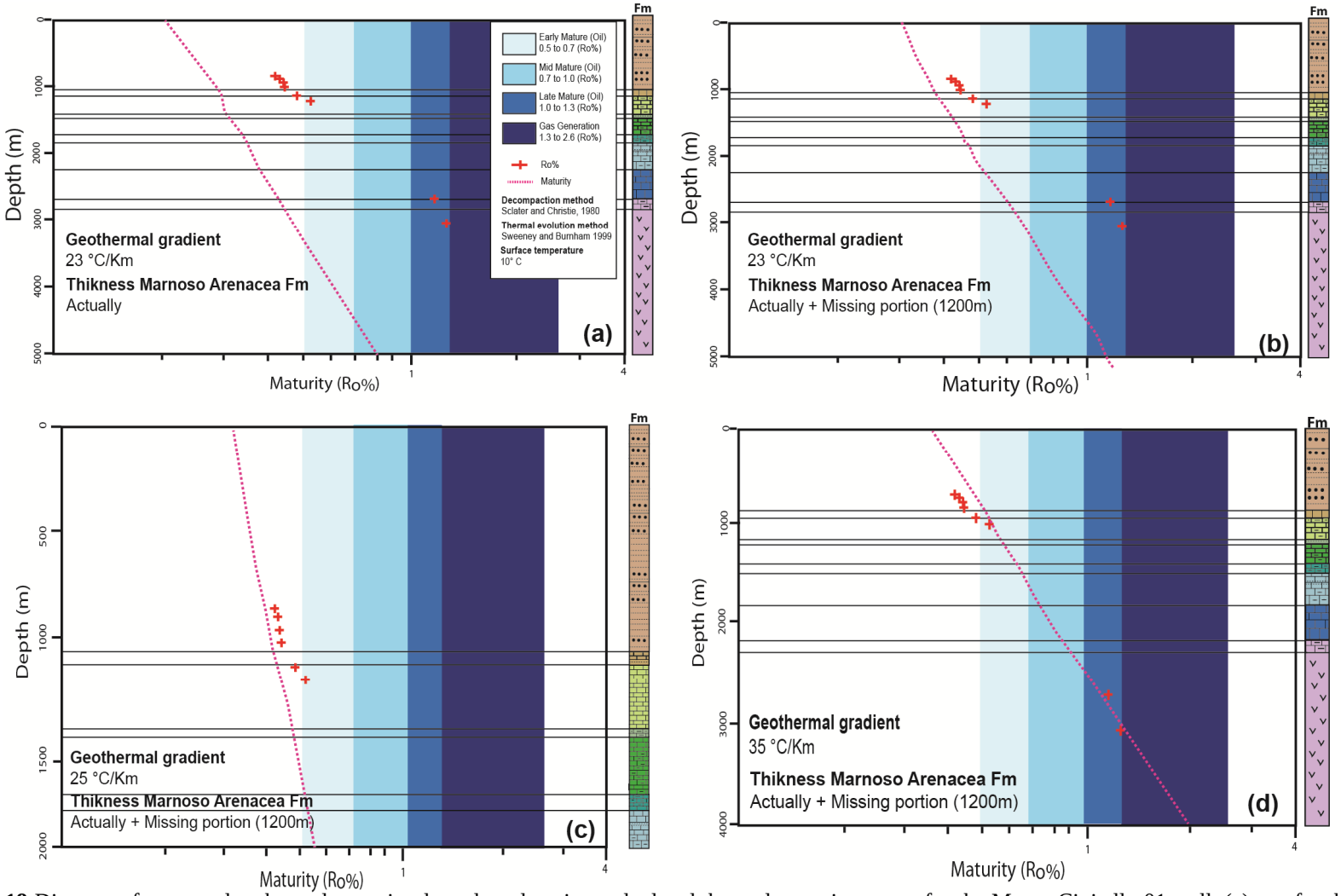

Fig. 3.18 Diagram of present-day thermal maturity data plotted against calculated thermal maturity curve, for the Monte Civitello 01 well. (a) test for the entire well length considering a geothermal gradient of 23 °C/Km and the preserved present-day thickness of Marnoso Arenacea Fm.; (b) test for the entire well length considering a geothermal gradient of 23 °C/Km and the preserved present-day thickness of Marnoso Arenacea Fm. with addition of an eroded portion; (c) test for the upper part of well considering a geothermal gradient of 25 °C/Km and the preserved present-day thickness of Marnoso Arenacea Fm.; with addition of an eroded portion; (d) test for the lower part of the well considering a geothermal gradient of 35 °C/Km and the preserved present-day thickness of Marnoso Arenacea Fm.with addition of an eroded portion.

To merge these tests into a fully calibrated model, it has been necessary to adopt a variable heat flow distribution through time. In detail the best fit was achieved using 100 mW/m^2 at 228 Ma gradually decreasing to 40 mW/m^2 at 11 Ma (Fig. 3.19).

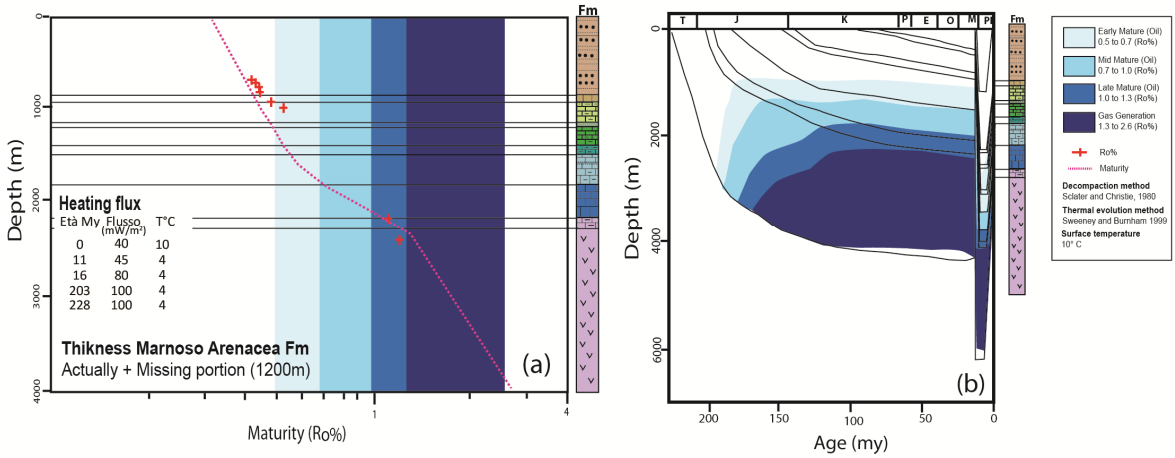

Fig. 3.19 (a) Diagram of present-day thermal maturity data plotted against calculated thermal maturity curve, for the Monte Civitello 01 well. (b) Representative one-dimensional burial and thermal modelling that fits thermal maturity data.

The thickness of the succession adding a missing portion of the Marnoso Arenacea Fm. has been considered. Thermal maturity versus depth diagram suggests a quite good fit of data. The burial history diagram shows that the basal part of the succession (Anidriti di Burano Fm.) reached a depth of 6.5 km and maximum burial temperatures of about 200 °C, entering the gas generation stage. Thermal maturity decreases toward the top of the succession. The Rhaetavicola contorta and the Calcare Massiccio Fms. reached the late thermal maturity zone of hydrocarbon generation, whereas the remaining part of the Jurassic succession reached mid-mature conditions at depths of 3.5 km and temperatures ranging between 120-140 °C. The early mature stage was reached by the Maiolica Fm. whereas younger deposits remained in the immature stage of hydrocarbon generation (i.e. Marnoso Arenacea Fm.). The exhumation started at about 5 Ma with a simplified constant erosion rate of about 0.5 mm/yr. Thus thermal maturity profile of Monte Civitello 01 agrees with a burial history of the Gubbio basin where present day geothermal gradient is about 25 °C (Zattin *et al.*, 2002) and a higher thermal regime during the pre-orogenic evolution of the succession. Here thermal maturity was acquired by sedimentary burial alone with erosion of the uppermost portion (about 1,2 km) of the Marnoso Arenacea Fm. in general agreement with surface data available in the Gubbio basin further to the south (west of Guado Tadino town). In the sector, to the east of the Gubbio fault, the Marnoso

Arenacea Fm. shows Ro% and I% in I-S values typical of the immature stage of hydrocarbon generation.

Concerning termocronological data to the east of Gubbio ridge, the AFT data are not reset and U-Th/He are totally reset with reliable ages of about 4.35 Ma (Fig. 3.17).

The evaluation of the exhumation rate has been performed, also in this case, using as input two geothermal gradient values (20 °C/Km in Fig. 3.20a; 30 °C/km in Fig. 3.20b) and considering the advection process. For a geothermal gradient of 20 °C/Km, the exhumation rates range between 0.58 and 0.53 mm/yr, with a mean rate of about 0.55 mm/yr (Fig. 3.20a). In contrast, exhumation rates are lower, from 0.53 mm/yr to 0.37 mm/yr, with a mean rate of about 0.45 mm/yr if a geothermal gradient of about 30 °C/km is applied (Fig. 3.20b).

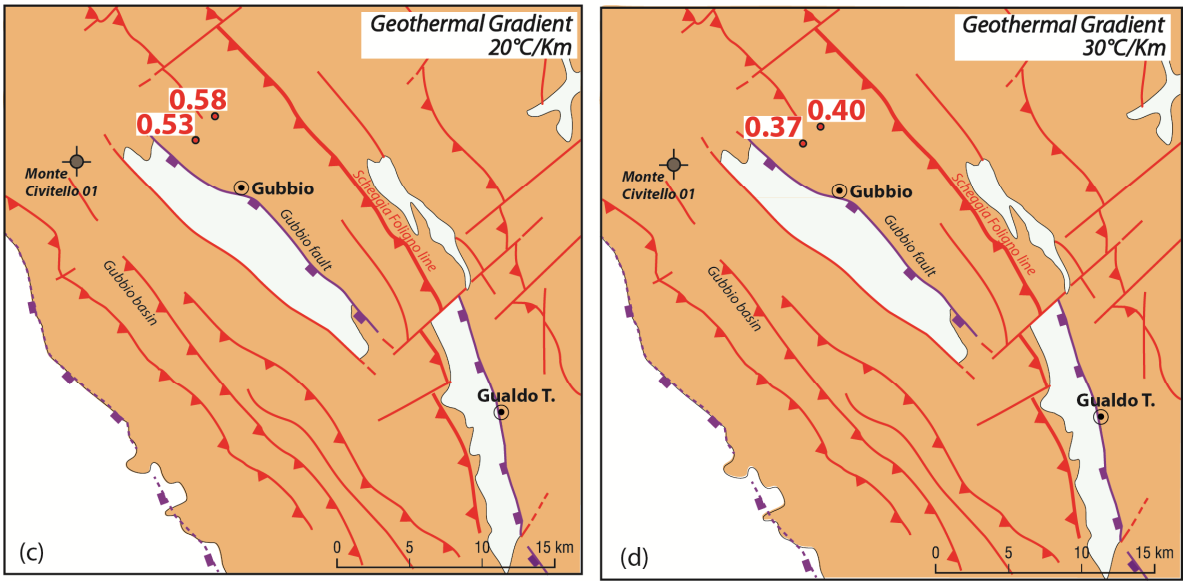

Fig. 3.20 Detail of the area to the east of the Tiber Valley with exhumation rates considering a gradient of 20 °C/Km (a) and 30 °C/Km (b).

3.6.2.3 Evolution of extensional tectonics and exhumation

In Fig. 3.21a the section from Mt. Acuto area to the east of the Gubbio ridge has been reported with the age and rates of the exhumation. It is evident that the internal sector (Massicci Perugini) has undergone a rapid and younger exhumation (3 Ma and 0.8 mm/yr) than that recorded in the external one (respectively 4.3 Ma and 0.5 mm/yr).

This trend is in contrast with what has been generally stated for external sedimentary portions of fold-and-thrust belts, where the exhumation age decreases toward the foreland (i.e., Thomson *et al*., 2010, Zattin *et al*. 2002 and Fig. 3.21b).

The exhumation rate of 0.8 mm/yr, in the western sector, can be considered as a threshold value between tectonically induced exhumation (>1.5 mm/yr) and exhumation rate of 0.1 mm/yr that indicates that erosion balances the rock uplift and the mean topography surfaces. Therefore, in this sector the contribution of local tectonics (normal faulting) to the exhumation processes is highly probable. A similar hypothesis has been proposed by Balestrieri *et al*. (2003) for the Mt. Falterona area with respect to the main normal faults acting in that area.

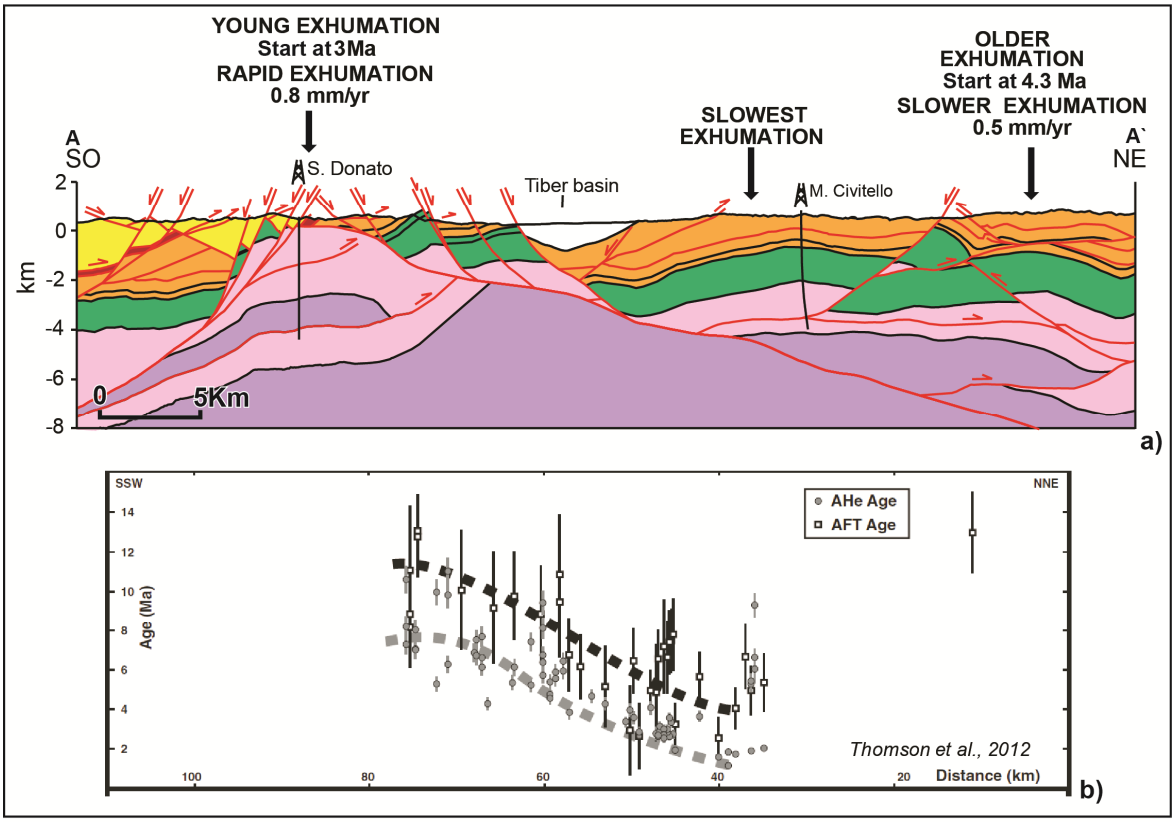

Fig. 3.21 a) Distribution of age and rate of exhumation from the Massicci Perugini area (Mt. Acuto) to east of the Gubbio fault; b) Apatite fission-track (AFT) ages and AHe ages distribution along the profile in the Northern Apennine chain (Mt. Cimone) (from Thomson *et al*., 2010).

The model proposed in this thesis suggests that to the west of the Tiber Valley, most of exhumation at shallower crustal levels is mainly due to the most recent extensional tectonics of the ATF system and not only to older compression and erosion.

This interpretation takes into account the anomalous bulge of upper Triassic units in the area of Mt. Malbe that is more uplifted if compared to the mean elevation of the same units in the surrounding thrust structures preserved in the subsurface (see for a review Barchi *et al*., 2010). Furthermore, it resembles -at a shallower structural level- what is envisaged in the exhumation ages distribution for the entire structure of the Northern

Apennines at the regional scale where at the rear of the sedimentary fold-and-thrust belt the uplift mid-crustal structure of the Alpi Apuane crops out.

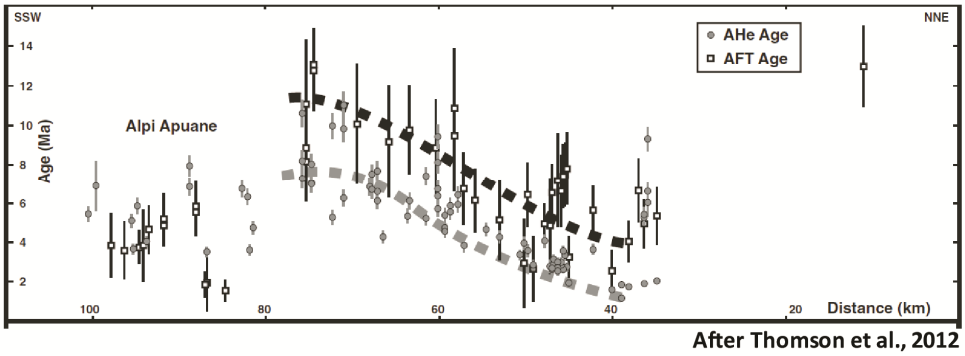

Fig. 3.22 Figure showing apatite fission-track (AFT) ages and AHe ages in the profile Alpi Apuane-Monte Cimone (from Thomson *et al*., 2010).

Thus the tectonic exhumation in the Mt. Malbe area can be achieved according to the following evolutionary stages:

1. the low angle Lisciano fault started acting at about 3 Myr ago and produced enough and enough quick extension to generate a strong isostatic instability. This quick and effective activity produced uplift and folding of the Lisciano fault itself. This folding inhibited the further activity of the Lisciano fault and extension migrated towards the foreland along the ATF system.
2. the strong isostatic instability caused by extension brought also to the activation of the W-dipping Corciano fault that separated and dissected the Lisciano from the Alto Tiberina fault systems. In this hypothesis the Corciano fault is not part of the antithetic faults of the Val di Chiana system (cfr. Mirabella *et al*., 2011) but can be interpreted as a kinematic adjustment of the rapid and effective extension accumulated along the long-lived Lisciano-ATF system.
3. At present extension acts mainly on the ATF system and its main antithetic faults (Gubbio fault) but I cannot exclude that the role played by the Corciano fault is totally over (e.g., possible reactivation of the Corciano fault as a result of localized strong crustal thinning in Corciano-Mt. Malbe –Perugia area).

In this framework I suggest that the Corciano fault may have adjusted isostatic instability in brittle regime that in analogous systems involving mid-crustal levels and on larger structures (core-complexes) is adjusted just by folding of the low angle extensional detachments. Nevertheless this last statement that is already strongly

supported by geometric, kinematic paleothermal and thermochronological studies, still needs to be numerically modelled to be fully validated from a dynamic point of view.

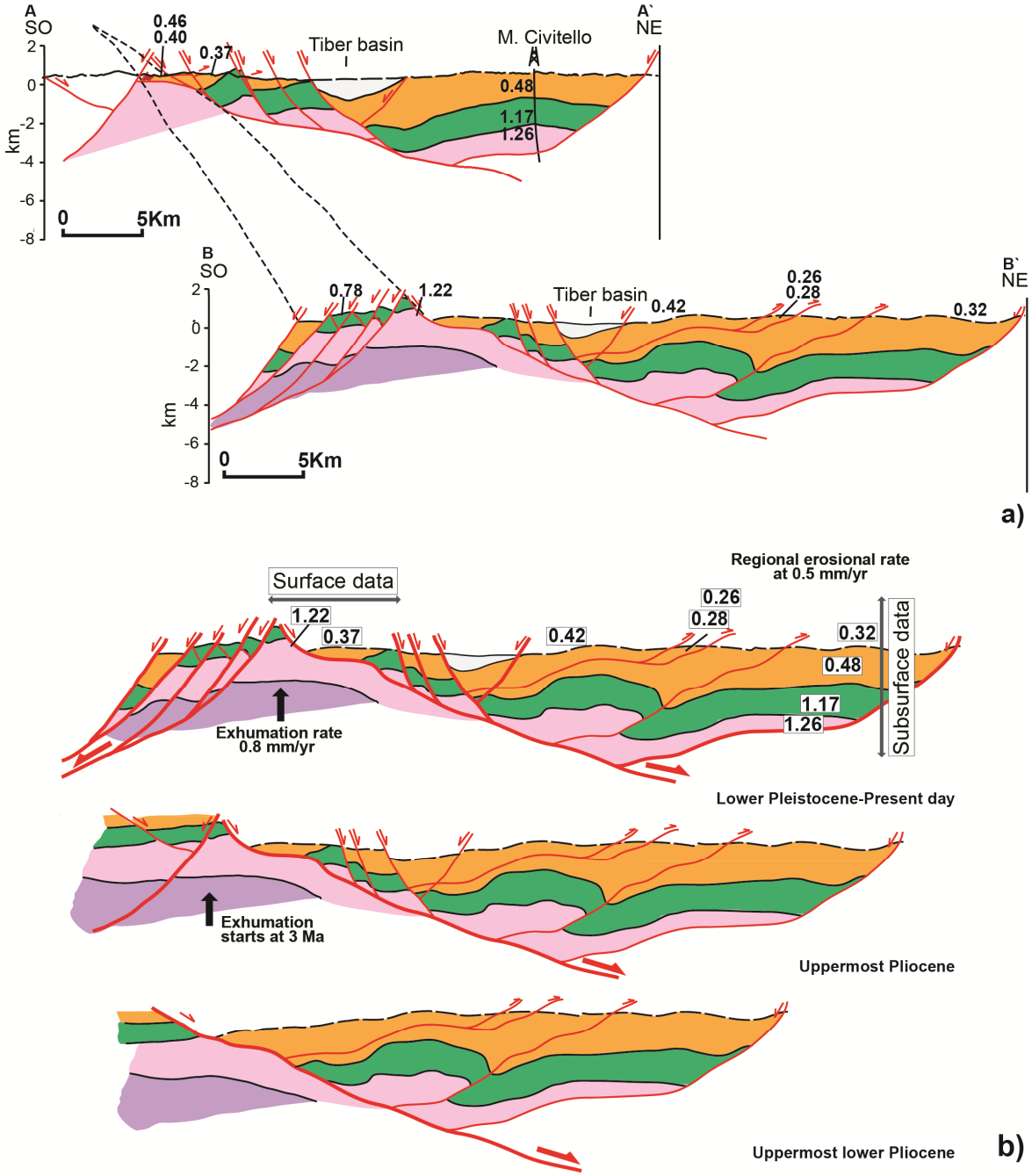

Fig. 3.23 a) Distribution of reflectance vitrinite data in section AA'(Mt. Acuto-Gubbio fault) BB' (Mt. Malbe-Gubbio fault) (traces in Fig. 3.1); b) evolutionary stages of tectonic exhumation in the Mt. Malbe area and distribution of maturity data (reflectance vitrinite) in section BB'.

3.7 Conclusion

In summary, the paleothermal and thermocronological data provide low temperature and time constraints on the late orogenic cooling and exhumation history of the ATF and Gubbio area.

The portion to the west of the Tiber Valley has been exhuming at least since 3 Ma, as indicated by AFT and (U-Th)/He ages. The exhumation rate is constant and of either about 0.80 mm/yr or about 0.56 mm/yr assuming respectively geothermal gradients of 20°C/Km and 30°C/Km. Moving from hinterland (west of Tiber Valley) toward the foreland (Gubbio basin and Gubbio ridge) the exhumation is characterized by older ages (4.3 Ma) and lower rates 0.55 mm/yr down to 0.45 mm/yr assuming geothermal gradients of 20 °C/Km and 30 °C/Km, respectively. Therefore, a reduction of the exhumation age has been recorded in this sector of the chain, moving from the external sector to the internal one, in contrast with has been generally observed in the external sedimentary portions of fold-and-thrust belts (i.e., Thomson *et al*., 2010, Zattin *et al*. 2002).

This different trend can be attributed to the contribution of the normal fault activity of the Altotiberina system to local exhumation. This hypothesis is supported by the evidence that the exhumation rate of 0.8 mm/yr in the western sector is closer to exhumation rates generally observed where tectonics enhance exhumation rather than those associated to erosion. Moreover, this interpretation takes into consideration that the area of Mt. Malbe is characterized by a strong exhumation of the upper Triassic unit if compared to the mean elevation of the same units in the subsurface. This arrangement is a result of the evolution that started at about 3 Ma with the Lisciano fault (LMF). Extension has generated isostatic instability that stopped the activity of LMF and caused the activation of the W-dipping Corciano fault that separated and dissected the Lisciano from the Altotiberina fault systems, with a migration of the extension towards the foreland.

Chapter 4

The Corsica-Sardinia rotation in the Northern Apennines: new paleomagnetic evidences

4.1 Introduction

The peculiar tectonic feature of the Mediterranean region is given by the coexistence of curved mountain belts and back-arc basins, which developed synchronously, in a plate-tectonics scenario dominated by the Africa-Eurasia convergence (Fig. 4.1). Such arcs and related back-arc basins formed as a consequence of trench rollback of dense and narrow slabs, resulting from the progressive fragmentation of the subducting African plate during Neogene and Quaternary (Malinverno and Ryan, 1986; Lonergan and White, 1997; Royden, 1993; Faccenna *et al*., 2004; Mattei *et al*., 2007). In the Central Mediterranean roll-back of the Ionian-Adriatic lithosphere, continuously subducted toward northwest underneath the Eurasia plate, caused the progressive closure of the intervening Mesozoic oceanic basins of Tethyan domain and the formation of the Apennines - Maghrebide orogenic belt and Ligure-Provençal and Tyrrhenian basin extensional back-arc basins (Faccenna *et al*., 2004 and references therein).

A large amount of paleomagnetic data from the Mediterranean region has proved that in most of the cases the curved shape of the orogens was acquired by means of opposite rotations along the two arms of the arcs and that the opening of back-arc basins was related to drifting of rigid blocks around an Eulerian rotation pole (among others, Kissel and Laj, 1988; Lonergan and White, 1997; Mattei *et al*., 2006, Cifelli *et al*. 2007, 2008). In this general context the Central Mediterranean represents a key area to understand these two

processes and both the Corsica-Sardinia and the Northern Apennines have been the place of a large number of paleomagnetic studies that investigated the amount and timing of CCW rotation of the Corsica-Sardinia block and the origin of the Northern Apennines curvature (see Gattacceca *et al*. 2007 and Cifelli and Mattei, 2010 for recent reviews on these subjects).

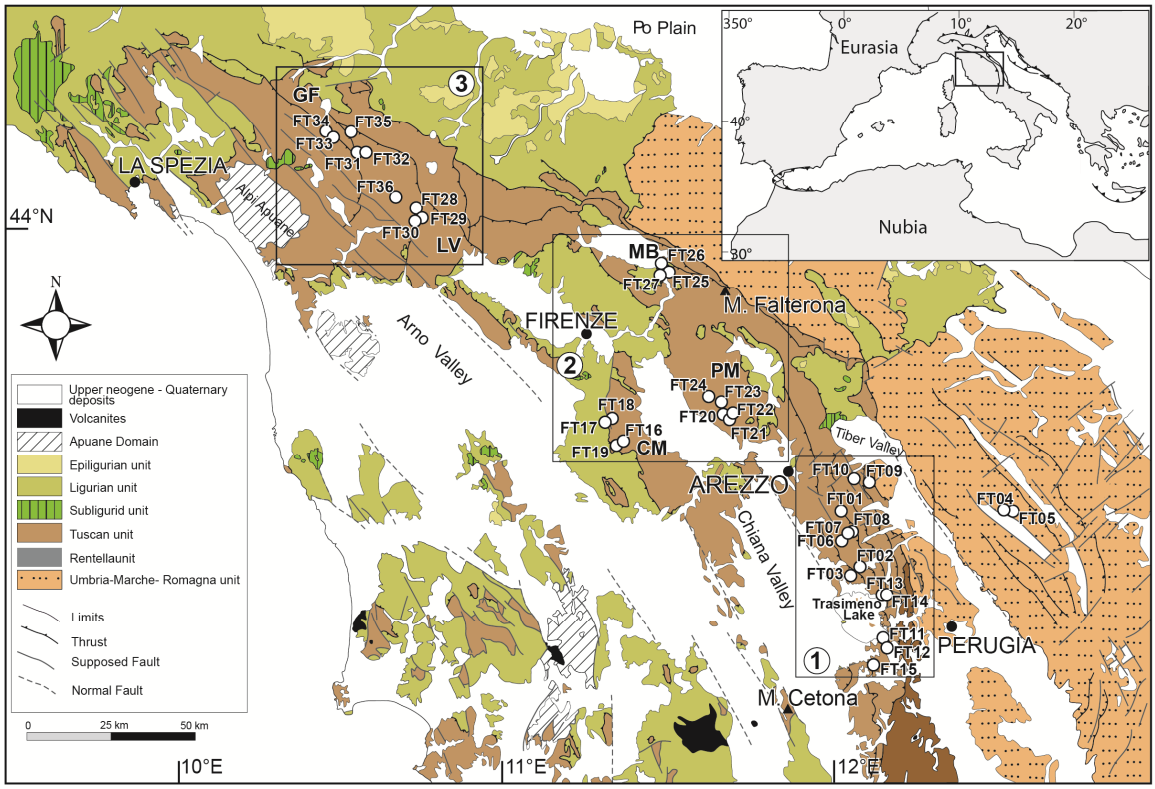

Fig. 4.1 Schematic map of the Northern Apennines and location of sampling sites. Areas in insets the Trasimeno Lake area (1), Chianti Mountains and Pratomagno (PM) area (2), and the Val di Lima (LV) and the Garfagnana (GF) area (3). MB = Mugello Basin. Inset, Schematic tectonic map of the Central Mediterranean

Vertical axis rotations in Central Mediterranean during the Neogene have been described as the result of two distinct events, which occurred in the area during different time as a consequence of the progressive eastward retreat of the subducting Ionian-Adriatic lithosphere. The first episode has been established by a large number of paleomagnetic data from Corsica and Sardinia, occurred during the Oligocene-Lower Miocene and was responsible of the opening of the Ligure-Provençal back-arc basin and the CCW rotation of the Corsica-Sardinia block. The second episode happened after the Upper Miocene and was responsible of the curvature of the Northern Apennine arc. This event has been described in the external portion of the Northern Apennines fold and thrust belt, where vertical axis rotations accompanied thrust activity (Speranza *et al.*, 1997).

Notwithstanding we knowledge about vertical axis rotations associated to these main tectonic episodes is very detailed, some important issues are still open and have not been faced in detail during the very long history of paleomagnetic research in Central Mediterranean. As an example we know precisely the amount and timing of the CCW rotation of the Corsica-Sardinia block, but we don't have any constrain on their geographic extension to the east, even if it has been suggested that the Tertiary Piedmont Basin (Maffione *et al*., 2008), and some external units of the Northern Apennines belt (Muttoni *et al*., 2000) were also involved in the CCW rotation of the Corsica-Sardinia block. This uncertainty is mostly due to the fact that most of the paleomagnetic data from the Northern Apennines come from the external portion of the chain, which was involved in the Apennine orogen after the ending of the Corsica-Sardinia CCW rotations. Conversely, only few data were collected in the internal sector of the chain, which experienced and recorded a continuous deformation history since the beginning of convergence in the Late Cretaceous, and which were already incorporated in the orogenic wedge during the Corsica-Sardinia rotation.

In order to provide new data for the internal sector of the curved belt and to investigate the possible spread of the Corsica-Sardinia CCW rotation in the Northern Apennines, an extensive paleomagnetic sampling was carried out in the Tuscan Nappe succession. Results show that Tuscan units underwent a larger amount of CCW rotations in the southern part of the arc than in the northern one. This rotation pattern contrasts with that measured in the external units of Northern Apennines and is not compatible with a simple oroclinal-bending model. On this base we propose that the Tuscan Nappe units were involved in the Corsica-Sardinia drifting and rotated CCW during the Lower Miocene, other than to participate in the vertical axis rotations which accompanied the main phases of emplacement and translation of the Apennine units that concurred to the final curved shape of the chain.

4.2. Geological setting

The Northern Apennines consists of several paleogeographic domains, organized in a fold and thrust belt forming a broad curved structure with an eastward (Adriatic) vergence (Fig. 4.1). The curvature of the arc follows the Adriatic margin of the belt, with the orientation of the main structures ranging from NW-SE/WNW-ESE in the north to almost N-S in the south. Several second-order arcs developed besides the principal arc, in response to heterogeneities in the stratigraphic sequences and out-of-sequence nappe

stacking (Baldacc*i et al.*, 1967; Elter, 1975; Boccaletti *et al.*, 1980; Principi and Treves, 1984; Barchi *et al.* 1998a, b; Costa *et al.*, 1998). The uppermost nappes of the Northern Apennines are represented by oceanic (Ligurian) and transitional (sub-Ligurian) domain units, characterized by the occurrence of Jurassic ophiolites and their Jurassic-early Cretaceous sedimentary cover, overlain by Cretaceous-Oligocene flysch sequences. The Ligurian domain units overthrust eastward the Tuscan domain units, formed by Upper Triassic to Eocene marine carbonates and by Oligocene-Lower Miocene foredeep sequences, which are deformed in an array of thrust sheets and ultimately thrust over the Umbria-Marche-Romagna units. The latter consists of sedimentary sequences deposited on a continental margin with basal late Triassic evaporites, platform carbonates (Lias) and pelagic sequences (Jurassic-Eocene) enriched upward in terrigenous deposits (Paleogene) and flysch sequences (Miocene) (Fig. 4.2).

The tectonic evolution of the Northern Apennines is characterized by the progressive migration of the orogenic front toward the Adriatic foreland, which is marked by the onset of siliciclastic deposits which get progressively younger toward the Adriatic foreland. The onset of siliciclastic deposition occurred in Northern Apennines during late Cretaceous in the oceanic Ligurian domain. The Ligurian oceanic domain was deformed during late Cretaceous to early Eocene time, and formed a double vergent accretionary wedge, now outcropping from Corsica to Italian peninsula (Treves 1984; Carmignani *et al.* 1994). Starting from the Oligocene onwards, foredeep basins migrated eastward and formed on the top of sedimentary sequences, belonging to the continental passive margin of Apulia. Their incorporation into the Apennines orogenic wedge marked the subduction of Adriatic continental lithosphere underneath Europe. Afterwards, during the Neogene, foredeep basins further migrated toward the Apulia foreland in front of the migrating thrust nappes. In Northern Apennines such process is well documented by stratigraphic and seismic studies, which precisely constrain the Neogene evolution of the foredeep basins in the front of the Apennines chain (e.g., Patacca *et al.* 1992). Foredeep basins formed on top of progressively easternmost (external) units, up to the Adriatic foreland. The formation and evolution of foredeep basins were driven by the loading of the adjacent thrust belt and related to subduction processes, such as the flexural retreat of the subducting lithosphere (Royden *et al.* 1987). This process was particularly severe during Plio-Pleistocene times as evidenced by the presence, in the external part of the Apennines chain, of a foredeep-basin system, which contains up to 8 km of Pliocene-Quaternary sedimentary rocks (Royden *et al.* 1987).

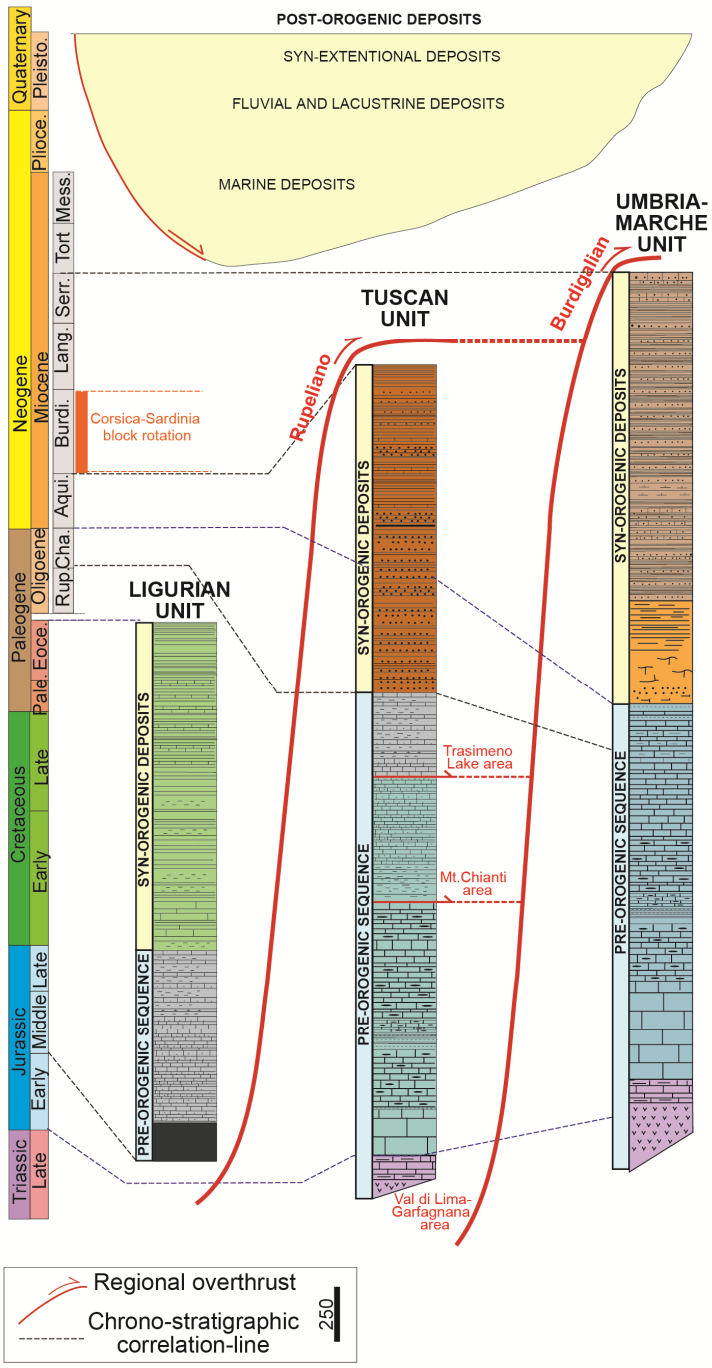

Fig. 4.2 Schematic stratigraphic sections and geometrical relationships of the different units of Northern Apennines

Extensional tectonics on the Northern Tyrrhenian sector was coeval with thrust emplacement in the external Umbria-Marche-Romagna chain, with both extensional and compressional fronts migrating toward the Adriatic foreland from middle Miocene up to Pleistocene (e.g., Elter *et al.* 1975). Extensional tectonics dissected the already formed Apennines chain and generated new NW-SE trending extensional basins filled by 'neoautochthonous' marine and continental sequences (Jolivet *et al.* 1998; Collettini *et al.*

2006 and references therein). Moreover, crustal thinning, high heat flow and upraise of magmatic bodies accompanied extensional tectonics along the Tyrrhenian margin. Today, active tectonics is represented by NW-SE normal faults, with a well documented historical and recent seismicity, mostly located in the internal sector of the Umbria-Marche-Romagna region, at the edges of intramontane basins (among others, Chiaraluce *et al.* 2004).

4.3 Paleomagnetic sampling and geological setting of the study areas

In this study, paleomagnetic sampling was carried out in the Tuscan Domain, in the internal sector of Northern Apennines. In particular, three main areas have been investigated: (1) the area around the Trasimeno Lake, (2) Chianti Mountains and Pratomagno area, and (3) the Val di Lima and Garfagnana area (Fig. 4.1). Thirty-six sites were sampled (528 oriented cylindrical samples). Samples were drilled using an ASC 280E petrol-powered portable drill with a water-cooled diamond bit. The cores were oriented in situ with a magnetic compass, corrected to account for a local ~2° magnetic declination according to the NOAA National Geophysical data center.

4.3.1 Trasimeno Lake area

This area is characterized by the presence of four major tectonic units, piled up during the Miocene that are from west (top) to east (bottom): the Ligurian units, consisting of Jurassic ophiolites; the Tuscan Nappe, an east-verging imbricate thrust-stack made up of pelagites and siliciclastic turbidites (Mirabella *et al*., 2011); a transitional unit (Mt. Rentella Unit) including polychromic marls of Mt. Rentella (Brozzetti *et al.,* 2000) and Aquitanian-Burdigalian foredeep siliciclastic turbidites of the Montagnaccia Fm. (Barsella *et al.,* 2009); and the Umbria unit, characterized by a Meso-Cenozoic carbonates succession followed by the foredeep turbidite succession of the Marnoso Arenacea Fm. (Early-Middle Miocene) (Mirabella *et al*., 2011). Some authors (e.g., Abbate and Bruni, 1989; Brozzetti, 2007) have suggested that the outermost part of the Tuscan Nappe belongs to a separate tectonic unit (Falterona-Cervarola Unit or Falterona Nappe). In this study, the Falterona-Cervarola Unit is considered as belonging to the Tuscan Nappe, according to Plesi *et al.* (2002).

In this area, the Tuscan Nappe succession has been sampled. Six sites (FT03, FT11-FT15) were sampled in the pelagic foreland ramp deposits of the Scaglia Toscana Fm.,

consisting of calcareous-marly turbidites and varicoloured shales and marly-shale layers (Ypresian-Lutetian). Seven sites (FT01, FT02, FT06-FT10) were sampled in the foredeep turbidite deposits of the Macigno Fm, which consists of thick coarse-grained siliciclastic turbidites alternating with siliciclastic thin and fine grained beds (Aquitanian) (Fig. 4.1).

Among the Scaglia Toscana Fm. sites two continues and well exposed section have been sampled (FT03 and FT15 sites). The first section is located in the Montanare Cave northern of Trasimeno Lake (site FT03 in Fig. 4.1). The section consists of alternating calcareous marls and marly-shales layers for a total thickness of about 70 m. The lithofacies is characterized by limestone nut-brown strata, generally 5–40 cm thick with grey chert in nodules and lens. The varicoloured marly-shale interstrata have a smaller thickness in the order of millimeters or centimeters. The samples have been collected in calcareous strata, in which a total of 44 samples were drilled considering a variable spacing ranging from 60 to 300 cm.

The second section is exposed at the NW of Mt. Solare in the Casilini Cave at south of Trasimeno Lake (site FT15 in Fig. 4.1). The section has a total thickness of about 50 m and it is mainly made up of an alternating calcareous and shale, marly-shales layers. The calcareous strata are mainly thin-bedded grey-red limestone (strata are normally 10–40 cm thick) with in some cases nodules and lens of chert, convolute lamina and bioturbations (at the top of the strata). These strata are interbedded with thin varicoloured shale and marly-shale layers (strata are normally 2–16 cm thick). A total of 53 samples are drilled from calcareous strata, with an average sampling spacing ranging from 60 to 120 cm.

4.3.2 Chianti Mountains and Pratomagno area

The structure of the Chianti Mountains has been interpreted as a result of thrust-and-fold deformation (Bonini, 1999) and it is characterized by the Tuscan Nappe succession, which in this area is largely exposed (from Upper Cretaceous to Lower Eocene members). The main structural feature of this region is an E-NE vergent steeply to moderately dipping, overturned anticline, which folds the Macigno sandstone and exposes Scaglia Toscana Fm. at its core (Bonini *et al*., 2012). Referring to Sagri *et al*., (2012), the Tuscan Nappe in this sector is thrust onto the more external Cervarola-Falterona unit. Falterona succession, cropping-out in the Pratomagno ridge, consists of Rupelian-Chattian varicoloured clays alternating mudstone layers (Villore Marls) at the bottom following by the Chattian-Burdigalian Falterona Fm.. This silicoclastic turbidites deposits have been subdivided into five member, on the base of thickness of the layers and arenites/pelites

ratio (Bortolotti *et al*., 2012). The succession ends with the Vicchio Marls Fm. that crops out mainly in the Mugello Basin area. This formation consist of gray marls and silty marls, interbedded by thin sandstone layers with calcareous component

In this area four sites (FT16-FT19) were sampled in the pelagic and ramp deposits of the Scaglia Toscana Fm., whereas 5 sites (FT20-FT24) were sampled in the foredeep turbidite deposits of the Falterona Fm., whereas 3 sites were taken from the Burdigalian thrust top deposit of the Marne di Vicchio Fm. (FT25-FT27) (Fig. 4.1).

4.3.3 Val di Lima and Garfagnana area

The main structural feature of Val di Lima area is a very large east-verging recumbent fold, with the hinge located in the Montale–Lucchio alignment (Fazzuoli *et al*., 1994; 1998). The second relevant characteristic of this area is represented by the several tectonic contacts between the Macigno Fm. and the Scaglia Toscana and Maiolica Fms. related to activity of low-angle thrust faults that cut these formations (Fazzuoli *et al*., 1998). Moreover this area is affected by large NW-SE and E-W normal fault that intersect the recumbent fold and create a tectonic boundary between the Mesozoic deposits and the Oligocene turbidite deposits (Macigno Fm.) (Fazzuoli *et al*., 1998). The stratigrafic succession with thick Jurassic formation, testify a subsident paleogeographic domain since Middle Jurassic until Oligocene time (Cerina Feroni and Patacca, 1975; Fazzuoli, 1980). In Val di Lima and Garfagnana areas the Jurassic-Cretaceous *condensed* and *reduced sequences* crop out, such as consequent of a non-uniform physiography. The consequent effect is a discordant deposition of Scaglia Toscana Fm. on top of Rosso Ammonitico Fm.. The upper part of Scaglia Toscana Fm. is interpreted as deposited in base-escarpment environment of an active margin. In this formation three lithofacies has been distinguished, the lithofacies sampled is *Argilliti dell'Orecchiella*, consisting of red, gray-green clays interbedded with centimeter calcareous strata. This lithofacies can be referred to Cenomanian-Rupelian time (Fazzuoli *et al*.,1998). This area is characterized by compressive deformation, starting from Eocene Time and culminating during upper Oligocene- late Miocene time, during which Ligurian unit thrusted on to more external domain and structuring of Falda Toscana occurred (Boccaletti *et al*., 1982; Carmignani *et al*., 1978; Chicchi and Plesi, 1991; 1992, Costa *et al*., 1998).

In Val di Lima area 4 sites have been collected in the Mesozoic core: (a) 3 sites (FT28-FT29-FT30) were collected in the Scaglia Toscana Fm., cropping out in a portion of the Mesozoic core south of Lucchio village; (b) one site (FT36) was sampled in the

northernmost part of the Mesozoic core, NE of Montefegatesi village (LV in Fig. 4.1). In the Garfagnana area three sites (FT33-34-35) have been sampled in the Corfino Mesozoic core while FT31 and FT32 sites have been sampled in the Mesozoic core near Sassorosso village (GF in Fig. 4.1).

4.4 Paleomagnetic methods and results

Paleomagnetic and rock magnetic analyses were carried out at the paleomagnetic laboratory of the Istituto Nazionale di Geofisica e Vulcanologia (INGV, Rome, Italy). The NRM of standard cylindrical specimens was measured using a 2-G Enterprises superconducting rock magnetometer (SRM) equipped with DCSQUID coils within a magnetically shielded room. In order to identify the main magnetic minerals in the study sediments, we carried out a series of rock magnetic analyses on selected specimens representative of the different sampled units. The measurements included: (1) Isothermal remnant magnetization (IRM) acquisition curves, carried out on 38 samples, and (2) stepwise thermal demagnetization of a three-component IRM carried out on 58 samples. The IRM was analysed by applying a stepwise increasing magnetic field (0-900 mT) along the z-axis sample with a pulse magnetizer and by measuring the remnant magnetization after each step with a 2G cryogenic magnetometer. The three-component IRM was produced by sequential application of pulsed magnetic fields of 2.1 T, 0.6 T and 0.12 T along z, y and x samples axes, respectively

4.4.1 Magnetic mineralogy analysis

In the Scaglia Toscana Fm. specimens, both low-coercivity and high-coercivity ferromagnetic minerals were identified. IRM curves show that most of the samples do not saturate at the maximum applied field (Fig. 4.3a). For these samples, the maximum unblocking temperature spectra is ~ 680 °C indicating the presence of high coercivity minerals, such as hematite (Fig. 4.3c). Some specimens are almost saturated at 0.4 T (Fig. 4.23a), indicating the occurrence of low-coercivity minerals. The maximum unblocking temperature spectra is ~ 580 °C or (rarely) 320 °C, suggesting the presence of magnetite and (in rare cases) iron sulphides, respectively (Fig. 4.3d,e). Some other samples show an intermediate behaviour, suggesting the presence of both high- and low-coercivity minerals (Fig. 4.3a).

The totality of the samples from Macigno Fm., Falterona Fm. and Vicchio Fm. saturate at 0.3 T (Fig. 4.3b), indicating that the high coercivity component is not significant

in these sediments. The stepwise thermal demagnetization of a three-component IRM in these samples show that the low-coercivity component is removed at 580 °C, suggesting that the magnetic mineralogy is dominated by magnetite (Fig. 4.3f-h).

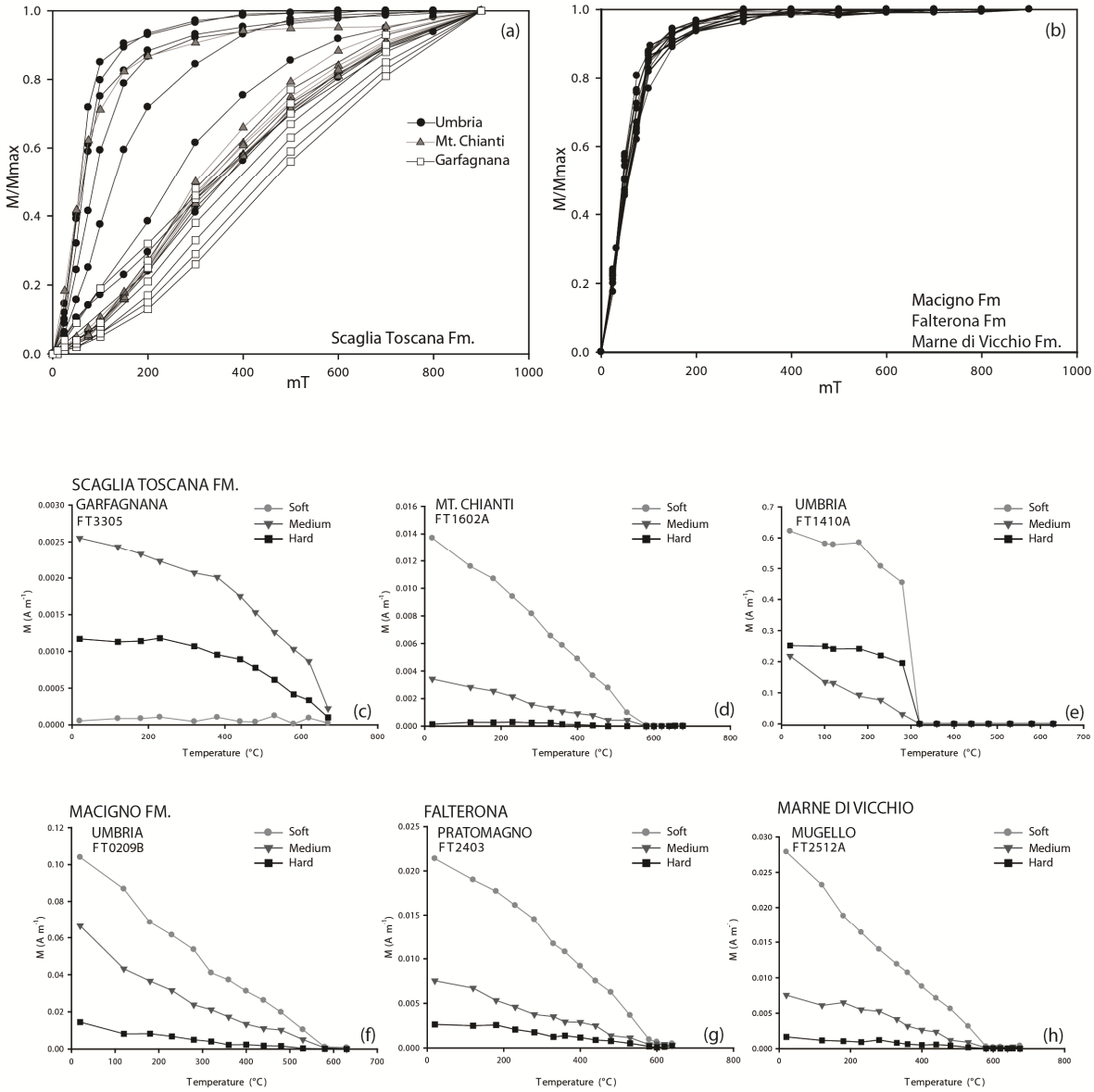

Fig. 4.3 Result of magnetic mineralogy. IRM acquisition curves showing the prevalence high-coercivity in the analyzed Scaglia Toscana Fm. (a) of low-coercivity in the analyzed Macigno Fm. (b).Thermal demagnetization curves of a three-component (hard, medium, soft) IRM (Lowrie, 1990) are shown for Scaglia Toscana formation (Fig. 3a–c), Macigno Fm. (Fig.3d), Falterona Fm. (Fig. 3f) and Marne di Vicchio Fm. (Fig. 3h).

4.4.2 Demagnetization of the Natural Remnant Magnetization and Vector Analysis

The natural remnant magnetization (NRM) of the studied samples was analyzed by both progressive stepwise thermal and alternating field (AF) demagnetization. Most of the samples have NRM intensities that range between 2 x 10^{-5} and 6 x 10^{-3} A/m. Demagnetization diagrams indicate stable paleomagnetic behavior with demagnetization vectors aligned along linear paths directed toward the origin of vector component diagrams, after removal of a viscous low coercivity remanence component at 120-180 °C or 10-15 mT (Fig. 4.4). However, some of the studied samples were too weakly magnetized (NRM values of about 1 x 10^{-5} A/m) to allow reliable complete stepwise demagnetization, or gave unstable directions during stepwise demagnetization. Such samples were discarded from further analyses. Demagnetization data were plotted using orthogonal vector diagrams (Zijderveld, 1967) and the characteristic remanent magnetization (ChRM) was determined by principal component analysis (Kirschvink, 1980) for 292 specimens. Most of these specimens yield a maximum angular deviation (MAD) <15°. Of these, the 70% show a MAD <10°. All the samples yielding MAD >17° were rejected and not considered in further analyses.

Most of the Scaglia Toscana Fm. samples are characterized by a single magnetization component. The characteristic remanent magnetization was generally isolated at temperature ranging from 650 °C to 700 °C suggesting the presence of hematite as main magnetic carrier. These samples, generally, show a reversed polarity (Fig. 4.4a-c). In some samples the decay of magnetization intensity was observed between 550-600 °C, indicating the presence of magnetite (Fig. 4.4d-e). When AF treatment is used, data for these samples decay linearly toward the origin up to 80–100 mT and do not evidently acquire any gyromagnetic remanent magnetization (GRM) (Fig. 4.4j). Other few samples are completely demagnetized at 320 °C, suggesting the presence of iron sulphides (Fig. 4.4f).

Samples from Macigno Fm., Falterona Fm. and Marne di Vicchio Fm. were completely demagnetized both in the range 480-530 °C and between 320-360 °C, likely due to the presence of magnetite (Fig. 4.4g-h) and iron sulphides (Fig. 4.4i), respectively. In most of the AF demagnetized samples from the Macigno Fm., the ChRM was generally isolated at 60-80 mT (Fig. 4.4k), whereas few samples show the acquisition of a gyromagnetic remanence, suggesting the presence of iron sulphides, as greigite (Fig. 4.4l).

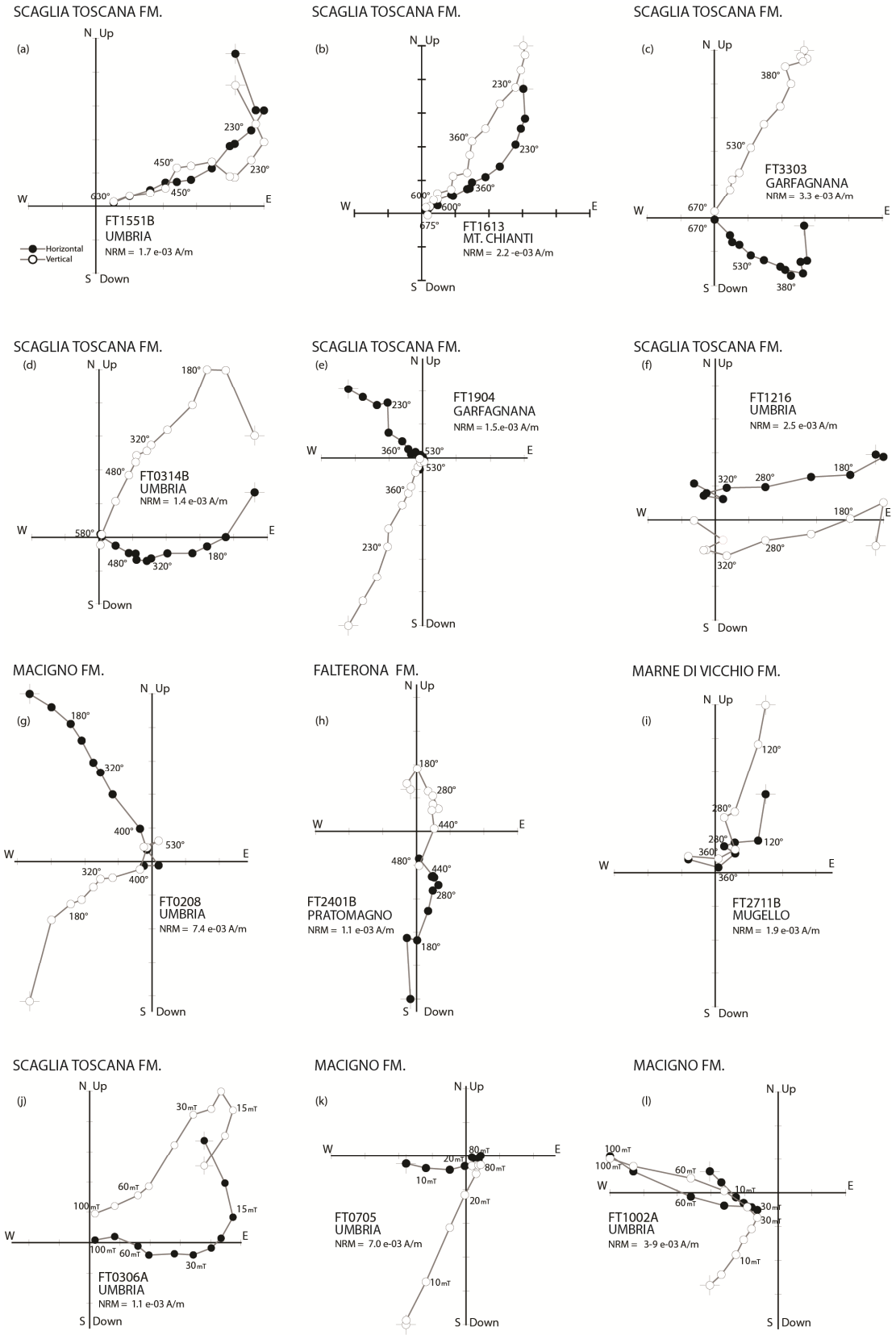

Fig. 4.4 Vector component diagrams (Zijdervald diagrams, after tectonic correction) for the progressive (a–i) thermal demagnetization and (j–n) AF of representative samples. Demagnetization step values are in degrees Celsius and mT, respectively. Open and solid symbols represent projection on the vertical and horizontal planes, respectively.

4.4.3 Paleomagnetic directions

The obtained directions of ChRM were analyzed using Fisher's statistic (1953). In sixteen sites we were not able to determine a well defined ChRM. In fifteen sites the mean directions are very well defined ($\alpha_{95} < 15^{\circ}$), whereas in five sites the α_{95} values range between 16° and 30.1°. The mean direction for each site and the statistics parameters α_{95} (95% confidence cone) and k (grouping parameter) are listed in Table 4.1. Paleomagnetic rotations for each site and for each sampled areas were evaluated by comparing paleomagnetic direction to coeval expected African poles from Besse and Curtillon (2002) as the Tuscan Nappe units were deposited onto the Adriatic lithosphere, and African poles are routinely used as proxy of Adria poles (e.g., Van der Voo, 1993; Channell *et al*., 1992; Channell, 1996; Muttoni *et al*., 2001). Rotation values and associated 95% confidence limits were calculated according to the method of Demarest (1983) and reported in Table 4.1.

4.4.3.1 Trasimeno Lake area

In the area around the Trasimeno Lake (area 1 in Fig. 4.1), reliable paleomagnetic results have been obtained from 9 out of the 15 sampled sites.

Sites from Scaglia Toscana Fm. show both normal and reversed polarities (FT03, 15), only normal polarity (FT11) and only reversed polarity (FT12), while sites from Macigno Fm. have normal polarity (FT02, 07, 09, 10) or normal and reversed polarities (FT01) (Tab. 4.1).

In all the mixed polarity sites the normal and reversed polarity are not antipodal and the reversed polarity directions show a larger amount of CCW rotation than the normal polarity ones (Fig. 4.5 and Tab. 4.1). The reversal test (McFadden and McElhinny, 1990) carried out in both the Scaglia Fm. (FT03,15) and in the Macigno Fm. (FT01) sites is negative. Taking into account this difference and in order to test a possible recent overprint which could affect the paleomagnetic directions, we have carried out fold test analyses considering together normal and reversed polarities and then separately the normal and reversed directions.

Table 4.1. Paleomagnetic direction from Tuscan Nappe.

Site	Coordinates (Lat-Long)	Lithology	Formation	Age	N° fit/N°	S_0	D_{BTC}	I_{BTC}	K	α_{95}	D_{ATC}	I_{ATC}	K	α_{95}	Rotation (± error)	Flattening (± error)
				Trasimeno Lake area - Scaglia Toscana Fm.												
FT03 r/n	43° 14' 32.3", 12° 04' 54.9"	Mudstone	Scaglia Toscana	Eocene	36/45	variable	324.8	56.3	17.9	5.8	284.6	51	18.5	5.7	-89.83 (13.79)	16.98(10.78)
r					21/45		130.8	-62.3	36.0	5.4	91.2	-49.5	32.6	5.7	-109.63 (11.73)	21.58 (9.68)
n					15/45		338.3	45.9	18.8	9.1	304.3	50.2	19.7	8.8	-60.33 (7.46)	16.88 (5.88)
FT11**	43° 05' 14.2", 12° 10' 50.0"	Mudstone	Scaglia Toscana	Eocene	4/13	variable	350.0	45.6	10.5	29.7	324.4	40.6	10.3	30.1	-	-
FT12	43° 04' 17.7", 12° 11' 22.6"	Mudstone	Scaglia Toscana	Eocene	6/16	variable	84.3	-60.0	27.2	13.1	75.0	-18.1	27.2	13.1	-103.12 (11.78)	33.52 (11.11)
FT15 r/n	43° 02' 38.7", 12° 08' 52.7"	Mudstone	Scaglia Toscana	Eocene	47/68	variable	355.4	67.4	15.7	5.4	264.6	31.1	15.9	5.4	-93.51 (6.87)	20.49 (6.07)
r					43/68		179.2	-69.4	17.6	5.3	81.6	-30.7	18.0	5.3	-61.51 (14.39)	20.89 (12.41)
n					4/68		336.4	42.9	30.4	16.9	296.6	30.7	39.1	14.9	-96.51 (6.79)	20.89 (6.02)
Mean					**3**		**312.8**	**66.2**	**14.8**	**33.2**	**266.0**	**33.9**	**16.0**	**31.9**	**-92.1±31.2**	**17.7 ± 25.3**
				Trasimeno Lake area – Macigno Fm.												
FT01 r/n	43° 20' 48.3", 12° 02' 09.2"	Sdt-Lms	Macigno	Aquitanian	12/14	263,42	312	69.1	8.6	15.7	274.7	38.3	11.9	13.1	-89.83 (13.79)	16.98 (10.79)
r					7/14		62.7	-74.8	35.7	10.2	74.9	-33.7	27.9	11.6	-60.33 (7.46)	16.88 (5.88)
n					5/14		339.8	43.6	159.1	6.1	304.2	38.4	158.1	6.1	-109.63 (11.73)	21.58 (9.69)
FT02	43° 14' 49.4", 12° 06' 28.1"	Sdt-Lms	Macigno	Aquitanian	8/11	246,30	351.5	42.8	15.3	14.6	322.5	43.4	15.3	14.6	-42.37 (16.41)	11.78 (11.90)
FT07	43° 17' 57.2", 12° 02' 30.4"	Sdt-Lms	Macigno	Aquitanian	7/13	235,30	336.7	35.1	29.8	11.2	314.8	35.5	29.8	11.2	-49.72 (12.50)	19.73 (11.60)
FT09	43° 27' 34.6", 12° 08' 12.2"	Mudstone	Macigno	Aquitanian	11/14	230,21	332.6	50.5	11.3	14.2	306.7	50.3	11.3	14.2	-57.85 (18.14)	5.09 (10.12)
FT10	43° 27' 46.8", 12° 07' 40.3"	Mudstone	Macigno	Aquitanian	10/15	160,11	314.6	41.6	16.1	12.4	309.1	51.3	16.1	12.4	-55.45 (16.25)	4.09 (10.26)
Mean					**5tot**		**331.5**	**48.6**	**23.4**	**16.2**	**305.4**	**45.0**	**28.5**	**14.6**	**-59.1±16.8**	**10.1 ± 11.9**
				Mt. Chianti area -Scaglia Toscana Fm.												
FT16	43° 32' 19.8", 11° 24' 32.9"	Mudstone	Scaglia Toscana	Eocene-Oligocene	7/8	248,09	66.2	-60.2	24.2	12.5	66.6	-51.2	24.2	12.5	-111.34 (16.48)	0.94 (10.66)
FT17	43° 35' 58.2", 11° 22' 02.1"	Mudstone	Scaglia Toscana	Eocene-Oligocene	9/10	73,17	297.8	6.5	40.6	8.2	300.5	18.3	40.4	8.2	-57.42 (8.29)	33.91 (7.71)
FT18 r/n	43° 36' 09.0", 11° 22' 21.2"	Mudstone	Scaglia Toscana	Eocene-Oligocene	6/7	24,23	259.6	37.3	10.8	21.3	278.9	47.2	10.8	21.3	-79.03 (25.66)	5.01 (10.26)
FT19 r/n	43° 32' 06.3", 11° 22' 41.0"	Mudstone	Scaglia Toscana	Eocene-Oligocene	6/6	220,22	325.3	64.2	31.8	10.9	281.1	61.4	31.9	10.9	-55.45 (16.25)	4.09 (17.16)
Mean					**4**		**281.4**	**45.9**	**5.6**	**42.7**	**279.6**	**46.5**	**11.2**	**28.8**	**-81.3±34.9**	**5.4 ± 22.9**
				Garfagnana and Val di Lima area -Scaglia Toscana Fm.												
FT28	44° 01' 53.1", 10° 43' 04.1"	Mudstone	Scaglia Toscana	Middle Eocene	8/9	28,50*	160.0	-69.6	12.7	16.7	191.4	-25.0	12.7	16.2	-25.87 (14.35)	4.09 (10.26)
FT30	44° 01' 14.9", 10° 43' 07.2"	Mudstone	Scaglia Toscana	U. Cretaceous- Paleocene	8/9	283,22	157.8	-46.2	50.2	7.9	144.4	-31.3	50.3	7.9	-21.12 (7.91)	17.40 (6.96)
FT31	44° 10' 52.6", 10° 24' 28.6"	Mudstone	Scaglia Toscana	U. Cretaceous- Paleocene	10/11	211,31*	138.5	-19.4	31.1	8.8	125.6	-25.5	31.1	8.8	-39.80 (8.27)	23.44 (7.58)
FT33	44° 11' 02.5", 10° 24' 17.0"	Mudstone	Scaglia Toscana	U. Cretaceous- Paleocene	9	263,37*	165.3	-71.4	36.5	8.6	110.7	-47	36.5	8.6	-54.69 (10.39)	1.98 (7.44)
FT34	44° 12' 50.5", 10° 22' 19.6"	Mudstone	Scaglia Toscana	U. Cretaceous- Paleocene	10/10	283,36*	161.3	-63.9	24.7	9.9	130.7	-36.2	24.7	9.9	-34.69 (10.12)	12.79 (8.36)
FT35	44° 12' 44.9", 10° 24' 43.1"	Mudstone	Scaglia Toscana	U. Cretaceous- Paleocene	10/10	39,29*	86.3	13.3	9.4	16.6	85.1	-6.8	9.4	16.6	-34.70 (10.13)	12.78 (8.36)
FT36	44° 04' 27.8", 10° 35' 28.5"	Mudstone	Scaglia Toscana	Middle Eocene	9	284,26*	61.4	6.7	5.4	24.5	56	25.2	5.4	24.5	-58.25 (21.82)	27.54 (19.57)
Mean					**4**		**151.9**	**-51.0**	**11.2**	**28.7**	**128.7**	**-35.6**	**32,4**	**16.4**	**-36.7±16.1**	**13.3±13.2**

N°fit/N° number of great circles/total number of studied samples at a site; D, I are site-mean declinations and inclinations calculated before (DBTC,IBTC) and after (DATC,IATC) tectonic correction;
k and α_{95} are statistical parameters after Fisher [1953]; S_0 is bedding attitude (azimuth of the dip and dip values), * deduced by AMS tensor; r/n indicates sites characterized both by samples with reversal and normal polarity;
** Sites not considered in further tectonic interpretation.

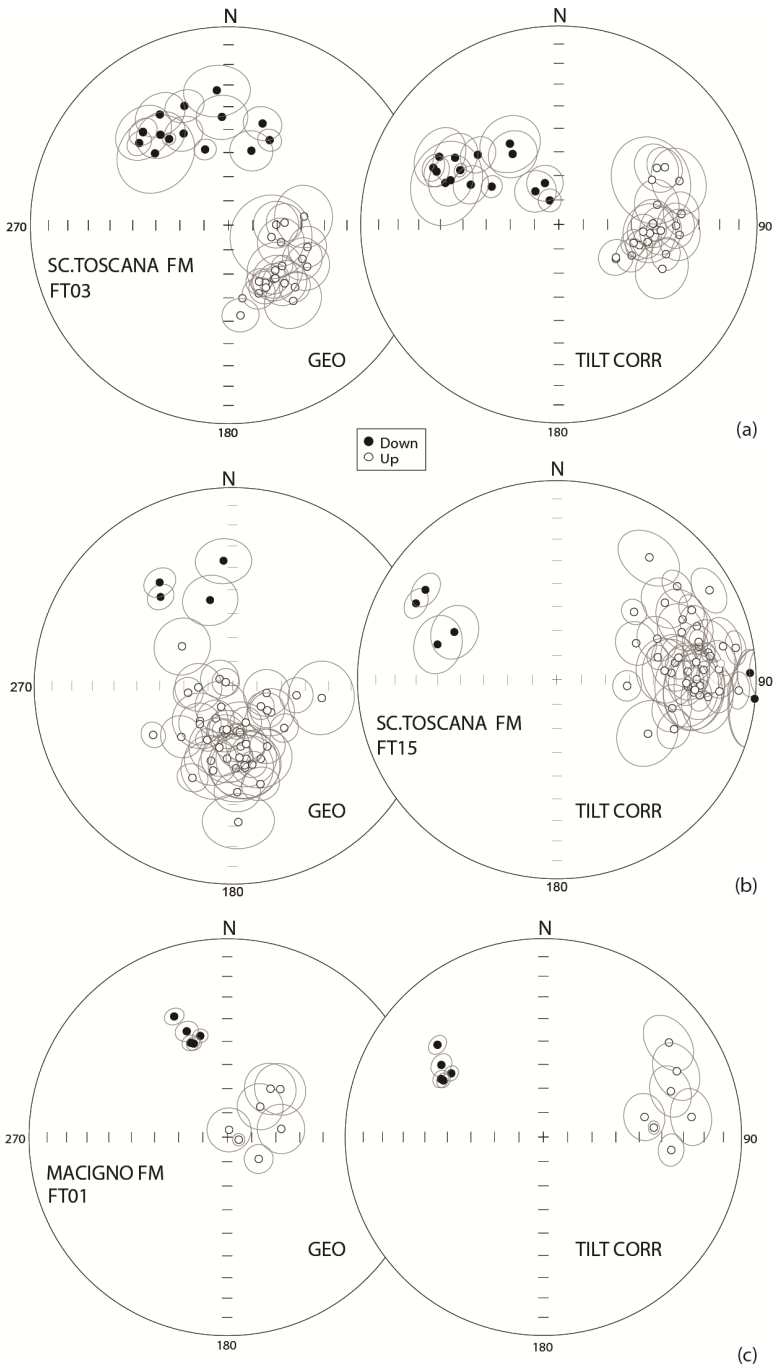

Fig. 4.5 Equal-area projection of sample characteristic remanent magnetization (ChRM) directions from the Scaglia Toscana Fm. (a-b) and Macigno Fm. (c). The 95% confidence ellipse for the normal and reversed directions is indicated.

In the Scaglia Toscana Fm. the mean site directions fold tests (McFadden, 1990) give inconclusive results either if we consider separately normal and reversed polarity directions or if we considerer together the normal and reversed polarity directions. In the latter case, however, the mean paleomagnetic directions are better grouped after (D = 266.0°, I = -33.9°, K = 16.0, $\alpha_{95\%}$= 31.9), than before tectonic correction (D = 312.8°, I =

66.2°, K = 14.8, $\alpha_{95\%}$= 33.2). It is also important to note that before tectonic correction the mean paleomagnetic direction is far from the GAD magnetic field expected for the sampling localities (Fig. 4.6a). Both these observations strongly suggest that the isolated ChRM for the Scaglia Toscana Fm. has been acquired before folding, and is probably of primary (syn-depositional) origin. When the mean ChRM direction is compared with the coeval (46.4 Ma) African paleopole (λ (°N) = 79.1; ϕ (°E) = 200.6, A_{95} = 5.2) a mean value of 92.1° ± 31.2° counterclockwise (CCW) rotation (F=17.7 ± 25.3) has been obtained.

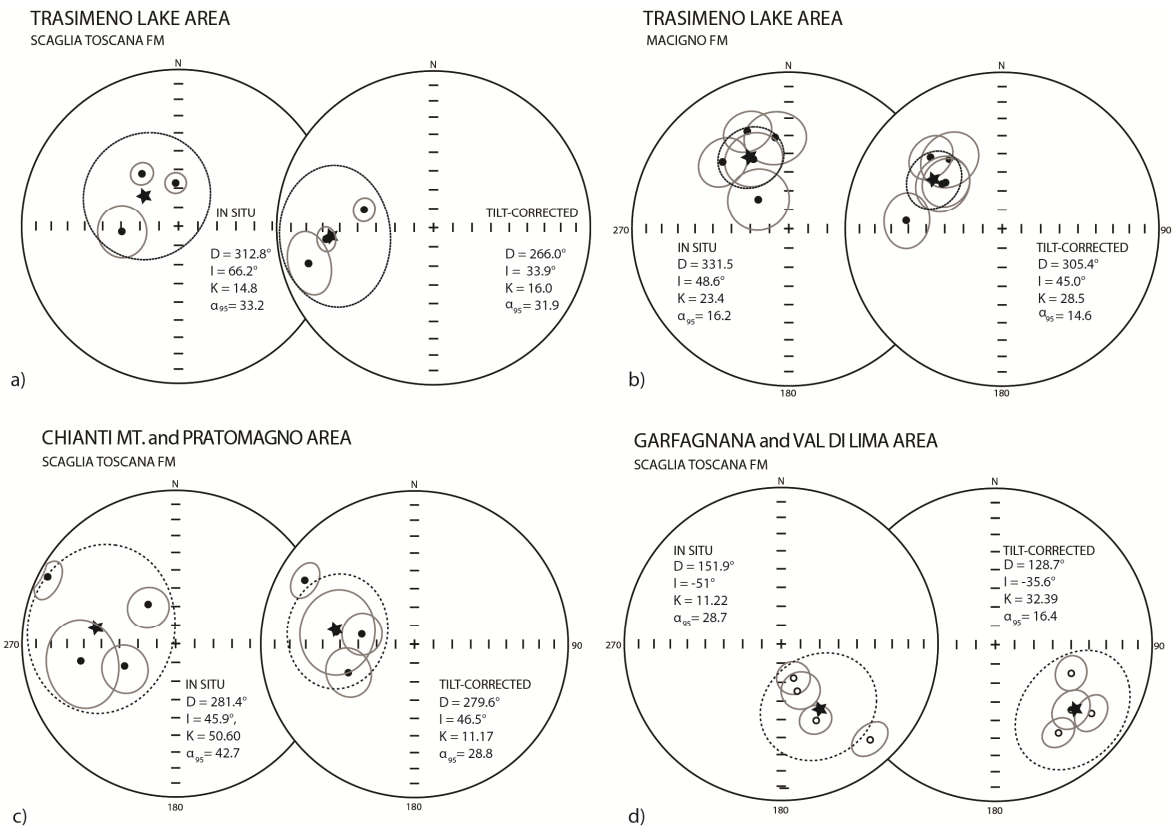

Fig. 4.6 Equal-area projection of the site-mean directions from Scaglia Toscana Fm. and Macigno Fm. of Trasimeno Lake area (a-b), from Scaglia Toscana Fm. of Mt. Chianti and Pratomagno area (c) and from Scaglia Toscana Fm. of the Val di Lima and Garfagnana area (d). White and black symbols represent projection onto upper and lower hemisphere, respectively. Ellipses are the projections of the α_{95} cone about the mean directions (the star is the mean for the area and the dotted ellipse the related α_{95} cone projection).

The McFadden (1990) fold test performed for the Macigno Fm. normal polarity mean directions is positive at the 95% confidence level ($\xi_{in\ situ}$ = 2.662; $\xi_{unfolded}$ = 1.418; $\xi_{95\%}$= 2.609), suggesting a pre-tilting age of magnetization for this magnetic component (Fig 4.6b). Normal polarity mean directions are better grouped after (D = 311.6°, I = 44°, K = 5.24, $\alpha_{95\%}$= 8.3), than before tectonic correction (D = 335.1°, I = 43.4°, K = 51.79, $\alpha_{95\%}$= 10.7). When the reversed directions of FT01 were also taken into

account, the McFadden (1990) fold test becomes indeterminate, although at the basin scale the mean paleomagnetic direction remains better grouped after (D = 305.4°, I = 45.0°, K = 28.5, $\alpha_{95\%}$= 14.6) than before tectonic correction (D = 331.5°, I = 48.6°, K = 23.4, $\alpha_{95\%}$= 16.2) (Tab. 4.1). Also in this case it is important to note that the mean paleomagnetic directions in *in-situ* coordinates are far from the GAD magnetic field expected for the sampling localities (Fig. 4.6a). Both these observations strongly suggest that the ChRM for the Macigno Fm. has been acquired before folding and the obtained directions can be used for tectonic interpretations. When the mean ChRM direction is compared with the coeval (19.6 Ma) African paleopole (λ (°N) = 81.7; ϕ (°E) = 165.7, A_{95} = 4.5), the value of rotation is 59.1° ± 16.8° CCW (F=10.1 ± 11.9).

4.4.3.2 Chianti Mountains and Pratomagno area

In the Chianti Mountains and Pratomagno area reliable paleomagnetic results have been obtained from all the 4 sampled sites from the Scaglia Toscana Fm., whereas in the 7 sites from Falterona and Marne di Vicchio Fms. we were not able to determine a well defined ChRM.

In the Scaglia Toscana Fm., one site (FT16) shows a reversed polarity, one site has a normal polarity (FT17) and two sites have both normal and reversed polarity components (FT18, 19). In these latter sites the reversal test (McFadden and McElhinny, 1990) is indeterminate. When we consider together the sites with reversed and normal mean directions the site-mean directions are better grouped after (D = 279.6°, I = 46.5°, K = 11.2, $\alpha_{95\%}$= 28.8), than before tectonic correction (D = 281.4°, I = 45.9°, K = 5.6, $\alpha_{95\%}$= 42.7) (Tab. 4.1, Fig. 4.6c), and the fold test (McFaddden, 1990) is positive at 95% confidence level ($\xi_{in\ situ}$ = 2.588; $\xi_{unfolded}$ = 1.641; $\xi_{95\%}$= 2.076) suggesting a pre-folding (syn-depositional) age for the magnetization. When the mean ChRM direction is compared with the coeval (46.4 Ma) African paleopole (λ (°N) = 79.1; ϕ (°E) = 200.6, A_{95} = 5.2) the mean site CCW rotation is 81.3° ± 34.9 (F = 5.4 ± 22.9) (Tab. 4.1).

4.4.3.3 Garfagnana and Val di Lima area

In the Garfagnana and Val di Lima area, well defined directions have been obtained from 7 (FT28,30,31,33,34,35) out of the 8 sampled sites from Scaglia Toscana Fm.. All the sites have a reversed polarity, except site FT36 that has a normal polarity.

Among the seven sites, four (FT30, FT31, FT32, FT33) show very well defined mean site directions (α_{95}< 10.0°), and are consistently rotated CCW. Conversely the other three sites (FT28, FT35 and FT36) show poorly defined mean site directions (α_{95}> 16.2°), which are far from the other four sites, being rotated CW (FT28 and FT36) or showing very large amount of CCW rotations (FT35) (Tab. 4.1). For these reasons, these sites have been not further considered for tectonic interpretations.

For the four coherent sites the McFadden (1990) fold test is indeterminate but the mean sites direction is much better grouped after (D = 128.7°, I = -35.6°, K = 32.3 $\alpha_{95\%}$ = 16.4) than before (D = 151.9°, I = -51.0°, K = 11.2, $\alpha_{95\%}$= 28.7) tectonic correction (Fig. 4.6d), strongly suggesting that the isolated magnetic component has a primary (syn-sedimentary) origin. When the mean paleomagnetic directions are compared with the Africa paleopole at 64 Ma (λ (°N) = 71.6; ϕ (°E) = 234.2, A_{95} = 3.6), a CCW rotation of 36.7° ± 16.1° (F=13.3± 13.2) is obtained (Tab. 4.1).

4.5. Tectonic interpretation of paleomagnetic results

Paleomagnetic rotations calculated for each site are reported in Fig. 4.7a, together with the overall set of paleomagnetic results already published in Northern Apennines and re-calculated by Cifelli and Mattei (2010). The complete paleomagnetic data set is analysed and discussed taking into account the spatial distribution of paleomagnetic declinations along the length of the arc and along two different profiles oriented orthogonal to the main structural axes of the chain (Fig. 4.7b and 4.7c). We then compare the amount of rotation displayed by paleomagnetic declinations with the change in strike of the structural trends (oroclinal test according to Schwartz and Van der Voo, 1983).

4.5.1 Distribution of paleomagnetic rotations along the Northern Apennines arc

The distribution of paleomagnetic rotations along the Northern Apennines arc is shown in Fig. 4.7a. Three different rotational domains can be recognized from the external toward the internal portion of the arc.

The first domain is represented by the external sector of the Northern Apennines, where a large amount of paleomagnetic data has been collected from the Oligocene-Lower Miocene Epiligurian Units, the Jurassic-Eocene Umbria-Marche domain and the Upper Miocene-Lower Pliocene Umbria-Marche foredeep units. Along this sector of the arc, a

progressive increase of CCW paleomagnetic rotations can be observed moving from the N-S oriented southern portion of the arc, toward the WNW-ESE oriented, northern sector of the arc, where up to 52° of CCW rotations have been measured in the Oligocene-Lower Miocene Epiligurian Units (Muttoni *et al*., 1998).

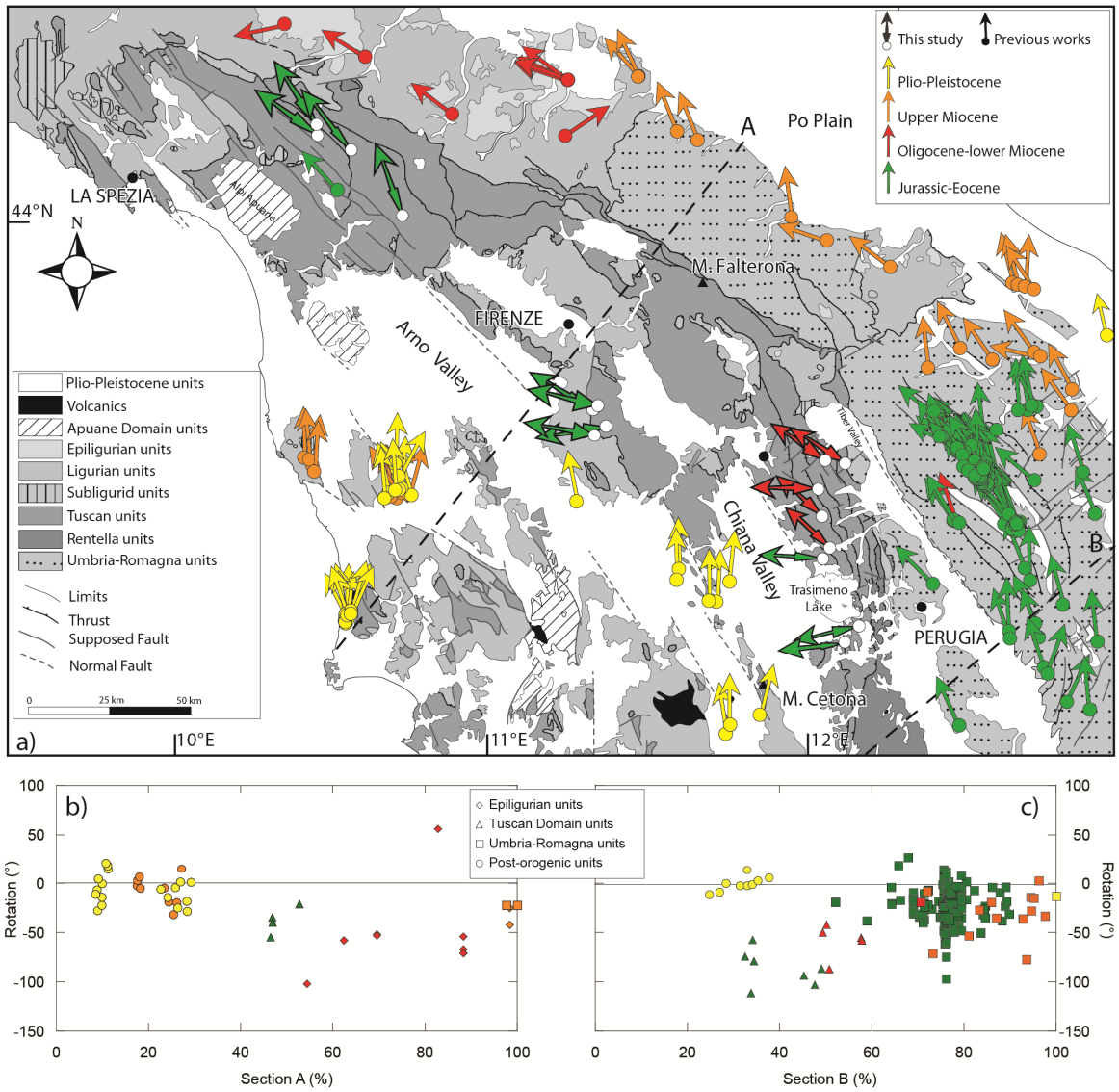

Fig.4.7 Paleomagnetic declinations from this study and from previous published results on the Northern Apennines. Rotations and confidence limits were calculated by comparing paleodirections to the coeval reference directions of the coeval expected African paleopole from Besse and Courtillot (2002) according to Demarest (1983).

The second sector is represented by the Tuscan units, which form the more internal domain of the Northern Apennines. In this area our results confirm the general trend of CCW rotations already measured in pre and syn orogenic units from the external Northern Apennines. However, the distribution of CCW rotation in the Tuscan Nappe units show a peculiar trend in comparison with data from the more external sector of the chain. In fact,

in the Tuscan units, the amount of CCW vertical axis rotations decreases from the southern sector of the arc (Trasimeno Lake and Chianti-Pratomagno areas), where we have measured a very large amount of CCW rotations in the Eocene Scaglia Toscana Fm. (92.1° ± 31.2° and 81.3° ± 34.9°, respectively) and in the lower Miocene Macigno Fm. (59.1° ± 16.8°), toward the northern part of the arc (Val di Lima area), where the mean CCW rotation is 36.7° ± 16.1° (Tab. 4.1).

The third sector is represented by the extensional Tyrrenian margin, where the Upper Miocene-Lower Pleistocene post-orogenic units show no significant vertical axis rotations (Mattei *et al*., 1996).

In order to analyze more in detail the distribution of paleomagnetic rotations in Northern Apennines we project paleomagnetic rotations along two profiles orthogonal to the main structural trend of the arc (Fig. 4.7b,c). Tectonic rotations are plotted as a function of their tectonic location in the orogenic wedge, making the reasonable assumption that moving away perpendicularly from the Tyrrhenian coast we progressively move from the more internal deformed sectors of the chain to the more external, less deformed sectors.

In the southern profile, CCW rotations measured in the orogenic units decrease significantly from the internal to the external sector of the chain (Fig. 4.7b). In particular, whereas CCW rotations up to 100° have been measured in the Tuscan units in the Trasimeno Lake and Chianti areas, CCW rotations measured in the more external Umbria-Marche units decreases to about 20°. These different paleomagnetic rotations are not related to the different age of the sampled sequences as both pre-orogenic and syn-orogenic units are systematically more rotated CCW in the Tuscan than in the Umbria-Marche units. On the other side, the boundary between these two different rotational domains is very sharp and corresponds with the tectonic boundary between the Tuscan and the Umbria-Marche units, suggesting that the larger amount of CCW rotations measured in the Tuscan units could be related to a geodynamic event that has not involved the more external units of the Northern Apennines. This event occurred before the Upper Miocene as the post orogenic units of the extensional Tyrrhenian margin are not rotated.

In the northern profile (Fig. 4.7c) we observe a different distribution of paleomagnetic rotations respect to the southern one. In fact, the different tectonic units of the Apennine orogenic wedge show a comparable amount of paleomagnetic rotations, which average between 25° and 50° CCW. In particular for what concern the internal Tuscan units, we have measured a mean paleomagnetic rotation of about 35° CCW, which

is comparable with the amount of CCW rotation measured in the middle Jurassic units of the Tuscan Nappe (Aiello and Hagstrum, 2001), and is of the same order of magnitude of paleomagnetic rotations measured in Oligocene to Miocene sites from the Epiligurian units (about 50° CCW) and from the Upper Miocene sites from the more external Umbria-Marche units (about 35° CCW). Also in this area paleomagnetic results collected from the extensional Tyrrhenian margin of Northern Apennines prove that CCW paleomagnetic rotations measured in the internal sector of the chain occurred before Late Miocene.

4.5.2 The oroclinal bending of the Northern Apennines

The origin of the Northern Apennine arc has been debated since Channell *et al*. (1978) observed that the increase in CCW rotations measured in the Cretaceous-Eocene "Scaglia" formation, from southern toward northern Umbria, probably reflected the oroclinal bending of an originally straight fold belt. This mechanism was first confirmed (Eldredge *et al.* 1985) and then rejected (Van der Voo and Channell 1980; Lowrie and Hirt 1986; Hirt and Lowrie 1988) on the base of different data sets from Mesozoic-lower Tertiary sediments in the Umbria-Marche domain of the chain. More recently, from the study of Messinian foredeep sediments of the external Umbria-Marche domain, Speranza *et al.* (1997) indicated that the present-day shape of the external part of the northern Apennines arc is related to the oroclinal bending of an originally N320° trending straight belt. These Authors suggested that vertical axis rotations accompanied the migration of the main thrust front toward the Adriatic foreland and characterized also the development of second-order curved thrust fronts in the Apennines.

In order to test a possible orocline origin for the curved shape of the Tuscan Nappe structures, an oroclinal test was carried out for our new results (Fig. 4.8). The relationship between paleomagnetic declinations and structural directions was investigated using the method originally proposed by Schwartz and Van der Voo (1983) for the Appalachians and later applied in different curved orogenic systems, Northern Apennines included (Eldredge *et al*. 1985; Lowrie and Hirt 1986; Speranza *et al.* 1997) (Fig. 4.8).

In this diagram we have chosen as reference rotation (Rr) 315°, as most of our results show large counterclockwise rotations. We remind that in this kind of diagram the exact value of the chosen references values (of declinations and structural directions) is not critical, only that is constant. As reference structural direction Sr we have used 315°, that is a perfect NW-SE trend, representative of the main orientation of the Northern Apennines tectonic structures.

As within-site structural directions (that must be considered as axis of the thrust-related folds in the Tuscan Units) we used the direction of the bedding strike (Fig. 4.8a) or the mean direction of the magnetic lineation of tectonic origin observed by AMS data (Fig. 4.8b), in analogies with Speranza *et al*., (1997).

The oroclinal test calculated for the Cretaceous- Eocene Scaglia Toscana Fm. shows that paleomagnetic rotation and bedding strike orientation are poorly correlated (correlation coefficient $r^2 = 0.22$) (Fig. 4.8a). The correlation slightly increases ($r^2 = 0.47$) when we calculate paleomagnetic rotation versus fold axis orientation (Fig. 4.8b).

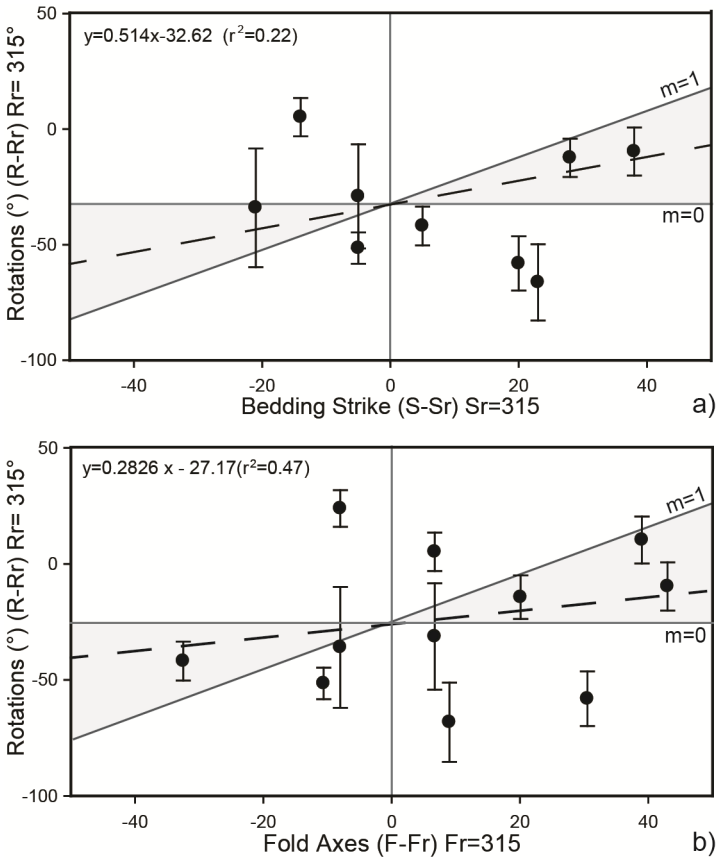

Fig. 4.8 Oroclinal test for the Tuscan Nappe considering rotations directly compared with fold axes deviation (a), and the structural strike deviation between the strike direction of bedding strike direction at each site (b). (see text for further details).

However, in both the cases the t test calculated comparing our results with the data distribution for zero slope gives negative results at the 99% significative level. These results indicate that the oroclinal test is negative and that there is no significant correlation between the orientation of tectonic structures and the measured paleomagnetic rotations.

Therefore a different model respect to the simple oroclinal bending hypothesis is required to explain the distribution of paleomagnetic rotation in the Tuscan Nappe units.

4.6 Paleomagnetic rotations of the Northern Apennines in the framework of Cenozoic evolution of the Central Mediterranean

Paleomagnetic results from the internal Tuscan units of Northern Apennines show a distribution of CCW rotations along the arc that cannot be explained using the oroclinal bending model, which has been successfully proposed for the evolution of the external portion of the arc (Speranza *et al.*, 1997).

On this base we propose a different model to explain the distribution of paleomagnetic rotation in the internal part of the Northern Apennines, which integrates in a single evolutionary model the Oligo-Miocene drifting and CCW rotation of the Corsica-Sardinia block and the curvature of the Northern Apennines arc (Fig. 4.9). The tectonic model takes into account: 1) the pre-drifting paleogeography of the Corsica-Sardinia block; 2) the timing of deformation of the different tectonic units of Northern Apennines; 3) the overall paleomagnetic data from Northern Apennines, and in particular the very large amount of CCW rotations measured in the southern portion of the Tuscan Units, when compared to the more external Umbria-Marche units.

The paleogeography of the Northern Apennine and Corsica-Sardinia block at the pre-drift stage (Chattian) is shown in Fig. 4.9a. At that time the more internal units (Ligurian oceanic domain), which were incorporated in the Apennine chain during Late Cretaceous, formed a double-verging orogenic wedge, related to northeastward subduction of the Adriatic-Ionian lithosphere. The proposed position of the Corsica-Sardinia block, located adjacent to southern France, was originally suggested by Argand in 1924 and has been later confirmed by a large amount of geological, geophysical and paleomagnetic evidences (De Jong and Manzoni, 1968; De Jong *et al*., 1969; Zijderveld *et al*., 1970; Alvarez, 1972; Alvarez *et al*., 1973; De Jong *et al*., 1973; Westphal *et al*., 1973; Montigny *et al*., 1981; Burrus, 1984; Edel, 1980; Vigliotti *et al*., 1990; Gattacceca *et al*., 2007).

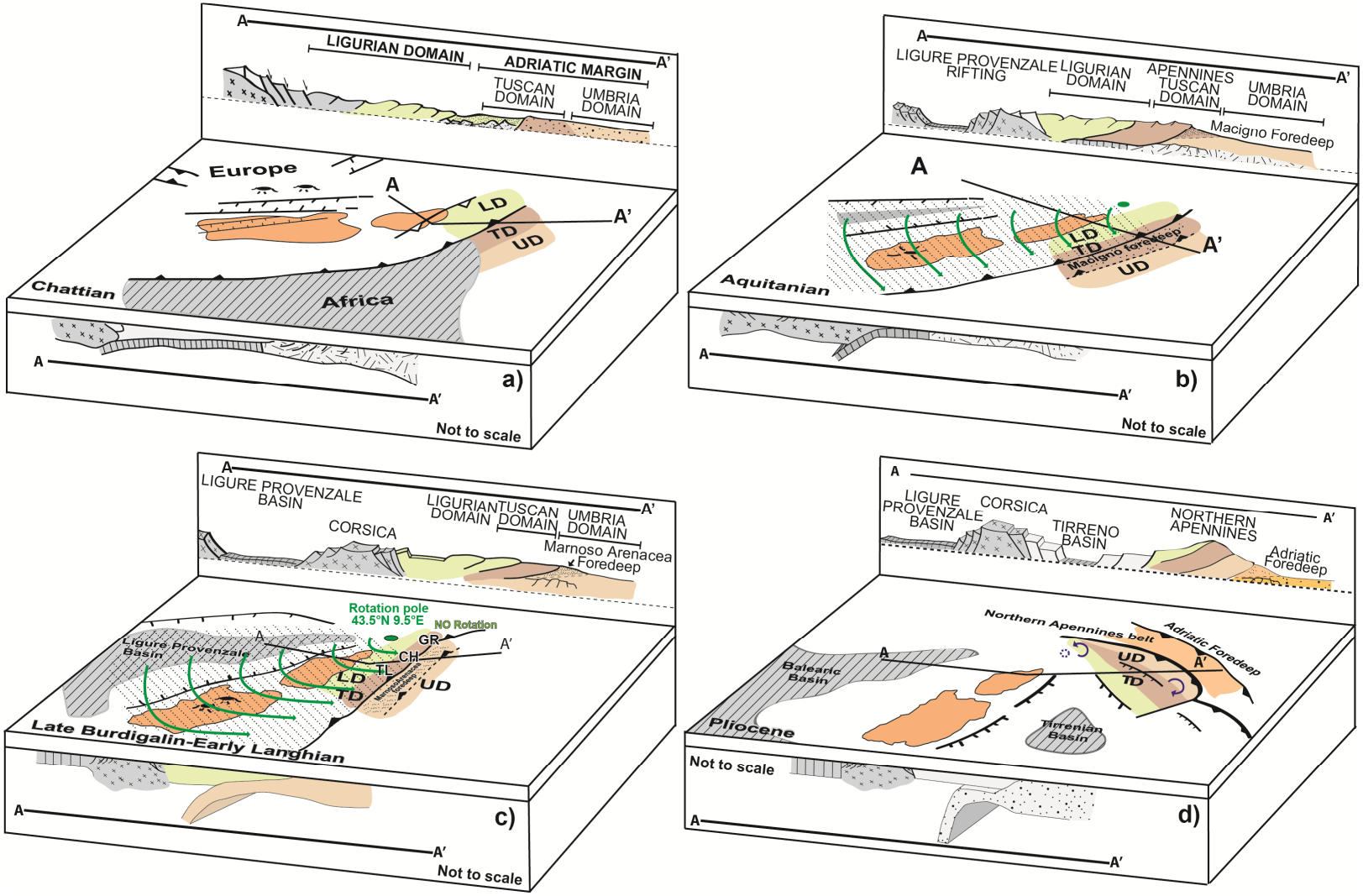

Fig. 4.9 Schematic cartoon of the tectonic evolution of the Northern Apennines with different stages of drifting and rotation of the Corsica Sardinia Block. LD=ligurian Domain; TD= Tuscan Domain; UD= Umbrian Domain. (GR= Garfagnana Area; CH= Chianti Mountains; TL= Trasimeno Lake)

These Authors, on the base of integrated paleomagnetic and geochronology investigations of Miocene volcanic sequences, have proven that 45° CCW rotation respect to stable Europe occurred after 21 My (Aquitanian), of which 30° CCW rotation occurred between 20.5-18 My, during the maximum volcanic events in Sardinia. At the same time, paleomagnetic analyses from sedimentary units from Corsica and from volcanic successions in Sardinia concur to demonstrate that the rotation was completed around 15 My ago (late Aquitanian-Langhian) (Vigliotti and Kent, 1990; Gattacceca *et al*. 2007). These results are fully compatible with a pre-drift palinspastic reconstruction where the Corsica Sardinia block is located adjacent to the coast of Southern, as deduced from morphological fit of the continental margins, oceanic crust extension defined by tectonic subsidence analysis (Pasquale *et al*., 1995) and compatible with 3D gravity inversion (Chamot-Rooke *et al*., 1999), and define a rotation pole during the drifting of the Corsica-Sardinia block located in the Ligurian Sea around 43.5°N, 9.5°E (4.10).

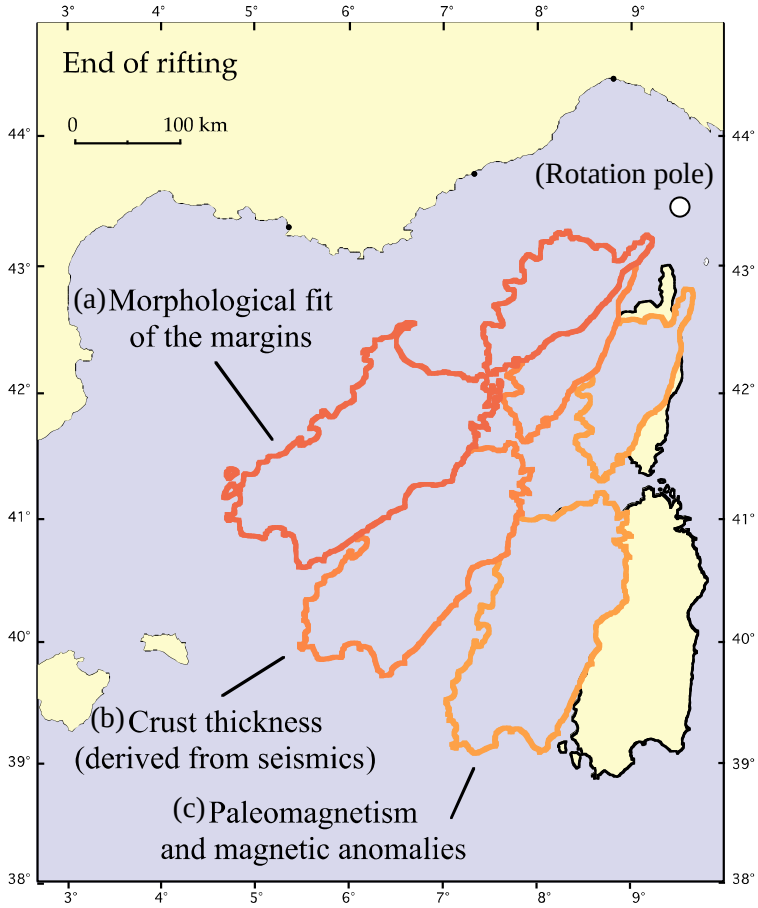

Fig. 4.10 Map of the Liguro-Provençal basin showing several reconstructions of the post-rift/pre-drift (~21.5 Ma) positions of Corsica and Sardinia, based on: (a) morphological fit of the continental margins of the basin (e.g. Westphal *et al*., 1973); (b) Oceanic crust extension defined by tectonic subsidence analysis (Pasquale *et al*., 1995); (c) paleomagnetic data of Corsica–Sardinia and basin magnetic anomalies (Edel, 1980) (from Gattacceca *et al*., 2007)

The Corsica-Sardinia CCW rotation has been coeval with the incorporation of the Tuscan domain succession in the Apennine orogenic wedge (Fig. 4.9b). Both these processes were induced by the westward subduction and eastward slab roll-back of the Adriatic-Ionian lithosphere. During Lower Miocene the trench was located to the east of the Tuscan Nappe, and this tectonic domain represented the external front of the Northern Apennines thrust and fold belt. Therefore, the Tuscan nappe, together with the Corsica-Sardinia block, formed the upper plate of the subducting system, while the Umbria-Marche units still represented the undeformed foreland domain. In this framework it appears reasonable that the CCW rotation of the Corsica-Sardinia block also extended to the Tuscan Nappe unit, which is also located in the upper plate in the subducting system. In this tectonic interpretation the Corsica-Sardinia CCW rotation has been recorded only by the southern part of the Tuscan units (Trasimeno Lake and Chianti areas), that is in the area located to the south of the Corsica-Sardinia pole of rotation (43.5°N, 9.5°E) (Fig. 4.9b,c). Conversely, the northern Apennine units located to the north of the rotation pole (Val di Lima area), didn't participate to this tectonic process and did not rotate. This interpretation explains the significant decreases of CCW rotations form the southern to the northern part of the Tuscan units.

The significant difference in the amount of CCW rotation between the Tuscan and the Umbria Marche units also demonstrates that the latter were not involved in the Corsica-Sardinia rotation. This is not surprising as, during the Lower Miocene, the Umbria-Marche units still represented the foreland of the Apennines orogeny and were located in the lower plate of the Adriatic-Ionian subducting system (Fig. 4.9b,c).

It is worth to note that the amount of CCW rotation Corsica-Sardinia (about 45-50°) is not sufficient to explain the entire CCW rotation measured in the Tuscan units (which reaches 80°-90°). Therefore, we suggest that, in analogy with what has been observed in the more external part of the northern Apennine, a portion of CCW rotations that we measured in the Tuscan Nappe units are related to local deformation and the stacking of Tuscan Nappe over the Umbria-Marche domain during the Lower–Middle Miocene. As a consequence, the huge CCW rotations (≈80°-90°) measured in the southern part of the Tuscan Nappe (Trasimeno Lake and Chianti Mts.) are related to two different processes: the Corsica-Sardinia CCW (≈50°) and the curvature of the Apennine arc (≈30° - 40°). The latter is also responsible of the entire CCW rotations measured in the northern Tuscan units (Val di Lima). During the Late Miocene and Pliocene vertical axis rotations accompanied thrust emplacement of the tectono-stratigraphic units located in the external sector of the

Northern Apennines as a consequence of slab roll-back of the subducting Adriatic lithosphere (Speranza *et al*., 1997; Muttoni *et al*, 1998) (Fig. 4.9d). These rotations did not involve the internal Tuscan units. In fact the late Miocene-Pleistocene post orogenic sequences that deposited on top of the deformed internal Apennines units during the rifting of the Tyrrhenian Sea basin did not undergo vertical-axis rotations (Sagnotti *et al*., 1994; Mattei *et al*, 1996) (Fig 4.9d).

4.6 Conclusions

The tectonic evolution of Central Mediterranean has been mainly characterized by two coeval processes, which occurred during the progressive slab roll-back of the subducting Adriatic-Ionian lithosphere. These processes are the drifting and CCW rotation of the Corsica-Sardinia block and the progressive curvature of the Northern Apennines chain. These two events have been usually considered separately, as paleomagnetic evidences of the first process derived from the Corsica-Sardinia block, not involved in the Apennines orogen, whereas the curvature of the arc was mainly described using paleomagnetic data from the more external units of the Northern Apennines, which during the Corsica-Sardinia rotation represented the foreland domain of the Apennines.

Paleomagnetic data from the Tuscan Nappe units, located in the internal portion of the Northern Apennines, allow filling this gap and demonstrate that during the Corsica-Sardinia drifting the Northern Apennines orogenic wedge also rotated CCW, suggesting that in this phase the Adriatic-Ionian subduction slab roll-back caused the CCW rotation of the whole upper plate of the Central Mediterranean subduction system. This scenario changed with the end of the Corsica-Sardinia drifting and CCW rotation, when back-arc extensional processes were transferred to the Northern Tyrrhenian basin. Since that time the vertical axis rotations were confined to the external part of the Apennines orogenic wedge, which progressively acquired its present-day curvature as a consequence of the slab roll-back of the subducting Adriatic slab, whereas the extensional basins located along the northern Tyrrhenian basin did not rotate during the same time interval. This difference is probably related to the different style of back-arc opening between the Ligure-Provencal basin, characterized by drifting and oceanic crust production, respect to the northern Tyrrhenian Sea, where extensional tectonics never evolved from the rifting to the drifting stage.

Chapter 5

The magnetic fabric of the Tertiary sediments of the internal Tuscan Nappe successions (Northern Apennines, Italy)

5.1 Introduction

The analysis of the anisotropy of magnetic susceptibility (AMS) represents a suitable tool to identify both the depositional (Rees, 1965; Schieber and Ellwood, 1988; Kissel *et al.*, 1997) and tectonic processes which occur in sediments (e.g., Kissel *et al*., 1986; Borradaile, 1988; Aubourg *et al*., 1991; Rochette *et al*., 1992; Housen *et al.*, 1993; Tarling and Hrouda, 1993; Pares and van der Pluijm, 2002; Cifelli *et al*., 2004, 2005). Generally, the magnetic susceptibility ellipsoid (with $K_{max} \geq K_{int} \geq K_{min}$) of undeformed sediments is oblate, with the foliation plane (K_{max}–K_{int}) parallel to the bedding plane. This fabric is attributed to depositional and/or compaction processes (Lowrie and Hirt, 1987; Lee *et al*., 1990; Paterson *et al.*, 1995) and may be controlled by flow regime. In these conditions, the magnetic lineation reflects the alignment of mineral long axes in the direction of the flow (e.g., Rees, 1965). If the sediments undergo tectonic deformation, a tectonic AMS sub-fabric will progressively develop, modifying the primary sedimentary magnetic fabric according to the amount and type of deformation. The magnetic fabric has a distinctive character in extensional and compressional tectonic settings (Kissel *et al*., 1986; Lowrie and Hirt, 1987; Sagnotti *et al.*, 1994b; Mattei *et al.*, 1997, 1999; Pares *et al*., 1999; Cifelli *et al.*, 2004). Consequently, it constitutes a valid tool in defining the deformation pattern in sedimentary rocks. In particular, this is the case of weakly deformed fine-grained sedimentary sequences, where no evident pervasive tectonic structures develop during

deformation (Graham, 1966; Borradaile and Tarling, 1981; Kissel *et al.*, 1986; Mattei *et al.*, 1997).

In the Italian Peninsula, several AMS studies have been carried out in sedimentary sequences of the Apenninic chain and the Tyrrhenian margin (Lowrie and Hirt, 1987; Sagnotti and Speranza, 1993; Sagnotti *et al.*, 1994b; Scheepers and Langereis, 1994; Winkler and Sagnotti, 1994; Averbuch *et al.*, 1995; Mattei *et al*, 1995; Sagnotti *et al*., 1998; Speranza *et al*., 1998; Mattei *et al.*, 2002; Cifelli *et al*. 2004, 2005, among others). All of these studies indicate a direct relationship between the magnetic fabric and the structural setting, showing that the AMS pattern is the result of the earliest stages of tectonic deformation and modification of the original sedimentary fabric, related to compaction processes.

In this study, a magnetic fabric study was carried out in the fine-grained sequences of the Tuscan Nappe succession, an internal area of Northern Apennines (Fig. 5.1). This area is located at the boundary between the more external Apenninic chain characterized by compressional regime and the internal Tyrrhenian margin where the extensional regime is predominant. Therefore the information on the tectonic regime recorded by sediments of this area represent an important element to reconstruct the geometry and timing of the deformation of this portion of the Apennine chain at local and regional scale, in the general framework of the geodynamic evolution of the Central Mediterranean area.

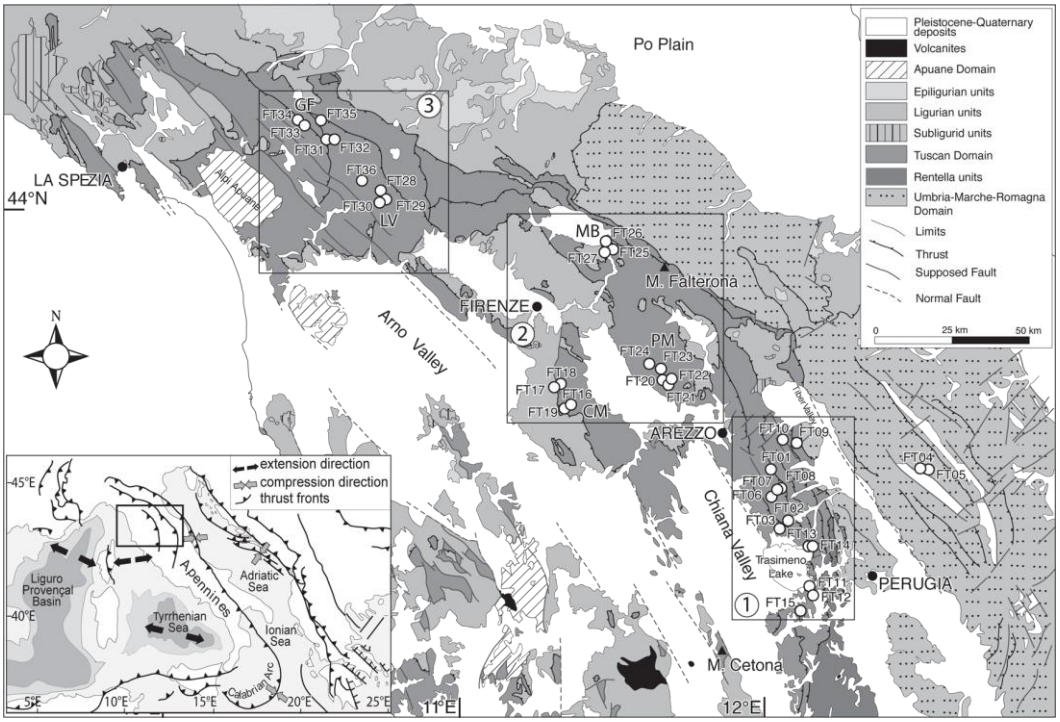

Fig. 5.1. Schematic map of the Northern Apennines and location of sampling sites.

5.2 Geological and tectonic setting

The Northern Apennines consists of several paleogeographic domains, organized in a fold and thrust belt forming a broad curved structure with an eastward (Adriatic) vergence (Fig. 5.1). The curvature of the arc follows the Adriatic margin of the belt, with the orientation of the main structures ranging from NW-SE/WNW-ESE in the north to almost N-S in the south. Several second-order arcs developed besides the principal arc, in response to heterogeneities in the stratigraphic sequences and out-of-sequence nappe stacking. The Northern Apennines is composed of a series of paleogeographic domains that form stacked structural units accreted onto the Adriatic foreland (Baldacci *et al.*, 1967; Elter, 1975; Boccaletti *et al*.,1980; Principi and Treves, 1984; Barchi *et al*., 1998a, b; Costa *et al.*, 1998) (Fig. 5.1). The uppermost nappes of the Northern Apennines are represented by oceanic (Ligurian) and transitional (sub-Ligurian) domain units, characterized by the occurence of Jurassic ophiolites and their Jurassic-early Cretaceous sedimentary cover, overlain by Cretaceous-Oligocene flysch sequences. The Ligurian domain units overthrust eastward the Tuscan domain units, formed by Upper Triassic to Eocene marine carbonates and by Oligocene-Lower Miocene foredeep sequences, which are deformed in an array of thrust sheets and ultimately thrust over the Umbria-Marche-Romagna units. The latter consists of sedimentary sequences deposited on a continental margin with basal late Triassic evaporites, platform carbonates (Lias) and pelagic sequences (Jurassic-Eocene) enriched upward in terrigenous deposits (Paleogene) and flysch sequences (Miocene).

The tectonic evolution of the Northern Apennines is characterized by the progressive migration of the orogenic front toward the Adriatic foreland, which is marked by the onset of siliciclastic deposits which get progressively younger toward the Adriatic foreland. The onset of siliciclastic deposition occurred in Northern Apennines during late Cretaceous in the oceanic Ligurian domain. The Ligurian oceanic domain was deformed during late Cretaceous to early Eocene time, and formed a double vergent accretionary wedge, now outcropping from Corsica to Italian peninsula (Treves 1984; Carmignani *et al.*, 1994). Starting from the Oligocene onwards, foredeep basins migrated eastward and formed on the top of continental sequences, belonging to the passive margin of Apulia. Their incorporation into the Apennines orogenic wedge marked the subduction of Adriatic continental lithosphere underneath Europe. Afterwards, during the Neogene, foredeep basins further migrated toward the Apulia foreland in front of the migrating thrust nappes. In Northern Apennines such process is well documented by stratigraphic and seismic studies, which precisely constrain the Neogene evolution of the foredeep basins in the front

of the Apennines chain (e.g., Patacca *et al.*, 1992; Calamita *et al.*, 1994; Pieri *et al*,. 1994). Foredeep basins formed on top of progressively easternmost (external) units, up to the Adriatic foreland. The formation and evolution of foredeep basins were driven by the loading of the adjacent thrust belt and related to subduction processes, such as the flexural retreat of the subducting lithosphere (Royden *et al.*, 1987). This process was particularly severe during Plio-Pleistocene times as evidenced by the presence, in the external part of the Apennines chain, of a foredeep-basin system, which contains up to 8 km of Pliocene-Quaternary sedimentary rocks (Royden *et al.*, 1987).

Extensional tectonics on the Northern Tyrrhenian sector was coeval with thrust emplacement in the external Umbria-Marche-Romagna chain, with both extensional and compressional fronts migrating toward the Adriatic foreland from middle Miocene up to Pleistocene (e.g., Elter *et al.*, 1975). Extensional tectonics dissected the already formed Apennines chain and generated new NW-SE trending extensional basins filled by 'neoautochthonous' marine and continental sequences (Jolivet *et al*,. 1998; Collettini *et al.*., 2006 and references therein). Moreover, crustal thinning, high heat flow and upraise of magmatic bodies accompanied extensional tectonics along the Tyrrhenian margin. Today, active tectonics is represented by NW-SE normal faults, with a well documented historical and recent seismicity, mostly located in the internal sector of the Umbria-Marche-Romagna region, at the edges of intramontane basins (among others, Chiaraluce *et al.*, 2004).

5.3 AMS sampling areas and methodology

In this study, AMS sampling was carried out in the Tuscan Domain, in the internal sector of Northern Apennines. In particular, three main areas have been investigated: (1) the area around the Trasimeno Lake, (2) Chianti Mountains and Pratomagno area, and (3) the Val di Lima and Garfagnana area (Fig. 5.1). In total, 36 sites were sampled (528 oriented cylindrical samples). Samples were drilled using an ASC 280E petrol-powered portable drill with a water-cooled diamond bit. The cores were oriented in situ with a magnetic compass, corrected to account for a local ~2° magnetic declination according to the NOAA National Geophysical data center.

5.3.1 Trasimeno Lake area

The Trasimeno Lake area is characterized by the presence of four major tectonic units, piled up during the Miocene that are from west (top) to east (bottom): the Ligurian

units, consisting of Jurassic ophiolites; the Tuscan Nappe (Tuscan allochthon), an east-verging imbricate thrust-stack made up of pelagites and siliciclastic turbidites (Mirabella *et al*., 2011); a transitional unit (Mt. Rentella Unit) including polychromic marls of Mt. Rentella (Brozzetti *et al.,* 2010) and Aquitanian-Burdigalian foredeep siliciclastic turbidites of the Montagnaccia Fm. (Barsella *et al.,* 2009); and the Umbria unit, characterized by a meso-cenozoic carbonates succession followed by the foredeep turbidite succession of the Marnoso Arenacea Fm. (Early-Middle Miocene) (Mirabella *et al*., 2011). Some authors (e.g., Abbate and Bruni, 1989; Brozzetti, 2007) have suggested that the outermost part of the Tuscan Nappe belongs to a separate tectonic unit (Falterona-Cervarola Unit or Falterona Nappe). In this study, the Falterona-Cervarola Unit is considered as belonging to the Tuscan Nappe, according to Plesi *et al.* (2002).

In this area, the Tuscan Nappe succession has been sampled. Six sites (FT03, FT11-FT15) were sampled in the pelagic foreland ramp deposits of the Scaglia Toscana Fm., consisting of calcareous-marly turbidites and varicoloured shales and marly-shale layers (Ypresian-Lutetian). Seven sites (FT01, FT02, FT06-FT10) were sampled in the foredeep turbidite deposits of the Macigno Fm, which consists of thick coarse-grained siliciclastic turbidites alternating with siliciclastic thin and fine grained beds (Aquitanian) (Fig. 5.1).

Among the Scaglia Toscana Fm. sites two continues and well exposed section have been sampled (FT03 and FT15 sites). The first section is located in the Montanare Cave northern of Trasimeno Lake (site FT03 in Fig. 5.1). The section consists of alternating calcareous marls and marly-shales layers for a total thickness of about 70m. The lithofacies is characterized by limestone nut-brown strata, generally 5–40 cm thick with grey chert in nodules and lens. The varicoloured marly-shale interstrata have a smaller thickness in the order of millimeters or centimeters. The samples have been collected in calcareous strata, in which a total of 44 samples were drilled considering a variable spacing ranging from 60 to 300 cm.

The second section is exposed at the NW of Mt. Solare in the Casilini Cave at south of Trasimeno Lake (site FT15 in Fig. 5.1). The section has a total thickness of about 50 m and it is mainly made up of an alternating calcareous and shale, marly-shales layers. The calcareous strata are mainly thin-bedded grey-red limestone (strata are normally 10–40 cm thick) with in some cases nodules and lens of chert, convolute lamina and bioturbations (at the top of the strata). These strata are interbedded with thin varicoloured shale and marly-shale layers (strata are normally 2–16 cm thick). A total of 53 samples are drilled from calcareous strata, with an average sampling spacing ranging from 60 to 120 cm.

5.3.2 Chianti Mountains and Pratomagno area

The structure of the Chianti Mountains has been interpreted as a result of thrust-and-fold deformation (Bonini, 1999) and it is characterized by the Tuscan Nappe succession, which in this area is largely exposed (from Upper Cretaceous to Lower Eocene members). The main structural feature of this region is an E-NE vergent steeply to moderately dipping, overturned anticline, which folds the Macigno sandstone and exposes Scaglia Toscana Fm at its core (Bonini *et al*., 2012). Referring to Sagri *et al*., (2012), the Tuscan Nappe in this sector is thrust onto the more external Cervarola-Falterona unit. Falterona succession, cropping-out in the Pratomagno ridge, consists of Rupelian-Chattian varicoloured clays alternating mudstone layers (Villore Marls) at the bottom following by the Chattian-Burdigalian Falterona Fm. This silicoclastic turbidites deposits have been subdivided into five member, on the base of thickness of the layers and arenites/pelites ratio (Bortolotti *et al.*, 2012). The succession ends with the Vicchio Marls Fm. that crops out mainly in the Mugello Basin area. This formation consist of gray marls and silty marls, interbedded by thin sandstone layers with calcareous component

In this area four sites (FT16-FT19) were sampled in the pelagic and ramp deposits of the Scaglia Toscana Fm, whereas 5 sites (FT20-FT24) were sampled in the foredeep turbidite deposits of the Falterona Fm, whereas 3 sites were taken from the Burdigalian thrust top deposit of the Marne di Vicchio Fm. (FT25-FT27) (Fig. 5.1).

5.3.3 Val di Lima and Garfagnana area

The main structural feature of Val di Lima area is a very large east-verging recumbent fold, with the hinge located in the Montale–Lucchio alignment. It has formed during two folding phases, the first referred to Late Tortonian and the second one to Messinian time (Fazzuoli *et al*., 1994; 1998). The second relevant characteristic of this area is represented by the several tectonic contacts between the Macigno Fm and the Scaglia Toscana and Maiolica Fms. related to activity of low-angle thrust faults that cut these formations (Fazzuoli *et al*., 1998). Moreover this area is affected by large NW-SE and E-W normal fault that intersect the recumbent fold and create a tectonic boundary between the Mesozoic deposits and the Oligocene turbidite deposits (Macigno fm.) (Fazzuoli *et al*., 1998). The stratigrafic succession with thick Jurassic formation, testify a subsident paleogeographic domain since Middle Jurassic until Oligocene time (Cerrina Feroni and Patacca, 1975; Fazzuoli, 1980). In Val di Lima and Garfagnana areas the Jurassic-Cretaceous *condensed* and *reduced sequences* crop out, such as consequent of a non-uniform physiography. The consequent

effect is a discordant deposition of Scaglia Toscana Fm. on top of Rosso Ammonitico Fm.. The upper part of Scaglia Toscana Fm. is interpreted as deposited in base-escarpment environment of a active margin. In this formation three lithofacies has been distinguished, the lithofacies sampled is Argilliti dell'Orecchiella, consisting of red, gray-green clays interbedded with centimeter calcareous strata. This lithofacies can be referred to Cenomanian-Rupelianan time (Fazzuoli *et al*., 1998). This area is characterized by compressive deformation, starting from Eocene Time and culminating during upper Oligocene- late Miocene time, during which Ligurian unit thrusted on to more external domain and structuring of Falda Toscana occurred (Boccaletti *et al*., 1980; Carmignani *et al.*, 1978; Chicchi and Plesi, 1991a,b; 1992, Costa *et al*., 1998).

In Val di Lima area 4 sites have been collected in the Mesozoic core: (a) 3 sites (FT28-FT29-FT30) were collected in the Scaglia Toscana Fm., cropping out in a portion of the Mesozoic core south of Lucchio village; (b) one site (FT36) was sampled in the northernmost part of the Mesozoic core, NE of Montefegatesi village (LV Fig. 5.1). In the Garfagnana area three sites (FT33-34-35) have been sampled in the Corfino Mesozoic core while FT31 and FT32 sites have been sampled in the Mesozoic core near Sassorosso village (GF Fig. 5.1).

5.3.4 Magnetic methods

AMS and rock magnetic analyses were carried out at the paleomagnetic laboratory of the Roma Tre University and Istituto Nazionale di Geofisica e Vulcanologia (INGV, Rome), respectively. The measurement of the low-field anisotropy of magnetic susceptibility (AMS) represents a cheap, rapid and non-destructive technique for the characterization of the mineral fabric of rocks (Hrouda, 1982). AMS is defined by a second rank tensor and represented geometrically in terms of an ellipsoid in which the greatest intensity of magnetization is induced along the long axis K_{max} and the weakest intensity along the short axis K_{min} (with the principal axes $K_{max} > K_{int} > K_{min}$). Several parameters have been defined both for the quantification of the magnitude of anisotropy and for defining the shape of the ellipsoid (see Tab. 5.1, Jelinek 1981 and Hrouda 1982). The mean susceptibility values K_m have been computed as $K_m=(K_{max}+K_{int}+K_{min})/3$. The magnetic lineation L (K_{max}/K_{min}) is defined by the orientation of K_{max}, while the magnetic foliation F (K_{int}/K_{min}) is defined as the plane perpendicular to K_{min}. T is the shape parameter and range from -1 (perfectly prolate ellipsoid with L >> F) to +1 (perfectly oblate ellipsoid with F << L) with zero values corresponding to a sphere (F ~ L). The anisotropy degree is expressed

by the parameter Pj (Jelinek, 1981) which is obtained considering all the three principal susceptibility values. Anisotropy of magnetic susceptibility (AMS) was measured for all samples using a KLY-3S kappabridge magnetic susceptibility meter. Results are shown on an equal area stereographic projection using the Jelínek and Kropáček (1978) statistics.

In order to identify the main magnetic minerals in the studied sediments, we carried out a series of rock magnetic analyses on selected specimens. The measurements included: (1) Isothermal Remnant Magnetization (IRM) acquisition curves, carried out on 38 samples; (2) stepwise thermal demagnetization of a composite isothermal remanent magnetization (IRM) produced by sequential application of pulsed fields of 0.12 T, 0.6 T and 2.7 T along three mutually orthogonal sample axes for 58 selected samples, and (3) hysteresis properties of small rock fragments from 6 selected samples for each formation. The hysteresis properties were measured on a Micromag alternating gradient magnetometer (AGM model 2900, Princeton Measurements Corporation) with a maximum applied field of 1 T.

5.4 Rock magnetism and AMS Results

Magnetic susceptibility (K) is highly variable within the sampled sites, with most of the samples characterized by susceptibility values in the 0-400 x 10^{-6} SI range (Fig. 5.2a). These values are typical of fine-grained sediments with low ferrimagnetic mineral content, whose susceptibility and magnetic fabric are mostly determined by paramagnetic and diamagnetic minerals in the clay matrix (Borradaile *et al*., 1986; Rochette, 1987; Sagnotti *et al*., 1998). Magnetic susceptibility values of the Scaglia Toscana Fm. display a wide distribution, with a main clustering at low values (K_m between 0 and 90 x 10^{-6} SI) (Fig. 5.2b). These susceptibility values are lower than those characterizing the distributions of the younger sediments of the Macigno, Falterona and Marne di Vicchio Fms. (K_m between 82 and 382 x 10^{-6} SI) (Fig. 5.2c). The different trends are related to the different magnetic minerals present in the rock matrix. Low susceptibility values can be observed in all the three analyzed areas of the Scaglia Toscana Fm. (Fig 5.2 d,e,f) and can be ascribed to the main contribution of diamagnetic minerals (i.e. calcite). However, in the Garfagnana area higher values of susceptibility indicate an additional contribution of paramagnetic minerals to the magnetic signal (Fig. 5.2f). On the other hand, paramagnetic minerals seem to be the most representative magnetic minerals in the Macigno, Falterona and Marne di Vicchio Fms. sediments. Turbidites deposits from the Macigno and Falterona Fms. show higher

susceptibility values (K_m between 120 x 10^{-6} SI and 382 x 10^{-6} SI) compared to the Marne di Vicchio Fm. thrust top deposits (K_m between 82 x 10^{-6} SI and 152 x 10^{-6} SI). This

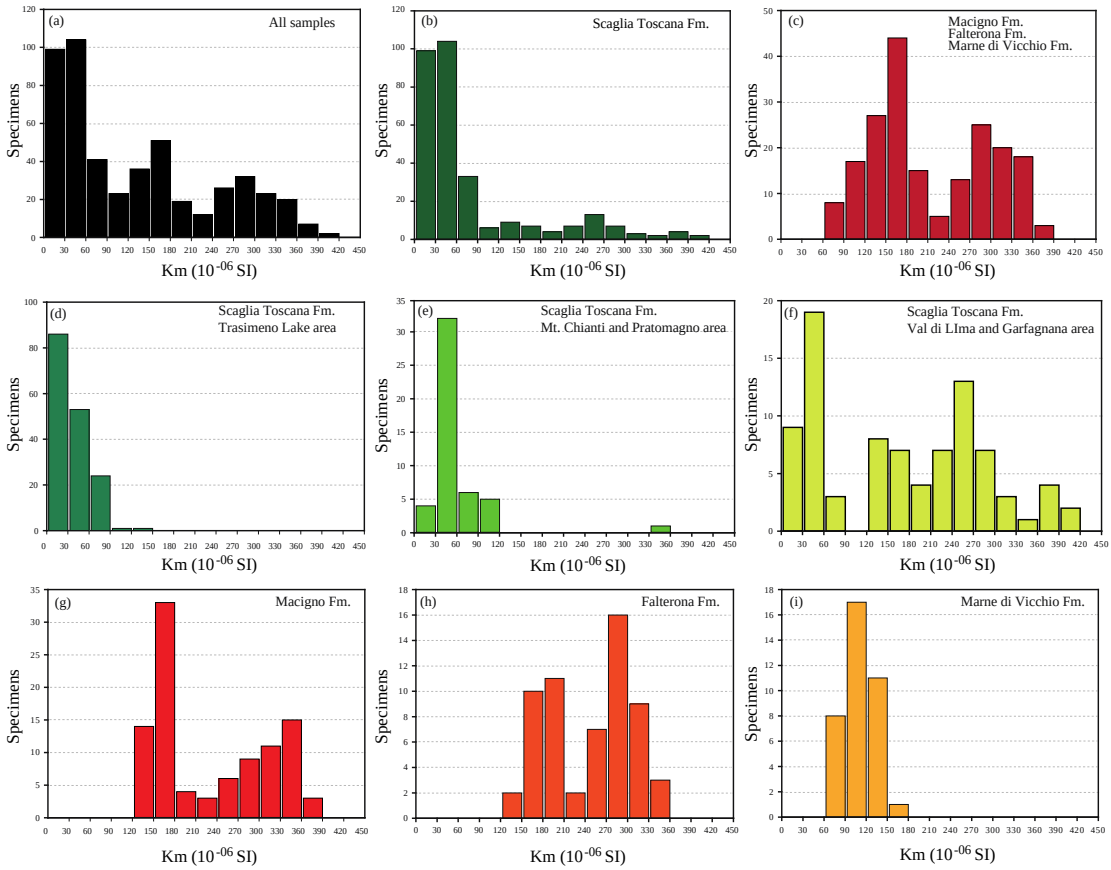

Fig. 5.2. Frequency distribution of the mean susceptibility (K_m) values for: (a) the entire set of 495 specimens; (b) Macigno, Falterona and Marne di Vicchio Fms.; (c) Scaglia Toscana Fm..

difference can be related to the higher contribution of diamagnetic minerals in marls (Fig. 5.2i) with respect to the sandstone and limestone of turbidite deposits (Fig. 5.2 g,h).

In the Scaglia Fm. samples, hysteresis loops show the prevalent paramagnetic behaviour, with a distinct ferromagnetic contribution (Fig. 5.3a-c). As already illustrated in chapter 4, IRM curves and the thermal demagnetization of a composite IRM (Lowrie, 1990) of these samples indicate that most of the samples do not saturate at the maximum applied field (Fig. 4.3a). For these samples, the maximum unblocking temperature spectra is ~ 680° indicating the presence of high coercivity minerals, such as hematite (Fig. 4.3c). This is confirmed by the high values of the remanence coercivity (Hcr) (Fig. 5.3d-f), which indicate hematite as the main ferromagnetic mineral.

Samples from Macigno Fm., Falterona Fm. and Vicchio Fm. show a ‘closed’ hysteresis loop, suggesting that the paramagnetic contribution is dominant (Fig. 5.3g-i). The totality of these samples saturate at 0.3T (Fig. 4.3b), indicating that the high coercivity component is not significant in these sediments. The stepwise thermal demagnetization of a three-component IRM shows that the low-coercivity component is removed at 580°C, suggesting that the magnetic mineralogy is dominated by magnetite (Fig. 4.3f-h). The presence of low-coercivity minerals (magnetite) is confirmed by the low values of Hcr (Fig. 5.3j-l).

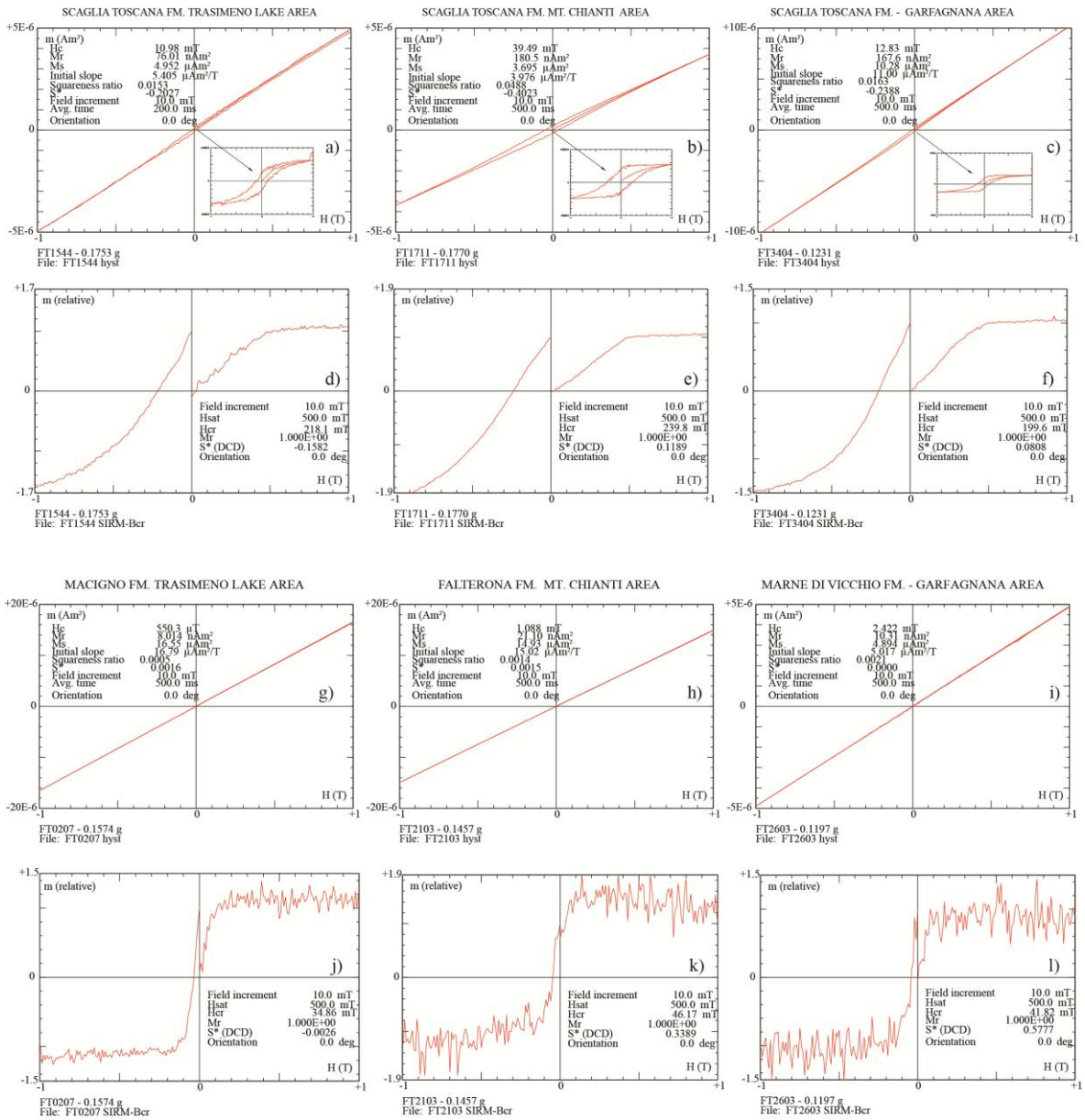

Fig. 5.3. Hysteresis loop for representative samples (a-f) of the Scaglia Toscana Fm.; (g) Macigno, Falterona (h) and Marne di Vicchio (i) Fms.. For each samples, the stepwise acquisition of an isothermal remnant magnetization (IRM) in fields up to 1 T and back-field demagnetization curves are also reported.

A weak correlation between site mean susceptibility values and the corrected anisotropy parameter Pj (as defined by Jelinek, 1981) is observed in the younger sediments, while it is not visible in the specimens from the Scaglia Toscana Fm., which show generally lower degree of anisotropy (Fig. 5.4a). In all the investigated samples, the Pj values are always relatively small, lower than 1.13, indicating a poorly developed magnetic fabric and therefore weakly deformed sediments. The shape and eccentricity of the susceptibility ellipsoids have been evaluated by plotting the Pj versus T parameters (Fig. 5.4b) and magnetic lineation (L) vs magnetic foliation (F) values (Fig. 5.4c). In general, T parameter is positive for all sites reflecting an oblate shape of the AMS ellipsoid (with F > L). Only site FT36 belonging to the Scaglia Toscana Formation from the Garfagnana area shows a prolate fabric. Samples from Macigno, Falterona and Marne di Vicchio Fms. are characterized by a strongly oblate fabric due to well developed magnetic foliation (1.03 < F< 1.11 and 1.00 < L < 1.01) (Fig. 5.4c). In contrast, Scaglia Toscana Fm. sites show lower values of the T parameter and higher values of L (1.01 < F < 1.06 and 1.00 < L < 1.03).

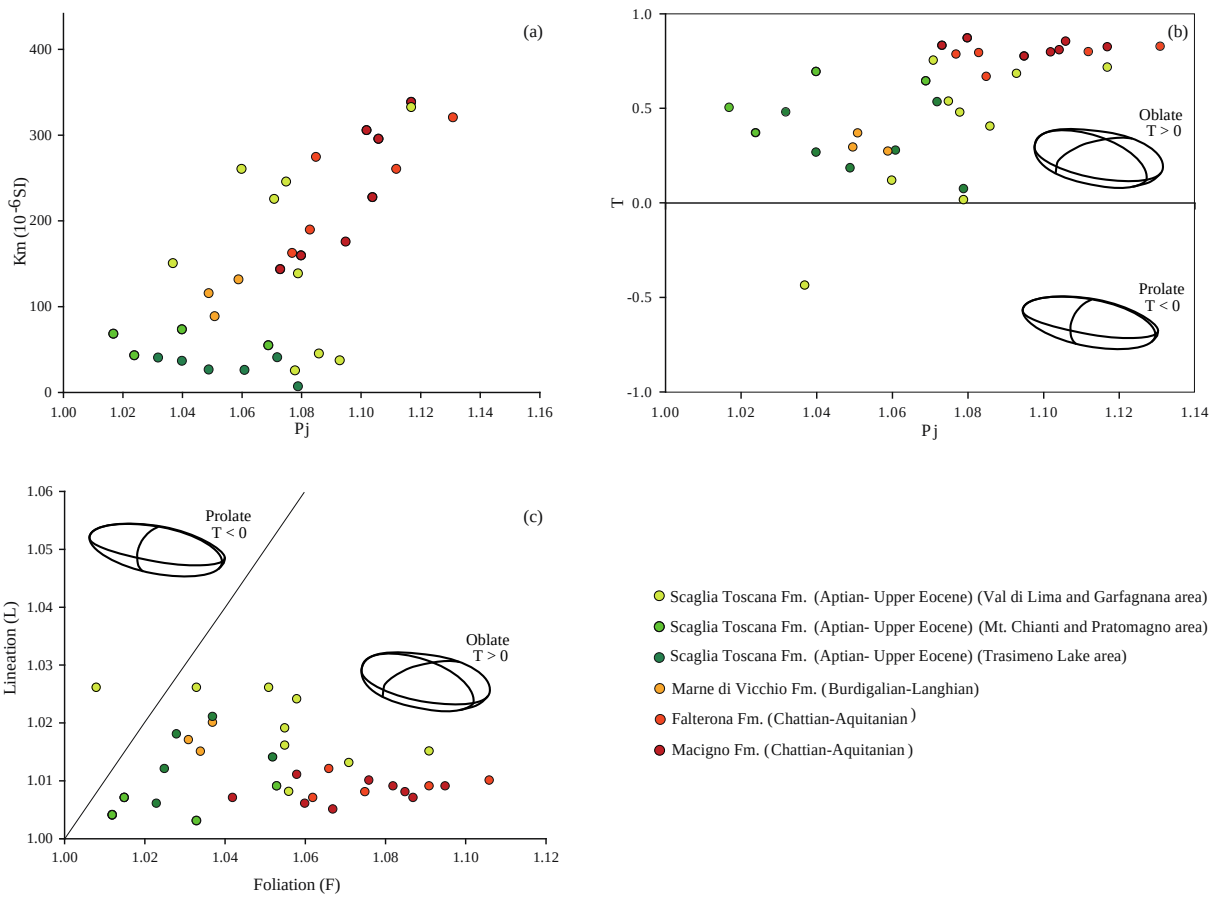

Figure. 5.4. Degree of anisotropy Pj vs. mean susceptibility K_m for at each site. (b) T- Pj plot for all investigated sites; (c) F-L plot for all investigated sites.

The main magnetic susceptibility directions for each site are tightly grouped with a well-defined magnetic foliation and magnetic lineation (Fig. 5.5). In most of the sites, the magnetic foliation is parallel to the bedding plane. Moreover, many sites clearly show distinct magnetic lineation as defined by clustering of the K_{max} axes. On the basis of the semi-angle of 95% confidence ellipse in the K_{max} - K_{int} plane (e_{12}) it is possible to distinguish the degree of lineation. We consider a lineation "well defined" when $e_{12} < 30°$, "poorly defined" when $30° \leq e_{12} \leq 45°$ and "not defined" when $e_{12} \geq 45°$ (Tab. 5.1).

In the Trasimeno Lake area (Tab. 5.1 and Fig. 5.5a,b), the lineation of Scaglia Toscana Fm. is well defined for 2 sites (FT13 and FT14), while it is poorly and not defined for FT11, FT12 and FT03, FT15 respectively. Among the 4 investigated sites of the Mt. del Chianti and Pratomagno area (Fig. 5.5c,d), two sites with poorly defined (FT16,18) and two sites with well defined lineation (FT17,19) have been recognized. Finally, in the Val di Lima and Garfagnana area (Fig. 5.5e,f), all the studied sites show a well defined lineation.

For Macigno Fm., in the Trasimeno Lake area, 5 sites show a well defined lineation (see site FT01 and FT02 in Fig. 5.5g, h,), whereas two sites show poorly defined (FT06) and not defined (FT07) magnetic lineation. In the Mt. Chianti and Pratomagno area, all the Falterona Fm. sites show a well defined lineation but one site showing a poorly defined lineation (Fig. 5.5 i,j). Finally, all the sites of the Marne di Vicchio Fm. display a well defined lineation (Fig. 5.5 k,l).

Table 5.1. List of anisotropy factors computed at each site.

Site	Coordinates (Lat-Long)	Lithology	Formation	Age	N.	S_0	Km	L	F	P'	T	Kmax (D, I)	Kint (D, I)	Kmin (D, I)	E1-2	E3-2
						Umbria Area										
FT01	43° 20' 48.3", 12° 02' 09.2"	Sand-limestone	Macigno (Mac3)	Aquitaniano	14	263,42	3.38E-04	1.009	1.095	1.117	0.822	305.1, 16.3	203.6, 34.5	56.2, 50.8	18.7	3.7
FT02	43° 14' 49.4", 12° 06' 28.1"	Sand-limestone	Macigno (Mac3)	Aquitaniano	11	246,30	3.05E-04	1.009	1.082	1.102	0.795	314.7, 5.3	221.6, 30.2	53.7, 59.2	6.3	2.5
FT03	43° 14' 32.3", 12° 04' 54.9"	Mudstone	Scaglia Toscana	Eocene	45	variable	3.61E-05	1.012	1.025	1.040	0.264	282.5, 16.4	186.0, 21.1	47.5, 62.8	60.3	14.0
FT04	43° 23' 10.4", 12° 33' 25.7"	Sand-limestone	Shlier	Aquitaniano	22	29,46	1.04E-04	1.007	1.042	1.053	0.683	324.6, 5.1	58.4, 36.6	227.9, 53.0	15.7	4.6
FT05	43° 23' 01.0", 12° 33' 52.4"	Sand-limestone	MarnosoArenacea	Burdig-Lang.	19	39,57	1.64E-04	1.011	1.058	1.075	0.665	324.2, 14.8	88.1, 64.5	228.6, 20.2	14.8	6.8
FT06	43° 17' 53.5", 12° 02' 22.6"	Sand-limestone	Macigno (Mac3)	Aquitaniano	19	variable	2.27E-04	1.008	1.085	1.104	0.813	310.5, 2.4	218.5, 38.6	43.5, 51.3	34.2	4.9
FT07	43° 17' 57.2", 12° 02' 30.4"	Sand-limestone	Macigno (Mac3)	Aquitaniano	13	235,30	2.95E-04	1.007	1.087	1.106	0.851	147.9, 4.7	241.1, 34.1	51.1, 55.4	45.6	3.9
FT08	43° 18' 13.8", 12° 04' 34.9"	Mudstone	Macigno (Mac3)	Aquitaniano	12	variable	1.75E-04	1.010	1.076	1.095	0.773	160.5, 14.0	257.1, 24.8	43.7, 61.0	7.0	3.2
FT09	43° 27' 34.6", 12° 08' 12.2"	Mudstone	Macigno (Mac3)	Aquitaniano	14	230,21	1.43E-04	1.006	1.060	1.073	0.828	245.0, 25.8	146.4, 17.1	26.6, 58.3	22.2	2.6
FT10	43° 27' 46.8", 12° 07' 40.3"	Mudstone	Macigno (Mac3)	Aquitaniano	15	160,11	1.59E-04	1.005	1.067	1.080	0.869	101.4, 10.0	193.6, 12.4	333.5, 74.0	21.5	3.8
FT11	43° 05' 14.2", 12° 10' 50.0"	Mudstone	Scaglia Toscana	Eocene	13	variable	6.37E-06	0.841	0.883	1.079	0.071	355.0, 14.5	128.8, 69.5	261.3, 14.1	30.9	18.7
FT12	43° 04' 17.7", 12° 11' 22.6"	Mudstone	Scaglia Toscana	Eocene	16	variable	2.60E-05	1.018	1.028	1.049	0.182	345.5, 16.2	204.1, 69.7	79.1, 12.0	31.9	22.6
FT13	43° 10' 54.6", 12° 10' 21.7"	Mudstone	Scaglia Toscana	Eocene	17	variable	4.03E-05	1.014	1.052	1.072	0.531	350.2, 2.4	257.6, 47.4	82.4, 42.5	22.5	6.8
FT14	43° 10' 53.3", 12° 10' 26.3"	Mudstone	Scaglia Toscana	Eocene	11	variable	2.55E-05	1.021	1.037	1.061	0.275	165.0, 5.3	67.2, 55.9	258.5, 33.6	13.4	12.1
FT15	43° 02' 38.7", 12° 08' 52.7"	Mudstone	Scaglia Toscana	Eocene	68	variable	3.99E-05	1.006	1.023	1.032	0.477	304.4, 31.5	165.3, 50.9	47.8, 20.6	57.2	7.4
						Monti del Chianti e Pratomagno Area										
FT16	43° 32' 19.8", 11° 24' 32.9"	Mudstone	Scaglia Toscana	Eocene-Oligoc.	13	248,09	$7.29E^{-05}$	1.003	1.033	1.040	0.691	251,2 / 20,7	156,2/ 13.0	36.3 / 65.2	33.2	6.3
FT17	43° 35' 58.2", 11° 22' 02.1"	Mudstone	Scaglia Toscana	Eocene-Oligoc.	11	73,17	$5.42E^{-05}$	1.009	1.053	1.069	0.641	155.1 / 1.0	64.7 / 24.2	247.4 / 65.8	21.5	4.0
FT18	43° 36' 09.0", 11° 22' 21.2"	Mudstone	Scaglia Toscana	Eocene-Oligoc.	13	24,23	$4.26E^{-05}$	1.007	1.015	1.024	0.367	307.0 / 6.3	38.6 / 13.8	193.2 / 74.7	42.8	14.5
FT19	43° 32' 06.3", 11° 22' 41.0"	Mudstone	Scaglia Toscana	Eocene-Oligoc.	11	220,22	$6.77E^{-05}$	1.004	1.012	1.017	0.501	141.7 / 5.3	232.4 / 7.4	16.2 / 80.9	26.7	7.6
FT20	43° 37' 28.7", 11° 40' 43.8"	Sand-limestone	Falterona (Fal 2)	Chattian.Aquit	16	variable	$2.60E^{-04}$	1.009	1.091	1.112	0.796	328.0 / 4.3	58.4 / 5.1	198.2 / 83.3	10.0	4.5
FT21	43° 37' 23.7", 11° 40' 59.1"	Sand-limestone	Falterona (Fal 2)	Chattian.Aquit	13	55,19	$2.74E^{-04}$	1.012	1.066	1.085	0.665	333.0 / 8.2	65.5 / 17.1	218.3 / 71.0	16.3	5.7
FT22	43° 37' 40.2", 11° 41' 00.1"	Sand-limestone	Falterona (Fal 3)	Chattian.Aquit	11	variable	$3.20E^{-04}$	1.010	1.106	1.131	0.824	127.9 / 3.6	37.2 / 11.2	235.5 / 78.2	33.0	4.0
FT23	43° 38' 13.5", 11° 40' 30.8"	Sand-limestone	Falterona (Fal 3)	Chattian-Aquit.	9	70,11	$1.62E^{-04}$	1.007	1.062	1.077	0.783	312.3 / 5.0	43.0 / 8.2	191.3 / 80.4	11.4	3.1
FT24	43° 38' 51.8" , 11° 39' 38.9"	Sand-limestone	Falterona (Fal 3)	Chattian-Aquit.	8	110,9	$1.90E^{-04}$	1.008	1.075	1.093	0.797	143.3 / 4.3	53.0 / 4.4	277.2 / 83.8	10.7	0.9
FT25	43° 55' 43.1", 11° 29' 57.9"	Marls	Marne Vicchio	Burdig-Lang.	12	340,25	$8.81E^{-05}$	1.015	1.034	1.051	0.366	299.4 / 16.9	30.4 / 3.4	131.5 / 72.7	5.2	1.8
FT26	43° 55' 5.1", 11° 29' 41.8"	Marls	Marne Vicchio	Burdig-Lang.	13	32,25	$1.15E^{-04}$	1.017	1.031	1.049	0.286	297.2 / 1.9	28.4 / 32.2	204.2 / 57.7	7.8	3.7
FT27	43° 54' 48.8" , 11° 27' 14.8"	Marls	Marne Vicchio	Burdig-Lang.	12	80,10	$1.31E^{-04}$	L	F	P'	T	324.6 / 1.2	234.5 / 4.7	69.2 / 85.1	9.1	3.7
						Garfagnana Area										
FT28	44° 01' 53.1", 10° 43' 04.1"	Mudstone	Scaglia Toscana	Mid. Eocene	9	28,50*	$4.46E^{-05}$	1.024	1.058	1.086	0.402	324.6 / 27.0	77.7 / 37.0	208.8 /40.5	13.1	3.8
FT29	44° 00' 54.6",10° 43' 14.0"	Mudstone	Scaglia Toscana	Mid. Eocene	9	250,26*	$3.67E^{-05}$	1.013	1.071	1.093	0.681	316.1 / 7.7	222.7 / 24.1	62.6 / 64.5	25.0	4.2
FT30	44° 01' 14.9", 10° 43' 07.2"	Mudstone	Scaglia Toscana	Upper Creta- Paleoc	9	283,22	$2.49E^{-05}$	1.019	1.055	1.078	0.476	329.3 / 15	235.3 /14.6	103 / 68.8	21.2	2.8
FT31	44° 10' 52.6", 10° 24' 28.6"	Mudstone	Scaglia Toscana	Upper Creta- Paleoc	11	211,31*	$2.60E^{-04}$	1.026	1.033	1.060	0.116	156.2 / 19	254.8/ 23.4	31.0 / 59.1	10.1	4.0
FT32	44° 11' 02.5", 10° 24' 17.0"	Mudstone	Scaglia Toscana	Upper Creta- Paleoc	9	210.82*	$1.50E^{-04}$	1.026	1.008	1.037	-0.439	122/9.3	260/77.6	30.7/8.2	15.4	2.7
FT33	44° 11' 02.5", 10° 24' 17.0"	Mudstone	Scaglia Toscana	Upper Creta -Paleoc	9	263,37*	$2.45E^{-04}$	1.016	1.055	1.075	0.534	178.4/3.6	271/36.7	83.5/53.1	8.0	2.6
FT34	44° 12' 50.5", 10° 22' 19.6"	Mudstone	Scaglia Toscana	Upper Creta- Paleoc	10	283,36*	$2.25E^{-04}$	1.008	1.056	1.071	0.751	354.4/13.2	255.7/32.6	103.4/54.1	6.8	4.1
FT35	44° 12' 44.9", 10° 24' 43.1"	Mudstone	Scaglia Toscana	Upper Creta- Paleoc	12	39,29*	$3.32E^{-04}$	1.015	1.091	1.117	0.714	318.2 / 4.6	50.7 / 28.5	219.8 / 61.1	17.5	5.1
FT36	44° 04' 27.8", 10° 35' 28.5"	Mudstone	Scaglia Toscana	Mid. Eocene	9	284,26*	$1.38E^{-04}$	1.026	1.051	1.079	0.013	322.3 / 21.3	226.4/ 14.7	104.3 / 63.7	5.0	3.6

N = number of specimens $k_m = (k_{max} + k_{int} + k_{min}) / 3$ (mean susceptibility, in 10^{-6} SI units); $L=k_{max} /k_{int}$; $F=k_{int} /k_{min}$

$P' = \exp\{2[(\eta_1 - \eta)^2 + (\eta_2 - \eta)^2 + (\eta_3 - \eta)^2]\}^{1/2}$ (corrected anisotropy degree; Jelinek, 1981)

$T = 2(\eta_2 - \eta_3) / (\eta_1 - \eta_3) - 1$ (shape factor; Jelinek, 1981)

$\eta_1 = \ln k_{max}$; $\eta_2 = \ln k_{int}$; $\eta_3 = \ln k_{min}$; $\eta = (\eta_1 + \eta_2 + \eta_3) / 3$

D= declination, I= inclination. For each locality the line shows the site arithmetic mean values.

S_0 bedding attitude (azimuth of the dip and dip values). S_0 with *symbol are deduced by AMS tensor.

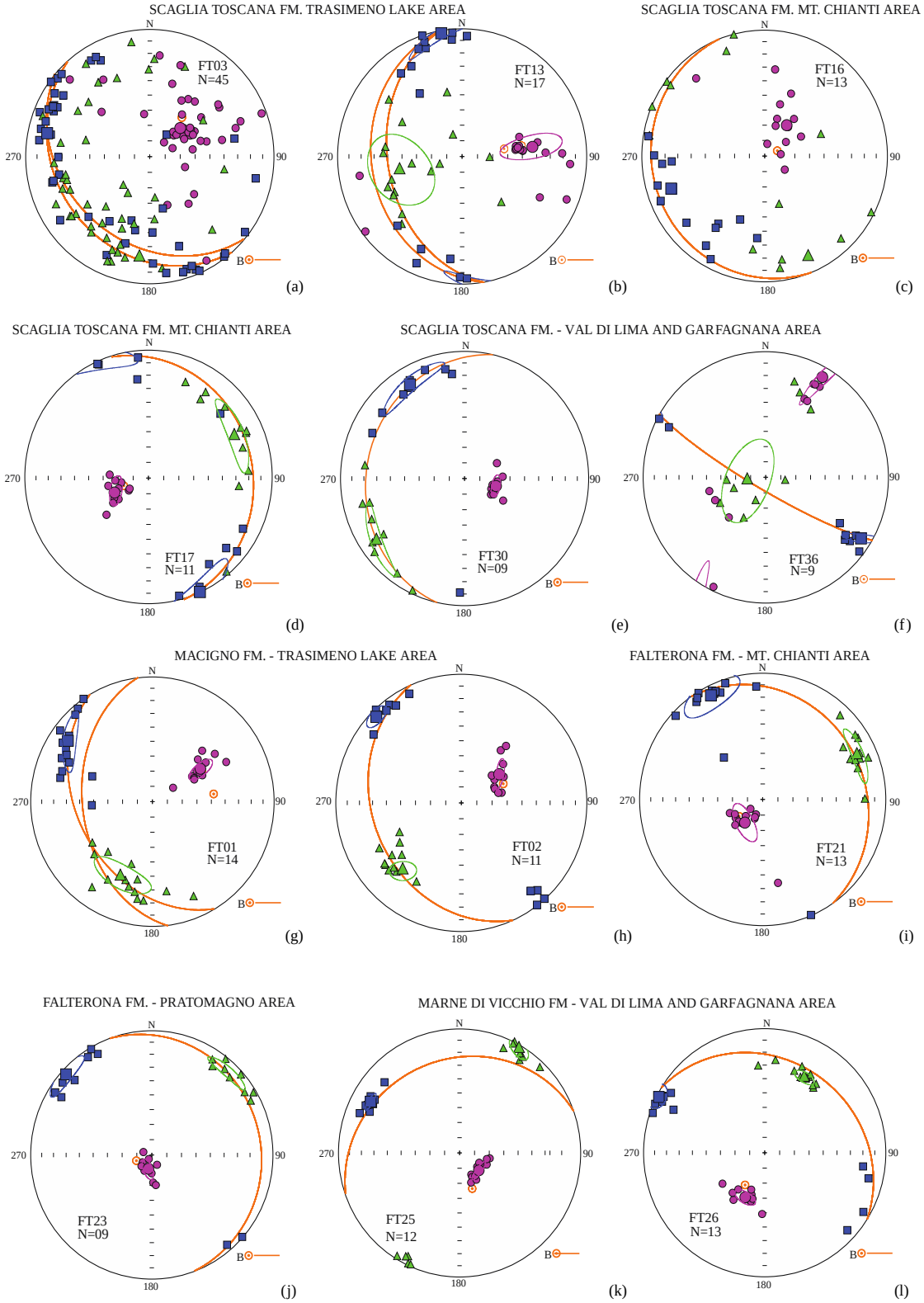

Figure.5.5. Magnetic anisotropy data for three representative sites (Equal-area Schmidt projection, lower hemisphere). The square represent the K_{max}; the triangle represents K_{int} and the circle represent K_{min}. The ellipses indicate the 95% region around the principal susceptibility axes.

5.5 Discussion

At the site scale, a well-defined magnetic lineation is well recognisable, even when the primary sedimentary fabric is still preserved, as is the case in most of the studied sites (Fig. 5.5). Such magnetic lineations in sedimentary rocks can be of depositional (related to depositional currents) or of tectonic origin. At all sites measured in this study the trend of the magnetic lineation is maintained through sequences that differ in sedimentological characters (carbonatic mudstone, marls or sandstone) and age (Upper Cretaceous - Paleogene; Oligocene - Middle Miocene). Furthermore, even though most of the samples sediments do not appear to be affected by deformation on the macroscopic scale, a magnetic fabric that can be related to the regional tectonic pattern is systematically observed. In fact, the distribution of magnetic lineation directions parallels the trend of folds and thrust faults at regional scale, supporting a tectonic origin for the observed magnetic lineation. The direction of the magnetic lineation strictly follows the present curved shape of the Northern Apennines from N-S in the southern sector to NW-SE in the northern sector of the chain (Fig. 5.6). In the southern area, the magnetic lineation of both Scaglia Toscana Fm. and Macigno Fm. assumed a NNW-SSE direction parallel to the thrust front and main fold axes, with the exception of two sites of Macigno Fm. that have about W-E directions. Moving northward, where the curvature of the arc is more accentuated, the lineation pattern for all three formations (Scaglia Toscana, Falterona and Marne di Vicchio Fms.) follow the same trend, except for one Scaglia Toscana site (FT16) in which the lineation is perpendicular to main fold axes. Finally, in the northernmost area (Garfagnana area), the magnetic lineation directions, of Scaglia Toscana Fm. sites, follow mainly the direction of the thrust front. This pattern indicates that the magnetic lineation formed during the early compressive phases of deformation of the Apennine chain. In few cases, such as of FT09,10 and FT16, the lineation is perpendicular at regional trend fold axes, possibly indicating that these sites are affected by local tectonic elements.

It is worth to note that the magnetic lineations found in the studied deposits are almost parallel to those published by Lowrie and Hirt (1987) for the pelagic marly limestones of the Cretaceous-Early Tertiary Scaglia Fm. in the Umbria region. Moreover, they are parallel to the magnetic lineations found in the foredeep Messinian clay-rich sediments from Marche-Romagna region (Sagnotti *et al*., 1998). These data suggest that, independently from the lithology, age and structural position, the development of the magnetic lineation in the studied deposits is not related to sedimentary processes but is

instead acquired as a result of a weak tectonic overprint on the primary sedimentary AMS fabric.

For this portion of the Northern Apennines, it is possible to propose the same model of evolution previously proposed by other authors (i.e. Sagnotti *et al*., 1998 and reference therein) for the external Central and Northern Apennines. In this model, sediments from the Tuscan Nappe succession, recorded the magnetic lineation in the early stage of their deformation during the early compressional phases, which progressively involved more external sector of the chain. Since the magnetic lineations agree with the actual tectonic setting (thrust front and fold axes directions), we suggest that the axes of magnetic lineations have been rotated following the formation of the arc during the involving of the sediment in the orogenic wedge.

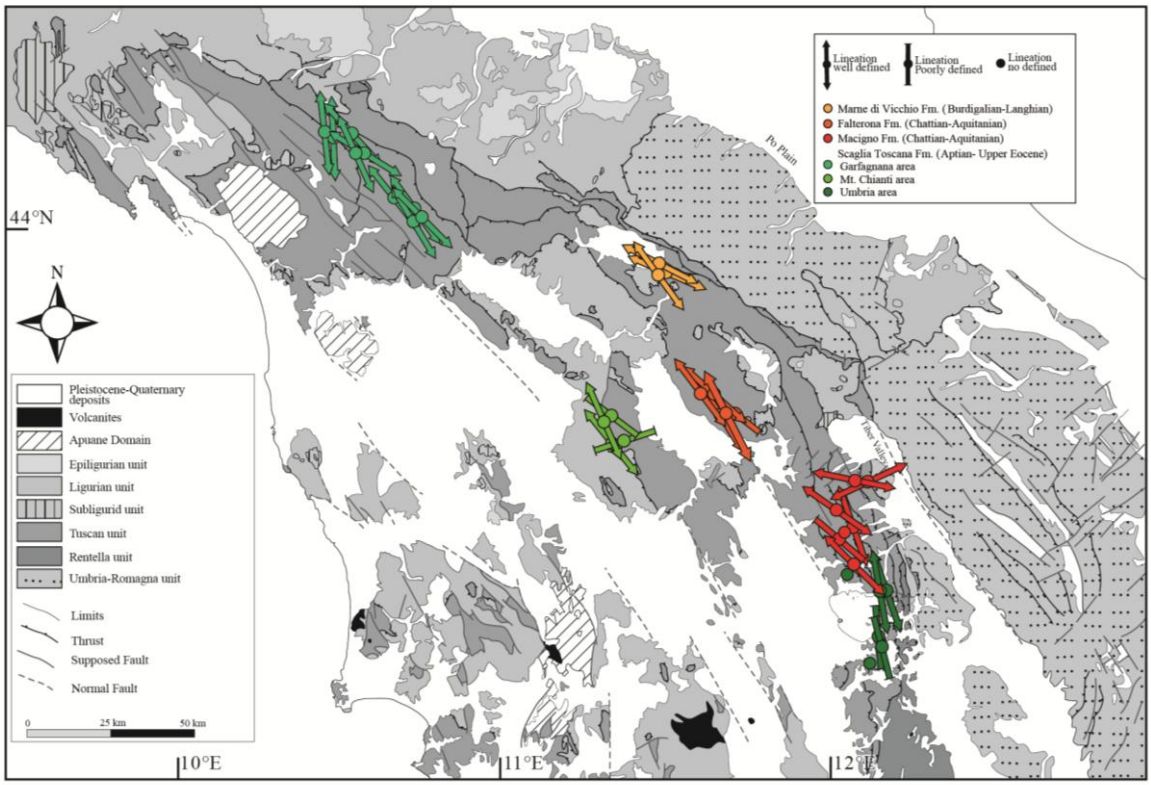

Fig. 5.6 Schematic map of the Northern Apennines and lineation distribution.

5.6 Conclusion

The study of the magnetic fabric of fine-grained sediments exposed in the internal sector of the Northern Apennine chain shows that AMS represent a suitable tool to study the deformation pattern in weakly deformed structures. The main points outlined in this study are:

- the magnetic susceptibility of the studied deposits and its anisotropy are, in most of the cases, controlled by the paramagnetic minerals.
- The magnetic fabric of the studied sediments mostly reflects the effects of compaction, showing a predominant magnetic foliation parallel to the bedding plane. In most of the sites, a distinct magnetic lineation was found, which is parallel to the fold axes and thrust fronts, both at local and regional scales.
- The same magnetic fabric is maintained in sequences that differ for sedimentological features and age, implying that the magnetic lineation was produced by a tectonic overprint of the primary sedimentary/compactional fabric. This result concurs with previous results (Lowrie and Hirt, 1988; Sagnotti *et al.*, 1998). In all the cases, the magnetic fabrics originated from the earliest stage of tectonic modification of an original compacted sedimentary fabric.
- The magnetic lineation follows the present curved shape of the northern Apennines over a total length of more than 300 km.

Chapter 6

Final remarks

In this thesis I adopted a multidisciplinary approach to reconstruct a kinematic evolution model of the internal portion of the Northern Apennines during Cenozoic. The integrated analyses, based on paleothermal and paleomagnetic methods, provided new data constraints in a sector of the chain not yet investigated, filling a gap in the existing literature. The elaboration and interpretation of the obtained data set enabled me to provide an important contribution to the evolution of the chain, in the geodynamic framework of the central Mediterranean.

A brief summary of the obtained results is reported below.

The paleothermal data, obtained along five sections across the Tuscan Nappe, in the most internal part of the belt, show two main thermal maturity trends (chapter 2). Organic and inorganic thermal indicators record both a decrease in thermal maturity from internal to the external sector of the chain and an increase of thermal maturity moving along the strike of the chain, from the SW (Trasimeno lake area) toward the NW (Pratomagno area). This pattern of thermal maturity is due to a variation of thickness of the allochthonous unit (Ligurian unit) that turns out to be thicker in the internal and in the northwestern sectors and tapers toward the east-southeast, as suggest by 1D thermal modelling based on both surface and subsurface data.

The studies focusing on the Alto Tiberina fault system, (chapter 3) is based on the integration between the paleothermal and low-T thermocronological data and allowed me to provide new constraints to reconstruct the exhumation history of the study area. The main result consists in an increase in the timing of exhumation, moving from the internal (Perugia area) to the external sector (Gubbio area) of the analysed portion of the chain in contrast to what is generally observed at a regional scale in the fold and thrust belts, where the exhumation ages decrease toward the external front. In particular younger ages are recorded at

the footwall of the ATF in the Perugia area where exhumation is bigger as testified by thermal indicators of maximum exposure. Here (U-Th)/He data indicate a mean age of exhumation of about 3 Ma, coeval with the activation of the fault system. The value of exhumation rate (0.8 mm/yr) can be considered as a threshold value between higher exhumation rate (>1.5mm/yr), where the uplift rate in rock is tectonically induced and lower exhumation rate (0.1 mm/yr) where erosion balances the rock uplift and the mean topography surfaces. Therefore, in this sector the local tectonics (normal faulting) has contributed to the exhumation processes. A similar hypothesis has been proposed by Balestrieri *et al.* (2003) for the Mt. Falterona Area.

Paleomagnetic analyses carried on onto Tuscan Nappe units allowed me to propose a new tectonic model for the internal sector of the chain (chapter 4). In the last decades, it has been assumed that the tectonic evolution of the Central Mediterranean has been mainly characterized by two coeval and distinct processes: the drifting and CCW rotation of the Corsica-Sardinia block and the progressive curvature of the Northern Apennines chain. The paleomagnetic evidence from Corsica-Sardinia block and data from more external portion of the Northern Apennines, have led to consider separately these two events. My paleomagnetic data demonstrate that during the Corsica-Sardinia drifting the Northern Apennines orogenic wedge also rotated CCW, suggesting that in this phase the Adriatic-Ionian subduction slab roll-back caused the CCW rotation of the whole upper plate of the Central Mediterranean subduction system. The distributions of the rotations show that the rotation values decrease with increasing latitude. In fact, at low latitudes (Umbria region) the mean rotations are higher, 99° ± 31°, and decrease toward north to 81° ± 35° and to 37° ± 16, in the Mt. Chianti and Garfagnana region, respectively. Our interpretation is that the CCW rotation of the Corsica-Sardinia block extended to the Tuscan Nappe but was limited to the southern Tuscan (Trasimeno Lake and Chianti Mts. And Pratomagno area), and did not involve the Tuscan units cropping out in the Garfagnana and Val di Lima area, which are located to the north of the Corsica-Sardinia rotation pole (located at N 43.5°).

In the same area, a study on the anisotropy of the magnetic susceptibility (AMS) has been conducted to determine the magnetic fabric of the rocks and the deformation pattern of the structures (chapter 5). These analyses indicated that the magnetic susceptibility is controlled mainly by the paramagnetic minerals. The analyzed sediment showed a predominant magnetic foliation parallel to the bedding plane, suggesting that the magnetic fabric is due to the compaction process during the diagenetic process that the sediments undergone. Moreover, a

distinct magnetic lineation was found, indicating an incipient deformation related to compressional deformation, overprinted on to the original magnetic fabric. In most cases the lineation is parallel to the fold axes and thrust fronts, both at local and regional scales, in agreement with previous results on the Northern Apennines (Lowrie and Hirt, 1988; Sagnotti et al., 1998).

References

Abbate E. (1969) - Il Gruppo della Val di Sambro (Serie Monghidoro«Auctt.») ed i terreni sovrastanti (Appennino modenese e bolognese). Dati preliminari. Boll. Soc. Geol. It., 88 (4), 637-644

Abbate E., Bortolotti V. and Passerini P. (1970) - Olistostromes and olistoliths. Sediment. Geol., 4, 521-557.

Abbate E. and Bruni P. (1989) - Modino-Cervarola o Modino e Cervarola? Torbiditi oligo-mioceniche ed evoluzione del margine Nord-appenninico. Mem. Soc. Geol. It., 39, 19-33.

Abbate, E., Balestrieri, M.L., Bigazzi, G., Ventura, B., Zattin, M., and Zuffa, G.G., (1999). An extensive apatite fission-trackstudy throughout the Northern Apennines nappe belt. Radiation Measurements 31, 673–676.

Aiello, I.W. and Hagstrum, J.T. (2001). Paleomagnetism and paleogeography of Jurassic radiolarian cherts from the northern Apennines of Italy**.** Geological Society of America Bulletin, 113, pp. 469–481

Aldega, L., Corrado, S., Di Paolo, L., Somma, R., Maniscalco, R., and Balestrieri, M. L. (2011). Shallow burial and exhumation of the Peloritani Mountains (NE Sicily, Italy): Insight from paleothermal and structural indicators. GSA, (1), 132–149. (doi:10.1130/B30093).

Alvarez, W. (1972). Rotation of the Corsica-Sardinia Microplate. Nature, 235,103–105.

Alvarez, W., F. G. Franks, and A. E. M. Nairn (1973). Paleomagnetism of Plio-Pleistocene basalts from NW Sardinia, Nature, 243,10–11.

Anelli, L., M. Gorza, M. Pieri, and M. Riva (1994), Subsurface well data in the Northern Apennines (Italy), Mem. Soc. Geol. Ital., 48, 461–471.

Argand, E. (1924), "La Tectonique de l'Asie", Extrait du Compte-rendu du XIIIe Congrès géologique international 1922 (Liège), 1(5), pp. 171-372

Argnani, A. and Ricci Lucchi, F., (2001). Tertiary silicoclastic turbidite systems of the Northern Apennines. In: Anatomy of an Orogen: the Apennines and Adjacent Mediterranean Basins. Dordrecht, Kluwer Academic Publishers, 327-350.

Aubourg, C., Rochette, P. and Vialon, P.(1991). Subtle stretching lineation revealed by magnetic fabric of Callovian–Oxfordian black shales (French Alps). Tectonophysics 185, 211–223.

Averbuch, O., Mattei, M., Kissel, C., Frizon de Lamotte, D. and Speranza, F. (1995). Cinematique des deformations au sein d’un systeme chevauchant aveugle: l’exemple de la ‘Montagna dei Fiori’ (front des Apennins centraux, Italie). Bull. Soc. Geol. Fr. 166, 5, 14, 451–461.

Baldacci F., Elter P., Giannini E., Giglia G., Lazzarotto A., Nardi R. and Tongiorgi M. (1967)- Nuove osservazioni sul problema della Falda Toscana e sulla interpretazione dei flysch arenacei tipo "Macigno" dell'Appennino settentrionale. Mem. Soc. Geol. It., 6 (2), 213 - 244.

Balestrieri, M.L., and Ventura, B. (2000). Apatite fi ssion- track data and exhumation ages across the main divide of the northern Apennines, Italy: Eos (Transactions, American Geophysical Union) Fall Meeting Supplement, v. 81, no. 48, p. T51C-12.

Balestrieri, M.L., Abbate, E., and Bigazzi, G., (1996). Insights on the thermal evolution of the Ligurian Apennines (Italy) through fi ssion-track analysis: Journal of the Geological Society of London, v. 153, p. 419–425, doi: 10.1144/gsjgs.153.3.0419.

Balestrieri, M. L., Bernet, M., Brandon, M. T., Picotti, V., Reiners, P., and Zattin, M. (2003). Pliocene and Pleistocene exhumation and uplift of two key areas of the Northern Apennines. Quaternary International, 102, 67–73.

Bambini A.M., Brogi A., Cornamusini G., Costantini A. and Lazzarotto A. (2009) - Nuovi dati litostratigrafici e biostratigrafici sulla Scaglia Toscana nella Toscana Meridionale (area di Rapolano Terme). Ital. J. Geosci., 128, 669-693.

Barchi, M.R. (2010). The Neogene-Quaternary evolution of the Northern Apennines: Crustal structure, style of deformation and seismicity [online], J. Virtual Explor., 36, paper 11, (doi:10.3809/jvirtex.2009.00220).

Barchi, M.R., and M. Ciaccio (2009). Seismic images of an extensional basin, generated at the hangingwall of a low-angle normal fault: The case of the Sansepolcro basin (Central Italy), Tectonophysics, 479,285–293, doi:10.1016/j.tecto.2009.08.024

Barchi M. R., Alvarez W. and. Shimabukuro D. H (2012). The Umbria-Marche Apennines as a Double Orogen: Observations and hypotheses. Ital. J. Geosci. (Boll. Soc. Geol. It.), 131, 2 ,. 258-271. (doi: 10.3301/IJG.2012.17).

Barchi, M.R., A. De Feyter, B. Magnani, Minelli, G. Pialli, G. and Sotera B. (1998a)- The structural style of the Umbria-Marche fold and thrust belt. Mem. Soc. Geol. Ital., 52, 557–578.

Barchi, M.R., De Feyter, A., Magnani B., Minelli, G. Pialli, G. and Sotera B. (1998b)- Extensional tectonics in the Northern Apennines (Italy): Evidence from the CROP03 deep seismic reflection line. Mem. Soc. Geol. Ital., 52, 528–538

Barchi, M.R., Paolacci S., Pauselli C.,. Pialli G, and Merlini S. (1999). Geometria delle deformazioni estensionali recenti nel bacino dell'Alta Val Tiberina fra S.Giustino Umbro e Perugia: Evidenze geofisiche e considerazioni geologiche. Boll. Soc. Geol. Ital., 118, 617–625

Barchi, M.R., Landuzzi, A., Minelli, G. and Pialli, G (2001)- Outer Northern Apennines. In: Anatomy of an Orogen: the Apennines and Adjacent Mediterranean Basins. Dordrecht, Kluwer Academic Publishers, 215-254.

Barchi, M.R., Pauselli C., Chiarabba C., Di Stefano R. and Federico C. (2006), Crustal structure, tectonic volution and seismogenesis in the Northern Apennines (Italy), Boll. Geofis. Teor. Appl., 47(3), 249–270.

Barnaba, P. (1958), Geologia dei Monti di Gubbio. Boll. Soc. Geol. Ital., 77,39–70.

Barsella, M., Boscherini, A., Botti, F., Marroni, M., Meneghini, F., Motti, A., Palandri, S. and Pandolfi, L., (2009). Oligocene-Miocene foredeep deposits in the Trasimeno Lake area (Central Italy): insights in the evolution of the Northern Apennines. Italian Journal of Geosciences 128, 341e352. doi:10.3301/IJG.2009.128.2.341

Basin Mod® 1-D for WindowsTM, (1996) A Basin Analysis Modelling System version 5.4 Software: Denver, Platte River Associates, 386 p.

Besse, J., and Courtillot V. (2002), Apparent and true polar wander and the geometry of the geomagnetic field over the last 200 Myr, J. Geophys. Res., 107(B11), 2300, doi:10.1029/2000JB000050.

Bettelli G., Boccaletti M., Cibin U., Panini F., Poccianti C., Rosselli S. and Sani F.(2002) – Note Illustrative della Carta Geologica d' Italia alla scala 1:50.000. Foglio 252 Barberino del Mugello. Servizio Geologico d'Italia, Roma, 130 pp

Boccaletti M., Coli M., Decandia F.A., Giannini E. and Lazzarotto A. (1980), - Evoluzione dell'Appennino Settentrionale secondo un nuovo modello strutturale. Mem. Soc. Geol. It., 21 359-373, 5 ff.

Boccaletti M. and Coli M. (1982) Carta strutturale dell'Appennino Settentrionale 1:250.000. CNR Progetto Finalizzato Geodinamica, SELCA, Firenze.

Boccaletti, M., Calamita, F., Deiana, G., Gelati, R., Massari, F., Moratti, G. and Lucchi, F.R. (1990) – Migrating Foredeep Thrust Belt System in the Northern Apennines and Southern Alps. Palaeogeography Palaeoclimatology Palaeoecology 77 (1), 3-14.

Boettcher S.S, and McBride, E.F. (1993). Thermal histories of piggy-back and foreland basins in the northern Apennines, Italy, derived from apatite fission track thermochronology: EOS, v. 74, no. 43, p. 547.

Boncio, P., Ponziani F., Brozzetti F., Barchi M.R., Lavecchia G., and Pialli G. (1998), Seismicity and extensional tectonics in the Northern Umbria Marche Apennines, Mem. Soc. Geol. Ital., 52, 539–555.

Boncio, P., Brozzetti F. and Lavecchia G. (2000), Architecture and seismotectonics of a regional low-angle normal fault zone in central Italy. Tectonics, 19, 1038–1055, (doi:10.1029/2000TC900023).

Bonini M. (1999) - Basement-controlled Neogene polyphase cover thrusting and basin development along the Chianti Mountains ridge (Northern Apennines, Italy). Geological Magazine, 136, 133-152.

Bonini M., Moratti G., Sani F. and Balestrieri M. L. (2012) - Compression-to-extension record in the Late Pliocene-Pleistocene Upper Valdarno Basin (Northern Apennines,

Italy): structural and thermochronological constraints. Ital.J.Geosci. (Boll.Soc.Geol.It.), 131, (doi: 10.3301/IJG.2011.18).

Borradaile G, Mothersill J, Tarling D and Alford C (1986). Sources of magnetic susceptibility in a slate; Earth Planet. Sci. Lett. 76 336–340.

Borradaile, G.J., (1988). Magnetic fabrics, petrofabrics and strain. Tectono- physics 156, 1–20.

Borradaile, G. J. and Tarling, D. H. (198l). The influence of deformation mechanisms on magnetic fabrics in weakly deformed rocks. Tectonophysics, 77, 151-168.

Bortolotti, V., Principi, G. and Treves, B. (2001) – Ophiolites, Ligurides and the tectonic evolution from spreading to convergence of Mesozoic western Tethys segment. In Vai, G. B., and Martini, I. P., eds., Anatomy of an orogen; The Appennines and adjacent Mediterranean Basins: London: Kluwer Academic Publischers, 151-164.

Bortolotti V., Poccianti C., Principi G. and Sani F., with contribution of Benvenuti M., Catanzariti R., Moretti S. and Reale V. (2009) – Note Illustrative della Carta Geologica d'Italia alla scala 1:50.000. Foglio 264 Borgo San Lorenzo. Servizio Geologico d'Italia, Roma, in stampa.

Botti, F., Aldega, L. and Corrado, S. (2004). Sedimentary and tectonic burial evolution of the Northern Apennines in the Modena-Bologna area : constraints from combined stratigraphic , structural , organic matter and clay mineral data of Neogene thrust-top basins. Geodinamica Acta, 3, 185–203.

Brandon, M.T. and Vance, J.A. (1992). Fission track ages of detrital zircon: implications for tectonic evolution of the Cenozoic Olympic subduction complex: Am. Journ. Sc., v. 292, p. 565-636.

Brandon, M.T., Roden-Tice, M.K. and Garver, J.I. (1998). Late Cenozoic exhumation of the Cascadia accretionary wedge in the Olympic Mountains, northwest Washington State: Geological Society of America Bulletin, v. 110, p. 985-1009.

Brozzetti, F. (1995), Stile strutturale della tettonica distensiva nell'Umbria occidentale: L'esempio dei Massicci Mesozoici Perugini, Studi Geol. Camerti (1) 105-109.

Brozzetti F., Luchetti L. and Pialli, G. (2000). La successione del Monte Rentella (umbria Occidentale) biostratigrafia a nannofossili calcarei ed ipotesi per un inquadramento tettonico regionale. Boll. Soc. Geol. It., 119 (12), 407-422.

Brozzetti F. (2007). The Umbria Preapennines in the Monte Santa Maria Tiberina area: a new geological map with stratigraphic and structural notes. Boll. Soc. Geol. It., 126 (3), 511-529.

Brozzetti, F., Boncio P., Lavecchia G., and Pace B. (2009). Present activity and seismogenic potential of a low-angle normal fault system (Città di Castello, Italy): Constraints from surface geology, seismic reflection data and seismicity, Tectonophysics, 463,31–46, doi:10.1016/j.tecto.2008. 09.023.

Burnham, A.K., and Sweeney, J.J., (1989). A chemical kinetic model of vitrinite maturation and refl ectance: Geochi- mica et Cosmochimica Acta, v. 53, p. 2649–2657, doi: 10.1016/0016-7037(89)90136-1.

Burrus, J. (1984) - Contribution to a geodynamic synthesis of the Provençal basin (north-western Mediterranean), Mar. Geol. 55 247–269.

Bustin, R.M., Barnes, M.A., and Barnes, W.C., (1990)- Deter mining levels of organic diagenesis in sediments and fossil fuels, in McIleareath, I.A., and Morrow, D.W., eds., Diagenesis: St. John's, Canada, Geoscience Canada Reprint, 4th series, p. 205–226

Butler, R.W.H., (1992), Hydrocarbon maturation, migration and tectonic loading in the western Alps, in England, W.A., and Fleet, A.J., eds., Petroleum Migration: Geological Society of London Special Publication 59, p. 227–244.

Butler, R.W.H., Mazzoli, S., Corrado, S., De Donatis, M., Di Bucci, D., Gambini, R., Naso, G., Nicolai, C., Scrocca, D., Shiner, P., and Zucconi, V. (2004). Applying thick-skinned tectonic models to the Apennine thrust belt of Italy: Limitations and implications. In: Thrust Tectonics and Petroleum Systems. American Association of Petroleum Geologists Memori 82, 647-667

Butler, R.W.H., Tavarnelli, E. and Grasso, M., (2006). Structural inheritance in mountain belts: An Alpine-Apennine perspective. Journal of structural Geology 28 (11), 1893-1908 10.1016/j.jsg.2006.09.006

Calamita, F., Cello, G., Deiana, G. and Paltrinieri, W., (1994). Structural styles, chronology rates of deformation and time- space relationships in the Umbria-Marche thrust system (central Apennines, Italy). Tectonics 13 (4), 873-881.

Carmignani L., Giglia G. and Kligfield R. (1978): Structural evolution of the Apuane Alps: an example of continental margin deformation. Journal of Geology, 86: 487-504

Carmignani, L., Carosi, R., Di Pisa, A., Gattiglio, M., Musumeci, G., Oggiano, G. and Pertusati, P. C., (1994). The Hercynian chain in Sardinia (Italy). Geodinamica Acta 7 (1), 31-47

Carrapa, B., Bertotti, G. and Krijgsman, W. (2003) Subsidence, stress regime and rotation(s) of a tectonically active active sedimentary basin within the western Alpine Orogen: the Tertiary Piedmont Basin (Alpine domain, NW Italy). Geological Society of London, Special Pubblications 208, 205-227.

Catanzariti, R., Cerrina Feroni, A.C., Marroni, M., Ottria, G. and Pandolfi, L., (2003). Ophiolites debris in the Aveto Unit (Trebbia Valley, northern Apennines, Italy): a record of the early Oligocene Apenninic foredeep. Geophysical Research Abstracts 5, 11978.

Cattuto, C., C. Cencetti, M. Fisauli, and L. Gregori (1995), I bacini pleistocenici di Anghiari e Sansepolcro nell'alta valle del Tevere, Quaternario, 8, 119–128.

Cerrina Feroni A. and Patacca E. (1975) - Considerazioni preliminari sulla paleogeografia del Dominio Toscano interno tra il Trias superiore e il Miocene medio. Atti Soc. Tosc. Sci. Nat., Mem., Ser. A, 82: 43-54.

Cerrina Feroni, A.C., Loni, L., Martelli, L., Martinelli, P., Ottria, G., and Sarti, G., (2001). The Romagna Apen- nines, Italy: An eroded duplex: Geological Journal, v. 36, no. 1, p. 39–54, doi: 10.1002/gj.874

Cerrina Feroni, A., Ottria, G., Martinelli, P. and Martelli, L. (2002). Structural geological map of the Emilia-Romagna Apennines, 1:250,000 Scale. Ed. S.EL.CA. Firenze.

Channell (1976). Umbrian paleomagnetism and the concept of the African-Adriatic promontory. Mem. Soc. Geol. It, 15, 119–128.

Channell J.E.T. and Tarling D.H. (1975). Paleomagnetism and the rotation of Italy, Earth Planet. Sci. Lett. 25 177–188.

Channell, J. E. T., Lowrie, W., Medizza, F. and Alvarez, W., (1978). Paleomagnetism and tectonics in Umbria, Italy. Earth and Planetary Science Letters 39, 199-210.

Channell, J. E. T., Brandner R., Spieler A., and Stoner J. S. (1992). Paleomagnetism and paleogeography of the Northern Calcareous Alps (Austria), Tectonics, 11, 792–810.

Channell, J. E. T. (1996), Paleomagnetism and paleogeography of Adria, in Paleomagnetism and Tectonics of the Mediterranean Region, edited by A. Morris and D. H. Tarling, Geol. Soc. Spec. Publ., 105, 119–132

Chamot-Rooke N., Gaulier J.-M., and Jestin F. (1999). Constraints on Moho depth and crustal thickness in the Liguro-Provençal basin from a 3D gravity inversion: geodynamic implications, in: B. Durand, L. Jolivet, F. Horvath, M. Seranne (Eds.), The Mediterranean Basins: Tertiary Extension Within the Alpine Orogen, Geol.Soc. London, Spec. Publ., vol. 156, pp. 37–61.

Chiaraluce, L., Amato, A., Cocco, M., Chiarabba, C., Selvaggi, G., Di Bona, M., Piccinini, D., Deschamps, A., Margheriti, L., Courboulex, F. and Ripepe, M., (2004). Complex normal faulting in the Apennines thrust-and-fold belt : the 1997 seismic sequence in central Italy. Bulletin of the Seismological Society of America 94, 99-116.

Chicchi S. and Plesi G. (1991a). Sedimentary and tectonic lineations as markers of regional deformation: an example from the Oligo-Miocene arenaceous flysch of Northern Apenines. Boll. Soc. Geol. It., 110: 601-616.

Chicchi S. and Plesi G. (1991b). Sovrascorrimenti e strutture associate dell'alto Appennino emilia- no fra il Passo del Lagastrello e il M. Cimone. Studi Geol. Camerti, Vol. Spec. 1990: 99-108.

Chicchi S. and Plesi G. (1992). Il Complesso di M. Modino nell'alto Appennino emiliano (tra il Passo del Lagastrello e il M. Cimone) e i suoi rapporti con la Falda toscana, l'Unità di Canetolo e le Liguridi. Mem. Descr. Carta Geol. d'It., 46 (1991): 139-163

Cibin, U., Spadafora, E., Zuffa, G.G., and Castellarin, A., (2001). Continental collision history from arenites of episutural basins in the Northern Apennines, Italy. Geological Society of America Bulletin 113 (1), 4-19. 10.1130/0016-7606(2001)113<0004:CCHFAO>2.0.CO;2

Cibin U., Di Giulio A., Martelli L., Catanzariti R, Poccianti C., Rosselli S. and Sani F. (2004) – Factors controlling foredeep turbidite deposition: the case of Northern Apennines (Oligocene-Miocene, Italy). In: A: Lomas and P: Joseph (Eds.), Confined Turbidite Systems, Geol. Soc. London, Spec. Publ. 222: 115-134.

Cifelli, F., Rossetti, F., Mattei, M., Hirt, A. M., Funiciello, R., and Tortorici, L. (2004). An AMS, structural and paleomagnetic study of quaternary deformation in eastern Sicily. Journal of Structural Geology, 26(1), 29–46. doi:10.1016/S0191-8141(03)00092-0.

Cifelli F., Mattei M., Chadima M., Hirt A.M. and Hansen A. (2005). The origin of tectonic lineation in extensional basins: combined neutron texture and magnetic analyses on “undeformed” clays. Earth and Planetary Science Letters, 235, 62– 78.

Cifelli, F., Mattei, M., and Rossetti, F. (2007). Tectonic evolution of arcuate mountain belts on top of a retreating subduction slab: The example of the Calabrian Arc. Journal of Geophysical Research, 112(B9), 1–20. doi:10.1029/2006JB004848.

Cifelli, F., Mattei, M. and Della Seta, M., (2008). Calabrian Arc oroclinal bending: The role of subduction. Tectonics 27 (TC5001).

Cifelli, F. and Mattei, M. (2010) Curved orogenic systems in the Italian Peninsula: a paleomagnetic review. In:(Eds.) Marco Beltrando, Angelo Peccerillo, Massimo Mattei, Sandro Conticelli, and Carlo Doglioni, Journal of the Virtual Explorer, volume 36, paper 17, doi:10.3809/jvirtex.2010.00239.

Collettini, C., De Paola, N., Holdsworth, H. R. and Barchi, M.R., (2006). The development and behaviour of low-angle normal faults during Cenozoic asymmetric extension in the Northern Apennines, Italy. Journal of Structural Geology 28, 333-352.

Cornamusini, G., Ielpi, A., Bonciani F. and Callegari I. (2011). Stratigraphic architecture of an outer ramp / basinal turbidite fan carbonate system in a foreland basin (“ Scaglia Toscana ” Fm ., Chianti Mts , Northern Apennines , Italy). Rend. Online Soc. Geol. It., Vol. 17 (2011), pp. 71-76, 5 fi gs., (DOI: 10.3301/ROL.2011.25)

Corrado, S., (1995). Optical parameters of maturity of organic matter dispersed in sediments: first results from the Central Apennines (Italy). Terra Nova 7(2), 338-347. 10.1111/j. 1365-3121.1995.tb00803.x

Corrado, S., Di Bucci, D., Naso, G., Giampaolo, C. and Adatte, T., (1998). Application of organic matter and clay mineral studies to the tectonic history of the Abruzzo-Molise- Sannio area, Central Apennines, Italy. Tectonophysics 285, 167-181. 10.1016/S0040-1951(97)00195-9

Corrado, S., Aldega, L., Balestrieri, M.L., Maniscalco, R. andGrasso, M., (2009). Structural evo- lution of the sedimentary accretionary wedge of the Alpine system in

Eastern Sic- ily: thermal and thermochronological constraints. Geological Society of America Bulletin 121, 1475–1490.

Corrado, S., Aldega, L. and Zattin, M. (2010a). Sedimentary vs . tectonic burial and exhumation along the Apennines (Italy)_ Journal of Virtual Explorer, 36. doi:10.3809/jvirtex.2010.00232

Corrado, S., Invernizzi, C., Aldega, L., D'Errico, M., Di Leo, P., Mazzoli, S. and Zattin, M. (2010b). Testing the validity of organic and inorganic thermal indicators in different tectonic settings from continental subduction to collision : the case history of the CalabriaLucania border (southern Apennines , Italy). Journal of the Geological Society, 167(August), 985–999. doi:10.1144/0016-76492009-137

Costa E., Pialli G. and Plesi G. (1998). Foreland basins of the Northern Apennines: relationships with passive subduction of the Adriatic lithosphere. Mem. Soc. Geol. It., 52, 595-606.

D'Agostino, N., Mantenuto, S., D'Anastasio, E., Avallone, A., Selvaggi, G., Barchi, M.R., Collettini, C., Radicioni, F., Stoppini, A. and Fastellini, F. (2009), Contemporary crustal extension in the Umbria-Marche Apennines from regional CGPS networks and comparison between geodetic and seismic deformation, Tectonophysics, 476,3–12, doi:10.1016/j. 1085 tecto.2008.09.033.

De Jong, K.A. and Manzoni (1968). Paleomagnetismo e cronologia delle collate basaltiche di Orosei. Boll. Soc. Geol. It 87, 713.717.

De Jong, K.A., Manzoni, M. and Zijderveld, J.D.A., (1969). Paleomagnetism of the Alghero Trachyandesites. Nature 224, 67–69.

De Jong, K.A., Manzoni, M., Stavenga, T., Van Dijk, F., Van der Voo, R., and Zijderveld, J.D.A., (1973). Palaeomagnetic evidence for rotation of Sardinia during the early Miocene. Nature 243, 281– 283.

Delle Donne, D., L. Piccardi, J. Odum, W. Stephenson, and R. Williams 1091 (2007), High-resolution shallow reflection seismic image and surface evidence of the upper Tiber basin active faults (Northern Apennines, Italy), Boll. Soc. Geol. Ital., 126, 323–331.

Demarest, H. H. (1983), Error analysis for the determination of tectonic rotation from paleomagnetic data, J. Geophys. Res., 88, 4321–4328.

Dessau, G. (1962) Geologia del M.Malbe nel quadro dei Massicci Mesozoici del perugino, Boll. Soc. Geol. Ital., 81, 225–315

Di Paolo, L., Aldega, L., Corrado, S. and Mastalerz, M. (2012). Maximum burial and unroofing of Mt . Judica recess area in Sicily : implication for the Apenninic – Maghrebian wedge dynamics. Tectonophysics, 530-531, 193–207. doi:10.1016/j.tecto.2011.12.020.

Dodson, M.H., (1973) Closure temperature in cooling geochronological and petrological systems: Contrib. Mineral. Petr., v. 40, p. 259-274.

Edel, J.B. (1980). Etude paléomagnétique en Sardaigne. Conséquences pour la géodynamique de la Méditerannée occidentale, Ph.D. Thesis, Institut de Physique du Globe, Université Louis Pasteur, Strasbourg (France).

Eldredge, S., V. Bachtadse, and. Van der Voo V (1985), Paleomagnetism and the orocline hypothesis, Tectonophysics, 119, 153–179

Elter, P., (1975). L'ensemble ligure. Bulletin de la Societe Geologique de France 17, 984-997

Elter, P., Giglia, G., Tongiorgi M., and Trevisan L., (1975). Tensional and compressional areas in the recent (Tortonian to Present) evolution of the Northern Apennines. Bollettino di Geofisica Teorica Applicata 17, 3-18.

Endignoux, L., and Wolf, S., (1990) - Thermal and kinematic evolution of thrust basins: A 2D numerical model, in Letouzey, J., ed., Petroleum Tectonics in Mobile Belts: Paris, Edit. Technip, p. 181–192.

Faccenna, C., Piromallo, C., Crespo-Blanc, A., Jolivet, L. and Rossetti, F. (2004)- Lateral slab deformation and the origin of the western Mediterranean arcs. Tectonics 23,1.

Farley, K. A. (2000) Helium diffusion from apatite: General behavior as illustrated by Durango fluorapatite. Journal Of Geophysical Research, Vol. 105, No. B2, P. 2903, Doi:10.1029/1999jb900348

Farley, K. A.; Rusmore M.E. and Bogue S.W. (2001) Post–10 Ma uplift and exhumation of the northern Coast Mountains, British Columbia. Geology v. 29 no. 2 p. 99-102 doi: 10.1130/0091

Fazzuoli M., Becarelli S., Burchietti G., Ferrini G., Garzonio C. A., Mannori G., Sani F. and Sguazzoni G. (1994). A short outline of the geology of the mesozoic inlier in the Lima Valley, Northern Apennines. Mem. Soc. Geol. It., 48 (1994): 79-85

Fazzuoli, M., Sani, F., Ferrini, G., Garzionio, C. A., Sguazzoni, G., Beccarelli, S. and Burchietti, G. (1998). Geologia del nucleo mesozoico della Val di Lima (provincie Pistoia e Lucca, Appennino Settentrionale). Note illustrative della carta geologica (scala 1:25.000). Boll. Soc. Geol. it., 117, 479–535.

Festa, A., Pini, G.A., Dilek Y., Codegone, G., Vezzani,L., Ghisetti, F., Lucente, C. and Ogata, K. (2010) - Peri-Adriatic me´langes and their evolution in the Tethyan realm. International Geology Review Vol. 52, Nos. 4–6, April–June 2010, 369–403.

Fisher, R. A. (1953), Dispersion on a sphere, Proc. R. Soc. London, Ser. A, 217, 295–305.

Fleischer, R.L., Price, P.B., and Walker, R.M., (1965) The ion explosion spike mechanism for formation of charged particle tracks: Journ. Appl. Phy., v. 36, p. 3645-3652.

Gailbraith, R.F. (1988) Graphical display of estimates having different standard errors: Technometrics, v. 30, p. 271-281

Gattacceca, J., Deino A., Rizzo R., Jones D. S., Henry B., Beaudoin B., and Vadeboin F. (2007), Miocene rotation of Sardinia: New paleomagnetic and geochronological constraints and geodynamic implications, Earth Planet. Sci. Lett., 258(3–4), 359–377.

Ghelardoni, R. (1962), Stratigrafia e tettonica del Trias di M. Malbe presso Perugia. Boll. Soc. Geol. Ital., 81,66–75.

Gleadow, A.J.W. and Duddy, I.R.(1981), A natural long-term track annealing experiment for apatite: Nucl. Tracks, v. 5, p. 169-174.

Gleadow, A. J.W., Duddy, I.R., and Lovering, J.F. (1983). Fission track analysis: a new tool for the evaluation of thermal histories and hydrocarbon potential: Austral. Petrol. Expl. Ass. J., v. 23, p. 93-102.

Geological Cartography Project (2011a). Città di Castello, in Carta Geologica d'Italia, sheet 289, scale 1:50,000, Ist. Super. per la Prot. e la Ric. Ambientale, Rome.

Geological Cartography Project (2011b). Umbertide, in Carta Geologica d'Italia, sheet 299, scale 1:50,000, Ist. Super. per la Prot. e la Ric. 1123 1124 Rome, in press.

Geological Cartography Project (2011c). Passignano, in Carta Geologica d'Italia, sheet 310, scale 1:50,000, Ist. Super. per la Prot. e la Ric. 1126 1127 Ambientale, Rome, in press.

Geological Cartography Project (2011d). Figline Valdarno, in Carta Geologica d'Italia, sheet 276, scale 1:50,000, Ist. Super. per la Prot. e la Ric. 1123 1124 Rome, in press.

Geological Cartography Project (2011e). Borgo San Lorenzo, in Carta Geologica d'Italia, sheet 264, scale 1:50,000, Ist. Super. per la Prot. e la Ric. Ambientale, Rome, in press.

Green, P.F., Duddy, I.R., Gleadow, A.J.W., Tingate, P.R., and Laslett G.M. (1986) Thermal annealing of fission tracks in apatite: 4. Quantitative modeling techniques and extension to geological scales: Chem. Geol., v. 79, p. 155-182.

Graham, J.W., (1966). Significance of magnetic anisotropy in Appalachian sedimentary rocks. In: Steinhart, J.S., Smith, T.J. (Eds.), The Earth Beneath the Continents. American Geophysical Union Geophysics, Monography 10, pp. 627–648.

Guenther, K., Reutter, K.J., (1985), Il significato delle strutture dell'unità di M. Modino-M. Cervarola tra il Passo delle Radici e il M. Falterona in relazione alla tettonica dell'Appennino Settentrionale: Giorn. Geol. serie 3a, 47 (1-2): 15-34.

Hillier, S., Màtyàs, J., Matter, A., and Vasseur, G., (1995) - Illite/smectite diagenesis and its variable correlation with vitrinite refl ectance in the Pannonian Basin: Clays and Clay Minerals, v. 43, p. 174–183, doi: 10.1346/ CCMN.1995.0430204.

Hirt, A. M. and Lowrie, A., (1988). Paleomagnetism of the Umbrian- Marches orogenic belt. Tectonophysics 146, 91-103.

Hrouda, F. (1982). Magnetic anisotropy of rocks and its application in geology and geophysics. Geophysical Survey 5, 37–82.

House, M.A.; Wernicke, B.P. and Farley, K.A. (1998)- Dating topography of the Sierra Nevada, California, using apatite (U-Th)/He ages. Nature, 369,66-96.

Housen, B.A., Richter, C. and Van der Pluijm, B.A. (1993). Composite magnetic anisotropy fabrics: experiments, numerical models, and implications for the quantification of rock fabrics. Tectonophysics 220, 1–12.

Hreinsdóttir, S. and R. Bennett (2009), Active aseismic creep on the Alto Tiberina low-angle normal fault, Italy, Geology, 37,683–686, doi:10.1130/G30194A.1.

Jelínek, V. and Kropáček, V. (1978). Statistical processing of anisotropy of magnetic susceptibility measured on groups of specimens. Studia Geophysica et Geodaetica 22, 50–62.

Jelinek, V. (1981). Characterization of the magnetic fabrics of rocks. Tectonophysics 79, 63–67.

Jolivet, L., Faccena, C., Goffé, B., Mattei, M., Rossetti, F., Brunet, C., Storti, F., Funiciello, R., Cadet, J. P., D'Agostino, N. and Parra, T., (1998). Midcrustal shear zones in postorogenic extension: example from the northern Tyrrhenian Sea". Journal of Geophysical Research 103, 12,123-12,160.

Keller, J., G. Minelli, and Pialli G. (1994), Anatomy of a late orogenic extension: The Northern Apeninnes case, Tectonophysics, 238, 275–294, doi:10.1016/0040-1951(94)90060-4.

Kirschvink, J.L. (1980) the last-square line and plane and the analysis of paleomagnetic data. Geophys. J. R. Astron. Soc. 62, 699-718.

Kissel, C., Barrier, E., Laj, C. and Lee, T.Q. (1986). Magnetic fabric in <<undeformed>> marine clays from compressional zones. Tectonics 5, 769–781.

Kissel, C., and Laj, C. (1988). The Tertiary geodynamical evolution of the Aegean arc: a paleomagnetic reconstruction. Tectonophysics 146, 1-4, 183-201.

Kissel, C., Laj, C., Lehman, B., Labyrie, L. and Bout-Roumazeilles, V. (1997). Changes in the strength of the Iceland–Scotland Overflow Water in the last 200,000 years: evidence from magnetic anisotropy analysis of core SU90-33. Earth and Planetary Science Letters 152, 25–36.

Klootwjjk, C.T. and Van den Berg (1975). The rotation of Italy: preliminary paleomegnetic data from the Umbrian sequence: Northern Appennines. Earth planetary Science Letters 25, 263-273.

Kligfield, R., Lowrie, W., Hirt, A. M. and Siddans, A. W. B., (1983). Effect of progressive deformation on remanent magnetization of Permian redbeds from the Maritime Alps (France). Tectonophysics 97, 59-85

Krijgsman, W. and Garcés, M. (2004). Paleomagnetic constraints on the geodynamic evolution of the Gibraltar Arc. Terra Nova,16, 281–287.

Lee, T., Kissel, C., Laj, C., Horng, C.S. and Lue, Y.T., (1990). Magnetic fabric analysis of the Plio-Pleistocene sedimentary formations of the Coastal Range of Taiwan. Earth and Planetary Science Letters 98, 23–32.

Lippolt H.,J; Leitz, M., Wernicke, R. S. and Hagedorn, B. (1994). (U-Th)/He dating of apatite: experience with samples from different geochemical environments. Chemical Geology, 112, 1–2, 179–191.

Lonergan, L., and N. White (1997). Origin of the Betic-Rif mountain belt, Tectonics, 16, 504–522.

Lowrie W. (1990). Identification of ferromagnetic minerals in a rock by coercivity and unblocking temperature properties. Geophys. Res. Let. 17, 159-162.

Lowrie W. and Alvarez, W. (1975). Paleomagnetic evidence for rotation of the Italian peninsula, J. Geophys. Res. 80, 1579-1582.

Lowrie, W. and Hirt, A. M. (1986). Paleomagnetism in arcuate mountain belts. In: The Origin of the Arcs (edited by Wezel, F. C.). Elsevier, New York, 141-158.

Lowrie, W., and Hirt, A.M. (1987). Anisotropy of magnetic susceptibility in the Scaglia Rossa pelagic limestone. Earth and Planetary Science Letters 82, 349–356.

Maffione, M., Speranza, F., Faccenna, C., Cascella, A., Vignaroli, G. and Sagnotti, L. (2008). A synchronous Alpine and Corsica-Sardinia rotation. Journal of Geophysical Research, 113(B3), 1–25. doi:10.1029/2007JB005214

Malinverno, A. and Ryan, W.B.F. (1986). Extension in the Tyrrhenian Sea and shortening in the Apennines as result of arc migration driven by sinking of the lithosphere. Tectonics 5, 227-245.

Marroni, M., Molli, G., Ottria, G. and Pandolfi, L., (2001). Tectono- sedimentary evolution of the External Liguride units (Northern Apennines, Italy): insights in the pre-collisional history of a fossil ocean-continent transition zone. Geodinamica Acta 14 (5), 307-320 10.1016/ S0985-3111(00)01050-0

Martinis, B. and Pieri M. (1964), Alcune notizie sulla formazione evaporitica dell'Italia centrale e meridionale, Mem. Soc. Geol. Ital., 4, 649–678

Marshak, S., (2004). Arcs, Oroclines, Salients, and Syntaxes -The origin of map-view curvature in fold-thrust belts: (in) McClay, K.R., (ed.), Thrust Tectonics and Petroleum Systems: Am. Assoc. of Petroleum Geologists Memoir 82, p. 131-156.

Mattei M., Funiciello R., Kissel C. and Laj C. (1994) - Strike-slip tectonics and Neogene block rotation in Central Italy. Mem. Soc. Geol.ca It., 48, 485-497. ISSN 0375-9857.

Mattei M., Funiciello R. and Kissel C. (1995). Paleomagnetic and structural evidence of Neogene block rotation in the Central Apennines, Italy. J. Geophy. Res., 100, 17863-17883. [doi:10.1029/95JB00864].

Mattei M., Kissel C. and Funiciello R. (1996.) No tectonic rotation of the Tuscan margin (Italy) since Upper Messinian: structural and geodynamical implications. J. Geophys. Res. 1996a; 101:2835-2845

Mattei, M., Sagnotti, L., Faccenna, C., and Funiciello, R. (1997). Magnetic fabric of weakly deformed clayey sediments in the Italian peninsula: relationships with compressional and extensional tectonics. Tectono- physics 271, 107–122.

Mattei, M., Speranza, F., Argentieri, A., Rossetti, F., Sagnotti, L. and Funiciello, R. (1999). Extensional tectonics in the Amantea basin (Calabria, Italy): a comparison between structural and magnetic anisotropy data. Tectonophysics 307, 33–49

Mattei, M., Cipollari, P., Cosentino, D., Argentieri, A., Rossetti, F., Speranza, F., and Di Bella, L., (2002). The Miocene tectono-sedimentary evolution of the southern Tyrrhenian Sea: stratigraphy, structural and palaeomagnetic data from the on-shore Amantea basin (Calabrian Arc, Italy). Basin Research 14, 147–168.

Mattei M., Cifelli F., Martín Rojas I., Crespo Blanc A., Comas M., Faccenna C. and Porreca M. (2006) – Neogene tectonic evolution of the Gibraltar Arc: New paleomagnetic constrains from the Betic chain. Earth and Planetary.Science Letters, (Elsevier, Amsterdam, NL), 250, 522-540, [doi:10.1016/j.epsl.2006.08.012]

Mattei M., Cifelli F. and D'agostino N. (2007). The Evolution of the Calabrian Arc: Evidence from paleomagnetic and GPS observations. Earth and Planetary Science Letters, (Elsevier, Amsterdam, NL), 263, 259–274. [doi:10.1016/j.epsl.2007.08.034];

Mazzoli, S., D'Errico, M., Aldega, L., Corrado, S., Invernizzi, C., Shiner, P., and Zattin, M., (2008). Tectonic burial and 'young' (< 10 Ma) exhumation in the southern Apennines fold-and- thrust belt (Italy). Geology 36 (3), 243-246

McFadden, P. L. (1990). A new fold test for paleomagnetic studies, Geo- phys. J. Int., 103, 163–169.

McFadden, P. L., and M. W. McElhinny (1990), Classification of the reversal test in paleomagnetism, Geophys. J. Int., 130, 725–729.

Meesters, A.G.C.A. and Dunai, T.J. (2002a). Solving the production - diffusion equation for finite diffusion domain of various shape. Part I. Implication for low-temperature (U-Th)/He termocronology. Chem. Geol. 186, 3-4, 333-334

Meesters, A.G.C.A. and Dunai, T.J. (2002b). Solving the production - diffusion equation for finite diffusion domain of various shape. Part II. Application to cases with α-ejection and non-homogeneous distribution of source. Chem. Geol. 186, 1.-2, 57-73

Meneghini, F., Botti, F., Aldega, L., Boschi, C., Corrado, S., Marroni, M. and Pandolfi, L. (2012). Hot fluid pumping along shallow-level collisional thrusts: The Monte

Rentella Shear Zone, Umbria Apennine, Italy. Journal of Structural Geology, 37, 36–52. doi:10.1016/j.jsg.2012.02.004

Merriman, R.J., and Frey, M. (1999). Patterns of very low- grade metamorphism in metapelitic rocks, in Frey, M., and Robinson, D., eds., Low Grade Metamorphism: Oxford, Blackwell, p. 61–107.

Minelli, G. and M. Menichetti (1990). Tectonic evolution of the Perugia massifs area (central Italy), Boll. Soc. Geol. Ital., 109, 445–453

Mirabella, F., Ciaccio M., Barchi M. R., and Merlini S. (2004). The Gubbio normal fault (central Italy): Geometry, displacement distribution and tectonic evolution. J. Struct. Geol., 26, 2233–2249, doi:10.1016/j.jsg. 2004.06.009.

Mirabella, F., Barchi M.R., Lupattelli A., Stucchi E., and Ciaccio M. (2008a). Insights on the seismogenic layer thickness from the upper crust structure of the Umbria-Marche Apennines (central Italy), Tectonics, 27, TC1010, 1200 doi:10.1029/2007TC002134.

Mirabella, F., Barchi M.R., and Lupattelli A. (2008b), Seismic reflection data in the Umbria-Marche region: Limits and capabilities to unravel the subsurface structure in a seismically active area, Ann. Geophys., 51(2/3), 383–396.

Mirabella, F., Brozzetti, F., Lupattelli, A. and Barchi, M. R. (2011). Tectonic evolution of a low-angle extensional fault system from restored cross-sections in the Northern Apennines (Italy). Tectonics, 30(6). doi:10.1029/2011TC002890

Molli, G., Giorgetti, G. and Meccheri, M., (2002). Tectono- metamorphic evolution of the Alpi Apuane Metamorphic Complex: New data and constraints for geodynamic models. Bollettino della Società Geologica Italiana, special volume 1, 789-800

Montigny, R., Edel, J. B. and Thuizat, R., (1981). Oligo-Miocene rotation of Sardinia: K-Ar ages and paleomagnetic data of tertiary volcanics. Earth Planetary Science Letters 54, 261-271.

Moore, D. M. and Reynolds, R. C., Jr. (1997). X-ray diffraction and the identification and analysis of clay minerals. Oxford, Oxford University Press, 378 p.

Muttoni, G., Argnani, A.,. Kent, D. V, Abrahamsen, N. and Cibin, U. (1998). Paleomagnetic evidence for Neogene tectonic rotations in the northern Apennines, Italy, Earth Planet. Sci. Lett., 154, 25–40.

Muttoni, G., Lanci L., Argnani A., Hirt A. M., Cibin U., Abrahamsen N., and Lowrie W. (2000), Paleomagnetic evidence for a Neogene two-phase counterclockwise tectonic rotation in the northern Apennines (Italy), Tectonophysics, 326, 241–253.

Muttoni, G., Garzanti E., Alfonsi L., Cirilli S., Germani D., and Lowrie W. (2001). Motion of Africa and Adria since the Permian: Paleomagnetic and paleoclimatic constraints from northern Libya, Earth Planet. Sci. Lett., 192, 159–174.

Pasquale, V., Verdoya, M., Chiozzi, P. (1995). Rifting and thermal evolution of the Northwestern Mediterranean. Annali di Geofisica, Vol. XXXVIII, N.1

Pares, J. M., Van der Pluijm, B. A. and Dinares-Turell, J., (1999). Evolution of magnetic fabrics during incipient deformation of mudrocks (Pyrenees, northern Spain), Tectonophysics, 307, 1-14.

Pares, J.M., van der Pluijm, B.A. (2002). Evaluating magnetic lineations (AMS) in deformed rocks. Tectonophysics 350, 283–298.

Patacca, E., Sartori, R. and Scandone, P. (1992). Tyrrhenian basin and Apenninic arcs: Kinematics relations since Late Tortonian times. Memorie Società Geologica Italiana 45, 425-451.

Patacca, E. and Scandone, P. (2001)- Late thrust propagation and sedimentary response in the thrust-belt-foredeep system of the Southern Apennines (Pliocene-Pleistocene). In: Anatomy of an orogen: The Apennines and adjacent Mediterranean basins (edited by Vai, G. B. & Martini, L. P.). Kluwer, Bodmin, 401-440.

Paterson, S.C., Yu, H. and Oertel, G. (1995). Primary and tectonic fabric intensities in mudrocks. Tectonophysics 247, 105–119.

Pialli, G., Barchi, M.R. and Minelli, G. (1998). Results of the CROP03 Deep Seismic Reflection Profile. Mem. Soc. Geol. Ital. vol. 52 (654 pp.)

Pieri, P., Sabato, L., Loiacono, F. and Marino, M., (1994). Il Bacino di Piggyback di Sant'Arcangelo: evoluzione tettonico- sedimentaria. Bollettino della Società Geologica Italiana 113, 465-481

Plesi G., Luchetti, L., Boscherini, A., Botti, F., Brozzetti, F., Bucefalo Palliani, R., Daniele, G., Motti, A., Nocchi, M. and Rettori, R. (2002). The Tuscan successions of the high Tiber Valley (Foglio 289 – Città di Castello): biostratigraphic, petrographic and structural features, regional correlations. Boll. Soc. Geol. It., Vol. Spec., 1, 425-436.

Principi G. and Treves B. (1984). Il sistema Corso-Appenninico come prisma di accezione. Riflessi sul problema generale del limite Alpi-Appennini. Mem. Soc. Geol. It., 28: 549-576.

Rees, A.I., (1965). The use of anisotropy of magnetic susceptibility in the estimation of sedimentary fabric. Sedimentology 4, 257–271.

Ricci Lucchi, F., (1975). Miocene Palaeogeography and basin analysis in the Periadriatic Apennines, in Squyres, C., editor, Geology of Italy, 2, PESL, Castelfranco Veneto—Tripoli, p. 129-236.

Ricci Lucchi, F., (1986). The Oligocene to Recent foreland basins of the northern Apennines: Special Publication International Association of Sedimentologists, v. 8, p. 105-139.

Ricci Lucchi, F. and. Pialli G (1973). Apporti secondari nella Marnoso-Arenacea: 1. Torbiditi di conoide e di pianura sottomarina a est-nord-est di Perugia, v.92, p. 669-712

Ridolfi A., Luchetti L., Menichetti M., Negri A. and. Pialli G (1995). Use of key beds in stratigraphical and structural analysis of the Marnoso arenacea of the Assino valley area (northern Umbria Preapennines) v.57, p. 113-129

Rochette, P (1987). Magnetic susceptibility of the rock matrix related to magnetic fabric studies. J. Struct. Geol. 9 (8), 1015–1020.

Rochette, P., Jackson, M.J. and Aubourg, C. (1992). Rock magnetism and the interpretation of anisotropy of magnetic susceptibility. Review of Geophysics 30 (3), 209–226.

Royden, L. E., Patacca, E. and Scandone, P. (1987). Segmentation and configuration of subducted lithosphere in Italy: an important control on thrust-belt and foredeep-basin evolution. Geology 15, 714–717.

Royden, L.H., (1993). Evolution of retreating subduction boundaries formed during continental collision. Tectonics 12, 629–638

Roure F., Andriessen P., Callot J.P., Faure J. L., Ferket H., Gonzales E., Guilhaumou N., Lacombe O., Malandain J., Sassi W., Schneider F., S. R. and V. N. (2010). The use of palaeo-thermo-barometers and coupled thermal, fluid flow and pore-fluid pressure modelling for hydrocarbon and reservoir prediction in fold and thrust belts.

Sagri, M. (2012). Note illustrative della Carta geologica d'Italia 1.50000. Figline Valdarno, sheet 276, scale 1:50,000, Ist. Super. per la Prot. e la Ric. 1123 1124 Rome.

Sagnotti, L. (1992). Paleomagnetic evidence for a Pleistocene counterclockwise rotation of the Sant'Arcangelo basin, southern Italy, Geophysical Research Letters, 19, No. 2, 135-138.

Sagnotti, L., and Speranza, F. (1993). Magnetic fabric analysis of the Plio- Pleiatocene clay units of Sant'Arcangelo basin, southern Italy. Physics and Earth Planetary Interior 77, 165–176.

Sagnotti L., Mattei M., Faccenna C. and Funiciello R. (1994a). Paleomagnetic Evidence for No Tectonic Rotation of the Central Italy Tyrrhenian Margin Since Upper Pliocene. Geophys. Res. Lett. 1994; 21:481-484

Sagnotti, L., Faccenna, C., Funiciello, R. and Mattei, M. (1994b). Magnetic fabric and structural setting of Plio-Pleistocene clayey units in an extensional regime: the Tyrrhenian margin of central Italy. Journal of Structural Geology 16, 1243–1257.

Sagnotti, L., Speranza, F., Winkler, A., Mattei, M. and Funiciello, R. (1998). Magnetic fabric of clay sediments from the external northern Apennines (Italy). Physics of the Earth and Planetary Interiors 105, 73–93.

Sagnotti, L., Winkler, A., Alfonsi, L., Florindo, F., and Marra, F. (2000). Paleomagnetic constraints on the Plio–Pleistocene geodynamic evolution of the external central–northern Apennines (Italy). Earth and Planetary Science Letters, 180 (3-4), 243–257. doi:10.1016/S0012-821X(00)00172-2

Scheepers, P.J.J., and Langereis, C.G. (1994). Magnetic fabric of the Pleistocene clays from the Tyrrhenian arc: a magnetic lineation induced in the final stage of the middle Pleistocene compressive event. Tectonics 13, 1190–1200.

Scheepers, P. J. J., Langereis, C. G. and Hilgen, F., (1993). Counter-clockwise rotations in the Southern Apennines during the Pleistocene: Paleomagnetic evidence from the Matera area. Tectonophysics 225, 379-410.

Scheepers, P. J. J., Langereis, C. G., Zijderveld, J. D. A. and Hilgen, F., (1994). Paleomagnetic evidence for a Pleistocene clockwise rotation of the Calabro-Peloritan block (southern Italy). Tectonophysics 230, 19-48.

Schieber, J. and Ellwood, B.B. (1988). Determination of basinwide paleocurrent patterns in a shale succession from anisotropy of magnetic suscepti- bility (AMS): a case study of the Mid-Proterozoic Newland Formation, Montana. Journal of Sedimentary Petrology 58, 830–835.

Schwartz, S. Y. and Van der Voo, R. (1983). Paleomagnetic evaluation of the orocline hypothesis in the central and southern Appalachians. Geophysical Research Letters 10, 505–508

Sclater, J.G., and Christie, P.A.F. (1980). Continental stretching: An explanation of post–Mid Cretaceous subsidence on the central North Sea Basin: Journal of Geophysical Research, v. 85, p. 3711–3739, doi: 10.1029/JB085iB07p03711.

Speranza, F., L. Sagnotti and M. Mattei (1997). Tectonics of the Umbria- Marche-Romagna Arc (central northern Apennines, Italy): New paleomagnetic constraints, J. Geophys. Res., 102, 3153–3166.

Speranza, F., Mattei, M., Naso, G., Di Bucci, D., and Corrado, S. (1998). Neogene–Quaternary evolution of the central Apennine orogenic system (Italy): a structural and palaeomagnetic approach in the Molise region. Tectonophysics, 299(1-3), 143–157. doi:10.1016/S0040-1951(98)00202-9

Speranza, F., Maniscalco R., Mattei M. Di Stefano A., Butler R.W. H., and Funiciello R. (1999). Timing and magnitude of rotations in the frontal thrust systems of southwestern Sicily, Tectonics, 18, 1178–1197.

Speranza, F., Mattei, M., Sagnotti, L. and Grasso, F. (2000). Rotational differences between the northern and southern Tyrrhenian domains: paleomagnetic constraints from the Amantea basin (Calabria, Italy). Journal Geological Society London 157, 327-334.

Speranza, F., I. Villa, L. Sagnotti, F. Florindo, D. Cosentino, P. Cipollari, and M. Mattei (2002). Age of the Corsica-Sardinia rotation and Liguro-Provençal basin spreading: New paleomagnetic and 40Ar/39Ar evidence. Tectonophysics, 347, 231–251.

Speranza, F., and Parisi, G. (2007). High-resolution magnetic stratigraphy at Bosso Stirpeto (Marche, Italy): Anomalous geomagnetic field behaviour during early Pliensbachian (early Jurassic) times? Earth and Planetary Science Letters, 256(3-4), 344–359. doi:10.1016/j.epsl.2007.01.006

Staplin, F.L., (1969). Sedimentary organic matter, organic metamorphism, and oil and gas occurrence. Bulletin of Canadian Petroleum Geology 17 (1), 47-66

Stockli, D. F., Farley, K. a., and Dumitru, T. A. (2000). Calibration of the apatite (U-Th)/He thermochronometer on an exhumed fault block, White Mountains, California. Geology,*28*(11),983–986.doi:10.1130/0097613(2000)028<0983:COTAUT>2.3.CO;2

Tarling, D.H. and Hrouda, F. (1993). The Magnetic Anisotropy of Rocks. Chapman and Hall, London, 217 pp.

Tavarnelli, E., Holdsworth, R.E., Clegg, P., Jones, R.R., McCaffrey, K.J.W., (2004). The anatomy and evolution of a transpressional imbricate zone, Southern Uplands, Scotland. Journal of Structural Geology 26 (8), 1341-1360 10.1016/j.jsg.2004.01.003

Thomson, S. N., Brandon, M. T., Reiners, P. W., Zattin, M., Isaacson, P. J., and Balestrieri, M. L. (2010). Thermochronologic evidence for orogen-parallel variability in wedge kinematics during extending convergent orogenesis of the northern Apennines, Italy. Geological Society of America Bulletin, 122(7-8), 1160–1179. doi:10.1130/B26573.1

Thio, H. K., (1987). Magnetotectonics in the Piemont Tertiary Basin. Phys. Earth Planet. Inter. 52, 308-319.

Treves, B., (1984). Orogenic belts as accretionary prisms: The example of the Northern Apennines. Ofioliti 9, 577-618.

Van der Voo, R. and Channell, J. E. T., (1980). Paleomagnetism in orogenic belts. Reviews of Geophysics and Space Physics 18, 455-481

Van der Voo, R. (1993), Paleomagnetism of the Atlantic, Thetys, and Iapetus Oceans, 411 pp., Cambridge Univ. Press, New York.

Van Hinsbergen, D.J.J., Krijgsman, W., Langereis, C.G., Cornée, J.-J., Duermeijer, C.E. and van Vugt, N. (2007). Discrete Plio-Pleistocene phases of tilting and counterclockwise rotation in the southeastern Aegean arc (Rhodos; Greece): early Pliocene formation of the south Aegean left-lateral strike-slip system, Journal of the Geological Society of London 164, 1133-1144.

Van Hinsbergen, D.J.J., Dupont-Nivet, G., Nakov, R., Oud, K. and Panaiotu, C. (2008). No significant post-Eocene rotation of the Moesian Platform and Rhodope (Bulgaria): implications for the kinematic evolution of the Carpathian and Aegean arcs: Earth Planet. Sci. Lett., 273, 345-358.

Vandenberg, J., Klootwijk, C. T. and Wonders, A. A. H., (1978). Late Mesozoic and Cenozoic movements of the Italian Peninsula: Further paleomagnetic data from the Umbrian sequence. Geological Society American Bulletin 89, 133-150.

Ventura, B., Pini, G.A., and Zuffa, G.G., (2001). Thermal history and exhumation of the northern Apennines (Italy): Evidence from combined apatite fi ssion track and vitrinite refl ectance data from foreland basin sedi- ments: Basin Research, v. 13, no. 4, p. 435–448, doi: 10.1046/j.0950-091x.2001.00159.x.

Vigliotti, L., and Kent, D.V. (1990). Paleomagnetic results of Tertiary sediments from Corsica : evidence of post-Eocene rotation. Physics of the Earth and Planetary Interiors, 62, 97–108.

Vigliotti L., Alvarez W. and McWilliams M. (1990). No relative rotation detected between Corsica and Sardinia, Earth Planet. Sci. Lett. 98 313–318.

Wagner, G.A., and Reimer, G.M. (1972). Fission track tectonics: the tectonic interpretation of fission track apatite ages: Earth Pl. Sci. Lett., v. 14, p. 263-268.

Wagner, G.A., and Van de Haute, P. (1992). Fission-track dating: Kluwer, Dordrecht, p. 286.

Warnock, A.C., Zeitler, P.K.,Wolf, R.A., and Bergman, S.C., (1997). An evaluation of low-temperature apa- tite U-Th/He thermochronometry. Geochimica et Cosmochimica Acta, v. 61, p. 5371–5377.

Westphal, M., Bardon C., Bossert A. and Hamzeh R. (1973). A computer fit for Corsica and Sardinia against Southern France, Earth Planet. Sci. Lett. 18 137–140.

Winkler A. and L. Sagnotti (1994). Anisotropy of anhysteretic remanence and magnetic susceptibility of marly clays from Central Italy, Annali di Geofisica, XXXVII, N.5, 1027-1035.

Wolf R., Farrley, K. and Silver, L. (1996a). Assesstment of (U-Th)/He thermocronometry: the low-temperature history of the San Jacinto Mountains, California. Geology, 25, 65-68.

Wolf R., Farrley, K. and Silver, L. (1996b). Helium diffusion and low-temperature thermocronometry of apatite. Geochimica and Cosmochimica Acta v. 60, p. 4231-4240.

Wolf R., Farrley, K. and Kass, D. (1998). Modeling of the temperature sensitivity of the apatite (U-Th)/He thermocronometr. Chem. Geol. 148, 105-114.

Zattin, M. (2003) Apatite fission-track analysis and the thermocronology of sedimentary Successions: Atti Ticinensi di Scienze della Terra - special series, v. 9, p. 33-42.

Zattin, M., Picotti, V. and Zuffa, G. G. (2002). Fission-track reconstruction of the front of the northern apennine thrust wedge and overlying ligurian unit. America journal of science, vol.302, 346–379.

Zattin, M., Landuzzi, A., Picotti, V. and Zuffa, G.G., (2000). Discriminat- ing between tectonic and sedimentary burial in a foredeep succession, Northern Apennines. Journal of the Geological Society of London 157, 629–633

Zeitler, P.K., Herczig, A.l., McDougall, I. and Honda, M. (1987). (U-Th)/He dating on apatite: a potential thermochronometer - Geochimica and Cosmochimica Acta v. 51, p. 2865-2868.

Zijderveld, J. D. A. (1967). A. C. demagnetization of rocks: Analysis of results, in Methods in Palaeomagnetism, edited by D.W. Collinson, K. M. Creer, and S. K. Runcorn, pp. 254–286, Elsevier, New York.

Zijderveld, J.D.A., De Jong, K.A., Van der Voo, R. (1970). Rotation of Sardinia: palaeomagnetic evidence from Permian rocks. Nature 226, 933–934.